



Terms and Conditions of Use of Digitised Theses from Trinity College Library Dublin

Copyright statement

All material supplied by Trinity College Library is protected by copyright (under the Copyright and Related Rights Act, 2000 as amended) and other relevant Intellectual Property Rights. By accessing and using a Digitised Thesis from Trinity College Library you acknowledge that all Intellectual Property Rights in any Works supplied are the sole and exclusive property of the copyright and/or other IPR holder. Specific copyright holders may not be explicitly identified. Use of materials from other sources within a thesis should not be construed as a claim over them.

A non-exclusive, non-transferable licence is hereby granted to those using or reproducing, in whole or in part, the material for valid purposes, providing the copyright owners are acknowledged using the normal conventions. Where specific permission to use material is required, this is identified and such permission must be sought from the copyright holder or agency cited.

Liability statement

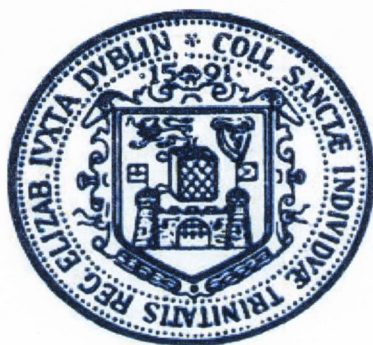
By using a Digitised Thesis, I accept that Trinity College Dublin bears no legal responsibility for the accuracy, legality or comprehensiveness of materials contained within the thesis, and that Trinity College Dublin accepts no liability for indirect, consequential, or incidental, damages or losses arising from use of the thesis for whatever reason. Information located in a thesis may be subject to specific use constraints, details of which may not be explicitly described. It is the responsibility of potential and actual users to be aware of such constraints and to abide by them. By making use of material from a digitised thesis, you accept these copyright and disclaimer provisions. Where it is brought to the attention of Trinity College Library that there may be a breach of copyright or other restraint, it is the policy to withdraw or take down access to a thesis while the issue is being resolved.

Access Agreement

By using a Digitised Thesis from Trinity College Library you are bound by the following Terms & Conditions. Please read them carefully.

I have read and I understand the following statement: All material supplied via a Digitised Thesis from Trinity College Library is protected by copyright and other intellectual property rights, and duplication or sale of all or part of any of a thesis is not permitted, except that material may be duplicated by you for your research use or for educational purposes in electronic or print form providing the copyright owners are acknowledged using the normal conventions. You must obtain permission for any other use. Electronic or print copies may not be offered, whether for sale or otherwise to anyone. This copy has been supplied on the understanding that it is copyright material and that no quotation from the thesis may be published without proper acknowledgement.

Noradrenaline acting on astrocytic β -adrenoceptors enhances neuronal complexity in primary cortical neurons



Jennifer Day

Thesis submitted for the degree of Doctorate of Philosophy at the University
of Dublin, Trinity College

Thesis submitted June 2012

Department of Physiology,
Trinity College Institute of Neuroscience
Trinity College,
Dublin 2.



Thesis 9665

In loving memory of:

Joan Flower
(1927-2012)

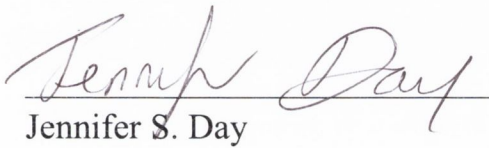
And

Keith Flower
(1984-2012)

I Declaration

I declare that this thesis has not been submitted as an exercise for a degree at this or any other university and it is entirely my own work.

I agree to deposit this thesis in the University's open access institutional repository or allow the library to do so on my behalf, subject to Irish Copyright Legislation and Trinity College Library conditions of use and acknowledgement.


Jennifer S. Day

II Summary

The complex structure of a neuron, comprising of an axon and dendrites (collectively termed neurites), is integral to the formation of functional networks in the central nervous system during development and after injury. Understanding the mechanisms involved in neuritic growth is imperative for regenerative neuroscience, and may lead to symptomatic cures for neurodegenerative diseases.

Noradrenaline (NA) is a catecholaminergic monoamine neurotransmitter which has been shown to have many neuroprotective properties via an action on the glial β_2 -adrenoceptor. The first aim of this thesis was to assess the ability of NA to induce neuritic growth of primary cortical neurons *in vitro* via (a) a direct action on neuronal adrenoceptors, and (b) an indirect action via glial adrenoceptors on primary mixed glial cells. Neurons were treated either directly with NA (1, 5, 10 μ M) or with the conditioned media (CM) from NA treated glial cells (NA CM). Any changes in neuronal morphology were determined using Sholl analysis, a method used to examine structure of primary neurites, neuritic branching and neuritic length of neurons. The results demonstrated that CM from NA treated glial cells, but not NA itself, increased the number of primary neurites, neuritic branching and the neuritic length of the primary cortical neurons when compared to control treated neurons.

The second aim of this study was to determine the receptor subtype and glial cell type by which NA-CM may be inducing its effect. It was determined that the effect of NA was mediated via the β_2 -adrenoceptor present on astrocytes as use of the β -adrenoceptor antagonist, propranolol, and not the α -adrenoceptor antagonist, phentolamine, attenuated NA CM-induced increases in neuritic growth. In addition, the selective β_2 -adrenoceptor agonists clenbuterol and salmeterol, but not the β_1 -adrenoceptor agonist, xamoterol, mimicked the NA CM-induced neuritic growth suggesting that it is in fact the β_2 -adrenoceptor and not the β_1 -adrenoceptor that is involved in this process. This was further supported by the finding that similar neuronal changes were found with the utilisation of the cell permeable cAMP analogue, dbcAMP, which is downstream of β_2 -adrenoceptor activation. Furthermore activation of the β -adrenoceptors on astrocytes but not on microglia led to increases in neuritic growth compared to control neurons, demonstrating that it is the astrocytes which are involved in this NA-mediated neuritic growth.

The ability of NA CM to induce neuritic growth was attributed to increased release of IL-6 and to a lesser extent GDNF and FGF-2 from the astrocytes, in combination with the presence of the neurotrophin, NGF- β . This was deduced as inhibition of each of these factors attenuated NA CM-induced neuritic growth to some degree. In addition to this, the phosphatidylinositol 3-kinase (PI3K), mitogen activated protein kinase (MAPK) and JAK-STAT signalling pathways have been implicated in NA CM-induced neuritic growth as phosphorylation of downstream mediators of each of these pathways was observed in NA CM-treated primary cortical neurons. Moreover, inhibition of these pathways via wortmannin and LY294002, PD98059 or S31-201 respectively attenuated the NA CM-induced neuritic growth previously observed.

Taken together, these results demonstrate a novel role for the astrocytic β_2 -adrenoceptor in inducing neuritic growth of cortical neurons. These findings may provide a therapeutic strategy for encouraging neuritic growth following neurodegeneration.

III Acknowledgements

I would first of all like to thank my supervisor, Professor Thomas Connor, for giving me the opportunity to complete my Ph.D. in his laboratory, and for all his guidance, support and well wishes over the years. Without him, this thesis would not have been possible, and so I am eternally grateful for his assistance.

I also wish to thank Professor Marina Lynch, TCIN, the department of Physiology and the HRB programme for taking me for this Ph.D. I have thoroughly enjoyed my time at TCIN and so would like to thank you for giving me this opportunity. I am also so grateful to all the staff in TCIN and physiology for all the assistance over the years.

In addition, a massive thank you to all the members of the TC/AH lab both past and present: Noreen, Karen, Dana, Lorna, Natacha, Alessia, Katie, Jen R, Aine, Valentina, Sinead, Éadaoin, Raasay, Eimear, Martina, Barry, Shane. Every single one of you has helped me bring this thesis to light, and for that I thank you. I would also like to thank my students over the years; Katie S., Katie M., Nick, Caroline and Eimear, thank you for your enthusiasm and hard-work, I wish you luck in all your future endeavours.

I would also like to take this opportunity to thank the other labs in TCIN. In particular Professor Mani Ramaswami and Dr. Joern Huelsmeier for their kindness in allowing use of their fluorescent microscope and all the assistance they gave me. Also to all the members of MAL, VAC, CC, Kelly, KKD and SOM labs for all the support over the years, both academic and social! In particular my HRB class: Ranya, Liz, Amy, Donal and Rodrigo, thank you guys, I couldn't have done this without you.

And last but by no means least, my family and friends. My parents; Janet and Colin, and my brothers; Andrew and Steven, thank you for your love, support and words of encouragement. Thank you also to Owen, for putting up with me, and for always being so supporting. To the rest of my family; my grandparents, aunts, uncles, cousins, nephew and sisters-in-law thank you for believing in me.

IV Table of Contents

I Declaration	i
II Summary	iii
III Acknowledgements	v
IV Table of Contents	vii
V List of Figures	xii
VI List of Tables	xiv
VII Abbreviations.....	xv
Chapter 1	1
1 Introduction	1
1.1 Cells of the central nervous system.....	1
1.1.1 Astrocytes	1
1.1.2 Microglia.....	3
1.1.3 Neurons and Neuronal Growth.....	4
1.1.4 The importance of neuronal protection and neuronal growth.....	7
1.2 Noradrenaline.....	9
1.2.1 Noradrenaline synthesis and metabolism	9
1.2.2 The adrenoceptors.....	10
1.2.3 Functions of NA.....	13
1.3 Serotonin	14
1.3.1 Serotonin synthesis and metabolism	14
1.3.2 Serotonin receptors	15
1.3.3 Functions of 5-HT	15
1.4 Pathways Associated with Neuronal Growth.....	16
1.4.1 The Mitogen Activated Protein Kinase Pathway	16
1.4.2 Phosphoinositide Signalling.....	20
1.4.3 Signalling via the receptor tyrosine kinases	22
1.5 Neuroprotective and neuronal growth inducing factors.....	23
1.5.1 Neurotrophins	23
1.5.2 Glial-derived neurotrophic factor.....	28
1.5.3 FGF-2.....	31
1.5.4 VEGF	34
1.5.5 Interleukin-6.....	35

1.6 Objectives of thesis.....	39
Chapter 2.....	41
<i>Materials and Methods</i>	41
2.1 <i>Materials</i>	39
2.1.1 <i>Animals</i>	39
2.1.2 <i>Experimental Treatments</i>	39
2.1.3 <i>Cell Culture Materials</i>	41
2.1.4 <i>Assay Kits</i>	42
2.1.5 <i>Molecular Reagents</i>	42
2.1.6 <i>General Laboratory Plastics</i>	43
2.1.7 <i>General Laboratory Chemicals</i>	43
2.1.8 <i>Western Blotting and Staining reagents and antibodies</i>	45
2.2 <i>Methods</i>	46
2.2.1 <i>Aseptic Technique</i>	46
2.2.2 <i>Preparation of Culture Media and Test Compounds</i>	47
2.2.3 <i>Preparation of coverslips</i>	49
2.2.4 <i>Preparation of Primary Cultures</i>	49
2.2.5 <i>Preparation of C6 glioma cells</i>	52
2.2.6 <i>Cell culture treatments</i>	53
2.2.7 <i>Harvesting glial cultures for mRNA analysis</i>	54
2.2.8 <i>Preparation of neuronal cultures for Western Immunoblotting</i>	54
2.2.9 <i>RNA Analysis</i>	54
2.2.10 <i>Fluorescent Immunocytochemistry and Sholl Analysis</i>	57
2.2.11 <i>Cell Viability assay: Alamar Blue</i>	61
2.2.12 <i>Sodium Dodecyl Sulphate Polyacrylamide Gel Electrophoresis (SDS-PAGE) and Western Immunoblotting</i>	61
2.2.13 <i>Enzyme-linked Immunosorbent assays (ELISA)</i>	64
Table 2.4 <i>ELISA antibodies and procedures</i>	65
2.2.14 <i>Statistical Analysis</i>	66
Chapter 3.....	67
3.1 Examination of the impact of neurotransmitters on neuronal complexity	69
3.1.1 <i>Effect of noradrenaline on neuronal complexity: A role for glial cells</i>	70
3.1.2 <i>NA has no effect on neuronal complexity of primary cortical neurons</i>	75
3.1.3 <i>5-HT CM has no effect on the morphology of primary cortical neurons</i>	79

3.1.4	<i>5-HT has no effect on neuronal complexity of primary cortical neurons</i>	82
3.1.5	<i>Amitriptyline CM increases some measures of neuronal morphology</i>	85
3.1.6	<i>Direct Amitriptyline treatment increases neuronal complexity</i>	88
3.2	<i>Examination of the glial adrenoceptor subtype involved in noradrenaline mediated neuronal morphology changes</i>	91
3.2.1	<i>NA CM-induced increases in neuronal morphology are primarily attributed to the β-adrenoceptor</i>	92
3.2.2	<i>Salbutamol CM increases measures of neuronal morphology</i>	96
3.2.3	<i>The β2-adrenoceptor agonists, salmeterol and clenbuterol, but not the β1-adrenoceptor agonist, xamoterol, increases measures of neuronal morphology</i>	99
3.2.4	<i>The cAMP analogue, dbcAMP, CM increases neuronal complexity</i>	102
3.3	<i>NA stimulation of astrocytic β-adrenoceptors are responsible for the NA CM-induced increases in neuronal complexity</i>	106
3.3.1	<i>NA CM from enriched astrocytes increases neuronal complexity</i>	107
3.3.4	<i>NA CM from enriched microglia does not increase neuronal morphology</i>	111
3.3.2	<i>Salbutamol CM from enriched astrocytes increases neuronal complexity</i>	114
3.3.3	<i>DbcAMP CM from enriched astrocytes increases neuronal complexity</i>	117
3.4	<i>C6 glioma cells as a model of primary astrocytes</i>	120
3.4.1	<i>C6 glioma cells express the astrocytic markers S100β and GFAP</i>	121
3.4.2	<i>The C6 glioma cells express the β2-adrenoceptor</i>	122
3.4.3	<i>NA CM from C6 glioma cells shows no effect on neuronal morphology</i>	123
3.5	<i>A role for glial-derived growth factors in mediating the effects of NA CM on neuronal morphology</i>	125
3.5.1	<i>NA and Salb treatment of glial cells induce the expression of growth factors</i>	126
3.5.2	<i>NA increases the release of growth factors from glial cells</i>	130
3.5.3	<i>GDNF increases neuronal complexity of primary cortical neurons</i>	131
3.5.4	<i>NGF-β increases neuronal complexity of primary cortical neurons</i>	134
3.5.5	<i>BDNF increases neuronal complexity of primary cortical neurons</i>	137
3.5.6	<i>FGF-2 increases neuronal complexity of primary cortical neurons</i>	140
3.5.7	<i>VEGF does not increase neuronal complexity of primary cortical neurons</i>	143
3.5.8	<i>IL-6 increases neuronal complexity of primary cortical neurons</i>	146
3.5.9	<i>Neutralization of GDNF attenuates some NA CM-induced increases in measures of neuronal complexity</i>	149
3.5.10	<i>Inhibition of NGF-β and BDNF signalling blocks NA CM-induced increases in neuronal complexity</i>	152
3.5.11	<i>Neutralization of FGF-2 attenuates NA CM-induced increases in neuronal complexity</i>	155

3.5.12 <i>Inhibition of IL-6 Signalling blocks NA CM-induced increases in neuronal complexity</i>	158
3.6 Signalling pathways mediating the ability of NA CM to increase the complexity of primary cortical neurons	161
3.6.7 <i>NA CM activates signaling pathways associated with neuronal growth in neurons</i>	162
3.6.1 <i>Inhibitors of the PI3K pathway blocks NA CM-induced increases in neuronal morphology</i>	164
3.6.2 <i>An inhibitor of the MAPK pathway attenuates NA CM-induced increases in neuronal morphology</i>	167
3.6.3 <i>An inhibitor of the STAT3 pathway blocks NA CM-induced increases in neuronal morphology</i>	170
4 Discussion	175
4.1 CM from NA treated glial cells but not a direct stimulation with NA, induces neuritic growth of primary cortical neurons	176
4.2 5-HT does not induce neuritic growth	177
4.3 The NA/5-HT reuptake inhibitor, AMI, induces neuritic growth via both an action on glial cells and a direct action on neurons	179
4.4 The β_2 -adrenoceptor is involved in NA CM-induced neuritic outgrowth	181
4.5 Astrocytes and not microglia are involved in the NA CM-induced neuritic growth	183
4.6 The C6 glioma cell line cannot be used as a model for the ability of primary astrocytes <i>in vitro</i> to induce neuritic growth	185
4.7 Factors involved in inducing neuronal growth by NA CM	186
4.7.1 <i>GDNF contributes to the NA CM increases in neuronal complexity</i>	187
4.7.2 <i>The presence of the neurotrophins; NGF-β and BDNF, are required for NA CM-induced increases in neuronal complexity</i>	188
4.7.3 <i>FGF-2 contributes to NA CM-induced increases in neuronal complexity</i>	191
4.7.4 <i>VEGF does not contribute to the NA CM-induced increases in neuronal complexity</i>	192
4.7.5 <i>IL-6 is required for the NA CM-induced increases in neuronal complexity</i>	193
4.7.6 <i>Cross-talk between the neuritic growth-inducing factors</i>	194
4.8 Signalling Pathways involved in NA CM-induced increases in neuronal morphology	196
4.8.1 <i>The PI3K pathway is involved in NA CM-induced increases in neuronal morphology</i>	196
4.8.2 <i>The MAPK pathway is involved in NA CM-induced increases in neuronal morphology</i>	198
4.8.3 <i>The STAT3 pathway is involved in NA CM-induced increases in neuronal morphology</i>	200
4.8.4 <i>Cross-talk between the PI3K, MAPK and STAT3 Pathways</i>	201
4.9 The induction of neuritic growth; the answer to neuronal degeneration?	202
4.10 Research Limitations and Future Directions	204

4.11 Conclusion 205

Chapter 5: References

V List of Figures

Figure 1.1	Functions of astrocytes	2
Figure 1.2	A typical neuron	5
Figure 1.3	The noradrenergic neuron	11
Figure 1.4	Signalling at the β_2 -adrenoceptor	13
Figure 1.5	Four main branches of MAPK Signalling	17
Figure 1.6	ERK1/2 Branch of MAPK Signalling	19
Figure 1.7	PI3K signalling leads to neuritic growth	21
Figure 1.8	Signalling via the Trk Receptors	24
Figure 1.9	Signalling via the p75 receptor	25
Figure 1.10	Signalling of GDNF	30
Figure 1.11	FGF-2 Signalling via the FGFR	33
Figure 1.12	IL-6 Signalling	37
Figure 2.1	C6 Glioma Cells growth and morphology	53

Figure 2.2	Neuron stained with β III tubulin and Hoescht (A) with overlaying Sholl analysis concentric circles (B)	59
Figure 2.3	Sholl profile of untreated rat primary cortical neurons	60
Figure 4.1	AMI leads to dimerisation of Trk receptors which may lead to neuritic growth via the PI3K and MAPK pathway	181
Figure 4.2	A unified theory for NA CM-induced neuritic growth	206

VI List of Tables

Table 2.1	Drug Interventions	40
Table 2.2	List of primers for PCR	57
Table 2.3	Antibody dilutions for western Immunoblotting	63
Table 2.4	ELISA antibodies and procedures	65

VII Abbreviations

5-HT	Serotonin
5-HTP	5-Hydroxytryptophan
AAAD	L-Aromatic amino acid decarboxylase
AD	Alzheimer's Disease
ALS	Amyotrophic lateral sclerosis
AMI	Amitriptyline
ANOVA	Analysis of Variance
Ask-1	Apoptosis signal-regulating kinase I
ATF2	Activating transcription factor 2
ATP	Adenosine triphosphate
BAD	Bcl-2-associated death promoter
BBB	Blood-brain-barrier
BDNF	Brain-derived neurotrophic factor
BSA	Bovine serum albumen
cAMP	Cyclic adenosine monophosphate
CBP	CREB-binding protein
CDMEM	Complete DMEM
Clen	Clenbuterol
CM	Conditioned medium
CNBM	Complete NBM
CNS	Central nervous system
CNTF	Ciliary neurotrophic factor
CREB	cAMP response element binding
DAPI	4',6-diamidino-2-phenylindole
dbcAMP	Dibutyryl adenosine 3',5'-cyclic monophosphate
DIV	Days in vitro
DMEM	Dulbecco's modified eagles medium
DOPA	3,4-dihydroxyphenylalanine
DPBS	Dulbecco's phosphate buffered saline
DRG	Dorsal root ganglion
EGF	Epidermal growth factor

Elk1	ETS-like transcription factor 1
EMT	Extraneuronal monoamine transporter
ERK	Extracellular signal-regulated kinases
EtOH	Ethanol
F-actin	Filamentous actin
FBS	Foetal bovine serum
FGF	Fibroblast growth factor
FGFR	FGF receptor
Frk	Forkhead-related transcription factor
FRS	Fibroblast growth factor receptor substrate
GAB	Grb-2 associated binder
GABA	γ -aminobutyric acid
GDNF	Glial-derived neurotrophic factor
GDP	Guanosine diphosphate
GFAP	Glial fibrillary acidic protein
GFL	GDNF family ligand
GFR- α	GDNF family receptor α -component
GPCR	G-protein coupled receptor
Grb-2	Growth factor receptor-bound protein 2
GSK3 β	Glycogen synthase kinase 3 β
GTP	Guanosine triphosphate
HCL	Hydrochloric acid
HPA	Hypothalamic-pituitary-adrenal
IFN	Interferon
IL-1 β	Interleukin 1 β
IL-6	Interleukin-6
IL-6R	Interleukin-6 receptor
IL-6R α	IL-6 receptor α
IRS	Insulin receptor substrate
JAK	Janus kinases
JNK	c-Jun NH2-terminal kinases
LPS	Lipopolysaccharide
MAP	Microtubule associated proteins

MAPK	Mitogen activated protein kinase
MAPKK	MAPK kinase
MAPKKK	MAPK kinase kinase
MEK	MAPK kinase
MHC	Major histocompatibility complex
MPTP	1-methyl-4-phenyl-1,2,3,6-tetrahydropyridine
mTOR	Mammalian target of rapamycin
NA	Noradrenaline
NBM	Neurobasal Medium
NCAM	Neural cell adhesion molecule
NET	Noradrenaline transporter
NFAT	Nuclear factor of activated T cells
NFκB	Nuclear factor kappa B
NGF	Nerve growth factor
NGS	Normal goat serum
NIK	NFκB inducing kinase
NT3	Neurotrophin 3
NT4/5	Neurotrophin 4/5
P90	S6 Kinase p90
Pak	p21-activated kinase
PBS	Phosphate buffered saline
PCR	Polymerase Chain Reaction
PD	Parkinson's Disease
PDK1	Phosphoinositide dependent kinase I
PI3K	Phosphatidylinositol 3-kinase
PIP2	Phosphatidylinositol 4,5-bisphosphate
PIP3	Phosphatidylinositol 3,4,5-trisphosphate
PKA	protein kinase A
PKC	Protein kinase C
PTEN	Phosphatase and tensin homolog
Rac	Ras-related C3 botulinum toxin substrate
Rap-1	Ras-related protein 1
RET	Rearranged during transfection

RT	Room temperature
RTK	Receptor tyrosine kinase
RT-PCR	Real-time PCR
Salb	Salbutamol
Salm	Salmeterol
SERT	Serotonin transporter
SH	Src homology
sIL-6R	Soluble IL-6 receptor
SMA	Spinal muscular atrophy
SOCS	Suppressors of cytokine signalling
SOS	Son of sevenless
TGF- β	Transforming growth factor β
TNF	Tumour necrosis factor
Traf6	TNF receptor associated factor 6
Trk	Tropomyosin receptor kinase
VEGF	Vascular endothelial growth factor
VMAT	Vesicular monoamine transporter
Xam	Xamoterol

Chapter 1

Introduction

1 Introduction

“Intellectual power, and its most noble expressions, talent and genius, do not depend on the size or number of cerebral neurons, but on the richness of their connective processes”

Santiago Ramon y Cajal: Recollections of My Life, 1884

As Cajal realised in the 1800s, the complex structure of a neuron is essential to all aspects of neuronal function (Cajal, 1937). Understanding the mechanisms of neuritic growth, that is, the growth of axons and dendrites, is important to many areas including developmental neuroscience and regenerative medicine. This thesis largely focuses on the ability of noradrenaline (NA), a neurotransmitter, to impact upon the growth and complexity of primary cultures of cortical neurons (herein called “primary cortical neurons”).

1.1 Cells of the central nervous system

The cells of the central nervous system (CNS) primarily consist of neurons and glia. A neuron, or nerve cell, is the fundamental building block of the CNS. Neurons carry signals both electrically via propagation of an action potential, and chemically via neurotransmitter release at a nerve terminal (Rang & Dale, 2003). Glial cells outnumber neurons, constituting 90% of the cells in the brain and comprising of more than half the volume. There are four subtypes of glial cells in the CNS; astrocytes, microglia, oligodendrocytes and ependymal cells. Traditionally, glia were seen as support cells for neurons and nothing more, however, it is now known that glia have many important functions including synapse formation (for review, see Barker & Ullian, 2008) and immunity (for review, see Graeber *et al.*, 2011).

1.1.1 Astrocytes

It was originally thought that astrocytes merely functioned as nutrient providers and buffers of ionic fluxes and neurotransmitter release. However, astrocytes are now known to be involved in neuronal development, synapse formation and upkeep, blood-brain-barrier (BBB) formation and upkeep, modulation of neuronal ionic signalling, support of neuronal metabolic pathways, neurotransmitter homeostasis, clearance of free radicals, immune function and also the provision of trophic support (see Figure 1.1; for reviews see Laming *et al.*, 2000; Abbott *et al.*, 2006; Markiewicz & Lukomska, 2006). Furthermore, astrocytes express receptors for most, if not all, neurotransmitters, and also demonstrate

functional downstream signalling following neurotransmitter binding. As such, astrocytes express functional receptors for NA (both α and β adrenoceptors), acetylcholine, serotonin (5-HT), dopamine, γ -Aminobutyric acid (GABA), glutamate, neuropeptides, histamine and the opioids (for review see Kimelberg, 1995).

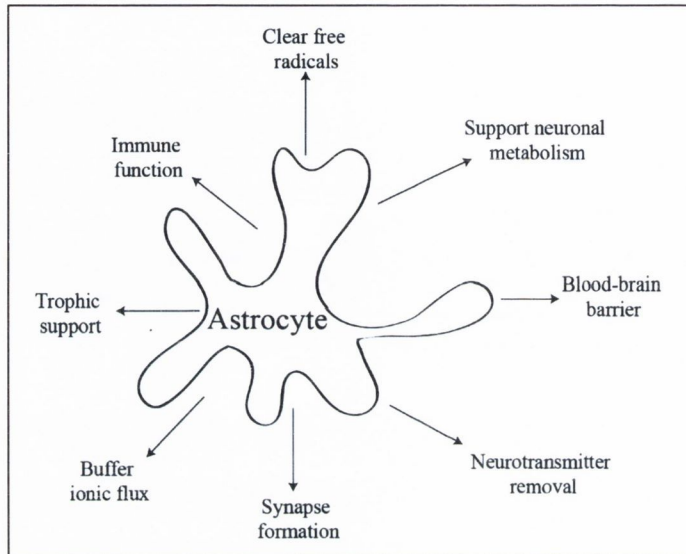


Figure 1.1: Functions of astrocytes

Astrocytes are involved in neuronal metabolism, the formation of the blood brain barrier, neurotransmitter removal, synapse formation, buffering ionic fluxes, trophic support, immune function and the clearance of free radicals.

1.1.1.1 Astrocytes and neuronal regeneration

Astrocytes are associated with the inability of neurons to regenerate following trauma. The astrocytes form a “glial scar” which is not only a physical barrier, but also an inhibitory environment as they secrete a number of inhibitory molecules that prevent axonal regrowth. These include tenascin, semaphorins and chondroitin sulphate proteoglycans (for review see Fitch & Silver, 2008). CNS neurons do however have the capacity for regeneration (Fitch & Silver, 2008), and so overcoming these inhibitory signals, or encouraging astrocytes to create a more permissive environment for neuronal regrowth is a promising strategy for neuronal regeneration research. Leading on from this, astrocytes are also vital for neuronal survival and growth. For example, astrocytes encourage a neuritic phenotype from neuronal cells in culture (Desagher *et al.*, 1996; Trentin *et al.*, 2003; Tom *et al.*, 2004; Oh *et al.*, 2009). Furthermore, astrocytes are capable of protecting neurons from toxic insults including amyloid- β toxicity (Yamamuro *et al.*, 2003) and oxidative stress (Desagher *et al.*, 1996; Tanaka *et al.*, 1999; Takano *et al.*, 2009), as well

as having the ability to produce and secrete a range of neurotrophic factors which provide protection to neurons. These include, for example; glial cell line-derived neurotrophic factor (GDNF), brain derived neurotrophic factor (BDNF), nerve growth factor β (NGF- β), neurotrophin-3 (NT-3) and fibroblast growth factor 2 (FGF-2) (Appel *et al.*, 1997; Basu & Yang, 2005; Toyomoto *et al.*, 2005; Delgado-Rivera *et al.*, 2009; Tanabe *et al.*, 2009; Mele *et al.*, 2010).

1.1.2 Microglia

Microglial cells, considered the brain's immune cells, belong to the monocytic lineage but their immune receptors are less prevalent compared to those of macrophages. Much of the focus on microglial cells is on their capacity to be highly activated upon toxic stimuli, such as inflammation or neurodegeneration. Upon activation, the microglia retract their processes, and become more amoeboid in morphology. They upregulate the expression of major histocompatibility complex (MHC) class II receptors, adhesion molecules and endocytotic receptors, release pro-inflammatory cytokines and reactive oxygen species, and increase their phagocytic capacity (for reviews, see Aloisi *et al.*, 2000; Galea *et al.*, 2007). In addition to this, activated microglial cells are capable of producing a range of pro-inflammatory mediators which are detrimental to neurons, for example; tumour necrosis factor- α (TNF- α), interleukin-1 β (IL-1 β) and interferon- γ (IFN- γ) (for review, see Liu & Hong, 2003). Further, microglial cells have been associated with many of the neurodegenerative diseases in the brain which can be considered as chronic inflammatory states. For example, activated microglial cells associate with amyloid plaques in Alzheimer's Disease (AD) and are found activated in the substantia nigra of Parkinson's Disease (PD), the main area of neuronal loss in this disease (for review, see Liu & Hong, 2003).

Unactivated microglial cells are considered as "resting", but are far from that. These "resting" microglial cells continuously extend and retract their processes, possibly sampling their environment for pathogens (Davalos *et al.*, 2005; Nimmerjahn *et al.*, 2005). In addition to a role in immunity, microglial cells are also vital for synaptic pruning during development, and may also be important for ongoing experience-driven synaptic remodelling (for review, see Tremblay *et al.*, 2011). Indeed, pruning of synaptic contacts by microglia requires the use of complement receptors, which are more commonly associated with the innate immune system (for review see Schafer & Stevens, 2010).

Interestingly, there is evidence to suggest that this process may become overactivated during neurodegenerative episodes, leading to excessive synaptic pruning (Stevens *et al.*, 2007). Furthermore, microglial cells express a large range of neurotransmitter receptors. These include receptors for glutamate, GABA, ATP, acetylcholine, cannabinoids, NA, dopamine and for the neuropeptides (for review, see Pocock & Kettenmann, 2007). These neurotransmitter receptors have many functions, for example activation of the adrenergic receptors reduces microglial activation and attenuates cytokine release upon LPS stimulation (Pocock & Kettenmann, 2007). In addition to this, microglial cells can also release trophic factors such as BDNF, GDNF, ciliary neurotrophic factor (CNTF), NGF and FGF-2 (Heese *et al.*, 1998; Batchelor *et al.*, 2002; Harada *et al.*, 2002).

1.1.3 Neurons and Neuronal Growth

Neurons are comprised of a cell body, an axon and dendrites (see Figure 1.2). Understanding the mechanisms of neuronal growth is vital firstly for unravelling the development of the nervous system and secondly, to develop strategies for encouraging neuronal growth following brain trauma, infection or neurodegenerative disorders. Neuronal growth can be divided into two main types; the elongation of a neurite, and the generation of new neuritic branches. Although much of the work on neuronal growth focuses on the growth of an axon, research shows that the same fundamental mechanisms (described below) also occur in dendrites (for review, see Scott & Luo, 2001).

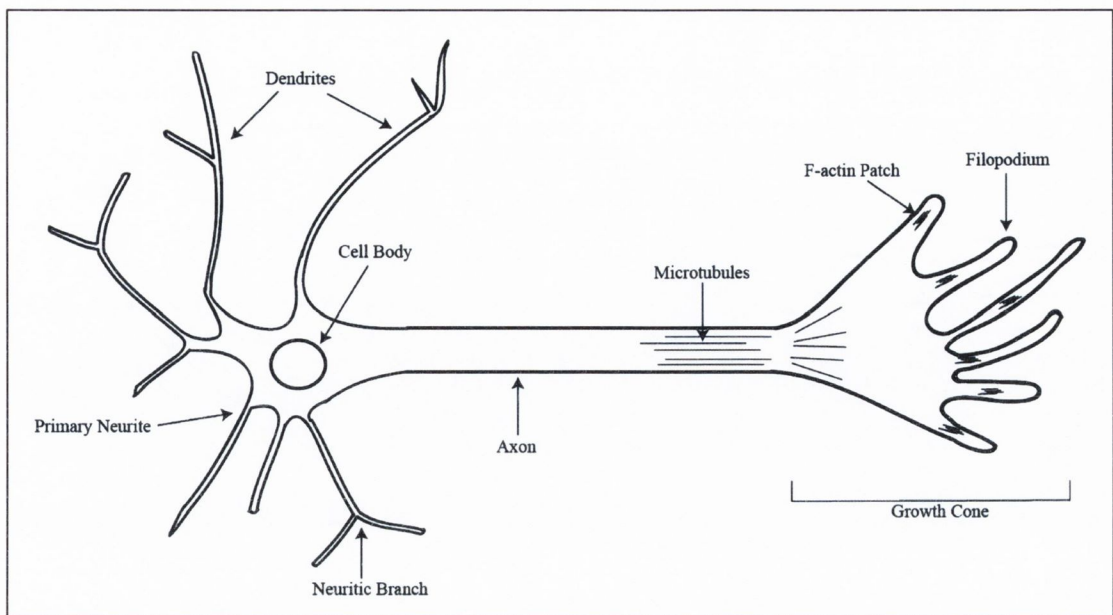


Figure 1.2: A typical neuron

Neurons contain a cell body off which stems dendrites and an axon (collectively termed neurites). Growth cones contain protruding F-actin filopodia and are invaded by microtubules to lengthen the neurite.

1.1.3.1 Mechanisms involved in increasing neuritic length

The lengthening of a neurite is fundamentally controlled by the growth cone. The growth cone located at the tip of the neurite is comprised of a central domain and a peripheral domain. The central domain contains a large concentration of the cytoskeletal protein microtubule similarly to as found in the main axon shaft, while the peripheral domain has a higher concentration of actin filaments (for review, see Goldberg, 2003). Growth cone advancement can be divided into three main stages; ‘protrusion’ of filamentous actin (F-actin)-containing filopodia into the environment; ‘engorgement’, where microtubules invade the F-actin peripheral domain often bringing essential membrane components and other machinery; and ‘consolidation’ where the growth cone has advanced and its remnants begin to reassemble the axon shaft. The F-actin polymers are composed of monomers of β -actin and γ -actin (for review, see Dent & Gertler, 2003). The peripheral domain actin filaments are continuously polymerising thus driving the growth cone forward. However, at the same time myosin motors at the central domain pull back the entire actin filament where it depolymerises. This backward flow of actin filaments prevents the central domain from moving forward and hence prevents advancement of the growth cone. It is the balance of the backward and forward actin polymerisation that drives growth cone advancement, with growth-promoting external cues pushing the

balance in favour of forward motion. The forward motion is accompanied by microtubule invasion into the peripheral zone, which moves the central domain forward and hence elongates the axon (for review, see Goldberg, 2003). Microtubules are composed of tubulin heterodimers of one α -tubulin and one β -tubulin unit (for review, see Dent & Gertler, 2003). Microtubules are formed into linear protofilaments of which 10-15 come together to form a protofilament. These heterodimers line up in a specific manner with the β -tubulin facing towards the growing end of the protofilament (plus end) and the α -tubulin facing the opposite end (minus end). Guanosine triphosphate (GTP) is bound to the tubulin heterodimer, and is hydrolysed to guanosine diphosphate (GDP) upon the dimer joining another dimer in a protofilament. Thus the protofilament has mainly GDP attached, with a GTP cap at the growing end ready to be hydrolysed by the addition of the next dimer. This GTP cap stabilises the structure, and if this is lost, the protofilament quickly depolymerises. Upon entering the growth cone, microtubules depolymerise and reorganise, a step which is essential for growth cone advancement and axonal elongation. The assembly of microtubules is regulated by microtubule assembly promoting factors, microtubule stabilising factors, microtubule associated proteins (MAPs), as well as microtubule associated motors (for review, see Conde & Caceres, 2009). Furthermore, the growth of an axon requires the insertion of new membrane which is primarily formed in the cell bodies and transported to the growing axon, or in endoplasmic reticulum at the axon itself. Also, the axon is capable of synthesising proteins which are required for neuronal growth (for review, see Goldberg, 2003).

1.1.3.2 Mechanisms involved in increasing axonal branching

The branching of an axon can occur via two main methods. Firstly, the axon can split into two at the growing growth cone at the axons tip. This method can occur for example if the growth cone approaches an inhibitory signal head-on. The signal halts straight-forward axonal growth but the growth cone at each side continues to advance, leading to uneven growth between the sides and the middle. Eventually the two sides will split to result in two independent branches.

The second mechanism is the formation of an axon collateral, that forms independently of the growth cone (for review, see Gallo, 2011). Axon collaterals are the branches of an axon occurring along its shaft rather than from the growth cone. It begins by the collection of F-actin, known as F-actin patches which will either eventually dissipate or form a

filopodium and thus a neuritic branch. It is not known how these patches turn into a filopodium but the actin-associated protein fascin might be involved (Ketschek *et al.*, 2011). For a filopodium to evolve into a mature neurite it must be stabilised to prevent its integration back into the main axon shaft, this is helped by the invasion of axonal microtubules into the filopodium. In addition to this, at points where the growth cone pauses, axon collaterals often emerge (for review, see Gallo, 2011). Most of the knowledge about collateral branching has focused on axonal branching; however collaterals also form on dendrites and the same mechanisms are thought to produce dendritic branches (Scott 2001). Furthermore, neurons also undergo the process of producing primary neurites, that is, neurites that extend directly from the cell soma. It is these neurites that will also eventually become the axon and the dendrites. However, surprisingly little is known about how a neuron initiates the formation of a primary neurite (for review, see Luo, 2002).

1.1.4 The importance of neuronal protection and neuronal growth

Although there is limited potential of the brain to produce new neurons during a lifetime (for review, see Gage, 2002), the neurodegeneration that occurs during brain injury, stroke, AD, PD, ageing and infection is permanent, and leads to debilitating symptoms. Therefore, developing methods of protecting neurons from cell death during these conditions, as well as methods to encourage the regrowth of damaged neurons are vital for a cure for these CNS conditions. Neurotrophic factors, for example, are often associated with an ability to protect neurons from toxicity (e.g. Nagahara *et al.*, 2009), and clinical trials for the use of, for example, the neurotrophin BDNF in neurodegenerative diseases are ongoing (for review, see Nagahara & Tuszynski, 2011). Unfortunately, neurotrophic factors cannot pass the BBB and so invasive procedures are required to directly utilise them in CNS disorders. Methods of indirectly increasing expression of neurotrophic factors via e.g. by encouraging neurotrophic factor release by glial cells following receptor activation could therefore prove beneficial for neuroprotective based therapies. As well as an ability to protect neurons from cell death, neurotrophic factors can also encourage neuritic growth of neurons both under basal conditions e.g. (Chao *et al.*, 2003; Lee *et al.*, 2009c; Cohen-Cory *et al.*, 2010), and following neurodegeneration (Cao *et al.*, 2008). Neuritic growth of neurons is vital for their integration into functional networks, and thus the use of neurotrophic factors would be of therapeutic value. For example, neuritic

growth is fundamental for memory formation, and thus encouraging neuritic growth could be beneficial to AD (for review, see Holtmaat & Svoboda, 2009). In line with this, the amyloid- β peptide induces neuritic loss from primary hippocampal neurons, which was attributed to activation of the p75 neurotrophin receptor (Knowles *et al.*, 2009). Furthermore, a long-term imaging study of neuronal morphology in a mouse model of AD demonstrated that neurites passing near amyloid- β plaques were thinner and terminated abruptly (Tsai *et al.*, 2004). Thus, an interesting strategy for neuronal regeneration could investigate means of enhancing neurotrophic factor production in the CNS without the need for an invasive procedure, and thus encourage neuritic growth.

1.2 Noradrenaline

Noradrenaline (NA) is a catecholaminergic monoamine neurotransmitter which is most abundantly expressed in the locus coeruleus complex, a cell group located in the brain stem. From this relatively small neuronal group, comprising only approximately 1,600 cells in the rat brain, the noradrenergic neurons project to almost all areas of the cerebral cortex, including; hippocampus, neocortex, amygdala, thalamus and hypothalamus, as well as to cerebellum and spinal cord (for review, see Feldman *et al.*, 1997). NA activates a wide range of so-called adrenergic receptors, which are broadly divided into the alpha-adrenoceptors and the beta-adrenoceptors based on agonist potency (Rang & Dale, 2003). All of the adrenoceptors are G-protein coupled receptors (GPCR) and can mediate the actions of both NA and adrenaline.

1.2.1 Noradrenaline synthesis and metabolism

NA is synthesised from the amino acid tyrosine via three enzymatic steps (see Figure 1.3). Tyrosine, a non-essential amino acid found in many foodstuffs such as dairy products, chicken, fish and nuts, is taken up into catecholaminergic neurons. The enzyme tyrosine hydroxylase converts the tyrosine into 3,4-dihydroxyphenylalanine (DOPA). This enzyme is confined to noradrenergic and dopaminergic neurons in the CNS, and sympathetic and adrenal cells in the periphery, and is the rate limiting step for catecholamine synthesis. The enzyme is also inhibited by NA leading to strict regulation of the pathway. DOPA is then converted to dopamine by L-aromatic amino acid decarboxylase (AAAD), a relatively nonspecific enzyme as it also decarboxylates other aromatic amino acids such as L-histidine and L-tryptophan. In noradrenergic neurons, the dopamine is transported into vesicles by the vesicular monoamine transporter (VMAT) and converted to NA by dopamine β -hydroxylase located inside the vesicles in membrane-bound form. Because of this, only a small amount of the enzyme is released with NA release (for reviews, see Eisenhofer *et al.*, 2001; Rang & Dale, 2003). VMATs, of which there is VMAT1 and VMAT2, package the monoamines into the vesicles in very high concentrations by use of a proton gradient across the membrane. Both transporters recognise all monoamines, with VMAT2 preferentially located in the nervous system (for review, see Iversen, 2006).

The catecholamines are metabolised via three enzymes; monoamine oxidase, catechol-O-methyltransferase and sulphotransferase (for review, see Eisenhofer *et al.*, 2001). These enzymes are mainly intracellular, therefore the main method of inactivation of synaptic

NA is via active transport into both nerve terminals and astrocytes by the neuronal NA transporter (NET) (Inazu *et al.*, 2003; Sager & Torres, 2011) or the extraneuronal monoamine transporter (EMT, also known as OCT3 in rat and mouse) which is expressed by astrocytes (Inazu *et al.*, 2003) and neurons (Shang *et al.*, 2003). The monoamine transporters function by using the electrochemical gradient of sodium and chloride ions. They transport the monoamine into the cell accompanied by both a sodium and chloride ion leading to a net increase in positive ion charges inside the cell (for review, see Iversen, 2006). These transporters are the targets of many antidepressant drugs which block the transporter and thus inhibit the reuptake of 5-HT (e.g. citalopram, fluoxetine), NA (e.g. reboxetine) or both (e.g. venlafaxine, amitriptyline) (for review, see Iversen, 2006).

1.2.2 The adrenoceptors

The adrenoceptors were first classified into α or β subtypes based on the potency of various synthetic amines on several physiological functions. For example, the α -adrenoceptors were shown to be mainly excitatory and to induce vasoconstriction, while the β -adrenoceptors were shown to be mainly inhibitory and to control vasodilation. The β -adrenoceptors were then further classified into β_1 and β_2 subtypes while further studies have since identified the β_3 subtype (for review, see Civantos Calzada & Aleixandre de Artinano, 2001).

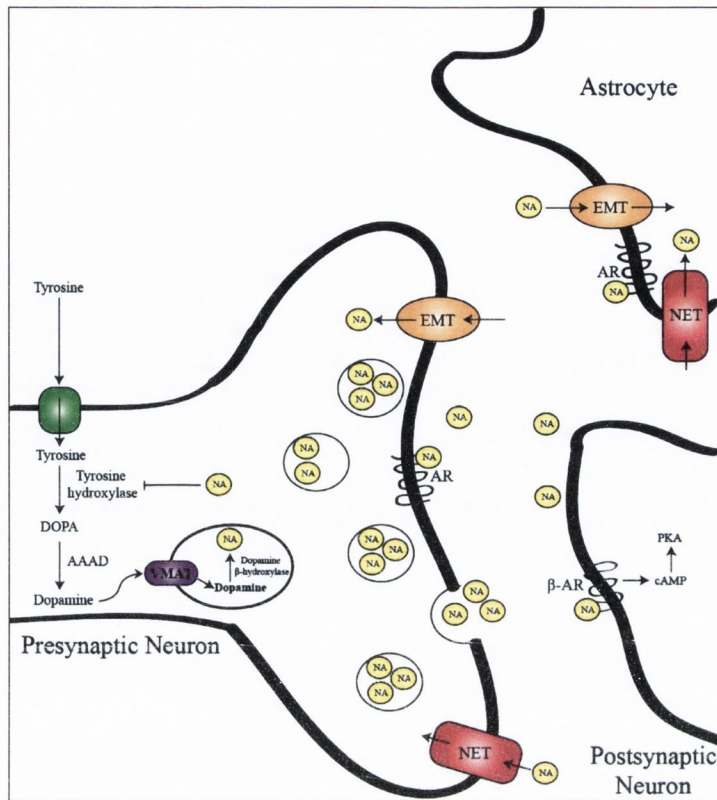


Figure 1.3: The noradrenergic neuron

NA is produced from tyrosine in noradrenergic neurons via a series of enzymatic steps. Upon stimulation, the neuron releases a vesicle of NA which can bind to adrenergic receptors on both postsynaptic neurons and on surrounding astrocytes. NA is removed from the synaptic cleft by active reuptake into the nerve terminal by NET and EMT present on neurons and astrocytes. AAAD L-aromatic amino acid decarboxylase; β -AR, β -adrenoceptor; cAMP, cyclic adenosine monophosphate; DOPA, 3,4-dihydroxyphenylalanine; EMT, extraneuronal monoamine transporter; NA, noradrenaline; PKA, protein kinase A; VMAT, vesicular monoamine transporter.

1.2.2.1 The Alpha-adrenoceptors

The α -adrenoceptors are further classified into the α_1 and the α_2 subclass of receptors based on agonist sensitivity. The α_1 -receptors all activate phospholipase C to produce inositol trisphosphate and diacylglycerol as secondary messengers (Rang & Dale, 2003). Each function via the $G_{q/11}$ GPCR. These α_1 receptors are the most abundant of the adrenoceptors in the CNS; however their function is not entirely clear. The lack of specific α_1 agonists and antagonists has led to inadequate functional profiles of the α_1 subtypes in the CNS (Tanoue *et al.*, 2003).

The α_2 -adrenoceptor agonists are widely used for the treatment of hypertension, glaucoma and attention deficit disorder (for review, see Gyires *et al.*, 2009). In general, the α_2 receptors lead to a reduction in cyclic adenosine monophosphate (cAMP) via coupling to G_i and G_o , however, they can also lead to an increase in cAMP via coupling to G_s . Most of the physiological effects of α_2 agonists can be attributed to function via the α_{2A} receptor. These receptors are involved in pre-synaptic inhibition of NA release, antinociception and hypothermia (for review, see Gyires *et al.*, 2009).

1.2.2.2 Beta adrenoceptors

Each of the β -adrenoceptors are classed as GPCRs. Activation of the β_1 -adrenoceptor stimulates salivation, increases heart rate and stimulates the breakdown of lipids (Rang & Dale, 2003). The β_3 -adrenoceptor shows strong expression in the heart but is also expressed in the brain. Activation of the β_3 -adrenoceptor has been associated with vasodilation of blood vessels and heart circadian rhythm regulation (for review, see Gauthier *et al.*, 2011). However, of the three subtypes of β -adrenoceptors, it is the β_2 -adrenoceptor which is primarily involved in the extra-synaptic functions of NA in the CNS. The β_2 -adrenoceptor is positively coupled to the membrane-bound enzyme adenylate cyclase through a trimeric G_s protein which has an α and $\beta\gamma$ subunit. Upon ligand binding, the receptor becomes stabilised which allows the α -subunit to preferentially bind GTP rather than GDP. The energy from GTP catalyzes the conversion of adenosine triphosphate (ATP) to cAMP via adenylate cyclase. This cAMP then activates protein kinase A (PKA) (See Figure 1.4, for review, see Johnson, 2001). The β_2 -adrenoceptor can also bind to G_i and G_q proteins (Daaka *et al.*, 1997; Wenzel-Seifert & Seifert, 2000). G_i protein coupling results in the stimulation of the mitogen-activated protein kinase (MAPK) pathway. It is thought that this occurs via the $\beta\gamma$ subunit of the β -adrenoceptor which acts as a scaffold protein for the tyrosine kinase proteins Src, Raf and Ras (for review, see Johnson, 2006). This pathway requires PKA phosphorylation of the β_2 receptor, as this impairs adenylate cyclase coupling. As adenylate cyclase activates PKA via G_s , this results in a negative feedback system, in which agonism at the β_2 -adrenoceptor can lead to PKA activation, which then shuts down the G_s pathway and activates the G_i pathway leading to MAPK activation (Daaka *et al.*, 1997). PKA results in the activation of the transcription factor cAMP response element-binding (CREB), which associates with the CREB-binding protein (CBP) and leads to the transcription of various genes (Herdegen & Leah, 1998).

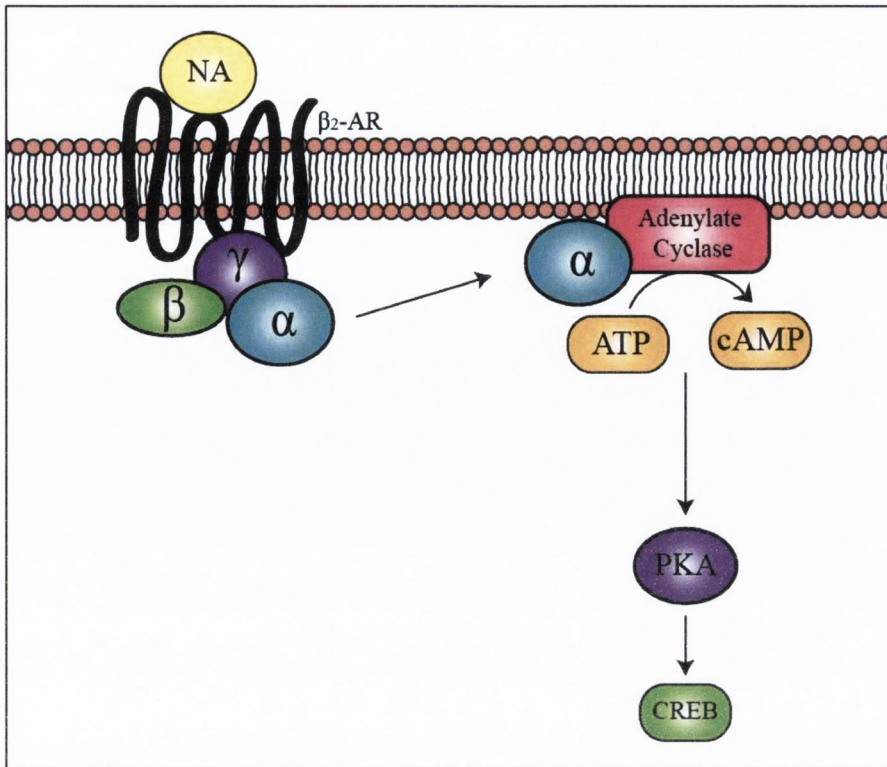


Figure 1.4: Signalling at the β_2 -adrenoceptor

NA binds to the β_2 -adrenoceptor and results in activation of adenylate cyclase via the α -subunit of the G-protein. ATP is then converted to cAMP by adenylate cyclase, which then activates PKA, and thus CREB.

1.2.3 Functions of NA

As noradrenergic neurons project to such a wide range of CNS regions, e.g. prefrontal cortex, hypothalamus, thalamus, hippocampus and spinal cord (for review, see Feldman *et al.*, 1997), it makes sense that NA is also involved in a wide range of CNS functions, for example; alertness, motivation, attention, sleep, the stress response and memory formation (for reviews, see Kobayashi & Yasoshima, 2001; Rang & Dale, 2003; Dunn & Swiergiel, 2008). For example, the hypothalamic-pituitary-adrenal axis (HPA), the main controller of stress, receives major input from noradrenergic neurons (for review, see Dunn & Swiergiel, 2008). NA also has an emerging role in memory consolidation. Activation of the cAMP/PKA pathway via β -adrenoceptor activation can modulate long-term potentiation, while depletion of the NA system can inhibit the formation of new memories (for review see Kobayashi & Yasoshima, 2001). Furthermore, there is a wealth of information linking NA to sleep, for example; blockade of adrenoceptors results in sedation, while knock-out mice for dopamine β -hydroxylase and thus for NA, show

altered sleep patterns (for reviews, see Gottesmann, 2008; Mitchell & Weinschenker, 2010). NA and in particular activation of the β -adrenoceptor is also associated with the dampening of the immune response in the CNS (for review, see Sanders & Straub, 2002). For example, NA induces the expression of the IL-1 receptor antagonist in primary cultures of mixed glial cells, which prevents IL-1 from binding to its receptor and thus limits pro-inflammatory downstream effects of IL-1 (McNamee *et al.*, 2010b). Reports also show that depression and anxiety are associated with downregulation of the noradrenergic system in the CNS (for review, see Goddard *et al.*, 2010)

Although there is only limited evidence that shows that NA might have a role in neuritic growth (Clarke *et al.*, 2010), there is a wealth of information on the neuroprotective potential of NA. Firstly, NA, via an action on the β_2 -adrenoceptors, induces the production of a range of neurotrophic factors (Schwartz & Costa, 1977; Follesa & Mochetti, 1993; Yamashita *et al.*, 1995; Culmsee *et al.*, 1999; Counts & Mufson, 2010; Manni *et al.*, 2011). Secondly, there is much evidence both *in vitro* (Semkova *et al.*, 1996; Junker *et al.*, 2002) and *in vivo* (Zhu *et al.*, 1998; Zeman *et al.*, 1999; Zhu *et al.*, 1999) demonstrating the ability of NA to protect neuronal cells from toxic insults. Therefore, the potential of utilising brain-permeable NA agonists, in particular β -adrenoceptor agonists, should be investigated as a possible means for encouraging neuronal regeneration.

1.3 Serotonin

Serotonin (5-hydroxytryptamine, 5-HT) is a monoamine neurotransmitter which is formed in serotonergic neurons originating in the raphe nuclei in the brainstem. These serotonergic nuclei can be divided into a rostral group, which mainly project to the cortex, hypothalamus, amygdala and hippocampus; and a caudal group which project to the brainstem and spinal cord (for review, see Hornung, 2003). 5-HT activates a wide range of receptors which are tentatively divided into seven families (5-HT₁₋₇) and includes GPCRs and ligand-gated ion channels (for review, see Hannon & Hoyer, 2008).

1.3.1 Serotonin synthesis and metabolism

5-HT is synthesised from the essential amino acid tryptophan via two enzymatic steps. First, tryptophan is converted to 5-hydroxytryptophan (5-HTP) by the enzyme tryptophan-5-hydroxylase. 5-HTP is then converted to 5-HT via the enzyme AAAD. Tryptophan is found in many foodstuffs including eggs, dairy, fish and seeds (Rang & Dale, 2003).

Synaptic 5-HT is taken back into the nerve terminal by the serotonin transporter (SERT), which is driven by sodium and chloride ions similarly to NET. 5-HT is also transported into synaptic vesicles by VMAT (for review, see Iversen, 2006).

1.3.2 Serotonin receptors

As previously mentioned, there are seven 5-HT receptor families (5-HT₁₋₇). The 5-HT₁ family has five members (5-HT_{1A, B, D, E, F}) all of which are GPCRs and preferentially bind to G_{i/o} and thus negatively regulate adenylate cyclase (for review, see Hannon & Hoyer, 2008). The 5-HT_{1A} receptor for example has high expression on neurons of the cortex and hippocampus, and there is some evidence that it is also expressed on glial cells (for review, see Barnes & Sharp, 1999). Interestingly, this receptor is associated with inducing the release of NA from the cerebral cortex and hippocampus, and also may have an antidepressant action (Barnes & Sharp, 1999). The 5-HT₂ family has three members 5-HT_{2A, B} and C which are also all GPCRs and bind to G_{q/11} and therefore increase inositol phosphates and intracellular Ca²⁺ (for review, see Hannon & Hoyer, 2008). For example, the 5-HT_{2A} receptor has high expression on both neurons and glial cells in the cortex, hippocampus and the caudate nucleus (for review, see Barnes & Sharp, 1999). In addition, activation of this receptor increases BDNF expression (Vaidya *et al.*, 1997). The 5-HT₃ family are all ligand-gated ion channels which upon activation trigger depolarization of a neuron. There are two members of the 5-HT₃ family, 5-HT_{3A, B}. Three of the other families, 5-HT_{4, 6} and 7, preferentially bind to G_s and so positively regulate adenylate cyclase leading to the formation of cAMP (for review, see Hannon & Hoyer, 2008), while the 5-HT₅ family has not been well characterised but is believed to also be a GPCR and is predominately expressed on astrocytes (Carson *et al.*, 1996).

1.3.3 Functions of 5-HT

5-HT is involved in a wide range of physiological functions including digestion and cardiovascular regulation, as well as many behavioural functions such as the sleep-wake cycle, appetite, pain modulation, mood, and learning and memory (for review, see Lucki, 1998). Of importance is the association of 5-HT with major depressive disorder. Selective serotonin reuptake inhibitors such as fluoxetine and sertraline remain the most commonly prescribed drugs for depression (Rang & Dale, 2003). 5-HT is also an emerging target for

managing chronic pain, with 5-HT_{1A} receptor agonists in particular being investigated as potential therapeutic agents (for review, see Bardin, 2011).

Many studies have also shown the ability of 5-HT to induce neuroprotection, in particular via the 5-HT_{1A} receptor. For example, 5-HT_{1A} receptor agonists have shown therapeutic efficacy against models of excitotoxicity (Oosterink *et al.*, 1998), ischemia (Semkova *et al.*, 1998) and staurosporine-induced apoptosis (Suchanek *et al.*, 1998). Furthermore, the neuroprotection mediated by activation of the 5-HT_{1A} receptor may occur via activation of both the phosphoinositide 3-kinase (PI3K) and the MAPK pathway (Druse *et al.*, 2005).

1.4 Pathways Associated with Neuronal Growth

Many molecules and signalling pathways have been associated with neuronal growth, of these, the MAPK pathway and PI3K pathways predominate (for reviews, see Redmond *et al.*, 2002; Read & Gorman, 2009).

1.4.1 The Mitogen Activated Protein Kinase Pathway

The MAPK pathway has many different branches; however each can be represented in a basic form, whereby the pathway is initiated by an activator or stimulus. This stimulus activates a MAPK kinase kinase (MKKK), which induces the activation via phosphorylation of a MAPK kinase (MKK) which activates a MAPK, which then activates a specific substrate, most commonly a component of a gene transcription factor (see Figure 1.5, for review, see Widmann *et al.*, 1999). The MAPK pathway has four main branches: the extracellular signal-regulated kinases (ERK) ERK 1 and ERK 2 (ERK1/2); the c-Jun NH2-terminal kinases JNK1, JNK2 and JNK3; the p38 enzymes p38 α , p38 β , p38 γ , p38 δ ; and ERK5 (for review, see Johnson & Lapadat, 2002). However, although each pathway has specific MKKKs, MKKs and MAPKs associated with it, there is much cross-over and complexity in MAPK signalling pathways (Widmann *et al.*, 1999). In addition to these four main branches, there are also atypical MAPK pathways leading to the activation of the MAPKs; ERK3, ERK4, nemo-like kinase, and ERK7 (Obara & Nakahata, 2010). The MAPK pathway, in particular the ERK1/2 branch, has been highly associated with neuronal growth. For example, MAPK activation is associated with the induction of a neuronal phenotype in rat PC12 cells (Traverse *et al.*, 1992; Cowley *et al.*, 1994; Ihara *et al.*, 1997; Sole *et al.*, 2004), the growth of neurites in sympathetic neurons

(Atwal *et al.*, 2000; O'Keeffe *et al.*, 2008), and the growth of neurites from primary cortical neurons (Abe *et al.*, 2001; Redmond *et al.*, 2002; Lee *et al.*, 2009c).

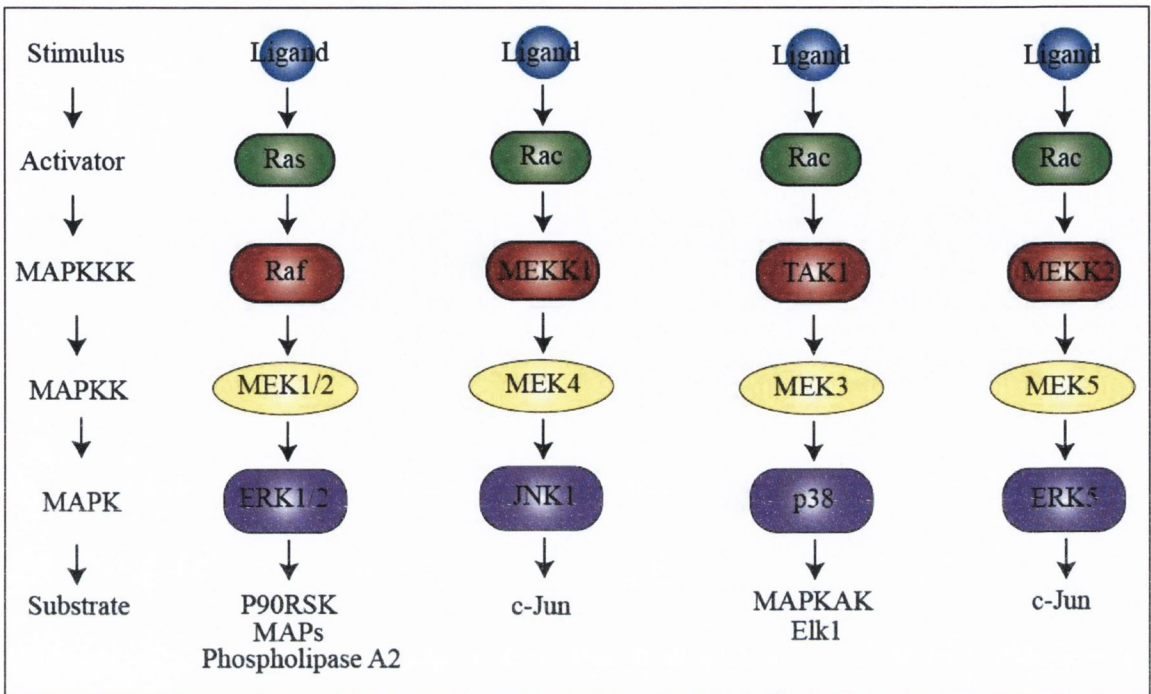


Figure 1.5: Four main branches of MAPK Signalling

MAPK signalling primarily occurs via the ERK1/2 branch, JNK branch, p38 branch and the ERK5 branch.

1.4.1.1 MAPK Signalling: ERK1/2 Branch

The ERK1/2 branch (see Figure 1.6) of the MAPK pathway is the most extensively studied branch and has roles in cell division, differentiation and cell survival. Activation of Ras by, for example, an activated receptor tyrosine kinase (see section 1.4.3) leads to the recruitment of Raf-1 (the MAPKKK) to the plasma membrane, where a tyrosine kinase such as c-Src phosphorylates and activates it. A second MAPKKK, B-raf, exists in neurons for the ERK1/2 branch of MAPK signalling. B-raf is activated not only by Ras but also via Ras-related protein-1 (Rap-1) (for review, see Widmann *et al.*, 1999). Activation of Raf-1 or B-raf then activates MAPKK1 (also known as MEK1/2 or ERK activator kinase I), which leads to the phosphorylation and activation of ERK1/2. ERK1/2 goes on to phosphorylate S6 kinase p90 (p90), phospholipase A2 and microtubule associated proteins (MAPs) such as MAP-1, MAP-2 and MAP-4. P90 goes onto phosphorylate c-Fos and inhibits glycogen synthase kinase 3 β (GSK3 β). As GSK3 β

normally inhibits c-Jun, p90 inhibition of GSK3 β activates c-Jun, and thus the transcription factor AP-1 activation, which is produced by the dimerisation of c-Jun and c-Fos. Phospholipase A2 phosphorylation catalyses the release of arachidonic acid and the subsequent production of eicosanoids such as prostaglandins. Negative feedback of the ERK1/2 pathway occurs as ERK1/2 can phosphorylate son of sevenless (SOS; the Ras exchange factor), Raf-1 and MKK1, thereby reducing their activity, and thus negatively controlling the MAPK pathway. ERK1/2 can also translocate to the nucleus and directly activate transcription factors such as ETS-like transcription factor1 (Elk1), Ets1, Sap1a, c-Myc, Tal and signal transducers and activators of transcription (STAT) proteins (for review, see Widmann *et al.*, 1999). Apart from direct interaction with the MAPs, the inhibition of GSK3 β activity, as occurs via the MAPK pathway, has been highly associated with the induction of neurite growth (for review, see Hur & Zhou, 2010). Furthermore the downstream transcription factors to ERK1/2; Elk1 and c-Myc, have also been associated with neuritic growth (Kim *et al.*, 1997; Vanhoutte *et al.*, 2001). Thus there appears to be many ways in which activation of the MAPK pathway can lead to changes in neuritic growth.

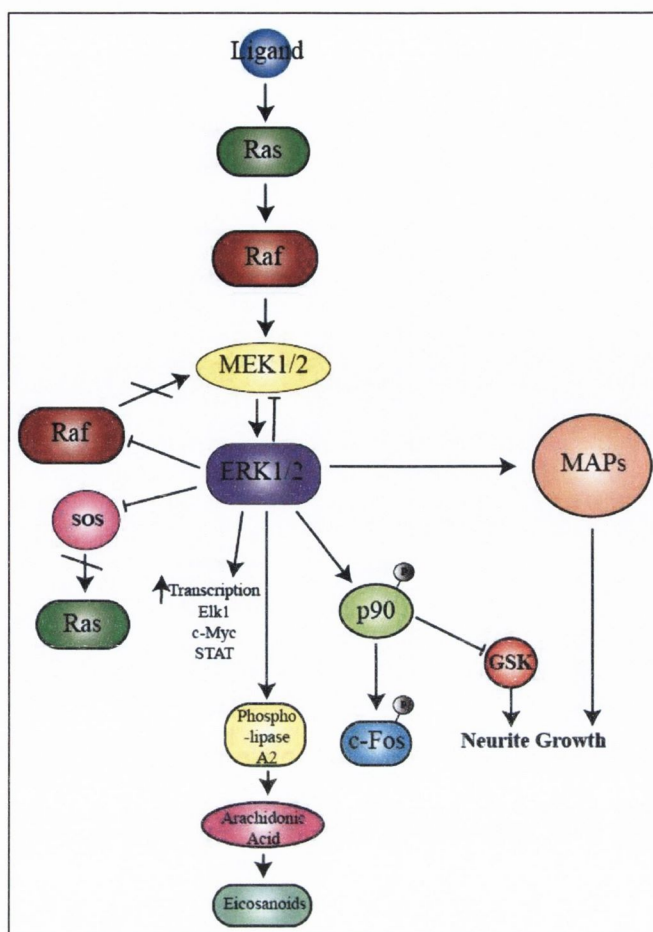


Figure 1.6: ERK1/2 Branch of MAPK Signalling

Activation of the ERK1/2 branch of MAPK signalling leads to the activation of microtubule associated proteins (MAPs), the inhibition of GSK, activation of c-Fos, increased transcription of Elk1, c-Myc and STATs, as well as the production of eicosanoids via phospholipase A2.

1.4.1.2 MAPK Signalling: JNK Branch

The JNK MAPKs are activated through a variety of cell surface receptors including GPCRs, cytokine receptors and the receptor tyrosine kinases (RTKs). JNK activity is regulated via two main activators; ras-related C3 botulinum toxin substrate (Rac) and Cdc42. These then go on to activate MEKK1 (a MAPKK) which in turn activates JNK. MEKK1 however has also been shown to activate nuclear factor kappa B (NF κ B) and ERK (for review, see Widmann *et al.*, 1999). Interestingly, the NF κ B pathway can also modulate neuritic growth (Sole *et al.*, 2004; Gutierrez *et al.*, 2008). Although normally associated with apoptosis, the JNK pathway can also mediate cell survival (for review, see Widmann *et al.*, 1999).

1.4.1.3 MAPK Signalling: p38 Branch

The p38 MAPKs are generally activated upon stressors to the cell such as heat shock, inflammation or ultraviolet radiation. The Rac1 and Cdc42 Rho kinases can also activate the p38 MAPK possibly via the p21-activated kinase (Pak). P38 then goes onto activate the MAPK activated protein kinase which induces the expression of heat shock proteins. P38 can also activate activating transcription factor 2 (ATF2), Elk1 and Max transcription factors. Furthermore, Max associates with c-Myc (induced by ERK 1/2) (for review, see Widmann *et al.*, 1999).

1.4.1.4 MAPK Signalling: ERK 5 branch

The ERK5 branch is the least researched branch but is thought to be activated by MKK5 and ultimately leads to the activation of c-Jun (Widmann *et al.*, 1999). The ability of Ras to induce ERK5 activation however remains controversial. Rap-1 has been shown however to induce ERK5 activity (Obara & Nakahata, 2010).

1.4.2 Phosphoinositide Signalling

Phosphoinositide signalling involves the enzyme PI3K (see Figure 1.7). There are three classes of PI3K, of which the class I PI3Ks are the best characterised and are generally activated in response to extracellular signals. This class can be further divided into class IA, regulated by RTKs, GPCRs and Ras, and the class IB which are regulated only by GPCRs. The class IA PI3K is comprised of a p85 regulatory subunit and a p110 catalytic subunit (Zhang *et al.*, 2011). PI3K is recruited to the plasma membrane by phosphorylated residues via its regulatory subunit. Upon binding to the phosphorylated residue, the regulatory subunit activates the catalytic subunit which is further activated by Ras. Activated PI3K then phosphorylates the membrane-bound lipid phosphatidylinositol 4,5-bisphosphate (PIP₂) into phosphatidylinositol 3,4,5-trisphosphate (PIP₃). PIP₃ is capable of activating many other kinases and is converted back to PIP₂ by many phosphatases including phosphatase and tensin homolog (PTEN) (for review, see Gallo, 2011). PIP₃ has docking sites for both AKT and phosphoinositide dependent kinase I (PDK1). PDK1 phosphorylates AKT at a tyrosine residue while mammalian target of rapamycin (mTOR) phosphorylates AKT in a serine residue leading to its full activation. AKT then translocates to the nucleus (Zhang *et al.*, 2011). For example, AKT phosphorylates Forkhead-related transcription factor 1 (Frk) and inhibits its activation, it also

phosphorylates Bcl-2-associated death promoter (Bad), which prevents cellular apoptosis. AKT inactivates the constitutively active GSK3 β and thus activating pathways which are normally inhibited by it. Separate to AKT signalling, the protein kinase C enzyme can be activated via PI3K by PDK1 and PIP3 also activates the GTPase, Rac, which is important for actin remodelling (for review, see Cantley, 2002). Similarly to MAPK ERK1/2 signalling, the PI3K pathway has many methods of influencing neuritic growth. PI3K, for example, also inactivates GSK3 β , which is highly associated with neuritic growth (for review, see Hur & Zhou, 2010). In addition to this, the PI3K pathway activates members of the Rho kinases family, of which Rac, Cdc42 and RhoA are particularly associated with neuritic growth via interactions with actin and microtubules, as well as interacting with various scaffolding proteins (for review, see Govek *et al.*, 2005). Furthermore, the phosphorylated AKT has many other downstream targets which are associated with neuritic growth, such as Ezrin and Tau (for review, see Read & Gorman, 2009).

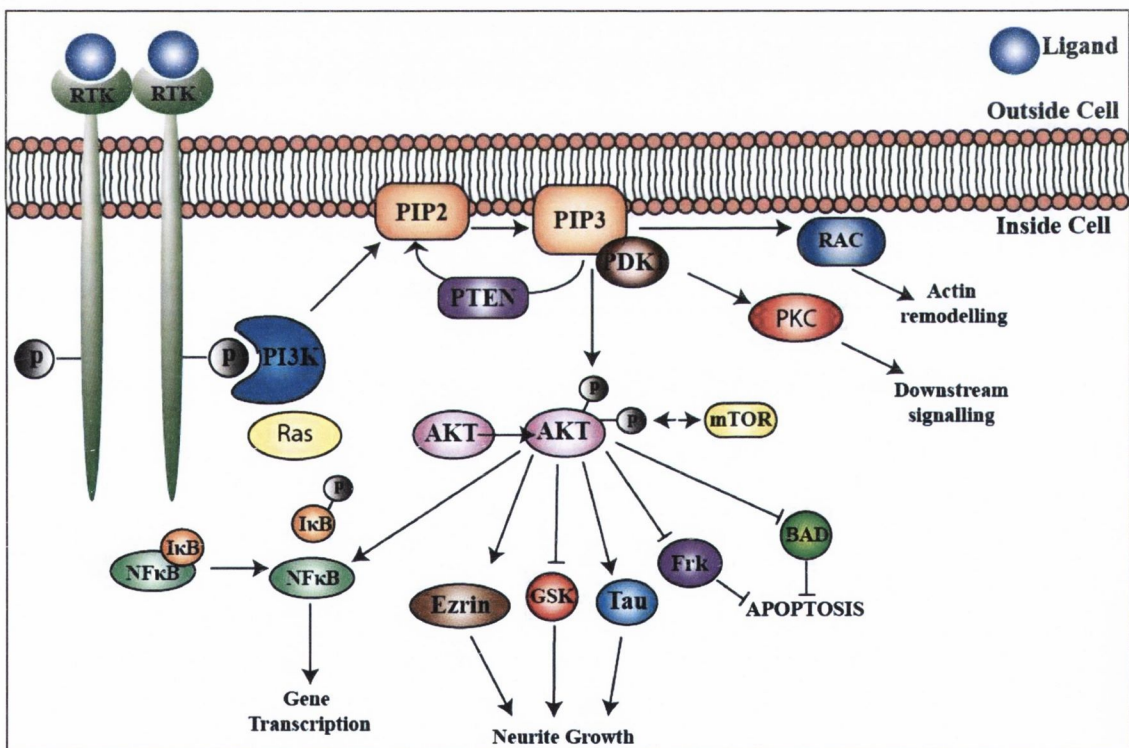


Figure 1.7: PI3K signalling leads to neuritic growth

Activation of the PI3K enzyme leads to the production of PIP3 and phosphorylation of AKT. This leads to the activation of NF κ B and downstream gene transcription, the activation of many proteins associated with neuritic growth, the inhibition of pro-apoptotic proteins and the activation of PKC.

1.4.3 Signalling via the receptor tyrosine kinases

Many growth factor receptors are RTKs. Upon ligand binding, two RTKs dimerise and auto-phosphorylate each other. This phosphorylation can recruit and activate enzymes and transcription factors, or can provide docking sites for adaptor proteins. Adaptor proteins generally lack their own catalytic activity but will associate with enzymes that do. They also associate with scaffolding adaptor proteins which can dock many signalling proteins (for review, see Gu & Neel, 2003). Scaffolding adaptor proteins can either contain several tyrosine phosphorylation sites to dock many signalling proteins or can contain Src homology (SH) 3 or SH2 domains to bind signalling proteins. Members of the first group include fibroblast growth factor receptor substrate 2 (FRS2), SH2 containing sequence Shc, Grb-2 associated binder (Gab), insulin receptor substrate (IRS) and downstream of kinase (Dok)-family proteins. The second group include growth factor receptor-bound protein 2 (Grb2) and Crk (for review, see Gotoh, 2008).

FRS2 for example is a scaffolding protein which upon activation is tyrosine phosphorylated. Activated FRS2 leads to recruitment of the adaptor protein Grb-2 and also Shp2; an Sh2 containing tyrosine phosphatase. Grb-2 is often associated with SOS, Cbl and Gab-1. SOS is a guanine nucleotide exchange (GEF) factor for Ras, thus activating the ERK MAPK pathway (see section 1.4.1.1). Cbl is a ubiquitin ligase which results in the degradation of the tyrosine kinase receptor via ubiquitination. While Gab-1 recruits PI3K and thus activates this pathway. Activation of the ERK pathway may also occur via Shp2 activation, although how Shp2 can activate Ras is controversial (for review, see Gotoh, 2008), but it might be more important in amplifying the pathway, rather than be utterly essential for it (for review, see Gu & Neel, 2003). The adaptor protein Gab-1 which associates with Grb-2 contains a binding site for the p85 subunit of PI3K and thus downstream activation of AKT. In addition to this, Gab-1 has been associated with phospholipase C (for review, see Gu & Neel, 2003). In this way, signalling via RTK can result in the activation of the MAPK pathway, PI3K and phospholipase C, for example see Figure 1.8 for the RTK tropomyosin receptor kinase (Trk) signalling.

1.5 Neuroprotective and neuronal growth inducing factors

There are many factors which have been shown to be involved in the regulation of neuronal protection and neuronal growth. Many of these induce the MAPK pathway, the PI3K pathway or indeed both. These include neurotrophic factors such as the neurotrophins and GDNF, and cytokines.

1.5.1 Neurotrophins

The neurotrophins are a group of neurotrophic factors consisting of BDNF, NGF- β , NT3 and neurotrophin 4/5 (NT4/5). They are all initially made as precursors or pro-neurotrophins which need to be cleaved intracellularly, by furin or pro-convertases, to reveal the mature neurotrophin protein. Additionally, the neurotrophins can be released in the pro-form and cleaved extracellularly by the extracellular endopeptidases tissue-plasminogen activator plasmin cascade or the extracellular matrix-metalloproteinases (for review, see Lessmann & Brigadski, 2009). For example, studies have shown that calcium-dependent release of NGF- β is primarily secreted in the pro-form from cortical neurons and is cleaved to the mature NGF- β protein extracellularly via a complex protease cascade (Bruno & Cuello, 2006). The neurotrophins are released in the CNS in an activity-dependent manner, and the inhibition of neurotrophin signalling can lead to neuronal death (for review, see Chao, 2003). They each bind to two types of receptors; the Trk receptors of which there are three; TrkA, TrkB and TrkC, and the p75 receptor. The Trk receptors show various affinities for the neurotrophins with TrkA preferentially binding to NGF- β , TrkB to BDNF and TrkC to NT-3 (Chao, 2003). The Trk receptors are all RTKs, see section 1.4.3.

1.5.1.1 Neurotrophin Signalling: Trk Receptors

Signalling of the neurotrophins via the Trk receptors is associated with neuronal survival (Chao, 2003). This receptor is activated when two neurotrophin ligands bind to two Trk receptors, resulting in autophosphorylation of tyrosine residues on the Trk receptors and thus the recruitment of various adaptor proteins, such as FRS2 and Shc (for reviews, see Reichardt, 2006; Gotoh, 2008). Both of these can recruit the Grb-2/SOS complex which leads to the activation of the MAPK pathway via Ras and Raf. Grb-2 can also be in a complex with Gab-1 which leads to the activation of the PI3K pathway (for reviews, see Gu & Neel, 2003; Reichardt, 2006). However, activation of the PI3K pathway via a Trk

receptor may also occur via the adaptor protein IRS-1 (for review, see Reichardt, 2006). Trk receptor signalling often leads to the sustained activation of ERK1/2 which may be associated with the internalisation of the Trk receptor to an endosome bringing the adaptor protein FRS2 close to Rap-1 (Chao, 2003; Reichardt, 2006). Phospholipase C is also recruited to and activated by the RTK leading to the subsequent activation of protein kinase C (for reviews, see Chao, 2003; Reichardt, 2006). There also exists a truncated form of the Trk receptors which lack the intracellular phosphorylation sites and so may act as negative regulators of the Trk receptors. Some reports however show that they may have their own signalling properties (for review, see Cohen-Cory *et al.*, 2010).

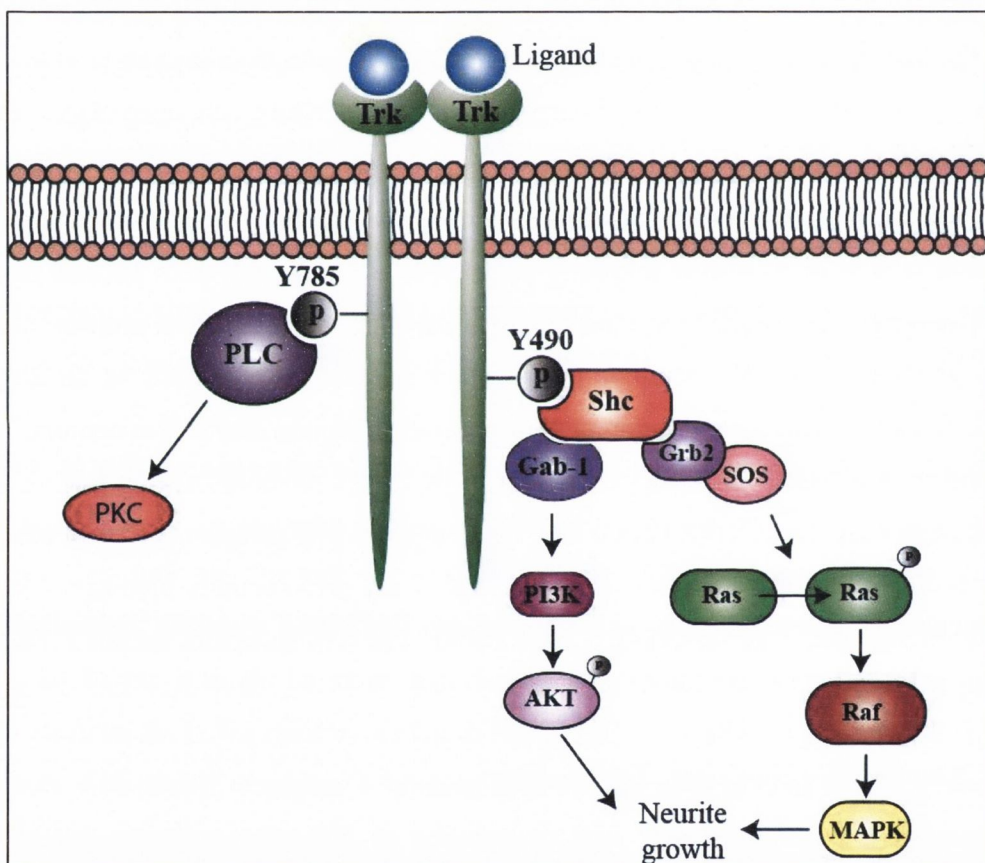


Figure 1.8: Signalling via the Trk Receptors

Two neurotrophin ligands bind to two Trk receptors, leading to the activation of phospholipase C, PI3K and MAPK.

1.5.1.2 Neurotrophin Signalling: p75 Receptor

The p75 receptor is a member of the TNF receptor superfamily and is associated with cellular apoptosis (see Figure 1.9; for review, see Dechant & Barde, 2002). P75 receptor activation leads to the activation of downstream pathways or can also increase the affinity of the neurotrophins for the Trk receptors. Interestingly, the p75 receptor has higher affinity for the pro forms of the neurotrophins which could be a mechanism of control over neurotrophin function as p75 signalling leads to the activation of other signalling pathways such as JNK and NF κ B (for review, see Chao, 2003). P75 activation results in the activation of the JNK branch of MAPK signalling via cdc42 and apoptosis signal-regulating kinase I (Ask-1), NF κ B activation via TNF receptor associated factor 6 (Traf6) and NF κ B inducing kinase (NIK), and the Rho kinases (Reichardt, 2006).

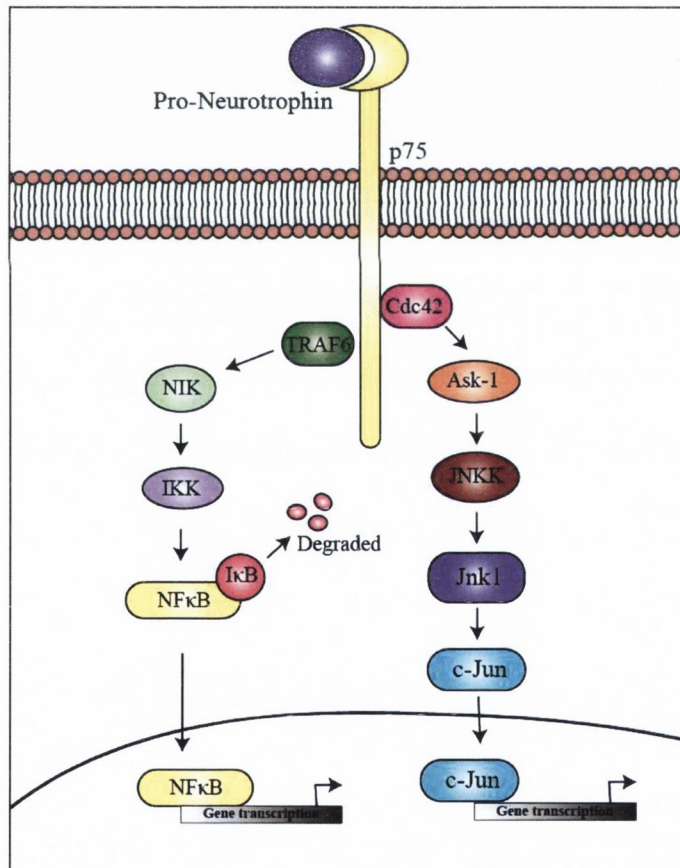


Figure 1.9: Signalling via the p75 receptor

Pro-neurotrophins bind to the p75 receptor and lead to the activation of the NF κ B and c-Jun MAPK pathways.

1.5.1.3 NGF- β and neuritic growth

NGF- β is an important potential therapeutic target for protecting neurons following degeneration and for encouraging neuritic growth. Early investigations demonstrated the ability of a factor from a mouse sarcoma, later identified as NGF- β , to induce neuritic growth of sensory neurons (Levi-Montalcini, 1964). Subsequently, much research has shown the ability of NGF- β to induce neuritic growth in both primary neurons and cell lines. For example, NGF- β was found to induce a neuronal-like phenotype in the rat neural crest pheochromocytoma cell, PC12 cells (Greene & Tischler, 1976). This phenomenon lent itself to a large amount of research on the signalling pathways involved in this NGF- β induction of neuritic outgrowth from the PC12 cells. Accordingly, it was then established that the MAPK pathway (Sole *et al.*, 2004), the PI3K pathway (Kimura *et al.*, 1994; Jackson *et al.*, 1996) and NF κ B activation (Wood, 1995; Hamanoue *et al.*, 1999) are involved in NGF- β induced outgrowth of PC12 cells. Interestingly, this differentiation into neuronal-like cells does not occur upon epidermal growth factor (EGF) receptor stimulation which has similar signalling to TrkA (for review, see Vaudry *et al.*, 2002). It is believed that this may be due to both sustained MAPK activation and PI3K activation upon NGF- β stimulation of TrkA which does not occur following EGF receptor activation (Qui & Green, 1992; Traverse *et al.*, 1992; York *et al.*, 2000). In relation to the use of NGF- β as a therapeutic agent, ongoing research is investigating the potential of utilising it for delaying cognitive decline during ageing. A promising study by Conner *et al.* found that delivering NGF- β to cholinergic neurons during ageing in the primate attenuates age-associated decreases in cholinergic innervations (Conner *et al.*, 2001). Studies such as this one led to the movement of utilising NGF- β in human trials for AD, a disorder which shows a huge loss of cholinergic innervation. The results of a phase I clinical trial investigating the efficacy of NGF- β gene therapy for patients with mild AD demonstrated safe administration in addition to a suggested attenuation of cognitive decline, warranting the continuation into phase II trials (Tuszynski *et al.*, 2005). The results from the Phase II clinical trial are yet to be finalised, but are due to be completed by May 2012.

1.5.1.4 BDNF and neuritic growth

The ability of BDNF to induce neuritic growth was identified in the 1980's by a study investigating the impact of the presence of BDNF on the growth of sensory neurons. The study demonstrated that BDNF led to a clear increase in neuritic growth (Davies *et al.*,

1986). Many other studies have since demonstrated that BDNF can also increase neuritic growth of central neurons such as retinal cells (Thanos *et al.*, 1989), cerebellar granule cells (Segal *et al.*, 1995) and primary cortical neurons (Horch & Katz, 2002). The ability of BDNF to induce neuritic growth, similarly to NGF- β , relies on activation of TrkB (Song *et al.*, 1997), and results in the activation of the MAPK and PI3K pathway with associated downstream effects as described previously (for review, see Cohen-Cory *et al.*, 2010). Furthermore, BDNF is important in developing synapses, and treatment of neurons *in vivo* with this neurotrophin increases synaptogenesis (Alsina *et al.*, 2001). Due to the widespread use of BDNF in the brain to encourage the growth of many neuronal types, BDNF has been investigated as a therapeutic agent for many CNS disorders which demonstrate neuritic loss, such as AD, PD and Amyotrophic Lateral Sclerosis (ALS) (for review, see Nagahara & Tuszynski, 2011). Clinical trials for the use of BDNF for ALS reached phase III, however, a large phase III trial failed to demonstrate any improvement in patient survival following systemic BDNF administration, however further trials using different delivery methods are ongoing (The BDNF Study Group, 1999; Nagahara & Tuszynski, 2011). In addition to ALS, BDNF has proved beneficial for AD in preclinical animal models. For example, aged primates treated with BDNF expressing lentiviral vectors, demonstrated increased cognitive function in tandem with attenuation of cortical loss (Nagahara *et al.*, 2009). Perhaps future clinical trials for BDNF against AD may demonstrate benefits to patients.

1.5.1.5 The Neurotrophins and NA

NA has previously been shown to induce the expression of neurotrophins in glial cells. An early study demonstrated that β -adrenergic stimulation of C6 glioma cells resulted in the release of NGF- β into the culture medium (Schwartz & Costa, 1977). In addition, Schwann cells increase NGF- β mRNA expression upon treatment with NA or cAMP activators (Matsuoka *et al.*, 1991). There is also much research on the ability of clenbuterol (Clen), a β_2 -adrenoceptor selective agonist to induce the secretion of NGF- β . For example *in vivo* Clen treatment results in increased NGF- β mRNA (Follesa & Mocchetti, 1993) and protein (Hayes *et al.*, 1995) in the cerebral cortex of rats. In addition, Clen treatment *in vitro* of rat hippocampal cells (mixed glia and neurons) results in the release of NGF- β protein which protects the hippocampal cells from glutamate toxicity (Semkova *et al.*, 1996). Furthermore, this protection was attenuated by treatment

with the β -adrenoceptor antagonist propranolol (Prop), or with an antibody against NGF- β (Semkova *et al.*, 1996).

NA has also been shown to induce the expression of BDNF. For example, NA treatment increases BDNF protein in primary hippocampal neurons (Chen *et al.*, 2007), and NA-induced BDNF is known to protect primary neurons against amyloid toxicity (Counts & Mufson, 2010). Furthermore, NA has also been shown to induce the expression of BDNF from primary astrocytes (Zafra *et al.*, 1992).

The ability of NA to induce the expression of NGF- β and BDNF may depend on the NA-induced increase in cAMP with the subsequent activation of PKA and the resultant activation of the transcription factor CREB (Rang & Dale, 2003). CREB then activates the CCAAT/enhancer-binding proteins which have been shown to be involved in NGF- β expression in the rat C6 astrocytoma cell line (Colangelo *et al.*, 1998; McCauslin *et al.*, 2006). Furthermore, an increase in CREB activity has also been demonstrated to result in BDNF expression in cultured cortical neurons (Tao *et al.*, 1998).

1.5.2 Glial-derived neurotrophic factor

GDNF is a neurotrophic factor which was isolated in 1993 by Lin *et al.* At this time it was shown to enhance cell survival of midbrain dopaminergic neurons and increase dopaminergic neurite outgrowth (Lin *et al.*, 1993). Subsequently GDNF has been found to have many other important roles both within the CNS; and outside the CNS such as kidney development and as a neurotrophic factor for the enteric nervous system (for review, see Baloh *et al.*, 2000). GDNF is not a member of the classical neurotrophin family but rather is a member of the GDNF family ligand (GFL) family; a sub-family of the transforming growth factor- β (TGF- β) superfamily due to the presence of seven repeating cysteine residues, a TGF- β characteristic. The GFL family also includes neurturin (NRTN), artemin (ARTN) and persephin (PSPN) (for review see Airaksinen & Saarma, 2002). All four of the GFLs signal via a multicomponent receptor complex comprising of the RTK rearranged during transfection (RET) and a GDNF family receptor α -component (GFR- α). The GFR- α , of which there are four subtypes, binds the ligand with high affinity but has no downstream signalling mechanisms, instead signalling occurs via the interaction of GFR- α with RET. GDNF preferentially binds to GFR- α 1 but there is

also evidence that it can bind to GFR- α 2 although functions of this pathway are unknown (for review, see Baloh *et al.*, 2000).

1.5.2.1 GDNF Signalling

As previously mentioned, GDNF primarily signals via the multicomponent complex GFR- α 1 and RET (see Figure 1.10). GDNF is secreted as a precursor preproGDNF protein which is cleaved to reveal the signalling sequence. The GDNF binds to the GFR- α which is linked to the plasma membrane via a glycosyl phosphatidylinositol anchor (for review see Airaksinen & Saarma, 2002). The activated GFR- α forms a complex with two RET molecules which activates their intracellular tyrosine kinase domains, inducing homodimerisation and tyrosine autophosphorylation. GFR- α and RET can however bind with low affinity in the absence of GDNF (Eketjall *et al.*, 1999). Soluble forms of the GFR- α receptors also exist which have been shown to bind GDNF in the extracellular space and present it to RET on the cell membrane. Furthermore, GFR- α 1 on the cell membrane can bind GDNF and present it to RET on an adjacent cell, and this signal may assist in the formation and maintenance of neuronal connections (Paratcha *et al.*, 2001). Phosphorylated tyrosines on the RET molecule provide docking sites for the adaptor proteins; FRS2, Grb7/10, phospholipase C, Shc and Grb2 (for reviews, see Airaksinen *et al.*, 1999; Gotoh, 2008). Thus activation of RET results in the activation of many signalling pathways, including the ERK1/2, JNK and PI3K pathways (for reviews, see Takahashi, 2001; Gu & Neel, 2003). There is also emerging evidence that GDNF can bind to and signal via the neural cell adhesion molecule (NCAM) receptor. GDNF was shown to increase phosphorylated Fyn, a Src family tyrosine kinase which is associated with the NCAM receptor, an association which requires GFR- α (Paratcha *et al.*, 2003).

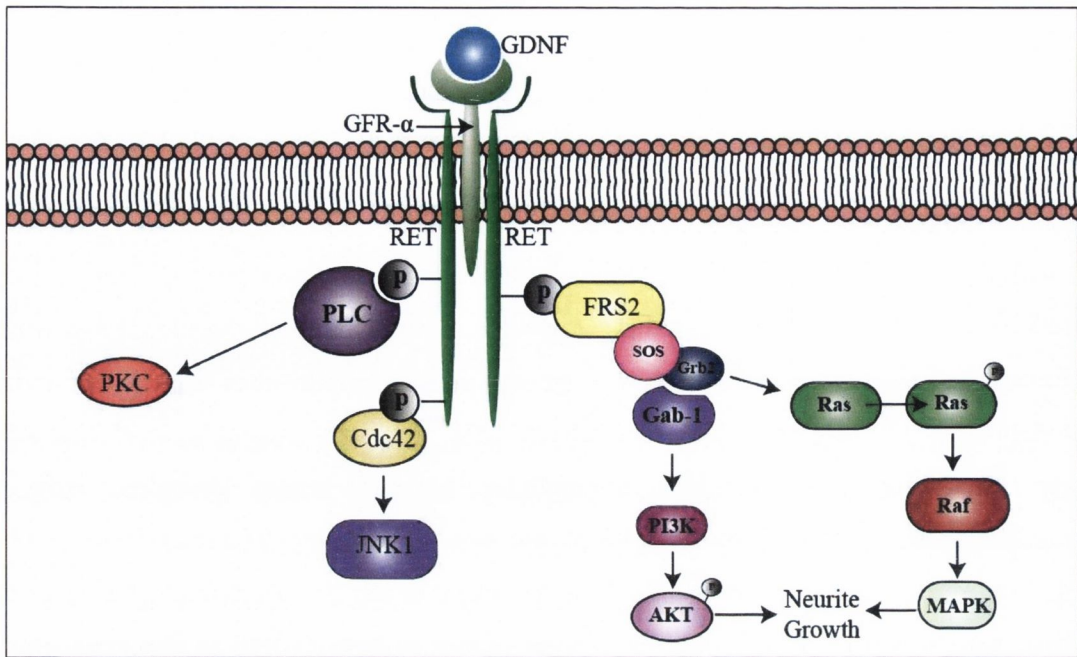


Figure 1.10: Signalling of GDNF

GDNF binds to GFR- α which associates with and activates the RET receptor. Activation of RET results in the activation of PKC, PI3K and MAPK pathways.

1.5.2.2 GDNF and Neuritic Growth

The ability of GDNF to impact upon neuritic growth was demonstrated early on in dopaminergic cortical neurons (Lin *et al.*, 1993; Hou *et al.*, 1996) and cerebellar purkinje cells (Mount *et al.*, 1995). However, the exact mechanism of GDNF-induced neuritic growth is not as clearly defined as for the neurotrophins. Some lines of evidence however suggest that the interaction between GDNF and NCAM is necessary for GDNF-induced neuritic growth (Chao *et al.*, 2003; Ditlevsen *et al.*, 2003; Cao *et al.*, 2008; Nielsen *et al.*, 2009). NCAM has no intracellular signalling capabilities, however the GDNF-induced neuritic growth via NCAM has been shown to involve the FGF-2 receptor (FGFR) (Nielsen *et al.*, 2009). Furthermore, the PI3K pathway is involved in GDNF-induced neuritic growth (Pong *et al.*, 1998; Ditlevsen *et al.*, 2003).

As GDNF is a potent protective factor for dopaminergic neurons, it is a prime candidate for PD therapy where there is profound loss of dopaminergic neurons in the substantia nigra (for review, see Barker, 2009). In two nonhuman primate models of PD, lentiviral GDNF treatment led to increased number of dopaminergic nigral neurons in aged primates and prevented neurotoxin 1-methyl-4-phenyl-1,2,3,6-tetrahydropyridine (MPTP)-induced

neuronal degeneration (Kordower *et al.*, 2000). These promising results led to the use of GDNF in human clinical trials. However, the clinical trials which have been performed utilising GDNF as a therapy for PD have been inconclusive. Early reports demonstrated efficacy of GDNF administration, however subsequently a larger double-blinded study showed no significant effect of GDNF over placebo (for review, see Barker, 2009). Furthermore, Amgen controversially halted some of its clinical trials prematurely, based on evidence of patients developing antibodies to GDNF and evidence of cerebellar degeneration in nonhuman primate models (Penn *et al.*, 2006).

1.4.2.3 GDNF and NA

At present, there are no reports of an ability of NA to induce the production and secretion of GDNF. However there is some indirect evidence; for example, GDNF mRNA has been detected in areas innervated by LC neurons, but not in the LC itself (Arenas *et al.*, 1995), suggesting perhaps that noradrenergic neurons might stimulate the production of GDNF. Furthermore, NA reuptake inhibitors such as amitriptyline, clomipramine and mianserin lead to an increase in GDNF, but it is unknown how this occurs (Hisaoaka *et al.*, 2007). It is also known that GDNF transcription is modulated by members of the CREB family (Baecker *et al.*, 1999; Hisaoaka *et al.*, 2008), which is downstream of β_2 -adrenoceptor activity.

1.5.3 FGF-2

FGF-2 is an 18kDa member of the FGF superfamily, which also includes 22 other ligands, and five receptors. Each FGF ligand contains a heparin binding site, which helps in the formation of a stable interaction between ligand and receptor (Ornitz *et al.*, 1996). The mechanism of release of FGF-2 into the extracellular space is somewhat controversial, due to the lack of a typical leader sequence which generally results in secretory proteins being transported to the endoplasmic reticulum and secreted. Early studies suggested that FGF-2 was released only upon cellular damage in an endoplasmic reticulum / Golgi independent manner (for review, see Powers *et al.*, 2000). However, it is now known that FGF-2 is directly translocated to the plasma membrane in a manner that requires both intracellular PIP2 and extracellular heparan sulphate proteoglycans (for review, see Nickel, 2010). Furthermore, FGF-2 is found extracellularly (for review, see Powers *et al.*, 2000), and can be released upon various stimuli (Delgado-Rivera *et al.*, 2009). FGF-2 has also been

shown to be expressed by both neurons and glial cells in the CNS but also displays expression in peripheral tissues (for reviews, see Reuss & von Bohlen und Halbach, 2003; Turner *et al.*, 2006).

1.5.3.1 FGF-2 Signalling

There are four FGF receptors (FGFR1-4) which are all RTKs. There are many splice variants of each receptor which lend to varying affinities of the FGFs to each receptor. The FGF receptors each display a distinct expression pattern, with the FGFR1 most abundantly expressed in the CNS (for review, see Turner *et al.*, 2006). FGF-2 can bind to all four receptor subtypes with varying affinities to each one, for example, FGF-2 has high affinity to the “c” type isoforms of FGFR1-3 and low affinity to the “b” isoforms (Ornitz *et al.*, 1996). Activation of the receptors only occurs when two receptors each with a bound FGF ligand, form a complex linked by a heparan sulphate proteoglycan molecule (for review, see Reuss & von Bohlen und Halbach, 2003). Phosphorylation and receptor activation follows (see Figure 1.11). SH2 domain proteins are known to bind to the activated FGFRs which can then recruit other proteins to the complex. Recruitment to the activated FGFR receptor includes phospholipase C and the adaptor protein FRS2. As described previously, FRS2 recruits Grb-2/SOS, which activates the MAPK pathway via Ras. Gab-1 is also recruited via Grb-2 which activates the PI3K pathway (for review, see Reuss & von Bohlen und Halbach, 2003). It is also important to note a high molecular weight FGF-2 exists which is not secreted and acts independently of the FGFR in the nucleus (for review, see Chlebova *et al.*, 2009).

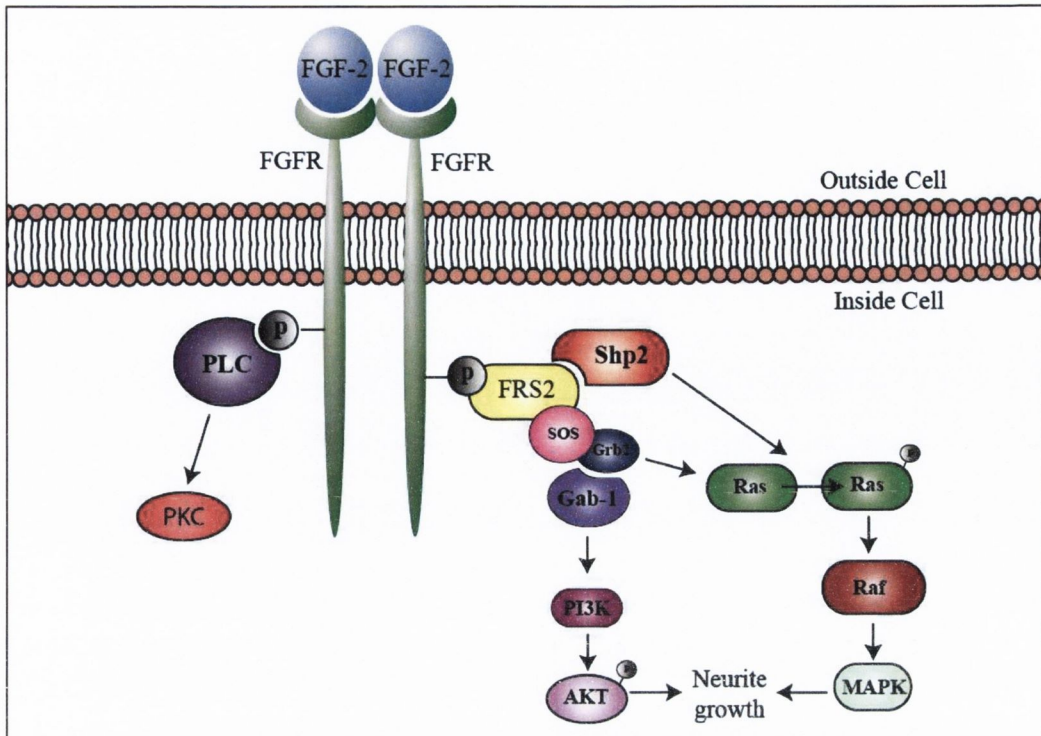


Figure 1.11: FGF-2 Signalling via the FGFR

FGF-2 binds to the FGFR which leads to the activation of the PI3K, MAPK and PKC pathways.

1.5.3.2 FGF-2 and Neuritic Growth

There is much research demonstrating the ability of FGF-2 to enhance neuritic growth of neurons, for example of rat hippocampal neurons (Walicke *et al.*, 1986; Aoyagi *et al.*, 1994; Patel & McNamara, 1995). In particular, FGF-2 appears to preferentially induce branching of axons and not dendrites (Patel & McNamara, 1995; Szebenyi *et al.*, 2001). Furthermore, the ability of cell adhesion molecules such as NCAM to induce neuritic growth appears to be mediated via the activation of the FGFR (for review see Viollet & Doherty, 1997). Both the MAPK and PI3K pathways have been demonstrated to be involved in FGF-2-induced neuritic growth (Abe *et al.*, 2001; Gilardino *et al.*, 2009). Interestingly, sustained activation of the MAPK is necessary for FGF-2-induced neuritic growth (Abe *et al.*, 2001), similarly to the sustained activity required for NGF- β -induced neuritic growth (Traverse *et al.*, 1992). In terms of therapeutic value, FGF-2 gene therapy has seen some amelioration of AD symptoms such as spatial learning deficits and hippocampal amyloid β deposition, as well as enhancement of neurogenesis, in a mouse model of AD (Kiyota *et al.*, 2011). It remains to be seen if the ability of FGF-2 to induce neuritic growth is also of therapeutic value to humans with AD.

1.5.3.3 FGF-2 and NA

There is limited evidence to show that FGF-2 can be produced upon noradrenergic stimulation. For example, rats injected with Clen show increases in FGF-2 mRNA in the cortex, hippocampus and cerebellum (Follesa & Mocchetti, 1993; Hayes *et al.*, 1995). Furthermore, primary rat cortical, hippocampal and cerebellar astrocytes show increases in FGF-2 mRNA expression and protein production following exposure with isoproterenol, a non-selective β -adrenoceptor agonist (Riva *et al.*, 1996). The ability of NA to induce FGF-2 expression also appears to rely on the increase in cAMP following β -adrenoceptor activation (Riva *et al.*, 1996).

1.5.4 VEGF

Vascular endothelial growth factor (VEGF), also known as VEGFA, belongs to a family which also includes placental growth factor, VEGFB, VEGFC and VEGFD. Alternative splicing of VEGF leads to four main isoforms in humans, all of which have slightly different properties. VEGF₁₆₅, the prototypical VEGF (herein referred to as VEGF), is a glycoprotein which although can be secreted, a large percentage of it also remains bound to the extracellular cell membrane and the extracellular matrix. The main role of VEGF is in angiogenesis, or the production of new blood vessels, therefore it is no surprise that VEGF is induced by hypoxic conditions and is a target for therapeutic relief of tumours (for review, see Ferrara *et al.*, 2003).

1.5.4.1 VEGF Signalling

VEGF has two receptors that it binds to and activates; VEGFR1 and VEGFR2, both of which are RTKs. VEGFR1 (also known as Flt1), undergoes a very weak phosphorylation response upon VEGF activation and thus it has been hypothesised that VEGFR1, as well as an alternatively spliced soluble VEGFR1 both function as decoy receptors to modulate the binding of VEGF to VEGFR2. Despite this, signalling via VEGFR1 has been associated with the recruitment of monocytes amongst other functions. VEGFR2 (also known as Flk1) on the other hand is crucial for the signalling of VEGF to induce vascular growth and induce BBB permeability (for review, see Ferrara *et al.*, 2003). Activation of VEGFR2 results in the phosphorylation of phospholipase-C γ , PI3K, Ras GTPase-activating protein and Src. It can also activate the ERK1/2 pathway. In addition to these receptors, VEGF associates with two other proteins known as neuropilin 1 (NRP1) and

NRP2, and it is thought that they function by increasing the binding activity of VEGF to VEGFR2 (for review, see Ferrara *et al.*, 2003).

1.5.4.2 VEGF and Neuritic Growth

Many reports have demonstrated the ability of VEGF to induce neuritic growth. For example, primary cortical neurons have been demonstrated to show increased neuritic growth following VEGF exposure (Rosenstein *et al.*, 2003; Khaibullina *et al.*, 2004; Jin *et al.*, 2006). The ability of VEGF to induce neuritic growth has been linked to activation of the VEGFR2 and retrograde transport of VEGF (Sondell *et al.*, 2000; Jin *et al.*, 2006). In addition, the Rho kinases have been implicated in the ability of VEGF to induce neuritic growth in primary cortical neurons (Jin *et al.*, 2006). Furthermore, overexpression of VEGF increased neuritic length and branching of newborn cortical neurons *in vivo* following an ischemic insult to rats (Wang *et al.*, 2009). Interestingly, a VEGF gene transfer protein has been investigated as a therapeutic agent for ALS. Clinical data from a phase II trial for SB-509 demonstrated the drug was both safe and showed efficacy in ALS patients (Benaim *et al.*, 2010), unfortunately however due to negative results for diabetic neuropathy this drug has been removed from all clinical trials.

1.5.4.3 VEGF and NA

Non-CNS cells have been shown to express VEGF following adrenergic stimulation. For example, brown adipose tissue induces VEGF mRNA following noradrenergic stimulation (Asano *et al.*, 1997), via the increase of cAMP and activation of PKA (Fredriksson *et al.*, 2000). VEGF is also upregulated following NA stimulation in many cancerous cell lines, for example see (Yang *et al.*, 2008). There is however, only one report which has demonstrated an increase in VEGF mRNA following direct NA stimulation in rat astrocytes (Wang & Yang, 2007). A second study however has shown that an increase in cAMP, as occurs downstream of adrenergic stimulation, can also increase VEGF mRNA in neurons in the hippocampus (Lee *et al.*, 2009b).

1.5.5 Interleukin-6

Interleukin-6 (IL-6) was first identified in the mid 1980's by Hirano and was classified as a cytokine due to its ability to differentiate immature B cells of the immune system to the fully mature antibody-producing cells (Hirano *et al.*, 1986). However, since then, IL-6

has been found to have many diverse functions, including the differentiation and proliferation of many cell types, in particular immune cells, and its involvement in normal metabolism and regulation of the HPA axis, and even a role as a neurotrophic factor (for reviews, see Chalaris *et al.*, 2011; Jones *et al.*, 2011; Spooren *et al.*, 2011). IL-6 is in a cytokine family which also includes CNTF, leukaemia inhibitory factor, oncostatin M, IL-11 and cardiotrophin-1, due to the fact that each signal via gp130 (Marz *et al.*, 1999).

1.5.5.1 IL-6 Signalling

The signalling of IL-6 occurs by two main mechanisms; classical signalling and trans-signalling. Classical signalling involves the interaction of IL-6 with a plasma membrane complex comprised of the non-signalling IL-6 receptor α (IL-6R α , also known as CD126) and glycoprotein 130 (gp130). IL-6 first interacts with the non-signalling IL-6R, which recruits two molecules of gp130 and facilitates downstream signalling of IL-6 (see Figure 1.12). IL-6 signalling is quite unique in that a soluble IL-6 receptor (sIL-6R) exists in the extracellular space which, upon IL-6 and subsequent gp130 binding, leads to viable downstream signalling. This is the trans-signalling of IL-6. As gp130 is ubiquitously expressed in all cell types, trans-signalling allows cell types which do not express the IL-6R to be activated by IL-6. The sIL-6R is generated by either alternative splicing of the IL-6R mRNA or by shedding of the membrane receptor by metalloproteinases known as A Disintegrin And Metalloproteinase (ADAM) family, in particular ADAM17 appears to be involved in cleaving the IL-6R from the membrane (for review, see Chalaris *et al.*, 2011).

Dimerisation of the gp130 molecules is followed by the recruitment of the Janus Kinases (JAK-1 and JAK-2) which leads to phosphorylation of tyrosine residues on the gp130 cytoplasmic domains and recruitment of STATs (for review, see Spooren *et al.*, 2011). In addition, phosphorylation of a specific tyrosine site on the gp130 molecule by JAK recruits Shp2 which activates the MAPK signalling pathway via Grb2-SOS. Furthermore, Gab-1, and therefore the PI3K pathway, is also activated upon ligand binding (Heinrich *et al.*, 2003).

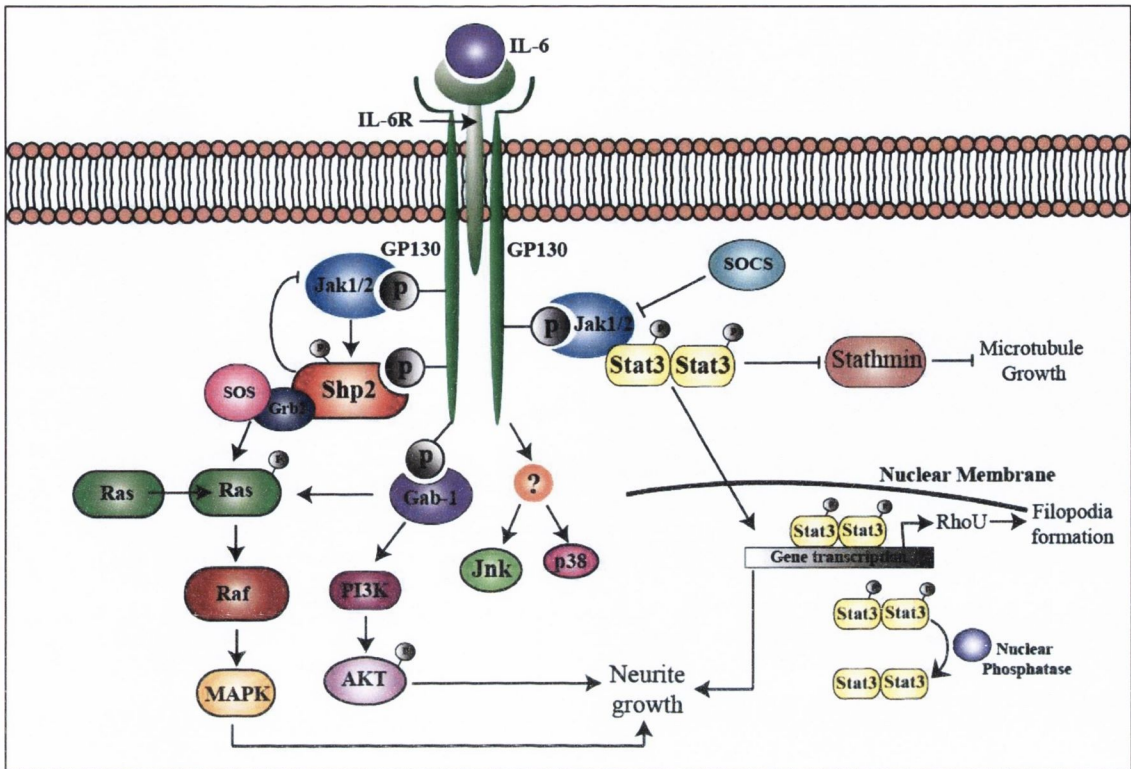


Figure 1.12: IL-6 Signalling

IL-6 binds to the IL-6 receptor, which leads to the phosphorylation of gp130. This then activates the JAK-STAT pathway. The PI3K and MAPK pathways are also activated upon ligand binding via Gab-1 and Grb-2 respectively.

1.5.5.2 IL-6 and Neuritic Growth

Early in its investigation, IL-6 treatment of PC12 cells was shown to induce a neuronal morphology of the cells in a manner similar to NGF- β treatment (Satoh *et al.*, 1988). This was later shown to occur via the STAT3 pathway (Wu & Bradshaw, 1996). Furthermore, primary hippocampal neurons demonstrate increased neuritic length and branching following IL-6 exposure (Sarder *et al.*, 1996). The ability of IL-6 to induce neuritic growth may be related to the transcription of the atypical Rho kinase RhoU following STAT3 phosphorylation and translocation to the nucleus (Schiavone *et al.*, 2009).

1.5.5.3 IL-6 and NA

NA has previously been shown to upregulate both IL-6 mRNA expression and protein production from rat neonatal primary astrocytes. Interestingly, NA was shown in this study to have no effect on the induction of IL-6 from microglia (Norris & Benveniste, 1993). Many other cells have shown modulation of IL-6 following adrenergic stimulation. For example, in the macrophage cell line RAW, adrenergic stimulation via the β_2 -adrenoceptor agonist salmeterol (Salm) resulted in a significant increase in the release of IL-6 protein from the cells. This ability was blocked by the β_2 -adrenoceptor selective antagonist ICI 118, 551 but not by a specific β_1 or β_3 antagonist (Tan *et al.*, 2007). Furthermore, β -adrenergic activation can both enhance (Szabo *et al.*, 1997; Manni *et al.*, 2011) and attenuate (van der Poll *et al.*, 1994) IL-6 production following an inflammatory stimulus. How NA stimulation leads to the induction of IL-6 expression is not known, however one study demonstrated that the ability was independent of PKA or NF κ B activation but is mediated via ERK1/2 and p38 MAPK pathways (Tan *et al.*, 2007).

1.6 Objectives of thesis

The major focus of this thesis was to examine the potential of NA, acting on glial β -adrenoceptors, to induce neuritic growth of primary cortical neurons through the release of neurotrophic factors. The specific aims were:

- 1) To investigate the ability of the monoaminergic neurotransmitters, NA and 5-HT, to induce neuritic growth of primary rat cortical neurons either directly or via an indirect action on glial cells.
- 2) To determine the glial adrenergic receptor subtype involved in NA-induced neuritic growth of neurons.
- 3) To determine the glial cell type (astrocyte vs. microglia) involved in NA-induced neuritic growth of neurons
- 4) To examine the potential use of the C6 glioma cell line as a model for investigating the ability of glial β -adrenergic stimulation to induce neuritic growth.
- 5) To determine a role for growth factors as the mechanism for NA-induced neuritic growth of primary cortical neurons.
- 6) To examine the signalling pathways involved in the regulation of NA-induced neuritic growth, specifically examining the PI3K, the MAPK and STAT3 pathways.

Chapter 2

Materials and Methods

2.1 Materials

2.1.1 Animals

Wistar rats (0-3 days old)

Bioresources, TCD

2.1.2 Experimental Treatments

Noradrenaline (99%) (NA)

Sigma-Aldrich, Ireland

STAT3 inhibitor VI, S31-201

Merck Chemicals, UK

Di-butyryl adenosine cyclic

monophosphate (db-cAMP)

Tocris Bioscience, UK

Goat IgG GDNF neutralizing antibody (GDNF nAB)

R&D systems, UK

Goat IgG

Santa-Cruz Inc., USA

LY294002 hydrochloride

Tocris Bioscience, UK

Mouse IgG1 κ fibroblast growth factor 2

neutralizing antibody (FGF-2 nAB)

Millipore, Ireland

Mouse IgG1 κ (isotype control)

Biolegend, USA

PD98049

Tocris Bioscience, UK

Phentolamine hydrochloride (Phent)

Sigma-Aldrich, Ireland

Propranolol hydrochloride (Prop)

Sigma-Aldrich, Ireland

Rat IgG2b κ CD126 (IL-6 R α chain) antibody

Biolegend, USA

Rat IgG2b κ , isotype control

Biolegend, USA

Recombinant rat BDNF

Biovision, USA

Recombinant rat FGF-2

Biovision, USA

Recombinant rat GDNF

R&D Systems, UK

Recombinant rat IL-6

R&D Systems, UK

Recombinant rat NGF- β	R&D Systems, UK
Recombinant rat VEGF	Biovision, USA
Rezazurin	Sigma-Aldrich, Ireland
Salbutamol hemisulfate (Salb)	Sigma-Aldrich, Ireland
Salmeterol (Salm)	Tocris Bioscience, UK
Y1036, Neurotrophin antagonist	Millipore, Ireland
Wortmannin (Wort)	Tocris Bioscience, UK
Xamoterol hemifumarate (Xam)	Tocris Bioscience, UK

Drug Name	Abbreviation	Function
Amitriptyline	Ami	Serotonin/Noradrenaline reuptake inhibitor
Clenbuterol	Clen	Agonist of β_2 adrenoceptor
Dibutyryl adenosine cyclic monophosphate	dbcAMP	cAMP analogue
LY294002	LY	PI3 Kinase Inhibitor
Noradrenaline	NA	Agonist of α and β adrenoceptors
PD98049	PD	MEK1 Inhibitor
Phentolamine	Phent	Antagonist of α adrenoceptor
Propranolol	Prop	Antagonist of β adrenoceptor
S31-201	S31-201	STAT3 Inhibitor
Salbutamol	Salb	Agonist of β_1 and β_2 adrenoceptors
Salmeterol	Salm	Agonist of β_2 adrenoceptor
Wortmannin	Wort	PI3 Kinase Inhibitor
Xamoterol	Xam	Agonist of β_1 adrenoceptor
Y1036	Y1036	Neurotrophin antagonist

Table 2.1: Drug Interventions

2.1.3 Cell Culture Materials

Acrodisc syringe filter (0.2µm)	Pall Corporation
Biocidal ZF™	WAK-Chemie
B-27 Supplement	Gibco, UK
Cell strainers (40µM)	BD Falcon, UK
Coverslips (plastic, 13mm)	Sarstedt, Ireland
Coverslips (glass; 13mm, 30mm)	VWR Int., Ireland
Dimethyl sulfoxide	Sigma-Aldrich, Ireland
Disposable sterile scalpels	Swann-Morton Ltd., UK
Dulbecco's modified Eagle's medium: F-12 (DMEM)	Biosera, UK
Dulbecco's phosphate buffered saline (PBS) (10X)	Sigma-Aldrich, Ireland
Ethanol, absolute	Hazmat, TCD
Foetal Bovine Serum (FBS)	Biosera, UK
Fungiozone	Gibco, UK
Glutamax	Gibco, UK
Haemocytometer	VWR Int., Ireland
Ham's F12 Nutrient Mixture	Gibco,UK
Neurobasal-media	Gibco, UK
Penicillin-streptomycin	Gibco, UK
Plastic syringe (50ml, 20ml and 1ml)	Becton Dickenson, UK
Poly-L-lysine	Sigma-Aldrich, Ireland
Poly-D-lysine	Sigma-Aldrich, Ireland
Serological pipette (25ml, 50ml)	Sarstedt, Ireland

Steri-Cycle CO ₂ Incubator	Bio-Sciences
Sterile 6, 24 well plates	Sarstedt, Ireland
Sterile falcon tubes (15ml, 50ml)	Sarstedt, Ireland
Sterile microtubes (2ml)	Sarstedt, Ireland
Sterile Petri dishes	Sarstedt, Ireland
Sterile transfer pipettes	Sarstedt, Ireland
Sterile T25cm ² , T75cm ² Flasks	Sarstedt, Ireland
Trypan Blue	Sigma-Aldrich, Ireland
Trypsin-EDTA	Sigma-Aldrich, Ireland

2.1.4 Assay Kits

GDNF Emax [®] Immunoassay System	Promega, UK
Human BDNF DuoSet ELISA	R&D Systems, UK
Human FGF-basic ELISA MAX [™] Deluxe Set	Biolegend, USA
NGF- β Emax [®] Immunoassay System	Promega, UK
Rat IL-6 ELISA SET	BD Biosciences, USA
Rat VEGF DuoSet ELISA	R&D Systems, UK

2.1.5 Molecular Reagents

96-well optical reaction plates	Applied Biosystems, UK
Absolute ethanol	Sigma-Aldrich, Ireland
Biosphere filter tips (1000, 100 and 10 μ l)	Sarstedt, Ireland
High capacity cDNA archive kit	Applied Biosystems

Molecular grade water	Sigma-Aldrich, Ireland
Optical adhesive covers	Applied Biosystems, UK
PCR tubes	Sarstedt, Ireland
RNase-free 1.5ml and 2ml microfuge tubes	Ambion, UK
RNase Zap wipes	Ambion, UK
Total RNA isolation kit	Macherney-Nagel GmbH & Co., Germany
TaqMan gene expression assays (see Table 2.2)	Applied Biosystems, UK
TaqMan universal PCR master mix	Applied Biosystems, UK

2.1.6 General Laboratory Plastics

Laboratory rolls	Fisher Scientific
Parafilm	Fisher Scientific
Microtest 96-well flat bottomed plates	Sarstedt, Ireland
Microtubes (1.5ml)	Sarstedt, Ireland
Microtubes (0.5ml)	Sarstedt, Ireland
Pipette tips	Sarstedt, Ireland
Plastic transfer pipettes	Sarstedt, Ireland
Plastic syringe (1ml)	Becton Dickenson
F96 Maxisorp immunoplates for ELISA	Sarstedt, Ireland

2.1.7 General Laboratory Chemicals

2-Propanol	Sigma-Aldrich, Ireland
------------	------------------------

Absolute ethanol (EtOH)	Sigma-Aldrich, Ireland
Acrylamide	Sigma-Aldrich, Ireland
Ammonium Persulfate (APS)	Sigma-Aldrich, Ireland
β -Mercaptoethanol	Sigma-Aldrich, Ireland
Bovine Serum Albumin (BSA)	Sigma-Aldrich, Ireland
Bromophenol Blue	Sigma-Aldrich, Ireland
Disodium hydrogen orthophosphate (Na_2HPO_4)	Sigma-Aldrich, Ireland
Glycerol	Sigma-Aldrich, Ireland
Glycine	Sigma-Aldrich, Ireland
Hydrochloric acid (HCl)	VWR Int., Ireland
N,N,N',N'-Tetramethylethylende-diamine (TEMED)	Sigma-Aldrich, Ireland
N'N' Bis Acrylamide	Sigma-Aldrich, Ireland
Normal goat serum	Vector, UK
NP-40 (([Octy]phenoxy)polyethoxyethanol)	Sigma-Aldrich, Ireland
Methanol (MeOH)	VWR Int., Ireland
Orthophosphoric acid	VWR Int., Ireland
Phosphatase inhibitor cocktail I & II	Sigma-Aldrich, Ireland
Potassium dihydrogen orthophosphate (KH_2PO_4)	VWR Int., Ireland
Potassium chloride (KCl)	Merck
Protease inhibitor cocktail	Sigma-Aldrich, Ireland
Sodium bicarbonate (NaHCO_3)	VWR Int., Ireland
Sodium carbonate (Na_2CO_3)	VWR Int., Ireland
Sodium Chloride (NaCl)	VWR Int., Ireland
Sodium dodecyl sulphate (SDS) 99%	Sigma-Aldrich, Ireland

Sodium hydroxide (NaOH)	Sigma-Aldrich, Ireland
Sodium phosphate monobasic monohydrate (NaH ₂ PO ₄)	Sigma-Aldrich, Ireland
Sulphuric acid (H ₂ SO ₄) 98%	BDH
Triton X-100	Sigma-Aldrich, Ireland
Trizma Base	Sigma-Aldrich, Ireland
Tris-HCl	Sigma-Aldrich, Ireland
Triton-X	Sigma-Aldrich, Ireland
Tween-20	Sigma-Aldrich, Ireland

2.1.8 Western Blotting and Staining reagents and antibodies

AKT Antibody	Cell Signalling, USA
Anti-mouse IgG	Sigma-Aldrich, Ireland
Anti-rabbit IgG	Amersham, UK
Anti- β III-tubulin IgG	Promega, UK
β -actin antibody	Santa-Cruz Inc., USA
β_2 -adrenoceptor antibody	Santa-Cruz Inc., USA
Broadrange molecular weight marker	Biorad, USA
CD11b antibody	Millipore, Ireland
ECL Western Blotting Substrate	Pierce, USA
GFAP antibody	Dako
Goat anti-rabbit Alexa 488	Invitrogen, USA
Goat anti-mouse Alexa 633	Invitrogen, USA
Goat anti-rabbit Alexa 546	Invitrogen, USA

Hoescht	Invitrogen, USA
Normal goat serum (NGS)	Sigma-Aldrich, Ireland
Polyvinylidene (PVDF)	Millipore, Ireland
Re-blot plus	Millipore, Ireland
STAT-3 Antibody	Cell Signalling, USA
Phospho-AKT Antibody	Cell Signalling USA
Phospho-p42/44 (ERK) Antibody	Cell Signalling, USA
Phospho-STAT-3 Antibody	Cell Signalling, USA

2.2 Methods

2.2.1 Aseptic Technique

Aseptic techniques were used during all cell culture work and also in the preparation of cell culture reagents to maintain a sterile environment which was free from fungal, bacterial and viral infections. This was necessary as infections can interfere with normal cellular function. Pipette tips and dH₂O were sterilised by autoclaving at 121°C for 20min prior to use in cell culture. Sterile disposable plastics were also utilised to ensure asepsis. Dissection equipment was cleaned with Virkon and then baked for a minimum of 1h at 200°C to ensure sterility. All cell culture work was carried out in a laminar flow hood (Hera Safe, category 2). This prevents contamination with airborne pathogens by only allowing filtered air to come into contact with cells. The interior of the hood was sterilized with 70% ethanol (EtOH; 30% ddH₂O and 70% EtOH v/v) before and after use. The hood surface was also exposed to ultraviolet (UV) light for 30min after use. Any items taken into the flow hood were lightly sprayed with 70% EtOH to prevent introduction of any pathogens to the hood work area. Disposable latex gloves were worn and sprayed with EtOH before use. Gloves were changed regularly during cell culture work. Cells were maintained in a sterile incubator (humidified 5% CO₂; 95% air environment at 37°C) and any items put in the incubator were lightly sprayed with EtOH to prevent contamination with any pathogens. Both the incubator and laminar flow hood were regularly cleaned with Biocidal ZF™, Mycoplasma off, virkon and EtOH to maintain a sterile environment.

2.2.2 Preparation of Culture Media and Test Compounds

Glial Culture Media: The glial culture media of 10% (v/v) heat-inactivated Fetal Bovine Serum (FBS), 1% (v/v) Penicillin-Streptomycin (P/S) in Dulbecco's modified Eagle's medium (DMEM:F12) and 0.1% (v/v) Fungizone was prepared by filter-sterilising 5ml P/S, 50ml FBS through a 0.2mm syringe filter into a 500ml bottle of DMEM:F12 and adding 500µl of Fungizone. This complete DMEM (cDMEM) was used in all glial preparations unless otherwise specified.

Neurobasal media: The neuronal culture media of 1% (v/v) P/S, 1% (v/v) Glutamax and 0.1% (v/v) Fungizone in neurobasal media (NBM, Invitrogen) was prepared by filter-sterilising 5ml P/S and 5ml glutamax through a 0.2mm syringe filter into a 500ml of NBM followed by addition of 500µl of Fungizone. When required, a working solution was prepared by adding 500µl of 100 X B-27 growth supplement to 50ml of complete-NBM.

Phosphate buffered saline (PBS): A working 1 X solution of PBS was prepared by adding 1ml Dulbecco's sterile 10 X PBS to 9ml ddH₂O.

Noradrenaline (NA): A 10mM stock solution was prepared by dissolving 0.034g NA (Formula weight 337g/mol) in 1ml NBM. This was then filter-sterilised using a 0.2mm syringe filter. NA was prepared fresh for each experiment.

Salbutamol: A 100mM stock solution was prepared by dissolving 25mg of salbutamol (β -AR agonist; Formula weight 228.35g/mol) in 1.71ml ddH₂O. Stock solution was frozen at -20°C in 15µl aliquots. Before use it was diluted to a working concentration in pre-warmed media and filter-sterilised using a 0.2mm syringe filter.

Salmeterol: A 100mM stock solution was prepared by dissolving 10mg salmeterol (selective β_2 -AR agonist; Formula weight 415.57g/mol) in 240.6µl DMSO. Stock solution was frozen at -20 °C in 12µl aliquots. Before use it was diluted to a working concentration in pre-warmed media and filter-sterilised using a 0.2mm syringe filter.

Xamoterol: A 50mM stock solution was prepared by dissolving 10mg xamoterol (selective β_1 -AR agonist; Formula weight 397.43g/mol) in 503.2µl ddH₂O. Stock solution was frozen at -20 °C in 12µl aliquots. Before use it was diluted to a working concentration in pre-warmed media and filter-sterilised using a 0.2mm syringe filter and.

Di-buteryl adenosine 3', 5'-cyclic monophosphate (db-cAMP): A 50mM stock solution was prepared by dissolving 25mg of db-cAMP (cyclic AMP analogue; Formula weight 491.4g/mol) in 1ml ddH₂O. Stock solution was frozen at -20 °C in 15µl aliquots. Before use it was diluted to a working concentration in pre-warmed media and filter-sterilised using a 0.2mm syringe filter.

Phentolamine: A 50mM stock solution of phentolamine (non-selective α -adrenoceptor antagonist; Formula weight 317.8g/mol) was prepared by adding 50mg to 3.38ml of ddH₂O. This solution was vortexed and filter-sterilised by using a 0.2µm syringe filter. Stock solution was frozen at -20 °C in 50µl aliquots for future use.

Propranolol: A 50mM stock solution was prepared by dissolving 50mg propranolol (non-selective β -AR antagonist; Formula weight 295.8g/mol) in 3.38ml ddH₂O. This was then filter-sterilised using a 0.2mm syringe filter. Stock solution was frozen at -20°C in 50µl aliquots for future use.

Alamar Blue (Resazurin): A 440µM stock solution of alamar blue was prepared by dissolving 25mg resazurin (C₁₂H₆NNaO₄, Formula weight 251.17g/mol) in 226.214ml ddH₂O. Stock solution was stored in a dark bottle for future use.

Wortmannin: A 10mM stock concentration of wortmannin was prepared by dissolving 1mg wortmannin (Formula weight 428.44g/mol) in 233.4µl of DMSO. Stock solution was frozen at -20°C in 5µl aliquots for future use. Before use it was diluted to a working concentration in pre-warmed media and filter-sterilised using a 0.2mm syringe filter.

LY294002: A 10mM stock concentration of LY294002 was prepared by dissolving 5mg LY294002 (Formula weight 343.81g/mol) in 1.45ml DMSO. Stock solution was frozen at -20°C in 15µl aliquots for future use. Before use it was diluted to a working concentration in pre-warmed media and filter-sterilised using a 0.2mm syringe filter.

PD98059: A 10mM stock concentration of PD98059 was prepared by dissolving 1mg PD98059 (Formula weight 267.28g/mol) in 374.14µl DMSO. Stock solution was frozen at

-20°C in 15µl aliquots for future use. Before use it was diluted to a working concentration in pre-warmed media and filter-sterilised using a 0.2mm syringe filter.

STAT3 Inhibitor VI, S31-201: A 10mM stock concentration of S31-201 was prepared by dissolving 10mg of S31-201 (Formula weight 365.4g/mol) in 2.74ml DMSO. Stock solution was frozen at -20°C in 15µl aliquots for future use. Before use it was diluted to a working concentration in pre-warmed media and filter-sterilised using a 0.2mm syringe filter.

2.2.3 Preparation of coverslips

Poly-L-lysine was firstly reconstituted with 3ml of sterile dH₂O and thoroughly mixed with a vortex. A further 22ml of sterile dH₂O was added to give a stock concentration of 1mg/ml. This solution was then filter-sterilised using a 0.2mm syringe filter and frozen at -20 °C in 1ml aliquots for future use. When required, this 1ml aliquot was diluted 1:25 by the addition of 24ml dH₂O to a final concentration of 40µg/ml. Poly-D-lysine was prepared by reconstituting 5mg with 50ml sterile dH₂O to make a stock concentration of 0.1mg/ml. This solution was then filter sterilized using a 0.2mm syringe filter and frozen at -20 °C in 5ml aliquots for future use. When required the aliquot was further diluted by addition of 5ml dH₂O to a working concentration of 50µg/ml. Glass coverslips were sterilised by baking at 200°C for at least 2h. Coverslips were then placed into sterile plates (24-well plates or 6-well plates) using a clean and sterile forceps and placed under the UV light for 30min for further sterilisation. A drop of 110µl (13mm diameter) or 1.5ml (25mm diameter) of poly-D-lysine (50µg/ml) or poly-L-lysine (40µg/ml) was added onto the centre of each coverslip and incubated at 37°C for at least 30min. The poly-D-lysine or poly-L-lysine was then aspirated and kept at 4°C to be re-used up to three times. The coverslips were then rinsed gently twice with sterile dH₂O and any residual dH₂O was discarded. The plates were left to fully dry for at least 2h at 37°C until use.

2.2.4 Preparation of Primary Cultures

Primary cultures for mixed glial cells, enriched astrocytes, enriched microglia and primary cortical neurons were prepared as described previously (McNamee *et al.*, 2010b) and see below.

2.2.4.1 Primary Mixed Glial Cells

Primary rat glial cells are prepared by dissection of the brain tissue and dissociation of the area of interest to obtain a glia enriched cell culture. The cells are allowed to grow and mature for between 10 – 14d and then used in experimental procedures. Glial cultures prepared in this manner generally contain astrocytes and microglia at 70% and 30% of total cell population respectively. Primary cultures are beneficial to use as they are untransformed cells, and are thus more representative of the natural brain environment.

The mixed glial enriched cultures were prepared from the brains of newborn Wistar rat pups (postnatal day 2-3), under sterile conditions, in the laminar flow hood. The pups were decapitated using a large sharp scissors. A smaller scissors was then used to cut the skin down the midline to reveal the skull which was then carefully cut on each side at ear level. A curved forceps was then used to gently pull away the skull to reveal the exposed brain. A straight fine toothed forceps was used to remove and discard the meninges. The cortical tissue on both hemispheres was then removed and placed into a drop of pre-warmed cDMEM. The cortical tissue from 3 pups was pooled and cross-chopped using a scalpel and any blood vessels were removed. The finely-chopped tissue was then transferred into a 50ml falcon tube with 6ml of pre-warmed cDMEM and incubated for 20min. After the incubation, the tissue was triturated until all visible clumps were removed, passed through a sterile mesh filter (40 μ m) and centrifuged at 2000 x RPM for 3min at 20°C. The supernatant was discarded and the pellet was re-suspended in 1ml pre-warmed cDMEM by gently triturating until a homogenous cellular suspension was obtained. At this stage the cell suspension was counted by the trypan blue exclusion method. 10 μ l of cell suspension was diluted with 90 μ l of trypan blue and viable cells were counted using a haemocytometer. The cell suspension was then diluted to approximately 5 x 10⁶ cells/ml and 5ml of this suspension was added into T75 flasks. The flasks were placed into an incubator (5% CO₂, 95% air at 37°C) for 2h to allow adherence to the bottom of the flask and then were flooded with 10ml cDMEM. Media was replaced after 3d and there-after every 4-6d.

For conditioned media studies, the T75 flasks were gently trypsinised by rinsing the cells with 1 X PBS, followed by addition of 5ml of trypsin-EDTA. The flasks were incubated at 37°C for approximately 10min, during which time the flasks were periodically checked under an inverted microscope to assess level of cell adherence to the plate. When approximately 95% of the cells were non-adherent, cDMEM was added to the flasks as the

FBS contains trypsin inhibitors. The resultant suspension was then centrifuged at 2000 x RPM for 3min at 20°C. The supernatant was discarded and the pellet was re-suspended in 1ml pre-warmed cDMEM by gently triturating until a homogenous cellular suspension was obtained. This cell suspension was diluted with a further 35ml cDMEM and re-plated into uncoated 6-well plates. Re-plated glial cells were treated at least 3d post trypsinisation and when cells were confluent.

For staining of primary glial cells, 75µl of the cell suspension (approximately 1×10^5 cells/ml) following trypsinization and centrifugation was plated onto poly-l-lysine pre-coated glass coverslips. After 2h to allow for cell adherence, 350µl of cDMEM was gently added.

2.2.4.2 Primary enriched astrocyte and microglia

Primary mixed glial cells were prepared as described before, with the exception that cultures for microglia were treated with GM-CSF (10ng/ml) and M-CSF (10ng/ml) to encourage microglial proliferation. When flasks reached confluency (approx d10-14), the flask caps were wrapped in parafilm and placed onto an orbital shaker for 2h at 110rpm to remove the loosely adherent microglial cells from the astrocytic monolayer. After which time, the flasks were brought back into the laminar flow, and tapped 10 times to encourage microglia to fully detach. The resultant suspension was centrifuged at 2000 X RPM for 5 min at 20°C. The supernatant was discarded and the pellet resuspended in 1ml cDMEM and counted by the trypan blue method. Cells were plated at a density of at least 1×10^6 cells/ml on poly-l-lysine pre-coated glass coverslips in 24-well plates and treated at least 2d post separation. Several coverslips were stained by fluorescent immunocytochemistry for CD11b, a marker for microglia, to assess for microglial purity. Cells prepared in this way yielded 95% pure microglia.

Mixed glial cultures for enriched astrocytes were not treated with GM-CSF or M-CSF. After 10-14d, microglia were removed as described above. The remaining astrocyte monolayer in the T75 flasks was then gently trypsinised and plated onto uncoated 6-well plates for treatments or poly-l-lysine pre-coated glass coverslips for fluorescent immunocytochemistry.

2.2.4.3 Primary Cortical Neurons

The cortex was dissected from 1d old Wistar rat pups as described previously. The tissue was finely cross-chopped in pre-warmed NBM and then transferred into 5ml of trypsin-EDTA, and incubated for 2min at 37°C. CDMEM (5ml) was then added and the tissue was triturated twice, followed by centrifugation at 2000 x RPM for 4min at 20°C. The resultant supernatant was discarded and the pellet re-suspended in 5ml cDMEM. This cell suspension was triturated until no visible clumps remained, passed through a sterile mesh filter (40µm) and centrifuged at 2000 x RPM for 3 min at 20 °C. The supernatant was discarded and the pellet was re-suspended in 1ml pre-warmed cNBM by gently triturating until a homogenous cellular suspension was obtained. The cell suspension was counted by the trypan blue exclusion method. For all Sholl analysis experiments, the cell suspension was diluted to 5×10^5 cells/ml and 75µl of this was gently pipetted onto the centre of a poly-d-coated coverslip in 24-well plates. The plate was placed into an incubator (5% CO₂, 95% air at 37°C) for 2h to allow adherence and then flooded with 300µl cNBM. For Western Immunoblotting experiments, the cell suspension was diluted to a concentration of 1×10^6 cells/ml, and 750µl of this was plated onto poly-d-coated coverslips in 6-well plates and allowed to adhere for 2h until the addition of 1.2ml cNBM. Neurons were treated after 3d *in vitro* (DIV).

2.2.5 Preparation of C6 glioma cells

C6 glioma cells (Banca Biologica e Cell Factory, Genova, Italy; passage 4; Figure 2.1) were first awakened by addition of 1ml pre-warmed Hams-F12 media to the vial, followed by a further 4ml and immediate transfer to a T-25 cm² flask and incubated at 37°C with 5% CO₂. All further experiments and re-animation of cells were performed in cDMEM. Upon reaching confluency (80-90%), the cells were trypsinised, and re-passaged into T-75cm² flasks or frozen down for future use. Briefly, the old media was discarded and the adherent cells were washed in pre-warmed sterile PBS. Trypsin (1:3 ratio in PBS) was added for 5min at 37°C. The trypsin was deactivated with cDMEM and the resultant cell suspension was centrifuged for 3min at 2000 x RPM at 20°C, to pellet the cells. The supernatant was removed, and the cells gently resuspended in cDMEM. Cells were counted using the haemocytometer. Aliquots of at least 1×10^6 cells/ml were frozen using the Nalgene Mr. Frosty box at -80°C for 24h and then transferred to a liquid nitrogen canister for future use. Cell suspensions were re-passaged into either T75cm² flasks (10ml of 1×10^5 cells/ml) for continued growth of the cell line, 6-well plates (2ml of

5×10^4 cells/ml) for cell treatments or glass coverslipped 24-well plates ($75 \mu\text{l}$ of 1×10^5 cells/ml followed by $300 \mu\text{l}$ after 2h). Cells were incubated for at least 24h prior to the addition of treatments.

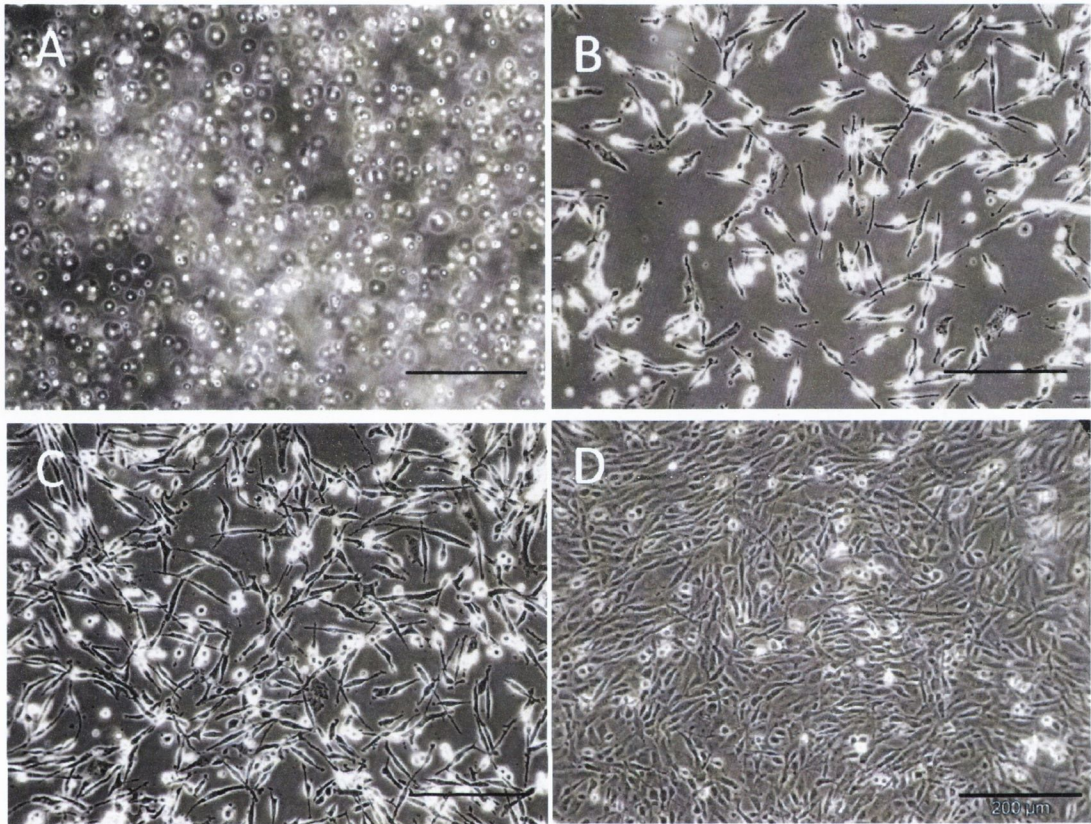


Figure 2.1 C6 Glioma Cells growth and morphology

C6 glioma cells immediately following re-animation (A), after 1 DIV (B), 2 DIV (C) and 3 DIV (D). Scale bar is equal to $200 \mu\text{m}$ in each case.

2.2.6 Cell culture treatments

For each experiment, 6-well tissue culture plates were prepared with mixed glial cultures as described in section 2.2.4. Each well was considered as $n=1$, and treated with 1.2 ml of drug. Pre-treatments were administered 30min prior to post-treatment. Cell cultures were incubated at $37 \text{ }^\circ\text{C}$ with $5\% \text{ CO}_2$ with the various drug treatments for either 6h to assess gene expression, or 24h for CM experiments, for protein production or cell viability. For CM experiments, after 24h, the CM was removed and filtered through a 0.2 mm syringe filter to remove cells and cellular debris. A full CM transfer was then performed on the neurons. B-27 supplement was added to every well after CM transfer. Neurons for cell viability and Sholl experiments were treated for 24h, neurons for Western Immunoblotting were treated for 5min. Control cultures were always treated with the addition of vehicle included in the drug treatments, e.g. DMSO. Cell numbers of glia (mixed glia, astrocytes

or microglia) for CM experiments were kept at approximately the same numbers across experiments (approx 1×10^6 cells/well). Where this was not possible (e.g. for enriched microglial cultures), CM volume was adjusted appropriately.

2.2.7 Harvesting glial cultures for mRNA analysis

The fumehood, equipment and gloves were wiped with RNase Away wipes prior to use to prevent RNA contamination. After 6h treatment, the supernatant from the 6-well plates was removed and the cells were lysed and then harvested using 350 μ l Lysis buffer (RA1 (Macherey-Nagel, Germany), 1% β -mercaptoethanol) per well. Samples were then frozen at -80°C to be extracted at a later time.

2.2.8 Preparation of neuronal cultures for Western Immunoblotting

Primary cortical neurons were prepared and treated as outlined previously. The treatments were removed by aspiration and cells rinsed gently in 1 x PBS at room temperature. 60 μ l of ice-cold lysis buffer (50mM Tris-HCl, pH8; 150mM NaCl; 1% ([Octyl]phenoxy)polyethoxyethanol (NP-40)) containing 1% protease and phosphatase inhibitors was added per well. Cells were scraped off using a clean pipette tip and collected in an ice-cold 1.5ml microtube. The samples were then centrifuged at 12,000 x RPM at 4°C for 10min. The supernatant was transferred to a clean ice-cold 1.5ml microtube and frozen at -80°C until later use. A 1:2 dilution of the supernatant was prepared and a protein assay was carried as outlined in section 2.2.12.1. Protein concentrations of samples were equalised to 1mg/ml using lysis buffer. Samples were then stored at -80°C until use for sodium dodecyl sulphate polyacrylamide gel electrophoresis (SDS-PAGE) and western immunoblotting as described in section 2.2.12.

2.2.9 RNA Analysis

2.2.9.1 RNA extraction

RNA was extracted from the cells using a NucleoSpin RNA II kit (Macherey-Nagel, Germany) according to the kit protocol. Standard precautions were taken to keep reagents, consumables and equipment free from RNAses. The lysate, as collected during cell harvesting (section 2.2.8), was filtered through the violet NucleoSpin Filter columns and centrifuged for 1min at 11,000 x g. 70% ethanol was then added to the lysate and mixed by gentle pipetting. This was then loaded into a NucleoSpin RNA II Column and centrifuged for 30sec at 11,000 x g. This membrane was then desalted using membrane desalting buffer and again centrifuged at 11,000 x g for 30sec. 95 μ l of Dnase reaction mixture was then added to the membrane and incubated for 15min to degrade any

contaminating DNA. The membrane was washed with buffer RA2 to inactivate the Dnase and centrifuged at 11,000 x g for 30sec. The column was placed in a new tube and the membrane was dried by the addition of 600µl RA3 and centrifuged at 11000 x g for 30sec, then 250µl RA3 was added and centrifuged at 11000 x g for 2min. The column was placed into a clean collection tube and the RNA was eluted using RNase-free water and centrifuged at 11,000 x g for 1min. The eluted RNA was reapplied to the column for a second elution step at 11,000 x g for 1min. The eluted RNA was then quantified using a nanospectrophotometer. The RNA was stored at -80 °C until RNA equalisation.

2.2.9.2 Measuring RNA concentration and Equalising RNA

The RNA concentration of each sample was measured using a NanoDrop® ND1000 spectrophotometer. Purity was demonstrated by the $A_{260/280}$ ratio. RNA samples (20 µl) were equalised to the lowest concentration of RNA detected by addition of RNase-free H₂O.

2.2.9.3 cDNA Preparation

Complementary DNA (cDNA), was reverse transcribed from the equalised RNA using ABI High Capacity cDNA archive kit according to the manufacturers protocol. Briefly an equal volume of RNA was mixed with cDNA Mastermix (containing RT Buffer (Reverse Transcriptase), dNTPs, random primers, multiscribe RT and RNase-free H₂O). The samples were mixed, briefly centrifuged and placed into a Thermal Cycler (PTC-200 Peltier Thermal Cycler DNA Engine) on the ABI-RT programme. The samples were kept at 25°C for 10min and then for 120min at 37 °C. Upon completion of the programme, the samples were removed, diluted 1:4 with RNase-free H₂O and frozen at -20°C until needed for further polymerase chain reaction (PCR) analysis.

2.2.9.4 Multi-target (Multiplex) quantitative Real Time-PCR (RT-PCR)

Quantitative PCR was performed on Applied Biosystems ABI Prism 7300 Sequence Detection System v1.3.1 in 96-well format and 25µl reaction volume per well as described previously (Boyle & Connor, 2007). Each sample included the target probe (see table 2.2) and the endogenous marker β-actin (VIC-labelled MGB Taqman probe, Applied Biosystems), to allow for normalisation of gene expression between samples. RT-PCR was performed using Taqman Gene Expression Assays (Applied Biosystems) which contain forward and reverse primers, and a FAM-labelled MGB Taqman probe to each gene of interest.

A 10 μ l volume of diluted cDNA was added to each well and 15 μ l of reaction mix (12.5 μ l Taqman Universal PCR Mastermix, 1.25 μ l β -actin primer, 1.25 μ l target primer) was added to give a final reaction volume of 25 μ l. Electronic pipettes (EDP3 2-20 μ l, 10-100 μ l and 20-200 μ l) were used to ensure pipetting accuracy. Samples were run on the ABI Prism 7300 Sequence Detection System (Applied Biosystems, Germany) for either 40 or 45 cycles. The samples were first heated to 95°C for 10min to start the process before the cycles began. The samples were heated to 95°C for 15 sec to allow denaturation of the double-stranded cDNA. The temperature was then decreased to 60°C to allow annealing and extension of the cDNA. The data were analysed using Applied Biosystems relative quantification software.

2.2.9.5 Realtime-PCR analysis

The $\Delta\Delta C_t$ method (Applied Biosystems RQ software, Applied Biosystems, UK) was used to assess gene expression, as calculated relative to the endogenous control β -actin, and the control samples to give a Relative Quantification value (RQ) ($2^{-\Delta\Delta C_t}$, where C_t is the threshold cycle). This method compares gene expression of treated samples to an untreated control sample instead of quantifying the exact copy number of the gene. This means that the fold-difference (increase or decrease) can be assessed between treated and untreated samples. The fold-difference is assessed using the cycle number (C_t) difference between samples. A threshold for fluorescence is set, against which C_t is measured. To accurately assess differences between gene expression, the threshold is set when the PCR reaction is in the exponential phase, when the PCR reaction is optimal or 100% efficient. Samples with low C_t readings demonstrate high fluorescence, indicating greater amplification and thus greater gene expression. To measure this fold-difference relative to control, the C_t of the endogenous control (β -actin) is subtracted from the C_t of the target gene for each sample, thus accounting for any difference in cDNA quantity that may exist. This normalised C_t value is called the C_t difference (ΔC_t). The ΔC_t of the control is subtracted from itself to give 0, and subtracted from all other samples, this is the $\Delta\Delta C_t$ value (cycle difference corrected for β -actin). The $\Delta\Delta C_t$ is then converted into a fold-difference. As a one-cycle difference corresponds to a two-fold increase or decrease relative to control, the fold-difference in gene expression between the control and treated samples is given by 2 to the power of the $-\Delta\Delta C_t$. Thus when PCR is 100% efficient a five-cycle difference between samples means a 5-fold difference is a 32-fold difference (2^5). The control sample always has a $\Delta\Delta C_t$ value of 0, thus 2^{-0} gives a $2^{-\Delta\Delta C_t}$ of 1, against which all other samples are referenced.

Target	Primer Code
B-actin (VIC)	4352340E
BDNF	Rn00560868_m1
CNTF	Rn00755092_m1
FGF-2	Rn00570809_m1
GDNF	RN00755092_m1
IGF-1	Rn00710306_m1
IL-10	Rn00563409_m1
IL-6	Rn00561420_m1
NGF- β	Rn01533872_m1
NT3	Rn00579280_m1
NT4/5	RN00566076_s1
TGF-beta 1	Rn00572010_m1
VEGF	Rn01511601_m1

Table 2.2 List of primers for PCR

2.2.10 Fluorescent Immunocytochemistry and Sholl Analysis

2.2.10.1 General fluorescent immunocytochemistry

Fluorescent immunocytochemistry was performed on both mixed glial cells and neurons grown on glass coverslips. Primary antibodies used were as follows; GFAP (1:2000), Cd11B (1:1000), β III-tubulin (1:850), S100 β (1:1000). All primary antibodies were diluted in 2.5% normal goat serum in PBS. Secondary antibodies used were; goat anti-rabbit Alexa Fluor 488, goat anti-mouse Alexa Fluor 633. All secondary antibodies were diluted in 2.5% normal goat serum in PBS.

Cells grown on glass coverslips were washed under sterile conditions twice with PBS. The cells were then fixed with ice-cold methanol for 15min at -20°C , and again washed twice with PBS. After the fixation step, all subsequent steps were performed on the normal

laboratory bench. Non-reactive sites were blocked for 2h at room temperature (RT) in blocking buffer (10% normal goat serum in PBS). The blocking buffer was removed and the primary antibody was immediately added. The cells were incubated in primary antibody overnight at 4°C. Cells were again washed three times in PBS. Cells were then incubated with an appropriate secondary antibody in a light protected environment for 2h at RT. The cells were again washed three times in PBS. The glass coverslips were then removed and mounted onto glass slides onto Vectashield fluorescent mounting media with DAPI. Each coverslip was sealed with nail varnish and stored in the dark at 4°C until viewed. All pictures were taken on epifluorescent microscope with AxioVision Rel 8 Software (Carl Zeiss MicroImaging).

2.2.10.2 Sholl Analysis

The Sholl analysis procedure was adapted from Gutierrez and Davies (2007). For the analysis, β III tubulin stained neuronal coverslips were viewed at 200 X on the epifluorescent microscope. For a coverslip to be utilised in Sholl analysis, the neurons must display a healthy network phenotype, following this, individual neurons, which were not in contact with any other neurons, were imaged at random. Five individual neurons from each coverslip were imaged, analysed and averaged for Sholl analysis. Where possible, groups were blinded. Neuronal images were imported into Microsoft PowerPoint where a calibrated image of concentric circles at 10 μ m distances (up to 165 μ m) was superimposed onto the cell body of the nucleus of the neuron (Figure 2.2). Primary neurites, neuritic branches and neurite termination points were all counted within each circle. Primary neurites were classified as those directly stemming from the cell body within circle number 1, while a branch was counted if a neurite clearly divides in two for at least 5 μ m (or half a circle width). The longest neurite was utilised as the neuritic length. If a neurite extended outside of the superimposed circles, the extended length was measured, however no further branches were recorded. Sholl analysis results were displayed for the number of primary neurites, the number of neuritic branches and the neuritic length. Furthermore, the Sholl profile was also displayed. For this, the total number of neurites for any segment was plotted against the distance from the cell soma.

The total number of neurites for any segment was calculated as follows:

$$X_i = X_{i-1} + B_i - T_i$$

Where X_i = the number of neurites for the “ith” segment

B_i = the number of branching events occurring in the “ith” segment

T_i = the number of branching terminations occurring in the “ith” segment

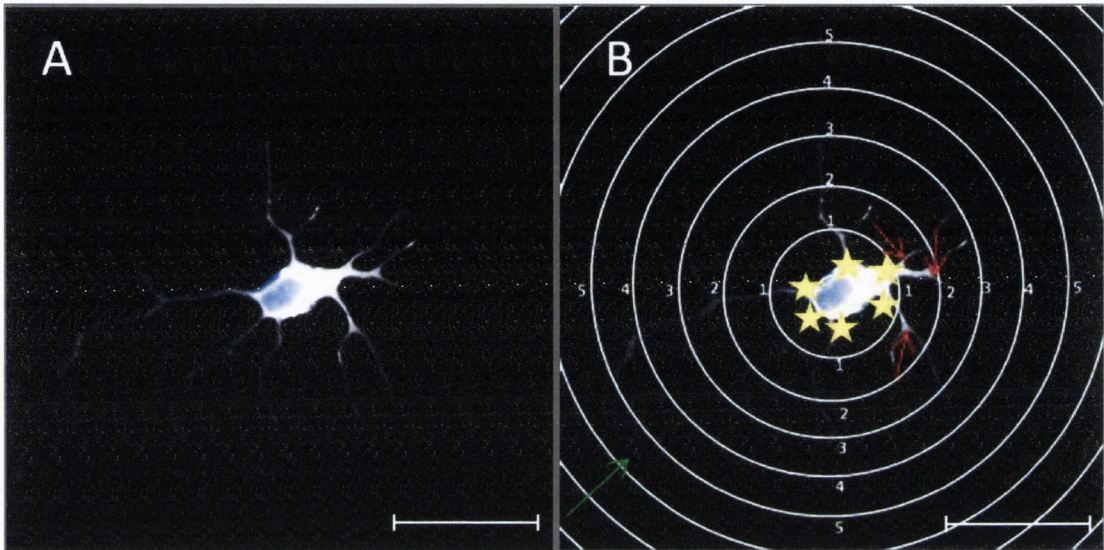


Figure 2.2: Neuron stained with β III tubulin and Hoescht (A) with overlaying Sholl analysis concentric circles (B)

Figure shows a neuron which has been stained with β III tubulin (white) with the cell body stained with Hoescht (blue). In this example, the neuron is considered to have six primary neurites (indicated with yellow stars), with three bifurcations between circles 1 and 2 (red arrows) and two more bifurcations between 2 and 3. The longest neurite terminates between circles 5 and 6 (green arrow). Scale bar = 30 μ m

As this was the first time Sholl analysis was performed in this laboratory it was important to examine the Sholl profile of the primary cortical neurons. As such the number of neuritic branches for untreated neurons was plotted against the distance from the cell soma to generate the Sholl profile. The resulting graph (Figure 2.3) shows a stereotypical Sholl profile as described in the literature (Gutierrez & Davies, 2007). Thus the Sholl analysis was utilised in subsequent studies.

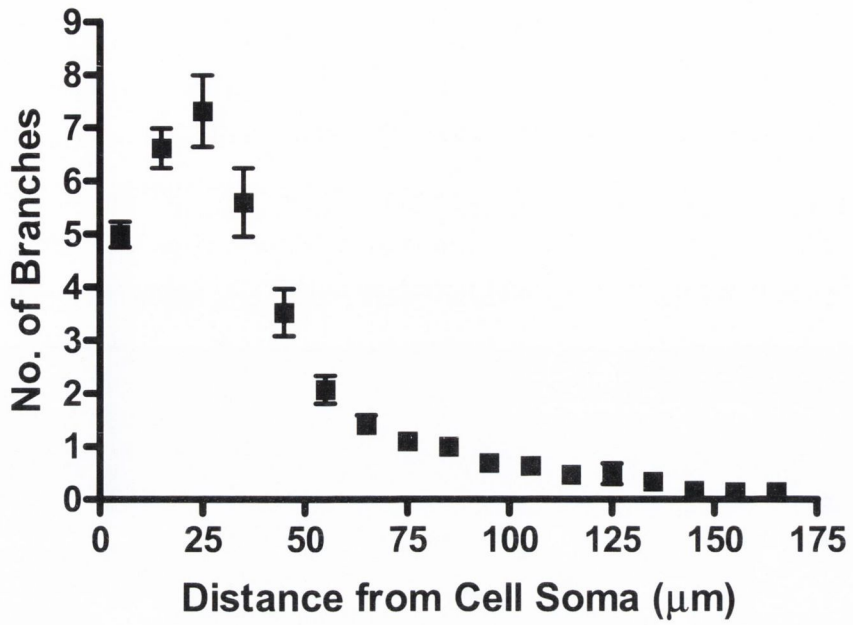


Figure 2.3: Sholl profile of untreated rat primary cortical neurons

A scatter plot of the number of branches plotted against the distance from the cell soma for control neurons demonstrate a stereotypical “Sholl profile”.

2.2.11 Cell Viability assay: Alamar Blue

The alamar blue assay is a metabolic assay for assessing the ability of living cells to convert a redox dye (resazurin, $C_{12}H_6NNaO_4$) into a fluorescent end product (resorufin). Viable cells can reduce resazurin into resorufin via mitochondrial metabolism. A 440 μ M solution of Alamar Blue dye was made by dissolving Resazurin in ddH₂O. Neurons were treated as required. Following treatment, medium was removed from the cultures and Alamar Blue dye in fresh NBM (As; 1:10 ratio, e.g. 30 μ l into 270 μ l) and incubated at 37°C and 5% CO₂ was added for 3h. The dye was also added to empty wells (Am) and untreated control cultures (Ac). When colour change had occurred, 200 μ l of supernatant was transferred to 96 well plates. Absorbance was read at 600nm using a microtitre plate reader (Elx 800 Bio-Tek instruments Inc.). Results were calculated as follows:

Am = Average absorbance of wells containing Media only

Ac = Average absorbance of wells containing Cells without treatments

As = Absorbance of a particular sample

% Viability = $((Am - As)/(Am - Ac)) * 100$

2.2.12 Sodium Dodecyl Sulphate Polyacrylamide Gel Electrophoresis (SDS-PAGE) and Western Immunoblotting

SDS-PAGE and Western Immunoblotting was performed as described previously (McNamee *et al.*, 2010a; McNamee *et al.*, 2010b).

2.2.12.1 Bradford Protein Assay

Protein concentration was determined by the Bradford assay method (Bradford, 1976). Standard protein concentrations (0-1000 μ g/ml) of Bovine Serum Albumin (BSA) were made. 5 μ l of standard and sample was pipetted into a 96-well plate in duplicate. 195 μ l of dye reagent was added on top of the standard and sample and the plate was incubated for 5 minutes at room temperature. After 5min, the plate was read using a standard plate reader (Bio-Tek microplate reader, BioTek Instruments, USA) and protein concentration was calculated.

2.2.12.2 Gel Preparation and SDS-Page

Samples to be analysed by western immunoblotting were added in a 4:1 v/v ratio to 4 x Laemmli sample buffer (1M Tris-HCL, pH 6.8; 25% (w/v) sodium dodecyl sulphate; 50% (v/v) glycerol; 10% (v/v) β -mercaptoethanol; 2% (w/v) bromophenol blue) and were boiled at 60°C for 5min prior to loading on gels for SDS-PAGE. Electrophoresis was performed using SDS-polyacrylamide gels (10% separating gel: 4% stacking gel). Briefly, gels were prepared, mixed by pipetting and quickly pipetted between two glass plates held firmly together with a casting frame. A layer of 2-propanol was poured on top of the gel to prevent evaporation. This separating gel was allowed to set for approximately 30min after which time the 2-propanol was removed and the top of the gel was rinsed with dH₂O. The stacking gel was then prepared and poured on top of the separating gel and a 10-well comb was placed into the gel to allow wells for loading to form. The stacking gel was left to set for 30min. The glass plates with gel were then removed from the casting frame and placed into an electrode assembly and clamped into place. This was then put into the gel rig. The inner and the bottom of the outer gel rig were filled with 1 x electrode running buffer (125mM Tris-Base, pH 8.3; 960mM glycine; 0.5% SDS) and the combs were removed. 30 μ l of sample was loaded per well. 5 μ l of Broadrange Molecular Marker was loaded onto gels alongside samples. Proteins were separated by applying a constant current of 33milliamps per gel for 60min or until the blue dye from the sample buffer had run to the bottom of the gel.

2.2.12.3 Semi-dry transfer

Following electrophoresis, separated proteins were transferred onto polyvinylidene fluoride (PVDF) membranes using a semi-dry blotter at a constant current of 225mA for 70min. Briefly, gels were removed from the glass plates and placed within a sandwich of filter paper and PVDF membrane. The PVDF was first activated by soaking the membrane in methanol for 30sec followed by soaking in dH₂O for 2min. To make the sandwich, two pieces of filter paper soaked in anode buffer I (0.3M Tris-Base, 10% methanol) were placed onto the anode (+) plate of the semi-dry blotter, one piece of filter paper soaked in anode buffer II (25mM Tris-Base, 10% methanol) was placed on top of this. The activated PVDF membrane was placed on next, followed by the gel. Lastly, three pieces of filter paper soaked in cathode buffer ((25mM Tris-Base, 40mM glycine, 10% methanol) was placed on top. Any bubbles which may have been present were removed by gently rolling a pasteur pipette over the top of the sandwich. The cathode (-) plate was then placed on top of the sandwich and the current was applied at 225mA for 70min. In this set-up the

proteins will migrate from the gel towards the anode plate and hence into the PVDF membrane.

2.2.12.4 Western Immunoblotting

Following transfer, membranes were immediately blocked in 5% milk in TBS-Tween20 (TBS-T) for 1h. The membrane was then washed 3 x 5min in 15ml TBS-T. The membrane was incubated with the primary antibody at the appropriate dilution (see Table 2.3) in 10ml of 5% BSA in TBS-T overnight at 4°C on a rocker-roller. The membrane was washed 3 x 10min in 15ml TBS-T and then the secondary antibody was applied to the membrane at the appropriate dilution (see Table 2.3) and incubated for 1h at RT. The membrane was washed 3 x 10min in 15ml TBS-T. The membrane was then exposed to ECL chemiluminescent solution and developed on Fujifilm Luminescent Image Analyzer LAS-3000. Blots were stripped in 10ml re-store Western blot Stripping Solution for 15min and then washed 3 x 10 min in 15ml TBS-T. After this, blots were ready to be re-blocked and re-probed with another antibody. Protein bands were quantified using ImageJ software, NIH.

Target	M. Wt (kDa)	Primary Antibody Conc	Secondary Antibody Conc
Akt	60	1:1000	1:2000
p-Akt	60	1:1000	1:2000
STAT3	79, 86	1:1000	1:2000
p-STAT3	79, 86	1:1000	1:2000
Erk	42, 44	1:1000	1:2000
P-Erk	42, 44	1:1000	1:2000
B2-adrenoceptor	55	1:1000	1:2000
B-actin	43	1:1000	1:2000

Table 2.3 Antibody dilutions for western immunoblotting

2.2.13 Enzyme-linked Immunosorbent assays (ELISA)

Protein concentrations were measured in the glial CM by ELISA. Each kit was chosen based on previous reports demonstrating successful protein quantification from primary rat astrocytes or rat brain homogenate (Park *et al.*, 2000; Hisaoka *et al.*, 2007; Griffin *et al.*, 2009; Guo *et al.*, 2009; Lee *et al.*, 2009a). Each ELISA was followed as per the manufacturers guidelines supplied in the kit (see table 2.4). Briefly, 50µl of the diluted capture antibody was added to each well of a 96-well plate and incubated for the appropriate amount of time. Following this, plates were washed with wash buffer and then blocked with block buffer to block any non-specific binding sites. The block was removed and the samples and diluted standards were then added to the plates (50µl) and incubated for the appropriate amount of time. Plates were washed again with wash buffer and the detection antibody (50µl) was added for the appropriate amount of time. The plates were again washed. Following this, the HRP-conjugated antibody (50µl) was added, incubated and then another wash was performed. TMB solution was then added (50µl) and colour development occurred. The reaction was stopped with stop solution (50µl) and absorbance was read at 450nm. Protein concentrations were calculated from the standard curve.

ELISA	FGF-2	NGF- β	GDNF
Capture Antibody	Diluted in coating buffer (supplied in kit), overnight at 4°C	NGF- β polyclonal antibody, diluted in coating buffer (0.025M NaHCO ₃ , 0.025M Na ₂ CO ₃ , pH 9.7), overnight at 4°C	GDNF monoclonal antibody, diluted in coating buffer (0.025M NaHCO ₃ , 0.025M Na ₂ CO ₃ , pH 9.7), overnight at 4°C
Block	Supplied in kit, 1h at RT	Supplied in kit, 1h at RT	Supplied in kit, 1h at RT
Standards and Samples	0-500pg/ml of standards, 2h at RT	0-250pg/ml of standards, 6h at RT	0-2000pg/ml of standards, 6h at RT
Detection Antibody	Diluted in blocking buffer, 1h RT	Anti-NGF- β monoclonal antibody, diluted in block buffer, overnight at 4°C	Anti-human GDNF polyclonal antibody, diluted in block buffer, overnight at 4°C
HRP-conjugated antibody	Avidin-HRP, diluted in blocking buffer, 30min RT	Anti-rat IgG-HRP, diluted in block buffer, 2.5h at RT	Anti-chicken IgY-HRP, diluted in block buffer, 2.5h at RT
Stop Solution	2N H ₂ SO ₄	1N HCl	1N HCl
Wash Buffer	PBS + 0.05% Tween-20	TBS + 0.05% Tween-20	TBS + 0.05% Tween-20

ELISA	IL-6	BDNF	VEGF
Capture Antibody	Diluted in coating buffer (0.1M NaHCO ₃ , pH 9.5)	Mouse anti-human BDNF diluted in PBS, overnight at RT	Mouse anti-rat VEGF diluted in PBS, overnight at RT
Block	PBS + 10% FBS, 1h at RT	PBS + 1% BSA, 1h at RT	PBS + 1% BSA, 1h at RT
Standards and Samples	0-5000pg/ml of standards, 2h at RT	0-1500pg/ml of standards, 2h at RT	0-1000pg/ml of standards, 2h at RT
Detection Antibody	IL-6 monoclonal antibody diluted in block buffer, 1h at RT	Anti-human BDNF diluted in block buffer, 2h at RT	Anti-rat VEGF diluted in block buffer, 2h at RT
HRP-conjugated antibody	streptavidin-HRP, 30min at RT	streptavidin-HRP, 20min at RT	streptavidin-HRP, 20min at RT
Stop Solution	2N H ₂ SO ₄	2N H ₂ SO ₄	2N H ₂ SO ₄
Wash Buffer	PBS + 0.05% Tween-20	PBS + 0.05% Tween-20	PBS + 0.05% Tween-20

Table 2.4 ELISA antibodies and procedures

2.2.14 Statistical Analysis

All data was analysed in GB-stat [Dynamic Microsystems Inc.] and all graphs created in Prism 4 (GraphPad Prism, California, USA). Analysis of variance (ANOVA), or student *t* tests were performed where appropriate. All Sholl profile graphs were analysed using a repeated measures ANOVA (two, or three-way where appropriate). If significant changes were observed, the data was further analysed using Newman-Keuls or Fisher's LSD *post-hoc* test as appropriate. A p value of less than 0.05 was deemed significant and all data are expressed as means + or ± standard error of the mean

Chapter 3

Results

3.1 Examination of the impact of neurotransmitters on neuronal complexity

Monoaminergic neurotransmitters, which include noradrenaline and serotonin, are classical transmitters which are released from nerve terminals to modulate post-synaptic signal transduction in neurons (Rang & Dale, 2003). However, both serotonin and noradrenaline have previously been shown to have extra-synaptic actions on glial cells and can promote the production of neurotrophic factors (for review, see Kimelberg, 1995). Much work has been performed to assess the roles of the monoamines in providing neuronal protection, however, there is little research examining monoamine-induced changes in neuronal outgrowth which could prove important for encouraging neuronal regeneration following brain injury, disease or neurodegeneration.

Therefore, the aims of these studies were as follows:

- 1) To determine if noradrenaline or serotonin promotes neurite outgrowth in primary rat cortical neurons either directly or via an indirect action on glial cells.
- 2) To determine if the antidepressant and NA/5-HT reuptake inhibitor, amitriptyline, promotes neuronal outgrowth in primary cortical neurons either directly or via an indirect action on glial cells.

3.1.1 Effect of noradrenaline on neuronal complexity: A role for glial cells

Noradrenaline is known to have extra-synaptic actions on glial cells, stimulating the release of supporting factors for neurons (for example (Madrigal *et al.*, 2009)). The purpose of these studies therefore was to determine if noradrenaline, via an action on glial cells, would provide a more trophic environment for primary cortical neurons. For that reason confluent primary mixed glial cells from P2-3 rat cortex were treated with control (complete neurobasal media (NBM)) or noradrenaline (NA; 10 μ M for viability assay, 1, 5, 10 μ M for Sholl analysis) in NBM. The cells were treated for 24h after which time the conditioned media (CM) was collected, filtered and then used to treat for 24h, primary cortical neurons which had been cultured for 4DIV. The neurons were then assessed for neuronal viability by the Alamar blue assay and for neuronal morphological changes by Sholl analysis.

3.1.1.1 NA CM increases neuronal viability

A Student's *t*-test demonstrated that CM from NA-treated cultures (NA CM) significantly increased neuronal viability when compared with control CM ($p=0.0097$, $t=2.893$, $d.f.=18$), while NA had no direct effect on neuronal viability ($p=0.0775$, $t=1.968$, $d.f.=10$). [Figure 3.1].

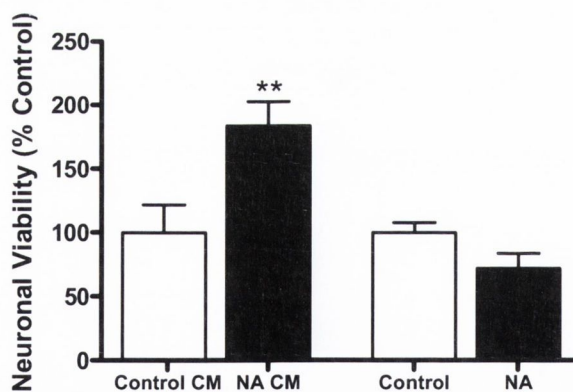


Figure 3.1: NA CM, but not a directly applied NA, increases neuronal viability

Primary cortical neurons were treated for 24h with either NA CM from glial cells or directly with NA (10 μ M for both). The Alamar blue assay was then performed. NA CM significantly increased neuronal viability as compared to control CM. Direct NA had no effect on neuronal viability. Data expressed as mean + SEM, $n=6-10$. ** $p<0.01$ vs. control CM (Student's *t*-test).

3.1.1.2 NA CM increases all measures of neuronal complexity of primary cortical neurons

Primary Neurites

A one-way ANOVA demonstrated a significant effect of NA CM on the number of primary neurites [$F_{(3,24)}=5.086$, $p=0.0072$]. *Post-hoc* analysis revealed that all doses of NA CM increased the number of primary neurites extending from the cell soma as compared to control CM treated neurons ($p<0.05$ for $1\mu\text{M}$ and $5\mu\text{M}$, $p<0.01$ for $10\mu\text{M}$). [Figure 3.2a, Newman-Keuls, $n=7$].

Neuritic Branches

A one-way ANOVA demonstrated a significant effect of NA CM on the number of neuritic branches [$F_{(3,24)}=6.113$, $p=0.0031$]. *Post-hoc* analysis revealed that all doses of NA CM increased the number of neuritic branches compared to control CM treated neurons ($p<0.05$ for $5\mu\text{M}$, $p<0.01$ for $1\mu\text{M}$, $10\mu\text{M}$). [Figure 3.2b, Newman-Keuls, $n=7$].

Neuritic Length

A one-way ANOVA demonstrated a significant effect of NA CM on the neuritic length [$F_{(3,24)}=12.82$, $p<0.0001$]. *Post-hoc* analysis revealed that all doses of NA CM significantly increased the neuritic length compared to control CM treated neurons ($p<0.01$). [Figure 3.2c, Newman-Keuls, $n=7$].

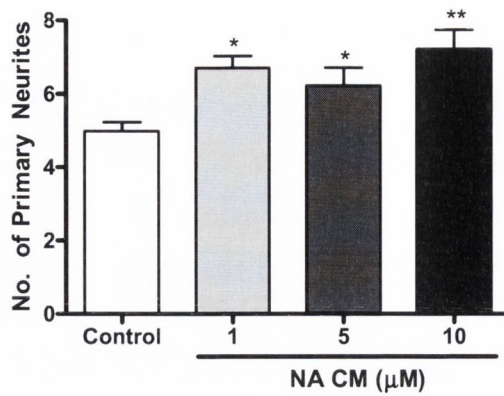
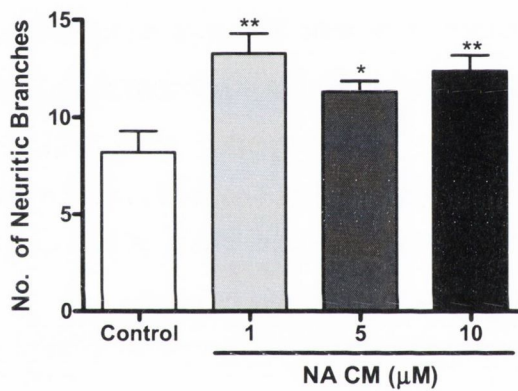
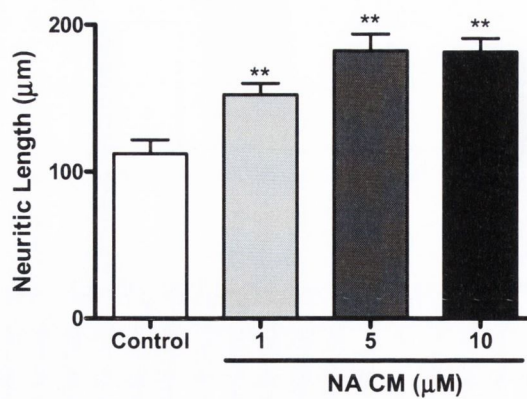
(a) Primary Neurites*(b) Neuritic Branches**(c) Neuritic Length*

Figure 3.2: NA CM increases all measures of neuronal complexity of primary cortical neurons

Primary cortical neurons were treated for 24h with NA CM from glial cells. Sholl analysis was then performed on the neurons. All doses of NA CM significantly increased (a) number of primary neurites (b) number of neuritic branches and (c) neuritic length. Data expressed as mean + SEM, $n=7$. * $p<0.05$, ** $p<0.01$ vs. control CM (One-way ANOVA followed by *post-hoc* Newman-Keuls).

3.1.1.3 Representative neurons for primary cortical neurons treated with NA CM

Primary cortical neurons were treated for 24h with NA CM from glial cells. Cells were then stained using fluorescent immunocytochemistry for the neuronal structural protein β III-tubulin and counter-stained with the cell body marker DAPI. Figure 3.3 shows representative images for neurons treated with control CM (A) and NA CM (B-D).

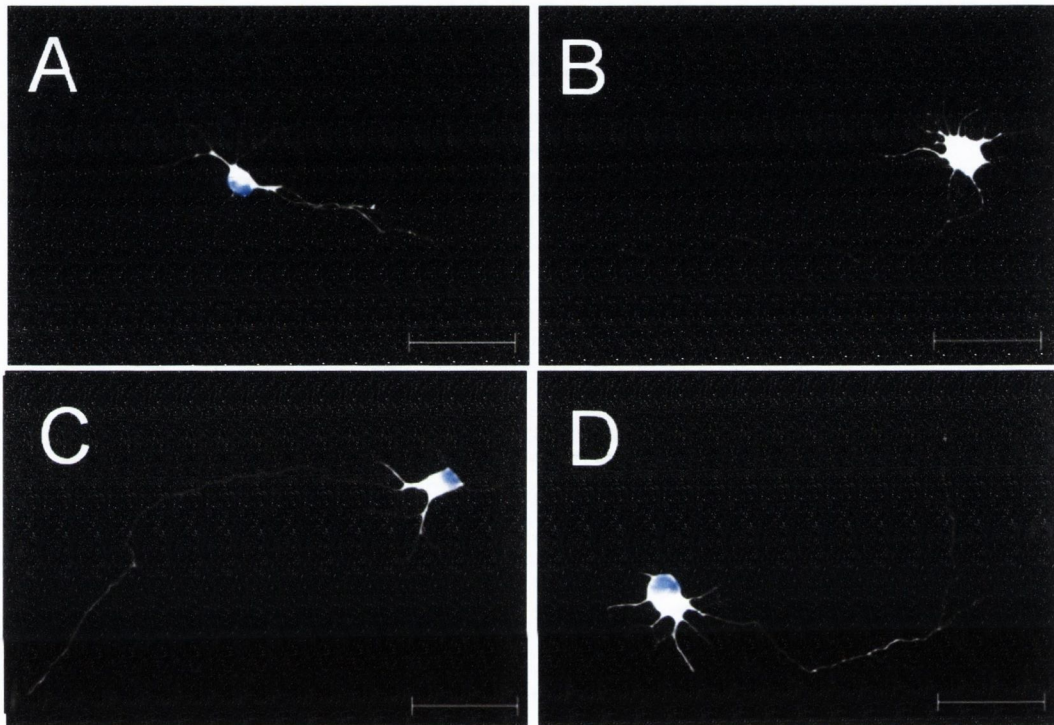


Figure 3.3: Representative neurons for primary cortical neurons treated with NA CM

Primary cortical neurons treated with NA CM from glial cells were stained using fluorescent immunocytochemistry for the neuronal structural protein β III-tubulin (white) and the cell body marker DAPI (blue). All neurons were imaged by 200X magnification. Pictures correspond to representative images for (A) control neuron treated with control CM and neurons treated with NA CM at $1\mu\text{M}$ (B), $5\mu\text{M}$ (C) and $10\mu\text{M}$ (D). Scale bars in each diagram are equal to $50\mu\text{m}$.

3.1.1.4 NA CM increases the Sholl profile of primary cortical neurons

A two-way repeated measures ANOVA demonstrated a significant effect of NA CM on the number of neuritic branches at specific distances from the neuronal cell soma [$F_{(3,384)}=14.306$, $p<0.0001$]. ANOVA also demonstrated a significant effect of distance [$F_{(16,384)}=362.21$, $p<0.0001$] and a significant distance by treatment interaction [$F_{(48,384)}=1.84$, $p=0.0009$]. Furthermore *post-hoc* analysis revealed that neurons treated with all doses of NA CM had significantly more branches than neurons treated with control CM at 5, 15 and 25 μm ($p<0.01$) from the cell soma while neurons treated with 1 μM NA also had significantly more branches at 35 μm ($p<0.05$). [Figure 3.4, Newman-Keuls, $n=7$].

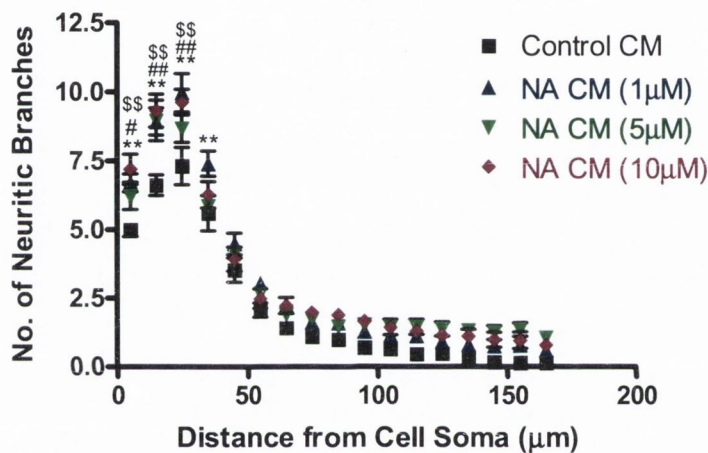


Figure 3.4: NA CM increases the Sholl profile of primary cortical neurons

Primary cortical neurons were treated for 24h with NA CM from glial cells. Sholl analysis was then performed on the neurons. NA CM (5 μM , 10 μM) significantly increased the number of branches at 5, 15 and 25 μm from the cell soma while NA CM (1 μM) significantly increased the number of branches at 5, 15, 25 and 35 μm from the cell soma compared to control CM. Data expressed as means \pm SEM, $n=7$. ** $p<0.01$ NA CM 1 μM vs. control CM, # $p<0.05$, ## $p<0.01$ NA CM 5 μM vs. control CM, ++ $p<0.01$ NA CM 10 μM vs. control CM (Two-way repeated measures ANOVA followed by *post-hoc* Newman-Keuls).

3.1.2 NA has no effect on neuronal complexity of primary cortical neurons

As primary cortical neurons are known to express the noradrenergic receptors (for review, see Gu, 2002), it was important to establish if a direct treatment of primary cortical neurons with NA can also lead to increases in morphological complexity. Therefore primary neurons were treated for 24h with control NBM or with NA (1 μ M, 5 μ M or 10 μ M) in NBM. As before, the neurons were stained using fluorescent immunocytochemistry for β III-tubulin and after image acquisition, were analysed by Sholl analysis specifically to determine the number of primary neurites extending from the cell soma, the number of neuritic branches and the length of the longest neurite.

3.1.2.1 Direct treatment of primary cortical neurons with NA does not alter neuronal complexity

Primary Neurites

A one-way ANOVA showed no significant effect of NA on the number of primary neurites [$F_{(3,24)}=1.386$, $p=0.2712$]. [Figure 3.5a, $n=7$].

Neuritic Branches

A one-way ANOVA showed no significant effect of NA on the number of neuritic branches [$F_{(3,24)}=1.675$, $p=0.1988$]. [Figure 3.5b, $n=7$].

Neuritic Length

A one-way ANOVA showed no significant effect of NA on the neuritic length [$F_{(3,24)}=2.075$, $p=0.1302$]. [Figure 3.5c, $n=7$].

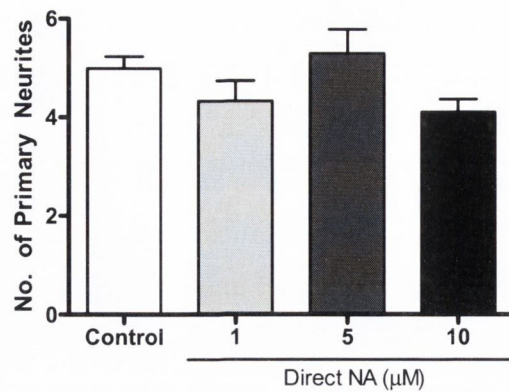
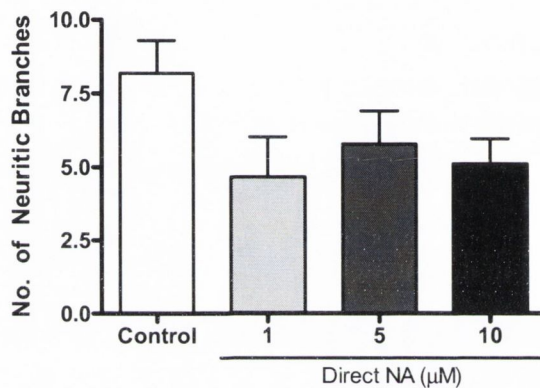
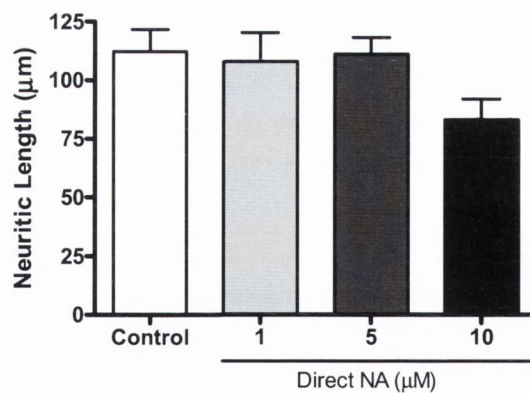
(a) Primary Neurites*(b) Neuritic Branches**(c) Neuritic Length*

Figure 3.5: Direct treatment of primary cortical neurons with NA does not alter neuronal complexity
 Primary cortical neurons were treated for 24h with NA. Sholl analysis was then performed on the neurons. NA treatment had no effect on (a) number of primary neurites, (b) number of neuritic branches or (c) the neuritic length of the neurons. Data expressed as mean \pm SEM, $n=7$. (One-way ANOVA).

3.1.2.2 NA reduces the Sholl profile of primary cortical neurons

A repeated measures ANOVA demonstrated a significant effect of NA on the number of neuritic branches at specific distances from cell soma [$F_{(3,384)}=3.34$, $p=0.036$]. ANOVA also demonstrated a significant effect of distance [$F_{(16,384)}=217.9$, $p<0.0001$] and a significant distance by treatment interaction [$F_{(48,384)}=1.75$, $p=0.0023$]. Furthermore, *post-hoc* analysis revealed that NA (1 μ M) treated neurons had significantly less branches than control treated neurons at 15 ($p<0.05$), 25 and 35 μ m ($p<0.01$) from the cell soma while NA (10 μ M) treated neurons had significantly less branches than control treated neurons at 15, 25, 35 ($p<0.01$) and 45 μ m ($p<0.05$) from the cell soma. [Figure 3.6, Newman-Keuls, $n=7$].

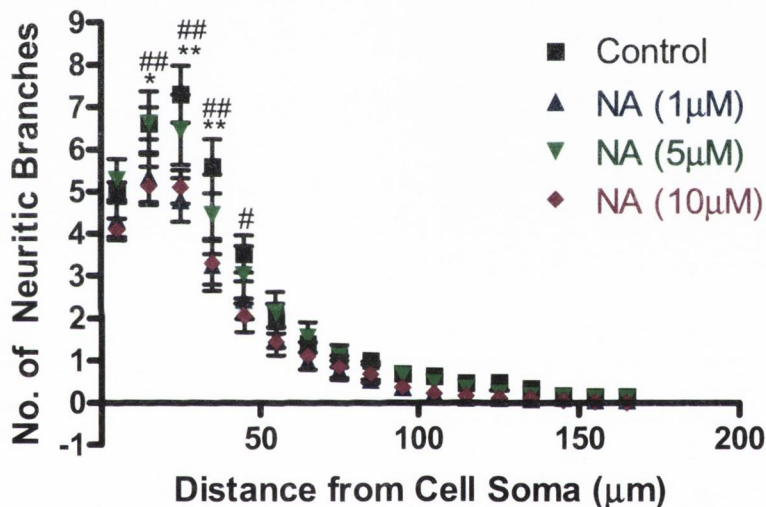


Figure 3.6: Direct treatment of primary cortical neurons with NA alters neuronal complexity

Primary cortical neurons were treated for 24h with noradrenaline. Sholl analysis was then performed on the neurons. NA (1 μ M) had significantly less branches than control at 15, 25 and 35 μ m from the cell soma while NA (10 μ M) had significantly less branches than control at 15, 25, 35 and 45 μ m from the cell soma. * $p<0.05$, ** $p<0.01$ NA 1 μ M vs. control, # $p<0.05$, ## $p<0.01$ NA 10 μ M vs. control. Data expressed as means \pm SEM, $n=7$. (Two-way repeated measures ANOVA followed by *post-hoc* Newman-Keuls).

3.1.2.3 Representative neurons for primary cortical neurons treated with NA

Primary cortical neurons were treated for 24h with NA. Cells were then stained using fluorescent immunocytochemistry for the neuronal structural protein β III-tubulin and counter-stained with the cell body marker DAPI. Figure 3.7 shows representative images for neurons treated with control (A) and NA (B).

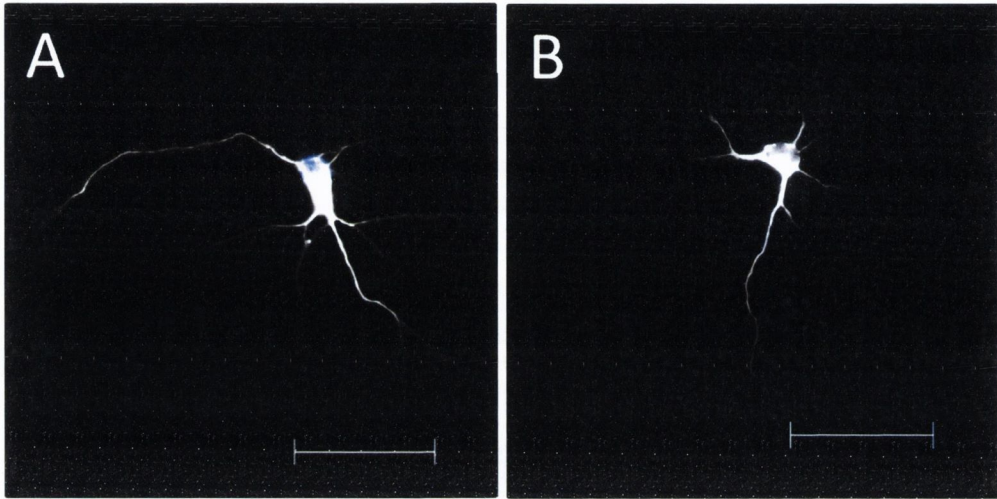


Figure 3.7: Representative images of primary cortical neurons treated with NA

Primary cortical neurons treated with NA were stained using fluorescent immunocytochemistry for the neuronal structural protein β III-tubulin (white) and the cell body marker DAPI (blue). All neurons were imaged by 200X magnification. Pictures correspond to representative images for (A) control neuron (B) NA (10 μ M). Scale bars in each diagram are equal to 50 μ m.

3.1.3 5-HT CM has no effect on the morphology of primary cortical neurons

As 5-HT has been shown to influence the expression of neurotrophic factors in glial cells it was of interest to determine if 5-HT could impact upon the morphology of primary cortical neurons. Confluent primary mixed glial cells were treated with control NBM or serotonin (1 μ M, 5 μ M or 10 μ M) in NBM. The cells were treated for 24h after which time the CM was collected, filtered and then used to treat 4 DIV primary cortical neurons for 24h. The neurons were then stained using fluorescent immunocytochemistry for β III tubulin and after image acquisition, were analysed by Sholl analysis specifically to determine the number of primary neurites extending from the cell soma, the number of neuritic branches and the length of the longest neurite.

3.1.3.1 5-HT CM has no effect on measures of neuronal complexity of primary cortical neurons

Primary Neurites

A one-way ANOVA demonstrated no effect of 5-HT CM on the number of primary neurites [$F_{(3,24)}=1.653$, $p=0.2037$]. (Figure 3.8a, $n=7$).

Neuritic Branches

A one-way ANOVA demonstrated no effect of 5-HT CM on the number of neuritic branches [$F_{(3,24)}=2.275$, $p=0.1056$]. (Figure 3.8b, $n=7$).

Neuritic Length

A one-way ANOVA demonstrated no effect of 5-HT CM on the neuritic length [$F_{(3,24)}=1.425$, $p=0.26$]. (Figure 3.8c, $n=7$).

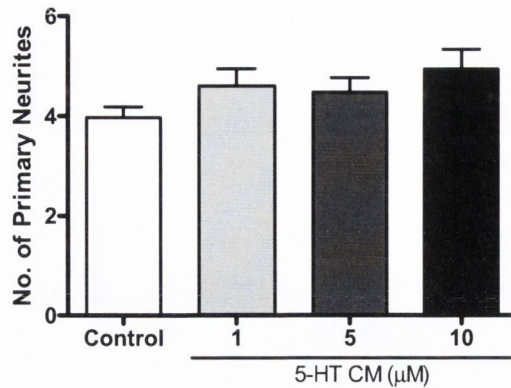
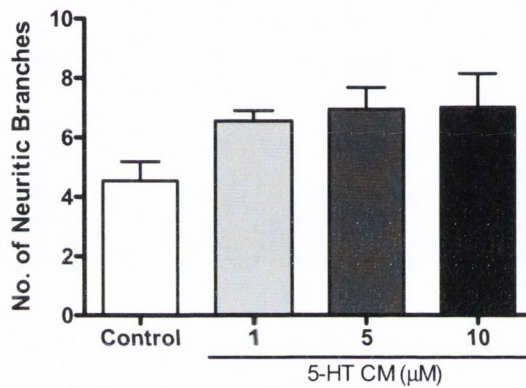
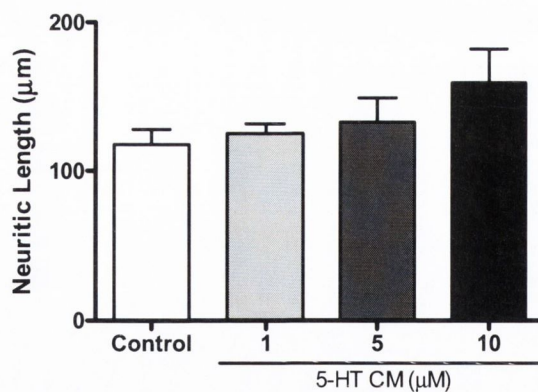
(a) Primary Neurites*(b) Neuritic Branches**(c) Neuritic Length*

Figure 3.8: 5-HT CM has no effect on measures of neuronal complexity of primary cortical neurons

Primary cortical neurons were treated for 24h with 5-HT CM from glial cells. Sholl analysis was then performed on the neurons. 5-HT CM had no effect on (a) number of primary neurites (b) number of neuritic branches or the (c) neuritic length. Data expressed as means \pm SEM, $n=7$. (One-way ANOVA).

3.1.3.2 5-HT CM increases the Sholl profile of primary cortical neurons

A repeated measures ANOVA demonstrated no significant effect of 5-HT CM on the number of neuritic branches at specific distances from cell soma [$F_{(3,384)}=2.62$, $p=0.074$]. ANOVA demonstrated a significant effect of distance [$F_{(16,384)}=246.24$, $p<0.0001$] with no significant distance by treatment interaction [$F_{(48,384)}=0.82$, $p=0.798$]. *Post-hoc* analysis revealed that 5-HT CM (1 μ M) treated neurons had significantly more branches than control CM treated neurons at 25 ($p<0.05$) and 35 μ m ($p<0.01$) while 5-HT (5 μ M) CM treated neurons had significantly more branches than control CM treated neurons at 25, 35 and 45 μ m ($p<0.05$) and 5-HT (10 μ M) CM treated neurons had significantly more branches than control CM treated neurons at 5, 35 ($p<0.05$) and 15 μ m ($p<0.01$) from the cell soma. [Figure 3.9, Newman-Keuls, $n=7$].

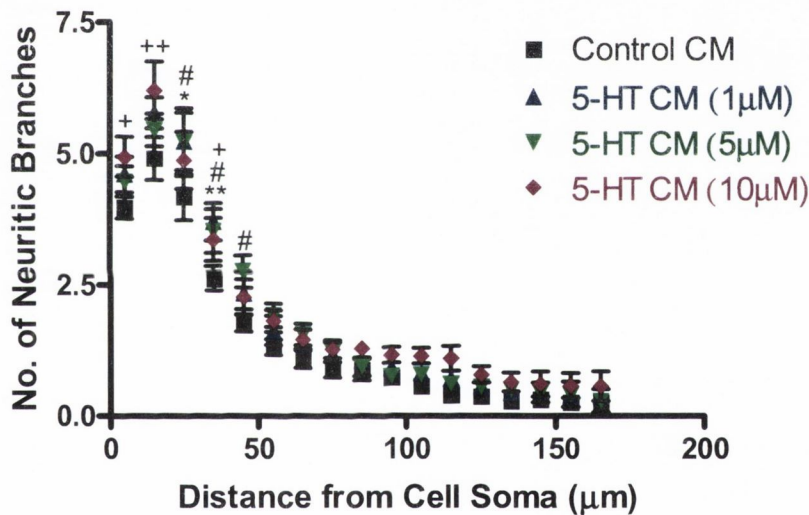


Figure 3.9: 5-HT CM increases the Sholl profile of primary cortical neurons.

Primary cortical neurons were treated for 24h with 5-HT CM from glial cells. Sholl analysis was then performed on the neurons. 5-HT CM (1 μ M) had significantly more branches than control at 25 and 35 μ m, while 5-HT CM (5 μ M) had significantly more branches than control at 25, 35 and 45 μ m, and 5-HT CM (10 μ M) had significantly more branches than control at 5, 15 and 35 μ m from the cell soma. * $p<0.05$, ** $p<0.01$ 5-HT CM (1 μ M) vs. control CM, # $p<0.05$, 5-HT CM (5 μ M) vs. control CM. \$ $p<0.05$, \$\$ $p<0.01$ 5-HT CM (10 μ M) vs. control CM. Data expressed as means \pm SEM, $n=7$. (Two-way repeated measures ANOVA followed by *post-hoc* Newman-Keuls).

3.1.4 5-HT has no effect on neuronal complexity of primary cortical neurons

Although serotonin CM had no effect on neuronal morphology, it was still important to assess any effect a direct treatment of 5-HT might have on neuronal morphology as neurons express the 5-HT receptors (for review, see Gu, 2002). Therefore neurons were treated for 24h with control NBM or with 5-HT (1 μ M, 5 μ M or 10 μ M) in NBM. As before, the neurons were stained using fluorescent immunocytochemistry for β III-tubulin and after image acquisition, were analysed by Sholl analysis specifically to determine the number of primary neurites extending from the cell soma, the number of neuritic branches and the length of the longest neurite.

3.1.4.1 5-HT has no effect on neuronal complexity of primary cortical neurons

Primary Neurites

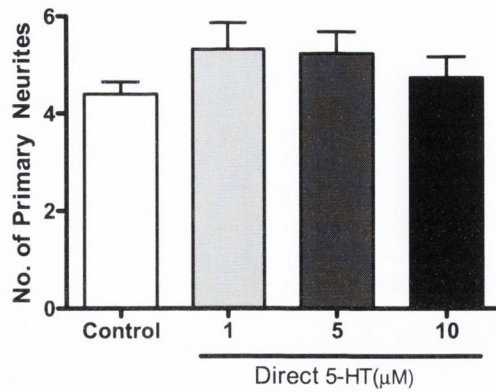
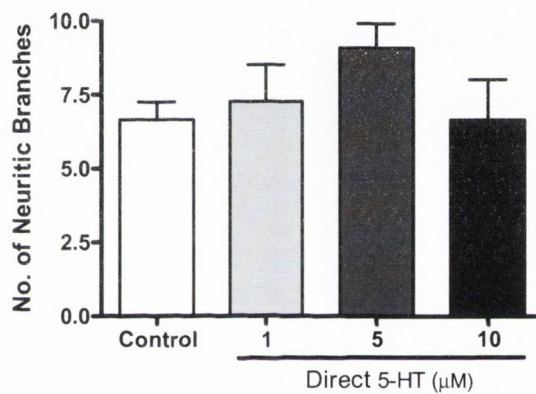
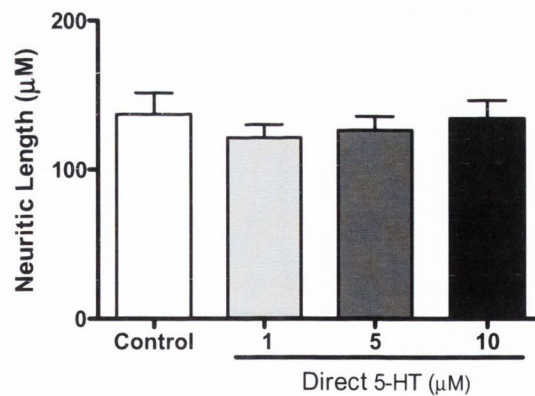
A one-way ANOVA demonstrated no effect of 5-HT on the number of primary neurites [$F_{(3,20)}=1.006$, $p=0.4109$]. [Figure 3.10a, $n=6$].

Neuritic Branches

A one-way ANOVA demonstrated no effect of 5-HT on the number of neuritic branches [$F_{(3,20)}=1.218$, $p=0.3289$]. [Figure 3.10 b, $n=6$].

Neuritic Length

A one-way ANOVA demonstrated no effect of 5-HT on the neuritic length [$F_{(3,20)}=0.318$, $p=0.7676$]. [Figure 3.10c, $n=6$].

(a) Primary Neurites*(b) Neuritic Branches**(c) Neuritic Length***Figure 3.10: 5-HT has no effect on neuronal complexity of primary cortical neurons**

Primary cortical neurons were treated for 24h with 5-HT. Sholl analysis was then performed on the neurons. 5-HT treatment had no effect on (a) number of primary neurites (b) number of neuritic branches and (c) neuritic length. Data expressed as mean \pm SEM, $n=6$. (One-way ANOVA).

3.1.4.2 5-HT increases the Sholl profile of primary cortical neurons

A repeated measures ANOVA demonstrated no effect of 5-HT on the number of neuritic branches at specific distances from cell soma [$F_{(3,320)}=2.57$, $p=0.0822$]. ANOVA demonstrated a significant effect of distance [$F_{(16,320)}=216.64$, $p<0.0001$] and a significant distance by treatment interaction [$F_{(48,320)}=1.618$, $p=0.0086$]. *Post-hoc* analysis revealed that 5-HT (5 μ M) had significantly more branches than control at 15, 25 ($p<0.01$) and 35 μ m ($p<0.05$) from the cell soma. [Figure 3.11, Newman-Keuls, $n=6$].

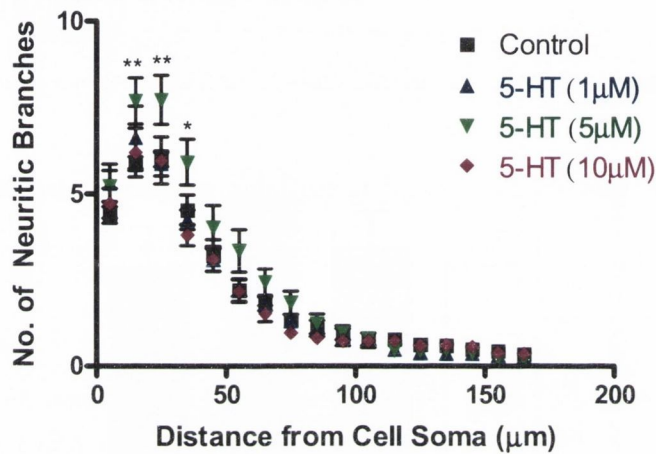


Figure 3.11: 5-HT increases the Sholl profile of primary cortical neurons.

Primary cortical neurons were treated for 24h with 5-HT. Sholl analysis was then performed on the neurons. 5-HT (5 μ M only) treated neurons had significantly more branches than control at 15, 25 and 35 μ m from the cell soma. Data expressed as means \pm SEM, $n=6$. ** $p<0.01$, * $p<0.05$ 5-HT (5 μ M) vs. control (Two-way repeated measures ANOVA followed by *post-hoc* Newman-Keuls).

3.1.5 Amitriptyline CM increases some measures of neuronal morphology

Amitriptyline (AMI), a tricyclic antidepressant, functions as both a serotonin and noradrenaline reuptake inhibitor (Iversen, 2006). Therefore, the ability of AMI to enhance neuronal complexity via actions on glial cells was assessed. Confluent primary mixed glial cells were treated with control NBM or AMI (1 μ M, 5 μ M or 25 μ M) in NBM. The cells were treated for 24h after which time the CM was collected, filtered and then used to treat 4 DIV primary cortical neurons for 24h. The neurons were then stained using fluorescent immunocytochemistry for β III-tubulin and after image acquisition, were analysed by Sholl analysis specifically to determine the number of primary neurites extending from the cell soma, the number of neuritic branches and the length of the longest neurite.

3.1.5.1 AMI CM increases the number of primary neurites and neuritic length but not branch number of primary cortical neurons

Primary Neurites

A one-way ANOVA demonstrated a significant effect of AMI CM on the number of primary neurites [$F_{(3,28)}=7.356$, $p=0.0009$]. *Post-hoc* analysis revealed that AMI CM (5 μ M) increased the number of primary neurites extending from the cell soma as compared to control CM treated neurons ($p<0.01$). [Figure 3.12a, Newman-Keuls, $n=8$].

Neuritic Branches

A one-way ANOVA demonstrated a significant effect of AMI CM on the number of neuritic branches [$F_{(3,28)}=3.363$, $p=0.0326$]. *Post-hoc* analysis revealed no significant effect of AMI CM on the number of neuritic branches. [Figure 3.12b, Newman-Keuls, $n=8$].

Neuritic Length

A one-way ANOVA demonstrated a significant effect of AMI CM on the neuritic length [$F_{(3,28)}=4.976$, $p=0.0068$]. *Post-hoc* analysis revealed that AMI CM (5 μ M) significantly increases the neuritic length compared to control CM treated neurons ($p<0.01$). [Figure 3.12c, Newman-Keuls, $n=8$].

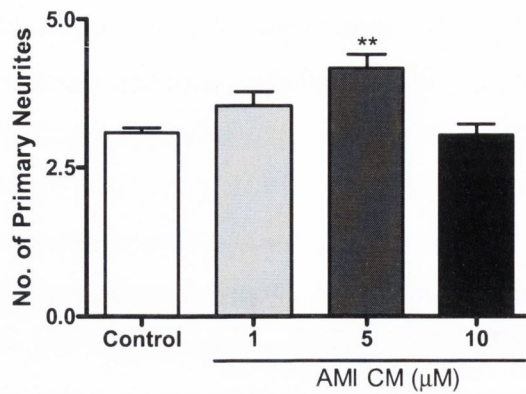
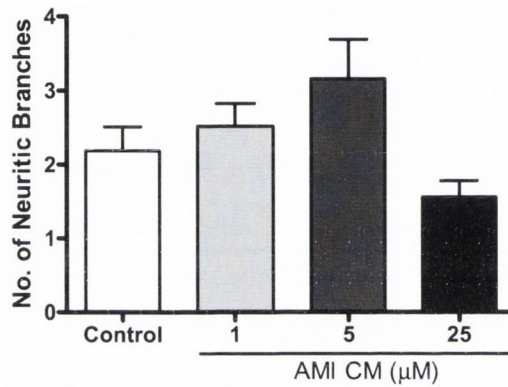
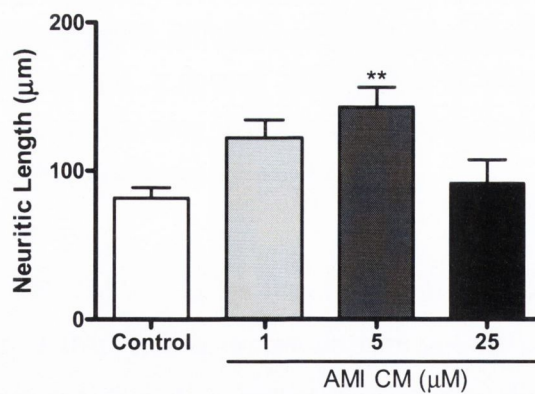
(a) Primary Neurites*(b) Neuritic Branches**(c) Neuritic Length*

Figure 3.12: AMI CM increases the number of primary neurites and neuritic length but not branch number of primary cortical neurons

Primary cortical neurons were treated for 24h with the AMI CM from glial cells. Sholl analysis was then performed on the neurons. AMI CM (5 μM) significantly increased (a) number of primary neurites and (c) neuritic length but not (b) number of neuritic branches. Data expressed as mean \pm SEM, $n=8$. ** $p<0.01$ vs. control CM (One-way ANOVA followed by *post-hoc* Newman-Keuls).

3.1.5.2 AMI CM increases the Sholl profile of primary cortical neurons

A repeated measures ANOVA demonstrated a significant effect of AMI CM on the number of neuritic branches at specific distances from cell soma [$F_{(3,448)}=8.606$, $p=0.003$]. ANOVA also demonstrated a significant effect of distance [$F_{(16,448)}=246.79$, $p<0.0001$] and a significant distance by treatment interaction [$F_{(48,448)}=1.614$, $p=0.0076$]. Furthermore *post-hoc* analysis revealed that AMI CM ($5\mu\text{M}$) had significantly more branches than control at 5, 15 and $25\mu\text{m}$ from the cell soma while AMI CM ($25\mu\text{M}$) had significantly less branches than control at $25\mu\text{m}$ from the cell soma. [Figure 3.13, Newman-Keuls, $n=8$].

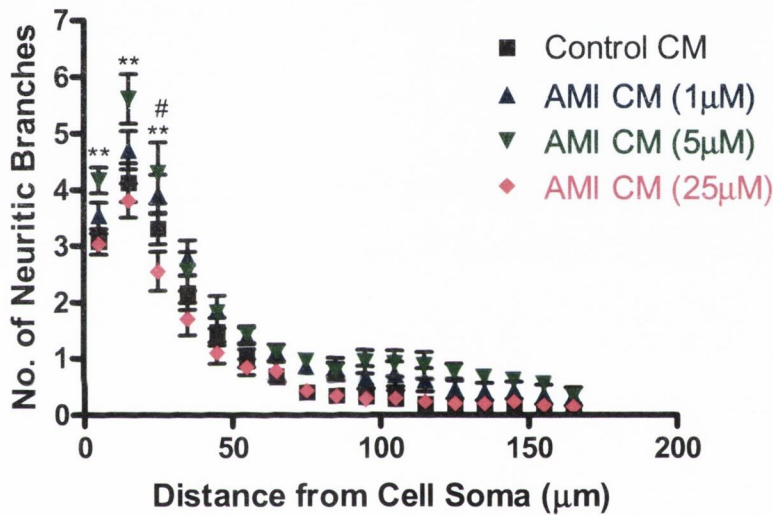


Figure 3.13: AMI CM increases the Sholl profile of primary cortical neurons.

Primary cortical neurons were treated for 24h with AMI CM from glial cells. Sholl analysis was then performed on the neurons. AMI CM ($5\mu\text{M}$) significantly increased the number of branches at 5, 15 and $25\mu\text{m}$ from the cell soma while AMI CM ($25\mu\text{M}$) significantly reduced the number of branches at $25\mu\text{m}$ from the cell soma compared to control CM. Data expressed as means \pm SEM, $n=8$. ** $p<0.01$ AMI CM $5\mu\text{M}$ vs. control CM, # $p<0.05$ AMI CM $25\mu\text{M}$ vs. control CM (Two-way repeated measures ANOVA followed by *post-hoc* Newman-Keuls).

3.1.6 Direct Amitriptyline treatment increases neuronal complexity

As AMI CM was shown to induce some morphological changes within the primary cortical neurons it was then important to assess if a direct treatment of primary cortical neurons with AMI could also induce morphological changes in the neurons or whether the glial cells were vital for this ability. Therefore primary neurons were treated for 24h with control NBM or with AMI (1 μ M, 5 μ M or 25 μ M) in NBM. As before, the neurons were stained using fluorescent immunocytochemistry for β III-tubulin and after image acquisition, were analysed by Sholl analysis specifically to determine the number of primary neurites extending from the cell soma, the number of neuritic branches and the length of the longest neurite.

3.1.6.1 Direct AMI increases all measures of neuronal complexity of primary cortical neurons

Primary Neurites

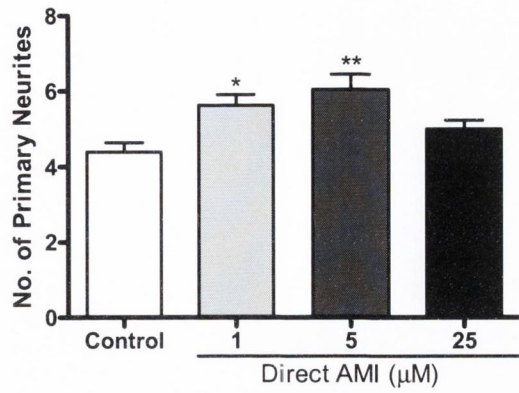
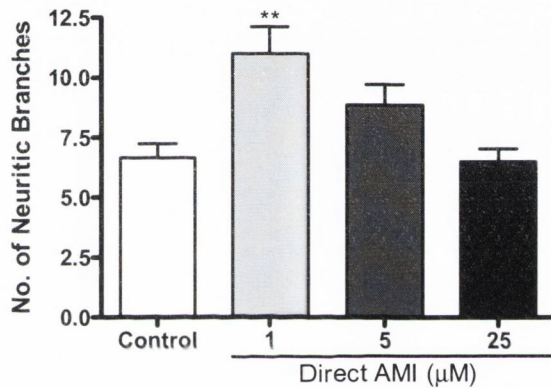
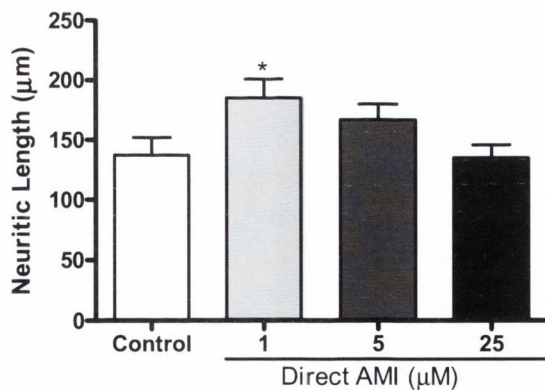
A one-way ANOVA demonstrated a significant effect of AMI on the number of primary neurites [$F_{(3,20)}=5.774$, $p=0.0052$]. *Post-hoc* analysis revealed that AMI (1 μ M, $p<0.05$) and (5 μ M, $p<0.01$) significantly increased the number of primary neurites extending from the cell soma as compared to control treated neurons. [Figure 3.14a, Newman Keuls, $n=6$].

Neuritic Branches

A one-way ANOVA demonstrated a significant effect of AMI on the number of neuritic branches [$F_{(3,20)}=6.838$, $p=0.0024$]. *Post-hoc* analysis revealed that AMI (1 μ M) increased the number of neuritic branches compared to control neurons ($p<0.01$). [Figure 3.14b, Newman Keuls, $n=6$].

Neuritic Length

A one-way ANOVA demonstrated a significant effect of AMI on the neuritic length [$F_{(3,20)}=3.181$, $p=0.0463$]. *Post-hoc* analysis revealed that AMI (1 μ M) increased the neuritic length compared to control treated neurons ($p<0.05$). [Figure 3.14c, Fishers LSD, $n=6$]

(a) Primary Neurites*(b) Neuritic Branches**(c) Neuritic Length***Figure 3.14: Direct AMI increases all measures of neuronal complexity of primary cortical neurons**

Primary cortical neurons were treated for 24h with AMI. Sholl analysis was then performed on the neurons. AMI significantly increased (a) number of primary neurites (b) number of neuritic branches and (c) neuritic length. Data expressed as mean + SEM, $n=6$. * $p<0.05$, ** $p<0.01$ vs. control (One-way ANOVA followed by *post-hoc* Newman Keuls [a and b] Fishers LSD [c]).

3.1.6.2 Direct AMI increases the Sholl profile of primary cortical neurons

A repeated measures ANOVA demonstrated a significant effect of AMI on the number of neuritic branches at specific distances from cell soma [$F_{(3,320)}=7.214$, $p=0.0018$]. ANOVA also demonstrated a significant effect of distance [$F_{(16,320)}=256.26$, $p<0.0001$] and a significant distance by treatment interaction [$F_{(48,320)}=2.11$, $p<0.0001$]. Furthermore *post-hoc* analysis revealed that AMI (1 μ M) treated neurons had significantly more branches than control treated neurons at 5, 35 ($p<0.05$), 15 and 25 μ m ($p<0.01$) from the cell soma while AMI (5 μ M) treated neurons had significantly more branches at 5, 15, 25 and 35 μ m from the cell soma. AMI (25 μ M) treated neurons were not significantly different to control treated neurons. [Figure 3.15, Newman-Keuls, $n=6$].

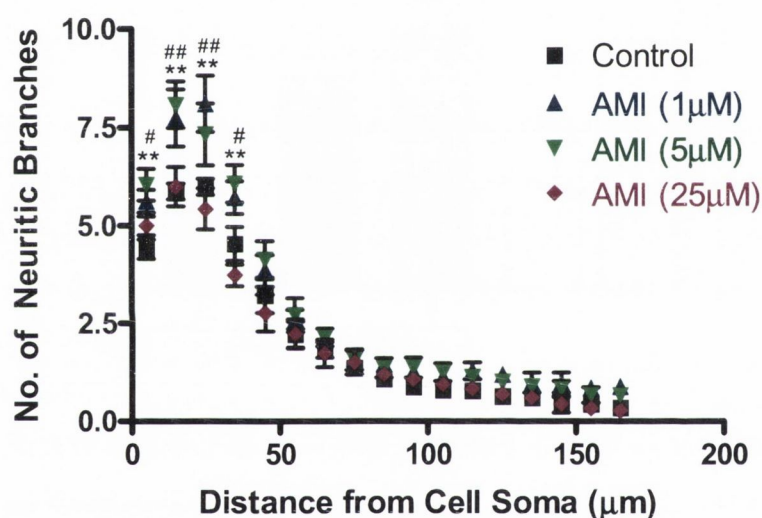


Figure 3.15: Direct AMI increases the Sholl profile of primary cortical neurons

Primary cortical neurons were treated for 24h with AMI. Sholl analysis was then performed on the neurons. AMI (1 μ M and 5 μ M) treated neurons had significantly more branches at 5, 15, 25 and 35 μ m from the cell soma compared to control treated neurons. Data expressed as means \pm SEM, $n=6$, # $p<0.05$, ## $p<0.01$ AMI (1 μ M) vs. control, ** $p<0.01$ AMI (5 μ M) vs. control. (Two-way repeated measures ANOVA followed by *post-hoc* Newman-Keuls).

3.2 Examination of the glial adrenoceptor subtype involved in noradrenaline mediated neuronal morphology changes

As NA elicited the most profound effect on neuronal morphology the remainder of the studies in this thesis are focused on the mechanisms and mediators that underlie the ability of CM from NA-treated glial cells to enhance neuronal morphology. NA can bind to either α - or β -adrenoceptor subtypes, both of which are present on glial cells (for review, see Kimelberg, 1995). Literature suggests that the neuroprotective properties of adrenergic stimulation are mediated mainly via the β -adrenoceptor subtype (Semkova *et al.*, 1996). Therefore, it was important to determine which glial adrenoceptor subtype was mediating the noradrenaline-induced effects on neuronal morphology in an attempt to understand the underlying mechanisms.

Therefore the aims of these studies were as follows:

- 1) To examine the ability of antagonism of the glial α - and β -adrenoceptors to attenuate NA CM-induced increases in complexity of primary cortical neurons.
- 2) To examine the ability of the non-selective β -adrenoceptor agonist, salbutamol, to induce morphological changes in neurons via an action on glial cells.
- 3) To examine the abilities of the specific β_1 -adrenoceptor agonist; xamoterol, and the specific β_2 -adrenoceptor agonists; clenbuterol and salmeterol, to induce morphological changes in neurons via an action on glial cells.
- 4) To examine the ability of the cell permeable cAMP analogue; dbcAMP, to induce morphological changes in neurons via an action on glial cells.

3.2.1 NA CM-induced increases in neuronal morphology are primarily attributed to the β -adrenoceptor

Propranolol (Prop, β -adrenoceptor antagonist) and phentolamine (Phent, α -adrenoceptor antagonist) were utilised in this study to block the ability of NA to bind to the β and α adrenoceptors respectively. Glial cells were pre-treated for 30min with Prop (10 μ M), Phent (10 μ M) or control followed by stimulation with NA (10 μ M) for 24h. This CM was then used to treat neurons for 24h, followed by Sholl analysis as before.

3.2.1.1 Antagonism of the β -adrenoceptor blocks all NA CM-induced increases in neuronal complexity while antagonism of the α -adrenoceptor attenuates NA CM-induced increases in neuritic length

Primary Neurites

A two-way ANOVA demonstrated a significant effect of NA CM treatment on the number of primary neurites [$F_{(1,42)}=18.45$, $p=0.0001$]. There was also a significant effect of antagonist treatment [$F_{(2,42)}=5.37$, $p=0.0084$] but no significant interaction [$F_{(2,42)}=1.51$, $p=0.2325$]. *Post-hoc* analysis revealed that NA CM had significantly more primary neurites compared to control CM ($p<0.01$) and that Prop in combination with NA CM had significantly less primary neurites compared to NA CM alone ($p<0.05$). Phent had no effect on NA CM-induced increases in the number of primary neurites [Figure 3.16a, Newman Keuls $n=8$].

Neuritic Branching

A two-way ANOVA demonstrated a significant effect of NA CM treatment on the number of neuritic branches [$F_{(1,42)}=28.83$, $p<0.0001$]. There was also a significant effect of antagonist treatment [$F_{(2,42)}=3.93$, $p=0.0273$] and a significant NA by antagonist interaction [$F_{(2,42)}=3.61$, $p=0.036$]. *Post-hoc* analysis revealed that NA CM treatment significantly increased the number of neuritic branches compared to control CM treated neurons ($p<0.01$) and that Prop with NA CM had significantly less neuritic branches compared to NA CM alone ($p<0.01$). Phent had no effect on NA CM-induced increases in the number of neuritic branches. [Figure 3.16b, Newman Keuls, $n=8$].

Neuritic Length

A two-way ANOVA demonstrated a significant effect of NA CM treatment on the neuritic length [$F_{(1,42)}=23.56$, $p<0.0001$]. There was also a significant effect of antagonist treatment [$F_{(2,42)}=4.93$, $p=0.0119$] and a significant NA by antagonist interaction [$F_{(2,42)}=6.92$, $p=0.0025$]. *Post-hoc* analysis revealed that NA CM treatment significantly increased the neuritic length compared to control treated neurons ($p<0.01$), while both Prop and Phent with NA CM had significantly reduced neuritic length compared to NA CM alone ($p<0.01$). [Figure 3.16c, Newman Keuls $n=8$].

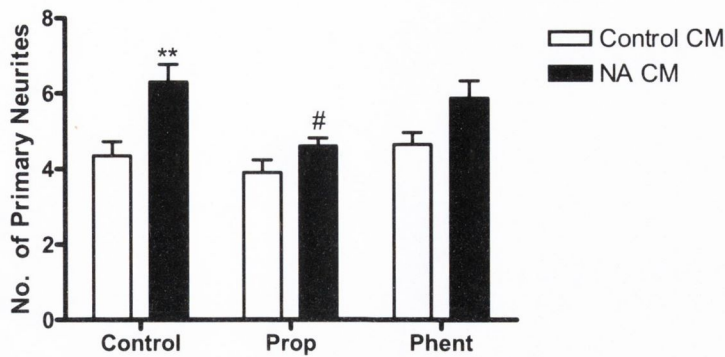
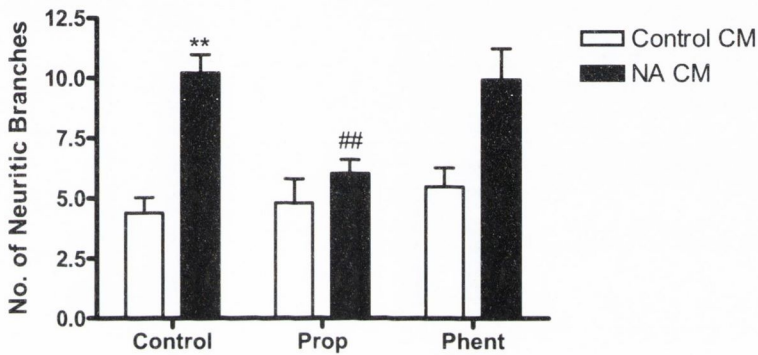
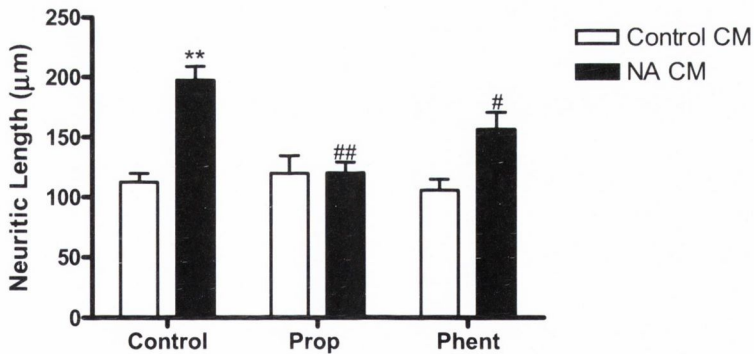
(a) Primary Neurites*(b) Neuritic Branches**(c) Neuritic Length*

Figure 3.16: Antagonism of the β -adrenoceptor blocks all NA CM-induced increases in neuronal complexity while antagonism of the α -adrenoceptor attenuates NA CM-induced increases in neuritic length

Primary cortical neurons were treated for 24h with the CM from glial cells pre-treated for 30 min with Prop (10 μM) or Phent (10 μM) followed by NA (10 μM) stimulation for 24h. Sholl analysis was then performed. Prop significantly reduced the NA CM-induced increases in (a) number of primary neurites, (b) number of neuritic branches and (c) neuritic length. While Phent significantly reduced the NA CM-induced increases in (c) neuritic length. Data expressed as mean + SEM, $n=8$. ** $p<0.01$ vs. control CM, # $p<0.05$, ## $p<0.01$ vs. NA CM alone. (Two-way ANOVA followed by *post-hoc* Newman-Keuls).

3.2.1.2 Antagonism of the β -adrenoceptor blocks all NA CM-induced increases in the Sholl profile of primary cortical neurons

A three-way repeated measures ANOVA demonstrated a significant effect of NA CM [$F_{(1,224)}=30.09$, $p<0.0001$] on the number of neuritic branches at specific distances from the cell soma. ANOVA also demonstrated a significant effect of Prop [$F_{(1,224)}=30.11$, $p<0.0001$] and of distance [$F_{(16,224)}=239.07$, $p<0.0001$]. Significant interactions were also found between NA CM and distance [$F_{(16,224)}=8.5$, $p<0.0001$], Prop and distance [$F_{(16,224)}=4.07$, $p<0.0001$], and between NA CM and Prop [$F_{(1,224)}=14.76$, $p=0.0018$]. Furthermore *post-hoc* analysis revealed that NA CM treated neurons had significantly more branches than control CM treated neurons at 5, 15, 25, 34 and 45 μm ($p<0.01$) from the cell soma. Prop with NA CM treated neurons had significantly less branches than NA CM treated neurons alone at 5, 15, 25, 35 ($p<0.01$) and 45 μm ($p<0.05$) from the cell soma. [Figure 3.17, Newman-Keuls, $n=8$].

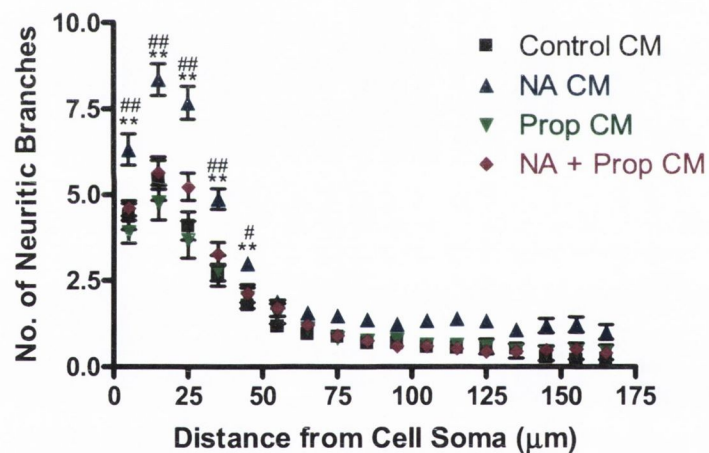


Figure 3.17: Antagonism of the β -adrenoceptor blocks all NA CM-induced increases in the Sholl profile of primary cortical neurons

Primary cortical neurons were treated for 24h with the CM from glial cells pre-treated for 30 min with Prop (10 μM) followed by NA (10 μM) stimulation for 24h. Sholl analysis was then performed. NA CM treated neurons had significantly more branches than control CM treated neurons at 5, 15, 25, 34 and 45 μm from the cell soma. Prop with NA CM treated neurons had significantly less branches than NA CM treated neurons alone at 5, 15, 25, 35 and 45 μm from the cell soma. Data expressed as means \pm SEM, $n=8$. ** $p<0.01$ NA CM vs. control CM, # $p<0.05$, ## $p<0.01$ NA CM + Prop vs. NA CM. (Three-way repeated measures ANOVA followed by *post-hoc* Newman-Keuls).

3.2.1.3 Antagonism of the α -adrenoceptor does not attenuate the NA CM-induced increases in the Sholl profile of primary cortical neurons

A three-way repeated measures ANOVA demonstrated a significant effect of NA CM [$F_{(1,224)}=58.45$, $p=0<0.0001$] but no significant effect of Phent on the number of neuritic branches at specific distances from the cell soma. ANOVA also demonstrated a significant effect of distance [$F_{(16,224)}=357.38$, $p<0.0001$] and a significant distance by NA CM treatment interaction [$F_{(16,224)}=7.26$, $p<0.0001$]. Furthermore *post-hoc* analysis revealed that NA CM treated neurons had significantly more branches than control at 5, 15, 25, 35 ($p<0.01$) and 45 μ m ($p<0.05$) from the cell soma. Phent treated neurons alone had significantly more branches than control CM treated neurons at 25 μ m from the cell soma ($p<0.05$). Importantly, there were no significant differences between NA CM in combination with Phent with NA CM treated neurons alone. [Figure 3.18, Newman-Keuls, $n=8$].

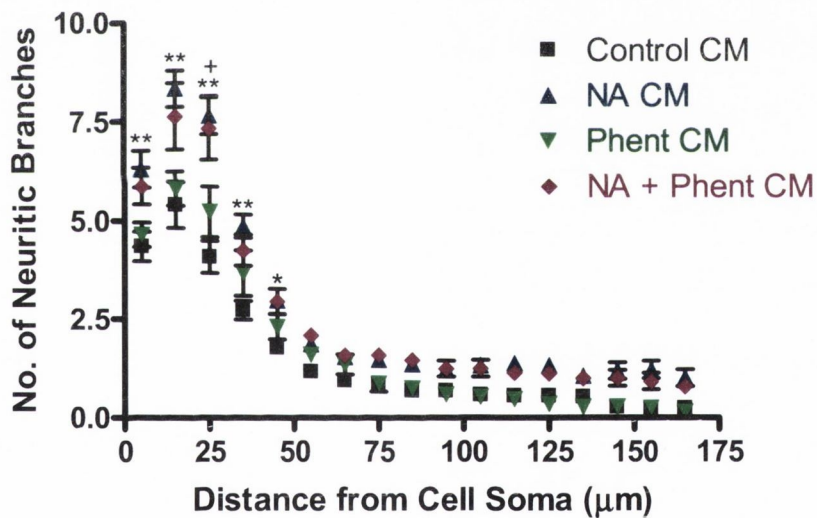


Figure 3.18: Antagonism of the α -adrenoceptor does not attenuate NA CM-induced increases in the Sholl profile of cortical neurons

Primary cortical neurons were treated for 24h with the CM from glial cells pre-treated with Phent (10 μ M) followed by NA (10 μ M) stimulation for 24h. Sholl analysis was then performed. NA CM treated neurons had significantly more branches than control CM treated neurons at 5, 15, 25, 34 and 45 μ m from the cell soma. Phent alone treated neurons had significantly more branches than control CM treated neurons at 25 μ m from the cell soma. There were no significant differences between NA CM alone and Phent with NA CM treated neurons. Data expressed as means \pm SEM, $n=8$. ** $p<0.01$ NA CM vs. control CM, + $p<0.05$ Phent vs. control CM (Three-way repeated measures ANOVA followed by *post-hoc* Newman-Keuls).

3.2.2 Salbutamol CM increases measures of neuronal morphology

Noradrenaline can signal via two main β -adrenoceptors, the β_1 -adrenoceptor and the β_2 -adrenoceptor (Rang & Dale, 2003). To assess the ability of activation of the glial β -adrenoceptors in enhancing neuronal complexity, the non-selective β -adrenoceptor agonist, Salbutamol (Salb), was utilised. As before, confluent primary mixed glial cells were treated with control NBM or Salb ($5\mu\text{M}$ or $10\mu\text{M}$) in NBM. The cells were treated for 24h after which time the CM was collected, filtered and then used to treat 4 DIV primary cortical neurons for 24h. The neurons were then stained using fluorescent immunocytochemistry for β III-tubulin and after image acquisition, were analysed by Sholl analysis specifically to determine the number of primary neurites extending from the cell soma, the number of neuritic branches and the length of the longest neurite.

3.2.2.1 Salb CM increases all measures of neuronal complexity of primary cortical neurons

Primary Neurites

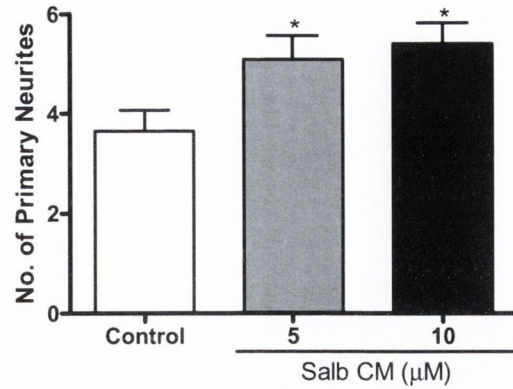
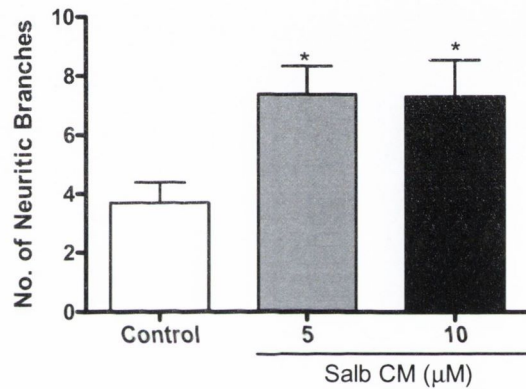
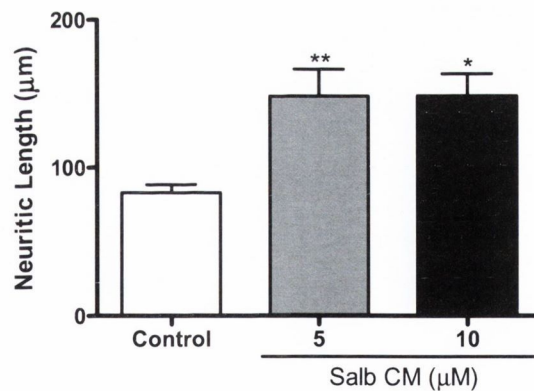
A one-way ANOVA demonstrated a significant effect of Salb CM on the number of primary neurites [$F_{(2,15)}=4.534$, $p=0.0288$]. *Post-hoc* analysis revealed that both doses of Salb CM increased the number of primary neurites extending from the cell soma as compared to control CM treated neurons ($p<0.05$). [Figure 3.19a, Newman-Keuls, $n=6$].

Neuritic Branches

A one-way ANOVA demonstrated a significant effect of Salb CM on the number of neuritic branches [$F_{(2,15)}=4.594$, $p=0.0278$]. *Post-hoc* analysis revealed that both doses of Salb CM increased the number of neuritic branches compared to control CM treated neurons ($p<0.05$). [Figure 3.19 b, Newman-Keuls, $n=6$].

Neuritic Length

A one-way ANOVA demonstrated a significant effect of Salb CM on the neuritic length [$F_{(2,15)}=7.367$, $p=0.0059$]. *Post-hoc* analysis revealed that both doses of Salb CM significantly increased the neuritic length compared to control CM treated neurons ($p<0.01$ for $5\mu\text{M}$ and $p<0.05$ for $10\mu\text{M}$). [Figure 3.19c, Newman-Keuls, $n=6$].

(a) Primary Neurites**(b) Neuritic Branches****(c) Neuritic Length****Figure 3.19: Salb CM increases all measures of neuronal complexity of primary cortical neurons**

Primary cortical neurons were treated for 24h with Salb CM (5, 10 μM) from glial cell. Sholl analysis was then performed on the neurons. Salb CM significantly increased (a) number of primary neurites (b) number of neuritic branches and (c) neuritic length. Data expressed as mean + SEM, $n=6$. * $p<0.05$, ** $p<0.01$ vs. control CM. (One-way ANOVA followed by *post-hoc* Newman-Keuls).

3.2.2.2 Salb CM increases the Sholl profile of primary cortical neurons

A repeated measures two-way ANOVA demonstrated a significant effect of Salb CM on the number of neuritic branches at specific distances from cell soma [$F_{(2,240)}=7.187$, $p=0.0065$]. ANOVA also demonstrated a significant effect of distance [$F_{(16,240)}=182.99$, but no significant distance by treatment interaction [$F_{(32,240)}=1.41$, $p=0.0755$]. Furthermore *post-hoc* analysis revealed that both doses of Salb CM treated neurons had significantly more branches than control CM treated neurons at 5, 15, 25 and 35 μ m ($P<0.01$) from the cell soma while Salb CM (5 μ M) treated neurons in addition had significantly more branches at 45 and 55 μ m ($p<0.01$). [Figure 3.20, Newman-Keuls, $n=6$].

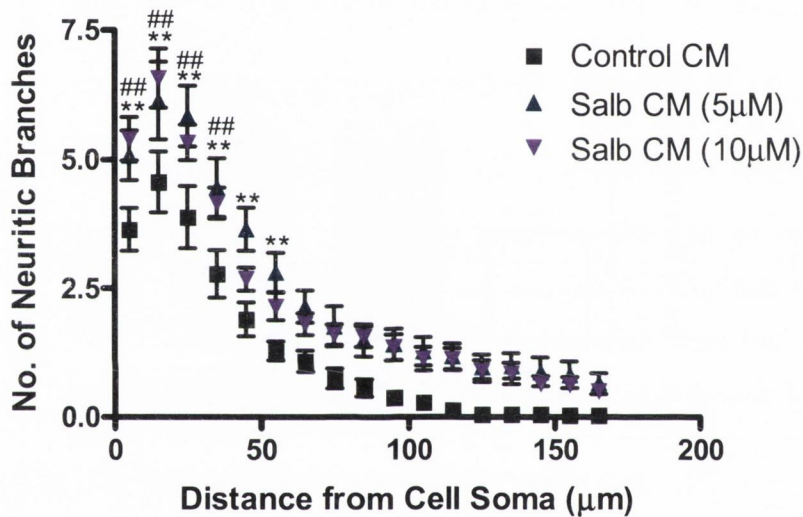


Figure 3.20: Salb CM increases the Sholl profile of primary cortical neurons

Primary cortical neurons were treated for 24h with Salb CM (5, 10 μ M) from glial cells. Sholl analysis was then performed on the neurons. Salb CM (5 μ M) treated neurons significantly increased the number of branches at 5, 15, 25, 35, 45 and 55 μ m from the cell soma while Salb CM (10 μ M) treated neurons had significantly more branches at 5, 15, 25 and 35 μ m from the cell soma compared to control CM. Data expressed as means \pm SEM, $n=6$. ** $p<0.01$ Salb CM (5 μ M) vs. control CM, ## $p<0.01$ Salb CM (10 μ M) vs. control CM (Two-way repeated measures ANOVA followed by *post-hoc* Newman-Keuls).

3.2.3 The β_2 -adrenoceptor agonists, salmeterol and clenbuterol, but not the β_1 -adrenoceptor agonist, xamoterol, increases measures of neuronal morphology

Salbutamol is considered both a β_1 and β_2 -adrenoceptor agonist; therefore it was important to further dissociate the ability of the β -adrenoceptors to induce morphological changes in the neurons. Therefore, the highly selective β_2 -adrenoceptor agonists salmeterol (Salm; 1 μ M) and clenbuterol (Clen; 1 μ M), and the highly selective β_1 -adrenoceptor agonist, xamoterol (Xam; 1 μ M) were utilised to treat primary mixed glial cells and thus the CM on primary neuronal cells. Sholl analysis was performed as before.

3.2.3.1 Salm CM and Clen CM but not Xam CM increase all measures of neuronal complexity of primary cortical neurons

Primary Neurites

A one-way ANOVA demonstrated a significant effect of treatment on the number of primary neurites [$F_{(3,21)}=6.664$, $p=0.0025$]. *Post-hoc* analysis revealed that Salm CM ($p<0.05$) and Clen CM ($p<0.01$) increased the number of primary neurites extending from the cell soma as compared to control CM treated neurons. Xam CM had no effect on the number of primary neurites. [Figure 3.21a, Newman-Keuls, $n=5-7$].

Neuritic Branches

A one-way ANOVA demonstrated a significant effect of treatment on the number of neuritic branches [$F_{(3,21)}=6.271$, $p=0.0033$]. *Post-hoc* analysis revealed that Salm CM ($p<0.01$) and Clen CM ($p<0.05$) increased the number of neuritic branches compared to control CM treated neurons. Xam CM had no effect on the number of neuritic branches. [Figure 3.21b, Newman-Keuls, $n=5-7$].

Neuritic Length

A one-way ANOVA demonstrated a significant effect of treatment on the neuritic length [$F_{(3,20)}=9.867$, $p=0.0003$]. *Post-hoc* analysis revealed that Salm CM ($p<0.01$) and Clen CM ($p<0.01$) increased the neuritic length compared to control CM treated neurons. Xam CM had no effect on the neuritic length. [Figure 3.21c, Newman-Keuls, $n=5-7$].

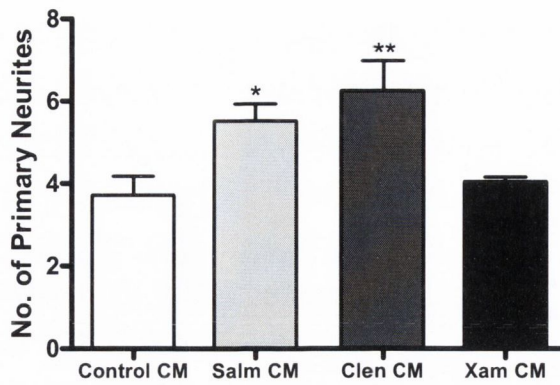
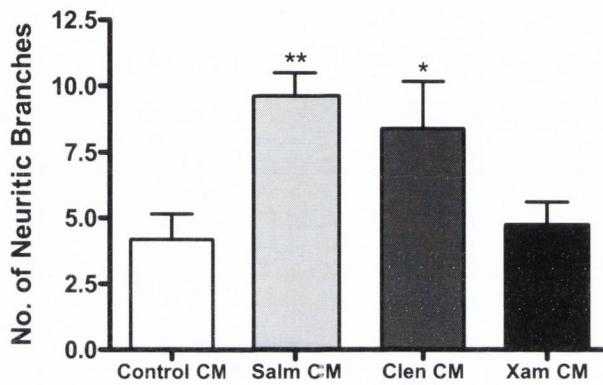
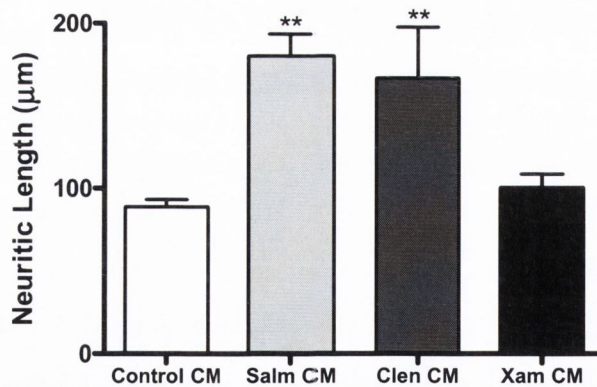
(a) Primary Neurites*(b) Neuritic Branches**(c) Neuritic Length*

Figure 3.21: Salm CM and Clen CM but not Xam CM increase all measures of neuronal complexity of primary cortical neurons

Primary cortical neurons were treated for 24h with the CM from glial cells treated with Salm ($1\mu\text{M}$), Clen ($1\mu\text{M}$) or Xam ($1\mu\text{M}$) for 24h. Sholl analysis was then performed on the neurons. Both Salm CM and Clen CM treated neurons significantly increased (a) number of primary neurites (b) number of neuritic branches and (c) neuritic length. Xam CM treatment of neurons had no effect on any parameter. Data expressed as mean + SEM, $n=5-7$. * $p<0.05$, ** $p<0.01$ vs. control CM (One-way ANOVA followed by *post-hoc* Newman-Keuls).

3.2.3.2 Salm CM and Clen CM but not Xam CM increases the Sholl profile of primary cortical neurons

A repeated measures two-way ANOVA demonstrated a significant effect of treatment on the number of neuritic branches at specific distances from cell soma [$F_{(3,336)}=10.96$, $p=0.0002$]. ANOVA also demonstrated a significant effect of distance [$F_{(16,336)}=157.53$, $p<0.0001$] and a significant distance by treatment interaction [$F_{(48, 336)}=2.748$, $p<0.0001$]. Furthermore *post-hoc* analysis revealed that Clen CM had significantly more branches at 5, 15, 25 and 35 μm from the cell soma than control CM treated neurons while Salm CM treated neurons had significantly more branches at 5, 15, 25, 35 and 45 μm from the cell soma. [Figure 3.22, Newman-Keuls, $n=5-7$].

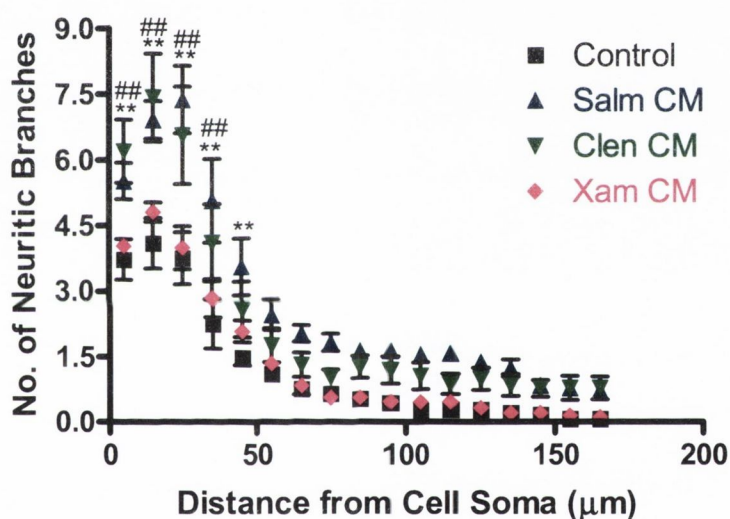


Figure 3.22: Salm CM and Clen CM but not Xam CM increases the Sholl profile of primary cortical neurons

Primary cortical neurons were treated for 24h with the CM from glial cells treated with Salm (1 μM), Clen (1 μM) or Xam (1 μM) for 24h. Sholl analysis was then performed on the neurons. Clen CM had significantly more branches at 5, 15, 25 and 35 μm from the cell soma than control CM treated neurons while Salm CM treated neurons had significantly more branches at 5, 15, 25, 35 and 45 μm from the cell soma. Data expressed as means \pm SEM, $n=5-7$, ** $p<0.01$ Salm CM vs. control CM, ## $p<0.01$ Clen CM vs. control CM (Two-way repeated measures ANOVA followed by *post-hoc* Newman-Keuls).

3.2.4 The cAMP analogue, dbcAMP, CM increases neuronal complexity

Stimulation of the β 2-adrenoceptor activates adenylate cyclase resulting in the subsequent production of cAMP (for review, see Johnson, 2001). To assess if an increase in the intracellular concentration of cAMP in glial cells is sufficient for the CM to enhance primary neuronal complexity, the cell-permeable cAMP analogue dbcAMP was utilised. Primary glial cells were treated with dbcAMP (300 μ M) for 24h after which time the CM was collected and used to treat neurons. Sholl analysis was performed as before.

3.2.4.1 DbcAMP CM increases all measures of neuronal complexity of primary cortical neurons

Primary Neurites

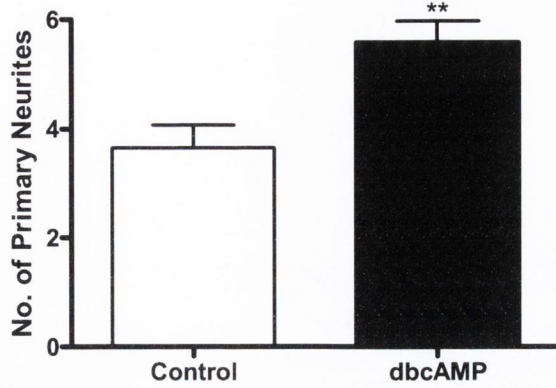
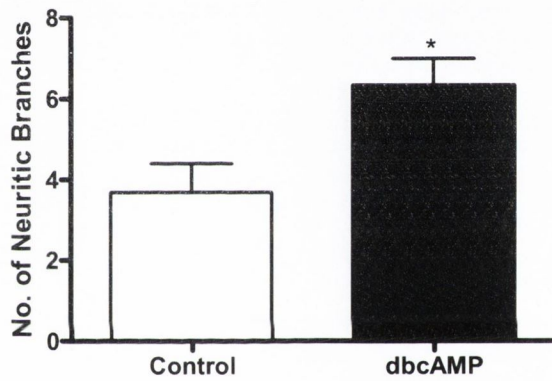
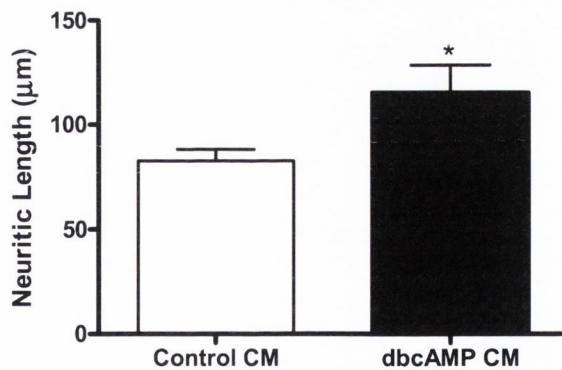
A Student's *t*-test demonstrated a significant effect of dbcAMP CM on the number of primary neurites compared to control CM treated neurons [$t=3.367$, $d.f.=9$, $p=0.0083$]. (Figure 3.23a).

Neuritic Branching

A Student's *t*-test demonstrated a significant effect of dbcAMP CM on the number of neuritic branches compared to control CM treated neurons [$t=2.727$, $d.f.=9$, $p=0.0023$]. (Figure 3.23b).

Neuritic Length

A Student's *t*-test demonstrated a significant effect of dbcAMP CM on the neuritic length compared to control CM treated neurons [$t=2.481$, $d.f.=9$, $p=0.0348$]. (Figure 3.23c).

(a) Primary Neurites*(b) Neuritic Branches**(c) Neuritic Length***Figure 3.23: DbcAMP CM increases all measures of neuronal complexity of primary cortical neurons**

Primary cortical neurons were treated for 24h with dbcAMP CM (300μM) from glial cells. Sholl analysis was then performed on the neurons. DbcAMP CM significantly increased (a) number of primary neurites (b) number of neuritic branches and (c) neuritic length compared to control CM treated neurons. Data expressed as mean + SEM, $n=5-6$. * $p<0.05$, ** $p<0.01$ vs. control CM (Student's t -test).

3.2.4.2 DbcAMP CM increases the Sholl profile of primary cortical neurons

A repeated measures two-way ANOVA demonstrated a significant effect of dbcAMP CM on the number of neuritic branches at specific distances from cell soma [$F_{(1,144)}=18.16$, $p=0.0021$]. ANOVA also demonstrated a significant effect of distance [$F_{(16,144)}=73.51$, $p<0.0001$] and a significant distance by treatment interaction [$F_{(16,144)}=3.45$, $p<0.0001$]. Furthermore *post-hoc* analysis revealed that dbcAMP CM had significantly more branches than control at 5, 15, 25, 35, 45 μ m ($p<0.01$) and 55 μ m ($p<0.05$) from the cell soma. [Figure 3.24, Newman-Keuls, $n=5-6$].

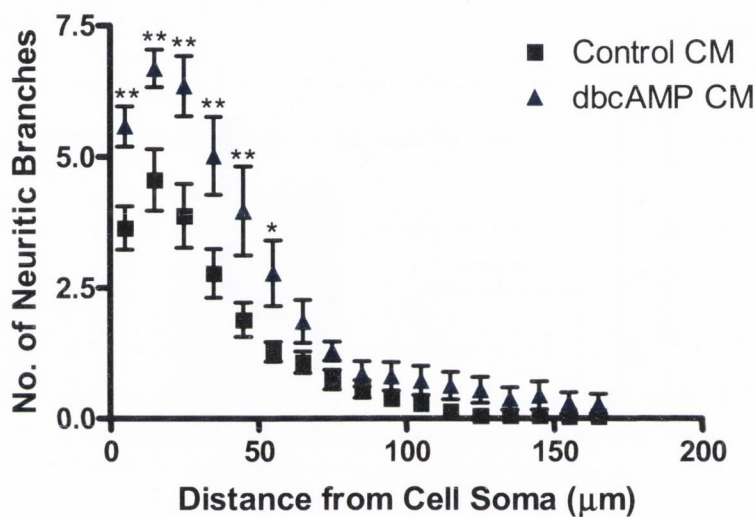


Figure 3.24: DbcAMP CM increases the Sholl profile of primary cortical neurons

Primary cortical neurons were treated for 24h with dbcAMP CM (300 μ M) from glial cells. Sholl analysis was then performed on the neurons. DbcAMP CM significantly increased the number of branches at 5, 15, 25, 35, 45 and 55 μ m from the cell soma compared to control CM treated neurons. Data expressed as means \pm SEM, $n=5-6$. ** $p<0.01$, * $p<0.05$ vs. control CM (Two-way repeated measures ANOVA followed by *post-hoc* Newman-Keuls).

3.2.4.3 Representative images for primary cortical neurons treated with dbcAMP CM

Primary cortical neurons were treated for 24h with dbcAMP CM from glial cells. Cells were then stained using fluorescent immunocytochemistry for the neuronal structural protein β III-tubulin and counter-stained with the cell body marker DAPI. Images (figure 3.25) show representative images for the dbcAMP CM experiment.

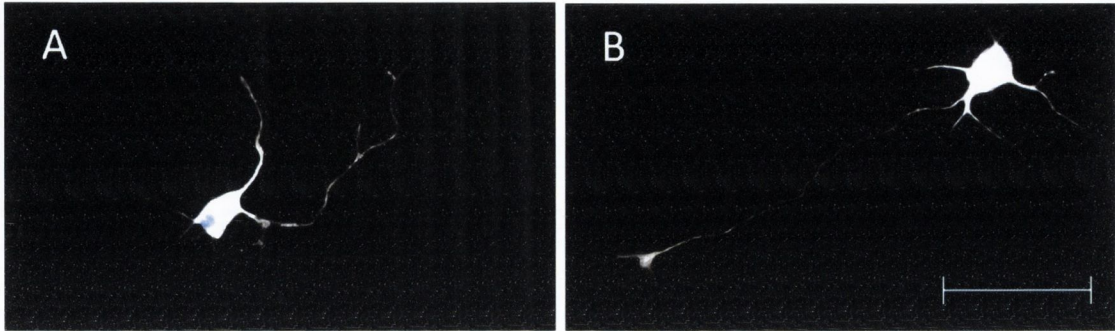


Figure 3.25: Representative images for primary cortical neurons treated with dbcAMP CM

Fluorescent immunocytochemistry with the neuronal structural protein β III-tubulin (white) and the cell body marker DAPI (blue) was carried out on primary cortical neurons treated with the CM from dbcAMP (300 μ M) treated mixed glial cells. All neurons were imaged by 200X magnification. Pictures correspond to representative images for (A) control neuron treated with control CM and neurons treated with dbcAMP CM (B), Scale bar is equal to 50 μ m.

3.3 NA stimulation of astrocytic β -adrenoceptors are responsible for the NA CM-induced increases in neuronal complexity

Primary mixed glial preparations are primarily composed of astrocytes (80-90%) and microglia (10-20%). As both cell types have been shown to express the β_2 -adrenoceptor (Kimelberg, 1995; Mori *et al.*, 2002), it was important to assess the roles of each cell type in enhancing neuronal complexity via the β_2 -adrenoceptor.

The aims of these studies were as follows:

- 1) To assess the ability of NA CM from cultures enriched in astrocytes and cultures enriched in microglia to induce morphological changes in primary cortical neurons.
- 2) To assess the ability of Salb CM and dbcAMP CM from enriched astrocytes to induce morphological changes in primary cortical neurons.

3.3.1 NA CM from enriched astrocytes increases neuronal complexity

Primary mixed glial cells were prepared as before. When cells reached confluency, the microglia were removed as described in the methods. Confluent astrocytes were then treated with control NBM or NA (10 μ M) in NBM. The cells were treated for 24h after which time the CM was collected, filtered and then used to treat 4 DIV primary cortical neurons for 24h. The neurons were then stained using fluorescent immunocytochemistry for β III-tubulin and after image acquisition, were analysed by Sholl analysis specifically to examine the number of primary neurites extending from the cell soma, the number of neuritic branches and the length of the longest neurite. In addition, cultures were stained using fluorescent immunocytochemistry for GFAP, to assess for astrocytic purity [figure 3.26].

3.3.1.2 NA CM from enriched astrocytes increases all measures of neuronal complexity of primary cortical neurons

Primary Neurites

A Student's *t*-test demonstrated a significant effect of NA CM on the number of primary neurites compared to control CM ($t=3.979$, d.f.=14, $p=0.0014$). [Figure 3.27a].

Neuritic Branching

A Student's *t*-test demonstrated a significant effect of NA CM on the number of neuritic branches compared to control CM ($t=3.711$, d.f.=14, $p=0.0023$). [Figure 3.27b].

Neuritic Length

A Student's *t*-test demonstrated a significant effect of NA CM on the neuritic length compared to control CM ($t=7.841$, d.f.=14, $p<0.0001$). [Figure 3.27c].

3.3.1.1 Representative images for enriched astrocyte culture

Primary enriched astrocytes were prepared as described in the methods. Cells were then stained using fluorescent immunocytochemistry for the astrocytic marker GFAP, the microglial marker CD11b and counter-stained with the cell body marker DAPI. No positive staining for CD11b was seen. Figure 3.26 shows representative images for enriched astrocytes.

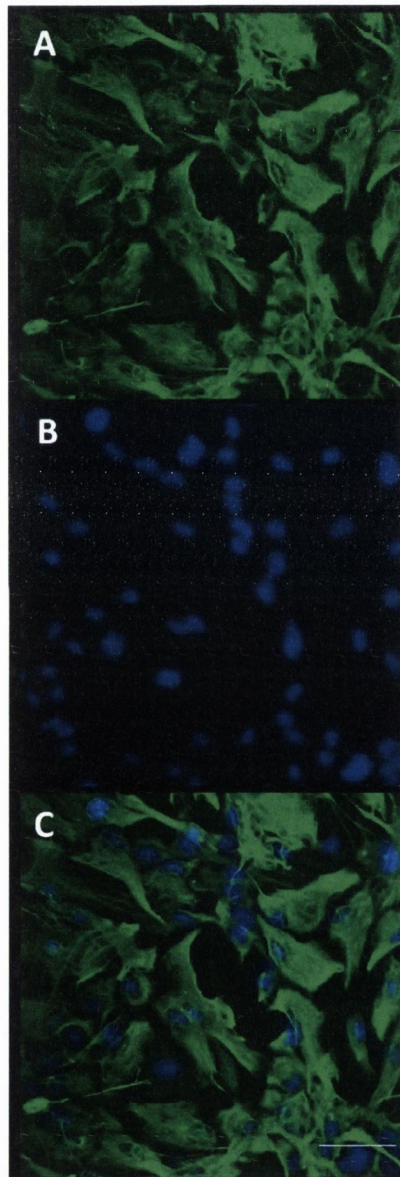


Figure 3.26: Representative images for enriched astrocyte culture

Primary enriched astrocytes were stained using fluorescent immunocytochemistry for the astrocytic marker GFAP (A, green) and counter-stained with DAPI (B, blue). Merged image C. Scale bar is equal to 50 μ m.

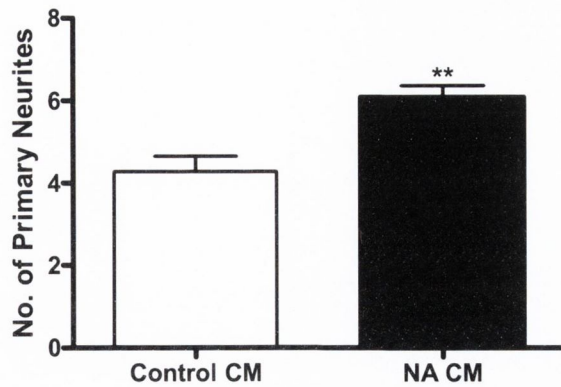
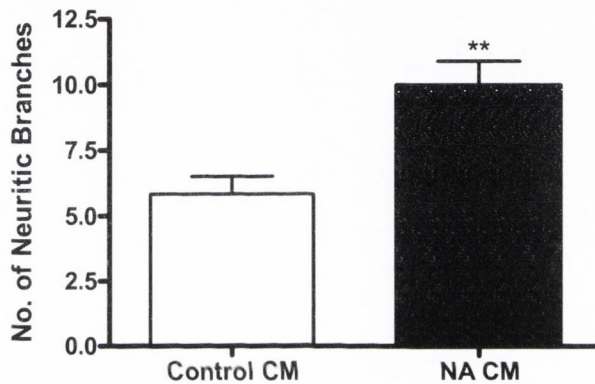
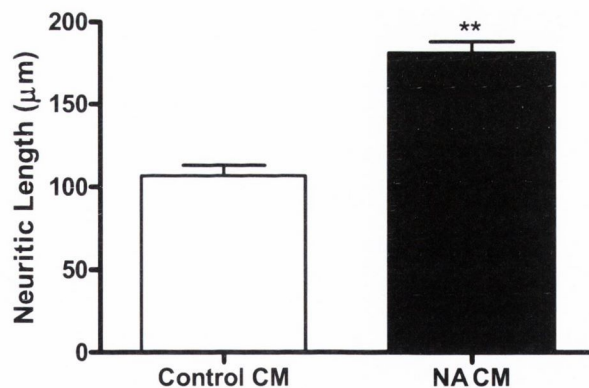
(a) Primary Neurites*(b) Neuritic Branches**(c) Neuritic Length*

Figure 3.27: NA CM from enriched astrocytes increases all measures of neuronal complexity of primary cortical neurons

Primary cortical neurons were treated for 24h with NA (10 μM) CM from astrocytes. Sholl analysis was then performed on the neurons. NA CM significantly increased (a) number of primary neurites (b) number of neuritic branches and (c) neuritic length compared to control CM treated neurons. Data are expressed as mean + SEM, $n=8$, ** $p<0.01$ vs. control CM (Student's t -test).

3.3.1.3 NA CM from enriched astrocytes increases the Sholl profile of primary cortical neurons

A two-way repeated measures ANOVA demonstrated a significant effect of NA CM on the number of neuritic branches at specific distances from cell soma [$F_{(1,224)}=25.988$, $p=0.0002$]. ANOVA also demonstrated a significant effect of distance [$F_{(16,224)}=200.339$, $p<0.0001$] and a significant distance by treatment interaction [$F_{(48, 224)}=3.455$, $p<0.0001$]. Furthermore *post-hoc* analysis revealed that NA CM had significantly more branches than control CM treated neurons at 5, 15, 25 μ m ($p<0.01$) and 35 μ m ($p<0.05$) from the cell soma. [Figure 3.28, Newman-Keuls, $n=8$].

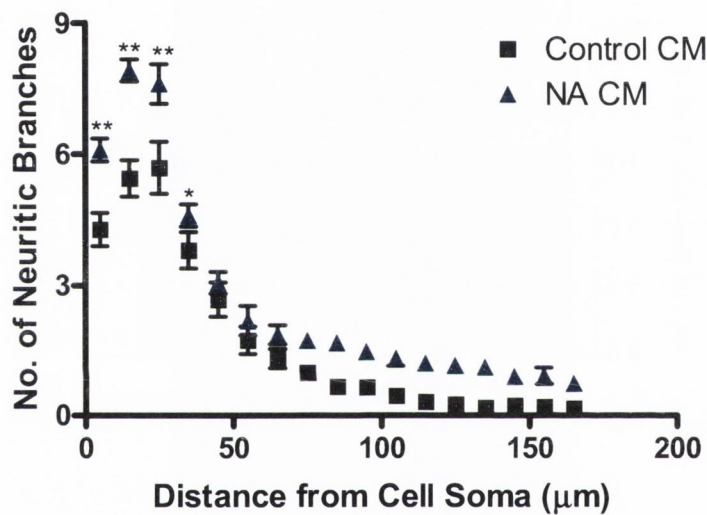


Figure 3.28: NA CM from enriched astrocytes increases the Sholl profile of primary cortical neurons
Primary cortical neurons were treated for 24h with NA (10 μ M) CM from astrocytes. Sholl analysis was then performed on the neurons. NA CM significantly increased the number of branches at 5, 15, 25 and 35 μ m from the cell soma compared to control CM treated neurons. Data expressed as means \pm SEM, $n=8$, ** $p<0.01$, * $p<0.05$ vs. control CM (Two-way repeated measures ANOVA followed by *post-hoc* Newman-Keuls).

3.3.4 NA CM from enriched microglia does not increase neuronal morphology

The previous section demonstrated that NA CM from enriched astrocytes enhanced the complexity of primary cortical neurons similarly to NA CM from a mixed glial culture. It was then important to establish if the microglia in a mixed glial culture are also involved in the enhancement of neuritic growth by NA CM. Therefore, purified primary microglia were prepared as described in the methods. Purified microglia were then treated with control or NA (10 μ M) in NBM. The cells were treated for 24h after which time the CM was collected, filtered and then used to treat 4 DIV primary cortical neurons for 24h. The neurons were then stained using fluorescent immunocytochemistry for β III-tubulin and after image acquisition, were analysed by Sholl analysis specifically to examine the number of primary neurites extending from the cell soma, the number of neuritic branches and the length of the longest neurite.

3.3.4.1 NA CM from enriched microglia had no effect on the number of neuritic branches or neuritic length and reduced the number of primary neurites of primary cortical neurons

Primary Neurites

A Student's *t*-test demonstrated a significant effect of NA CM on (A) number of primary neurites ($t=3.088$, d.f.=14, $p=0.0081$). [Figure 3.29a].

Neuritic Branching

A Student's *t*-test demonstrated no significant effect of NA CM (B) number of neuritic branches ($t=0.5246$, d.f.=14, $p=0.608$). [Figure 3.29b].

Neuritic Length

A Student's *t*-test demonstrated no significant effect of NA CM neuritic length ($t=0.004408$, d.f.=14, $p=9965$). [Figure 3.29c].

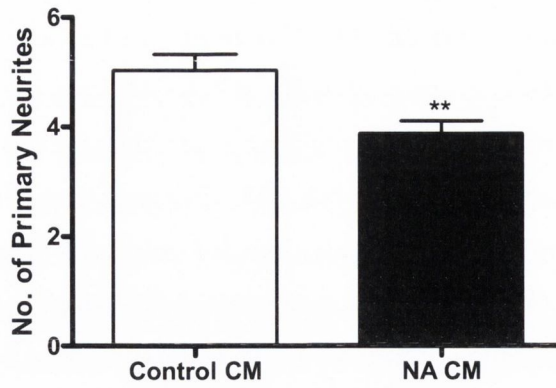
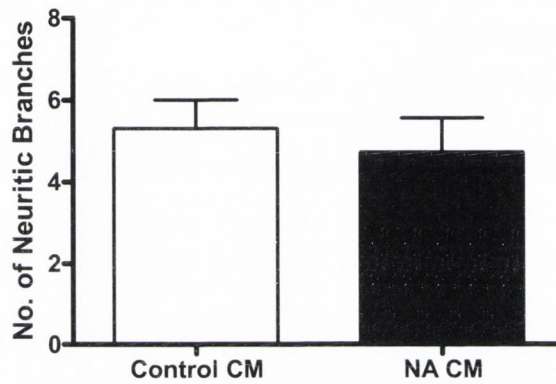
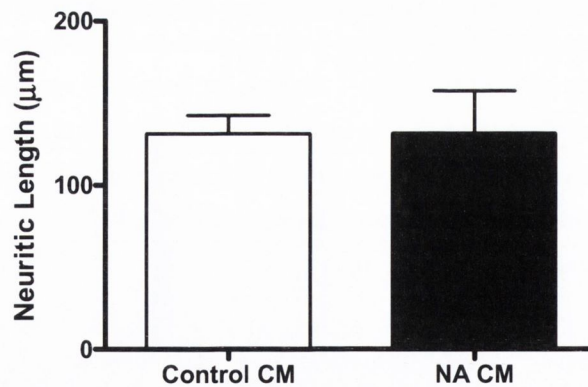
(a) Primary Neurites*(b) Neuritic Branches**(c) Neuritic Length*

Figure 3.29: NA CM from enriched microglia had no effect on the number of neuritic branches or neuritic length and reduced the number of primary neurites of primary cortical neurons

Primary cortical neurons were treated for 24h with the NA CM (10 μ M) from microglia. Sholl analysis was then performed on the neurons. NA CM significantly reduced the number of primary neurites and had no effect on the number of neuritic branches or the neuritic length. Data are expressed as mean + SEM, $n=8$ (Student's t -test).

3.3.4.2 NA CM from enriched microglia significantly reduced the Sholl profile of primary cortical neurons

A two-way repeated measures ANOVA demonstrated no significant effect of NA [$F_{(1,224)}=2.5148$, $p=0.1351$] but a significant effect of distance [$F_{(16,224)}=195.7$, $p<0.0001$]. There was no significant interaction between the two. Furthermore, *post-hoc* analysis revealed that NA CM had significantly less branches than control CM at 5 and 15 μm ($p<0.01$) from the cell soma. [Figure 3.30, Newman-Keuls, $n=8$].

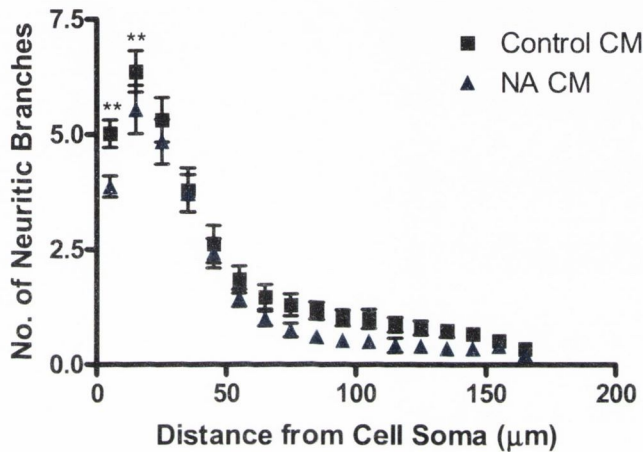


Figure 3.30: NA CM from enriched microglia significantly reduced the Sholl profile of primary cortical neurons

Primary cortical neurons were treated for 24h with NA CM (10 μM) from enriched microglia. Sholl analysis was then performed on the neurons. NA CM significantly reduced the number of neuritic branches at 5 and 15 μm from the cell soma compared to control. Data are expressed as mean \pm SEM, $n=8$ (Two-way repeated measures ANOVA followed by *post-hoc* Newman Keuls).

3.3.2 Salbutamol CM from enriched astrocytes increases neuronal complexity

Primary enriched astrocytes were prepared as described in the methods. Confluent astrocytes were then treated with control or Salb (10 μ M) in NBM. The cells were treated for 24h after which time the CM was collected, filtered and then used to treat 4 DIV primary cortical neurons for 24h. The neurons were then stained using fluorescent immunocytochemistry for β III tubulin and after image acquisition, were analysed by Sholl analysis specifically to examine the number of primary neurites extending from the cell soma, the number of neuritic branches and the length of the longest neurite.

3.3.2.1 Salb CM from enriched astrocytes increases the neuritic branching and neuritic length but not primary neurites of primary cortical neurons

Primary Neurites

A Student's *t*-test demonstrated no significant effect of Salb CM on the number of primary neurites compared to control CM ($t=1.45$, $d.f.=14$, $p=0.1692$). [Figure 3.31a].

Neuritic Branching

A Student's *t*-test demonstrated a significant effect of Salb CM on the number of neuritic branches compared to control CM ($t=2.388$, $d.f.=14$, $p=0.0316$). [Figure 3.31b].

Neuritic Length

A Student's *t*-test demonstrated a significant effect of Salb CM on the neuritic length compared to control CM ($t=3.712$, $d.f.=14$, $p=0.0023$). [Figure 3.31c].

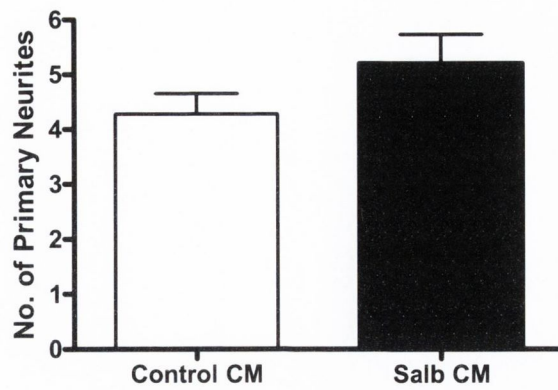
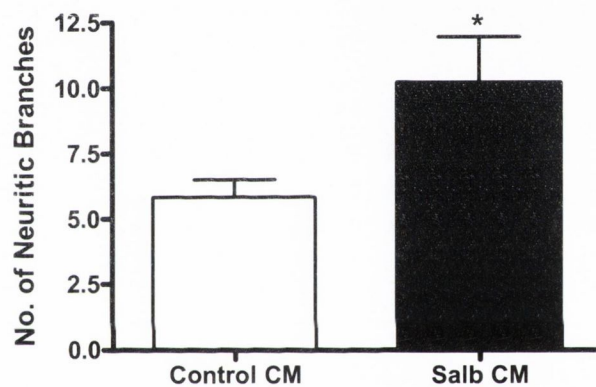
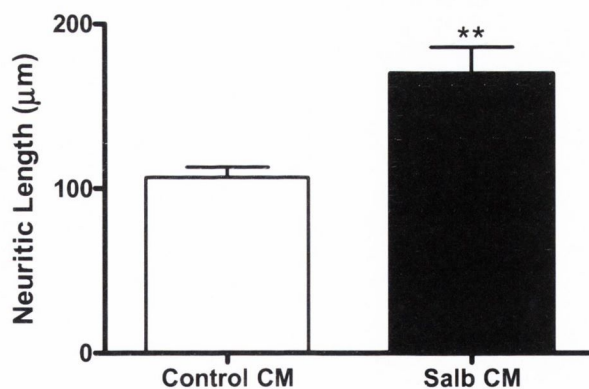
(a) Primary Neurites*(b) Neuritic Branches**(c) Neuritic Length*

Figure 3.31: Salb CM from enriched astrocytes increases the neuritic branching and neuritic length but not primary neurites of primary cortical neurons

Primary cortical neurons were treated for 24h with Salb (10µM) CM from astrocytes. Sholl analysis was then performed on the neurons. Salb CM significantly increased (b) number of neuritic branches and (c) neuritic length, but not (a) number of primary neurites. Data are expressed as mean + SEM, $n=8$, ** $p<0.01$, * $p<0.05$ vs. control CM (Student's t -test).

3.3.2.2 Salb CM from enriched astrocytes increases the Sholl profile of primary cortical neurons

A two-way repeated measures ANOVA demonstrated a significant effect of Salb (10 μ M) CM on the number of neuritic branches at specific points from the cell soma [$F_{(1,224)}=12.195$, $p=0.0036$]. ANOVA also showed that distance was significant [$F_{(16,224)}=99.58$, $p<0.0001$] but no significant distance by treatment interaction [$F_{(16,224)}=1.215$, $p=0.2571$]. Furthermore *post-hoc* analysis revealed that Salb CM had significantly more branches than control CM treated neurons at 5 ($p<0.05$), 15, 25, 35 and 45 μ m ($p<0.01$) from the cell soma. [Figure 3.32, Newman-Keuls, $n=8$].

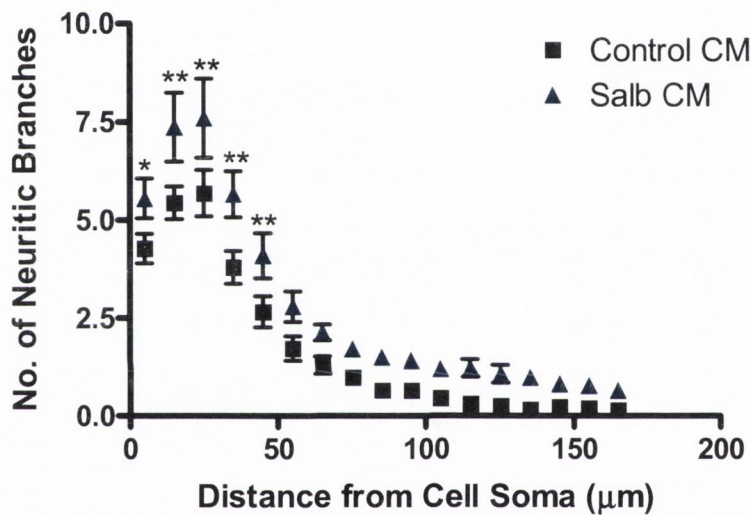


Figure 3.32: Salb CM from enriched astrocytes increases the Sholl profile of primary cortical neurons
Primary cortical neurons were treated for 24h with Salb (10 μ M) CM from enriched astrocytes. Sholl analysis was then performed on the neurons. Salb CM had significantly more branches than control CM treated neurons at 5, 15, 25, 35 and 45 μ m from the cell soma. Data are expressed as mean \pm SEM, $n=8$, * $p<0.05$, ** $p<0.01$ vs. control CM (Two way repeated measures ANOVA followed by *post-hoc* Newman-Keuls).

3.3.3 DbcAMP CM from enriched astrocytes increases neuronal complexity

Primary astrocytes were prepared as described in the methods. Confluent astrocytes were then treated with control or dbcAMP (300 μ M) in NBM. The cells were treated for 24h after which time the CM was collected, filtered and then used to treat 4 DIV primary cortical neurons for 24h. The neurons were then stained using fluorescent immunocytochemistry for β III-tubulin and after image acquisition, were analysed by Sholl analysis specifically to examine the number of primary neurites extending from the cell soma, the number of neuritic branches and the length of the longest neurite.

3.3.3.1 DbcAMP CM from enriched astrocytes increases all measures of neuronal complexity of primary cortical neurons

Primary Neurites

A Student's *t*-test demonstrated a significant effect of dbcAMP CM on the number of primary neurites ($t=4.511$, $d.f.=14$, $p=0.0005$). [Figure 3.33a].

Neuritic Branching

A Student's *t*-test demonstrated a significant effect of dbcAMP CM on the number of neuritic branches ($t=3.853$, $d.f.=14$, $p=0.0018$). [Figure 3.33b].

Neuritic Length

A Student's *t*-test demonstrated a significant effect of dbcAMP CM on the neuritic length ($t=6.009$, $d.f.=14$, $p<0.0001$). [Figure 3.33c].

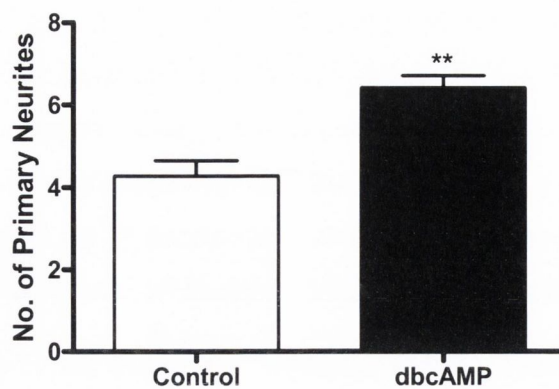
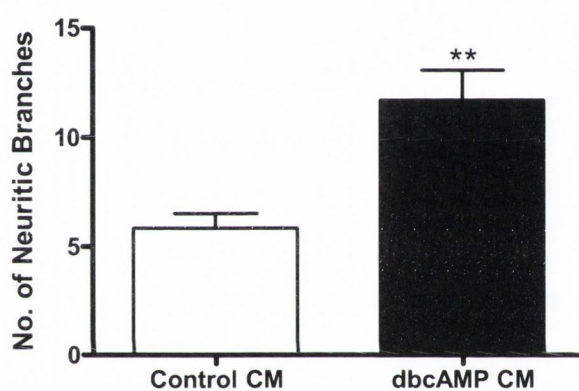
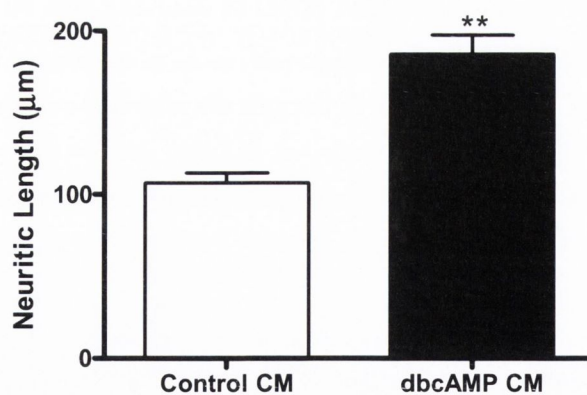
(a) Primary Neurites*(b) Neuritic Branches**(c) Neuritic Length*

Figure 3.33: DbcAMP CM from enriched astrocytes increases all measures of neuronal complexity of primary cortical neurons

Primary cortical neurons were treated for 24h with dbcAMP (300µM) CM from enriched astrocytes. Sholl analysis was then performed on the neurons. DbcAMP CM significantly increased (a) number of primary neurites (b) number of neuritic branches and (c) neuritic length compared to control CM treated neurons. Data expressed as mean + SEM, $n=8$. ** $p<0.01$ vs. control CM (Student's t -test).

3.3.3.2 DbcAMP CM from enriched astrocytes increases the Sholl profile of primary cortical neurons

A two-way repeated measures ANOVA demonstrated a significant effect of dbcAMP (300 μ M) on the number of neuritic branches at specific points from the cell soma [$F_{(1,224)}=41.958$, $p<0.0001$]. ANOVA also demonstrated a significant effect of distance [$F_{(16,224)}=148.566$, $p<0.0001$] and a significant distance by treatment interaction [$F_{(16,224)}=5.44$, $p<0.0001$]. Furthermore *post-hoc* analysis revealed that dbcAMP CM had significantly more branches than control CM treated neurons at 5, 15, 25, 35 ($p<0.01$) and 45 μ m ($p<0.05$) from the cell soma. [Figure 3.34, Newman-Keuls, $n=8$].

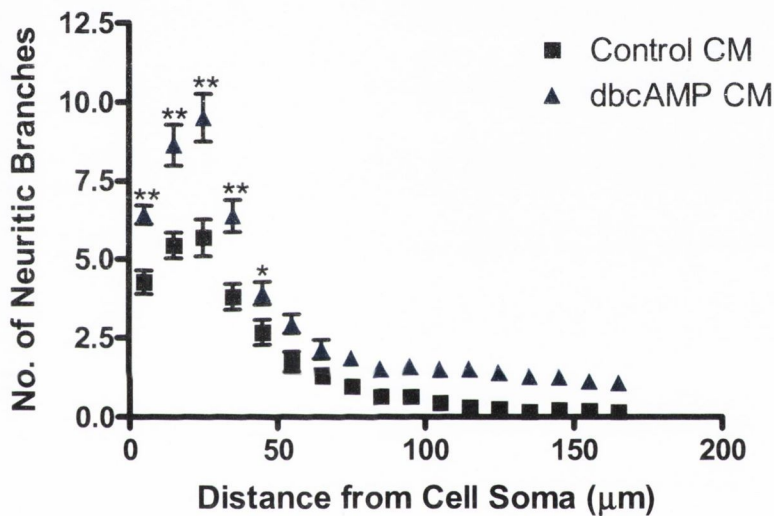


Figure 3.34: DbcAMP CM from enriched astrocytes increases the Sholl profile of primary cortical neurons

Primary cortical neurons were treated for 24h with dbcAMP (300 μ M) CM from enriched astrocytes. Sholl analysis was then performed on the neurons. DbcAMP CM had significantly more branches than control at 5, 15, 25, 35 and 45 μ m from the cell soma compared to control CM treated neurons. Data are expressed as mean \pm SEM, $n=8$, * $p<0.05$, ** $p<0.01$ vs. control CM (Two-way repeated measures ANOVA followed by *post-hoc* Newman-Keuls).

3.4 C6 glioma cells as a model of primary astrocytes

The previous section demonstrated that astrocytes in primary mixed glial culture are responsible for the ability of NA to induce morphological changes in primary cortical neurons. Therefore use of the C6 glioma cell line was examined as an alternative to primary astrocytes for studying the impact of β_2 -adrenoceptor activation on neuronal morphology.

The aims of these studies were as follows:

- 1) To assess the expression of the astrocytic markers S100 β and GFAP in the C6 glioma cell line.
- 2) To assess the expression of the β_2 -adrenoceptor in C6 glioma cells.
- 3) To assess the ability of NA CM from C6 glioma cells to induce morphological changes in primary cortical neurons.

3.4.1 C6 glioma cells express the astrocytic markers S100 β and GFAP

C6 glioma cells were fixed in methanol and stained using fluorescent immunocytochemistry for S100 β , GFAP and the nuclear marker DAPI. C6 glioma cells were shown to strongly express both S100 β and GFAP [Figure 3.35].

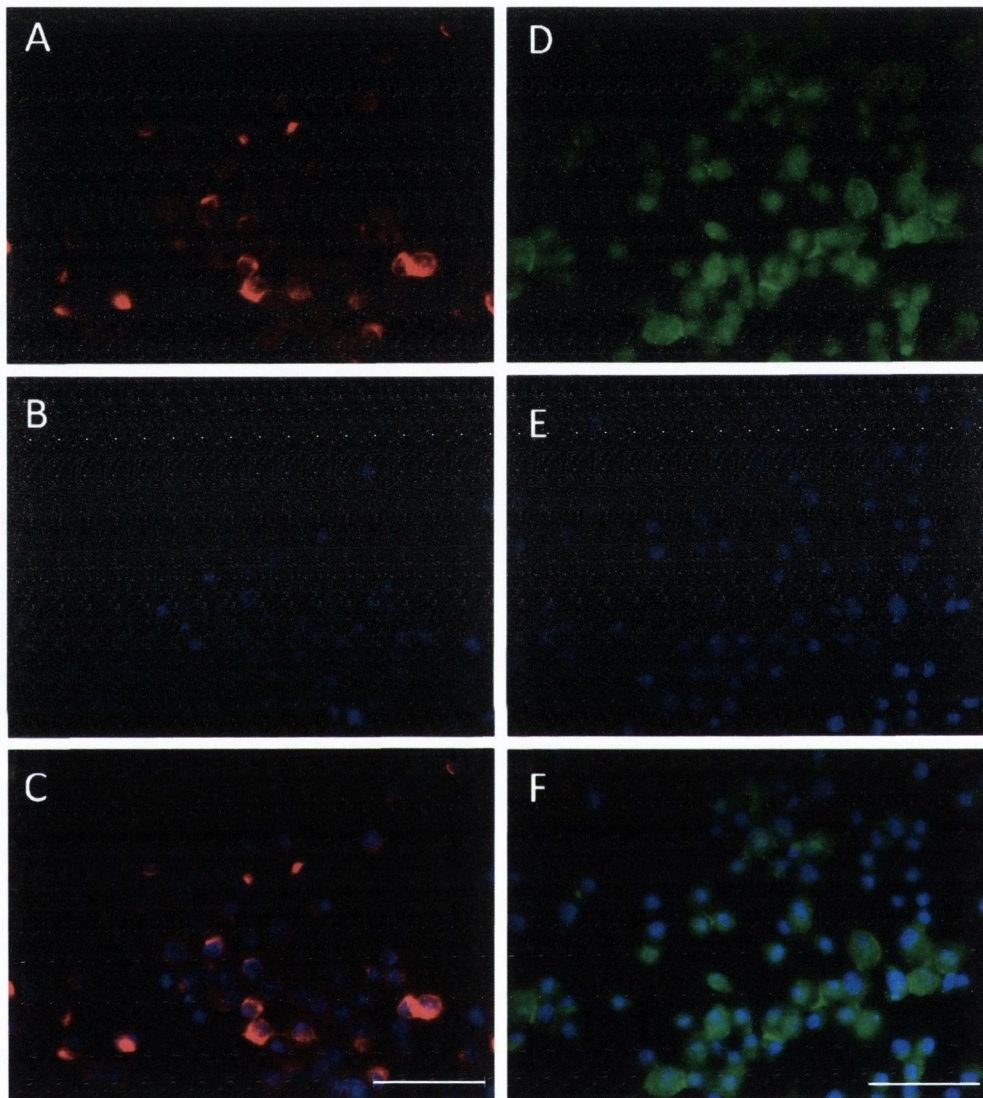


Figure 3.35: C6 glioma cells expression of S100 β and GFAP

C6 glioma cells were stained using fluorescent immunocytochemistry with S100 β (A, C), GFAP (D, F) and DAPI (B, C, E, F). C6 cells were shown to express the astrocytic marker S100 β . (A) S100 β , red (B) DAPI, blue and (C) co-localisation of S100 β and DAPI in C6 cells. Scale bar is equal to 50 μ m.

3.4.2 The C6 glioma cells express the β_2 -adrenoceptor

As the C6 cells were to be used to measure NA-induced morphological changes in neurons via the β_2 -adrenoceptor, it was imperative to examine if they express the β_2 -adrenoceptor. Therefore, C6 cells were grown in serum-free DMEM for 48h. Following this, the cells were harvested and prepared for Western blotting as described in the methods. Western immunoblot visualisation clearly shows the expression of the β_2 -adrenoceptor in all C6 glioma cell line samples at the 55kDa mark. β -actin was also clearly expressed at 43kDa. [Figure 3.36].

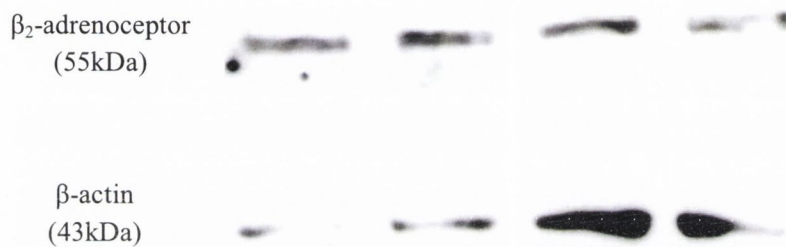


Figure 3.36: C6 glioma cells express the β_2 -adrenoceptor

Western blot analysis of C6 glioma cell lysates show that the β_2 adrenoceptor was expressed by the cells. β -actin was also expressed. ($n=4$).

3.4.3 NA CM from C6 glioma cells shows no effect on neuronal morphology

As with the primary astrocytes, the C6 cells were treated with NA (1, 10 μ M) for 24h. Following this, the CM was removed, filtered and used to treat primary cortical neurons for 24h. The neurons were then stained and assessed for changes in neuronal morphology by Sholl analysis.

Primary Neurites

A one-way ANOVA demonstrated no significant effect of NA treatment on the number of primary neurites extending from the cell soma [$F_{(2,13)}=1.019$, $p=0.388$]. [Figure 3.37a, $n=5-6$].

Neuritic Branches

A one-way ANOVA demonstrated no significant effect of NA treatment on the number of neuritic branches [$F_{(2,13)}=0.469$, $p=0.636$]. [Figure 3.37b, $n=5-6$].

Neuritic Length

A one-way ANOVA demonstrated no significant effect of NA treatment on the neuritic length [$F_{(2,13)}=0.95$, $p=0.4117$]. [Figure 3.37c, $n=5-6$].

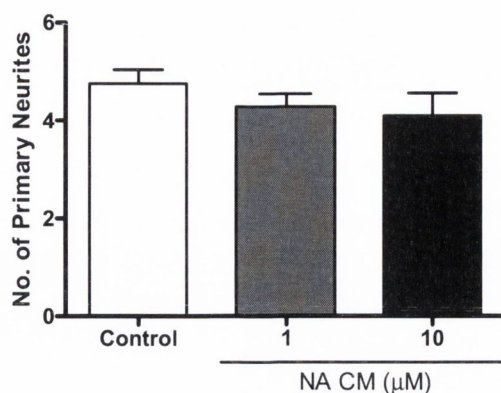
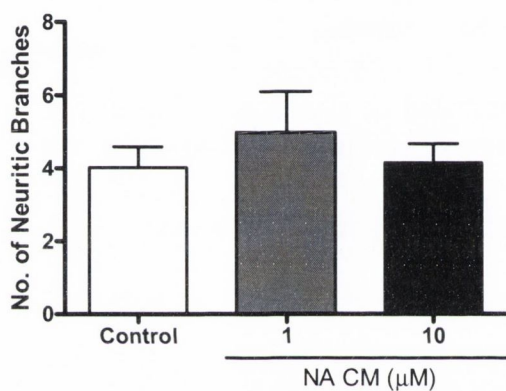
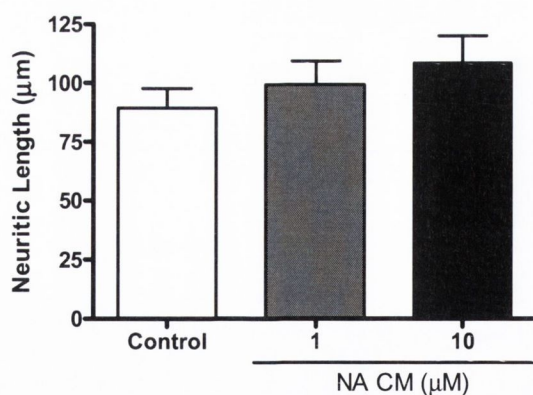
(a) Primary Neurites*(b) Neuritic Branches**(c) Neuritic Length*

Figure 3.37: NA CM from C6 cells had no effect on neuronal morphology

Primary cortical neurons were treated for 24h with the CM from C6 cells treated with NA (1, 10μM) for 24h. Sholl analysis was then performed on the neurons. NA CM had no effect of (a) Primary neurites, (b) neuritic branches or (c) neuritic length compared to control CM treated neurons. Data are expressed as mean + SEM, $n=5-6$. (One-way ANOVA).

3.5 A role for glial-derived growth factors in mediating the effects of NA CM on neuronal morphology

As the previous sections have described, NA treatment of primary glial cells via an action on the astrocytic β_2 -adrenoceptor, results in the release of soluble factors which induces morphological changes in primary cortical neurons. It was therefore important to examine potential mediators which might be resulting in these changes, to assess if the mediators could directly stimulate neuronal growth, and to see if neutralisation of these mediators could prevent NA CM-induced morphological changes.

The aims of these studies were as follows:

- 1) To examine the expression of a range of neuronal growth factors in glial cells following treatment with NA and the β -adrenoceptor agonist, salbutamol.
- 2) To examine the ability of a direct treatment of the selected growth factors to mimic the morphological changes induced by β -adrenoceptor activation.
- 3) To assess if neutralization of these growth factors in the NA CM could attenuate NA CM-induced increases in neuronal morphology.

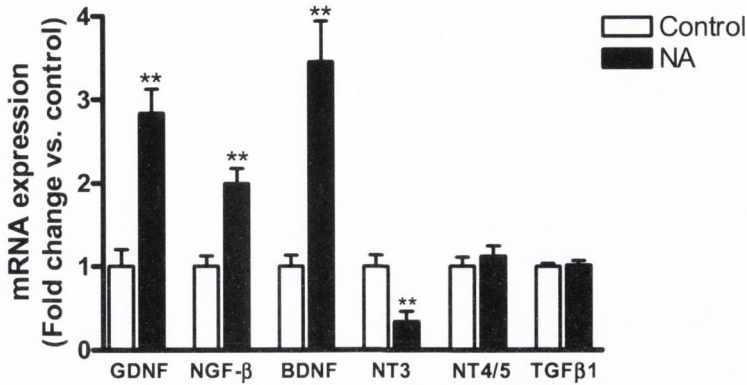
3.5.1 NA and Salb treatment of glial cells induce the expression of growth factors

Examination of any changes in mRNA levels of a particular protein is a rapid method of assessing the potential of a particular stimulus to increase the production of a protein (Guo *et al.*, 2008). Therefore, primary mixed glial cells were treated for 6h with NA or Salb and then harvested for mRNA expression as described in the methods.

3.5.1.1 NA treatment of glial cells leads to the increase in mRNA expression of several growth factors

A Student's *t*-test demonstrated a significant increase in the expression of GDNF ($t=5.263$, $p=0.0004$, $d.f.=10$), NGF- β ($t=4.518$, $p=0.0011$, $d.f.=10$), BDNF ($t=4.897$, $p=0.0006$, $d.f.=10$), FGF-2 ($t=6.534$, $p<0.0001$), VEGF ($t=8.68$, $p<0.0001$, $d.f.=10$) and IL-6 ($t=5.258$, $p=0.0005$, $d.f.=9$) and a significant decrease in expression of NT3 ($t=3.73$, $p=0.0039$, $d.f.=10$) and IGF-1 ($t=2.564$, $p=0.0282$, $d.f.=10$) in NA treated glial cells. No significant effect of NA treatment was found in NT4/5 ($t=0.7674$, $p=0.4606$, $d.f.=10$), TGF- β 1 ($t=0.2518$, $p=0.8063$, $d.f.=10$), CNTF ($t=2.031$, $p=0.0768$, $d.f.=8$) or IL-10 ($t=1.898$, $p=0.0869$, $d.f.=10$). [Figure 3.38, $n=5-6$].

(a)



(b)

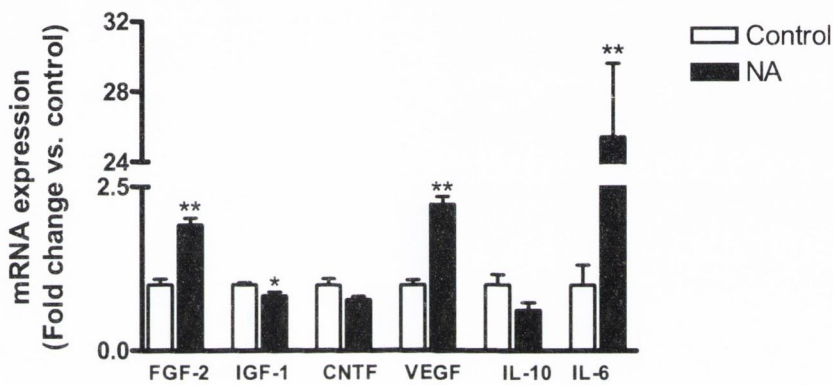


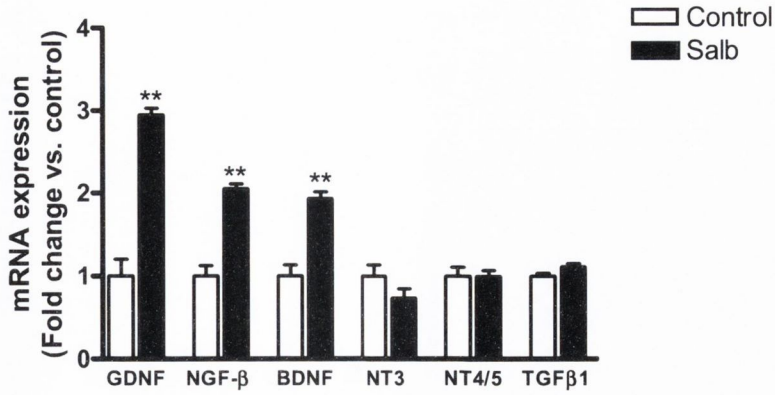
Figure 3.38: NA treatment of glial cells leads to the increase in mRNA expression of several growth factors

Glial cells were treated for 6h with noradrenaline and then harvested for mRNA expression. NA increased the expression of GDNF, NGF-β, BDNF (a) and FGF-2, VEGF and IL-6 (b). NA significantly reduced mRNA expression of NT3 (a) and IGF-1 (b). NT4/5, TGF-β1, CNTF and IL-10 remained unchanged. Data expressed as means + SEM, $n=5-6$, * $p<0.05$ vs. control, ** $p<0.01$ vs. control (Student's *t*-test).

3.5.1.2 Salb treatment of glial cells leads to the increase in mRNA expression of several growth factors

A Student's *t*-test demonstrated a significant increase in the expression of GDNF ($t=8.865$, $p<0.0001$, $d.f.=10$), NGF- β ($t=7.624$, $p<0.0001$, $d.f.=10$), BDNF ($t=5.809$, $p=0.0003$, $d.f.=10$) FGF-2 ($t=4.171$, $p=0.0019$), VEGF ($t=10.28$, $p<0.0001$, $d.f.=10$) and IL-6 ($t=4.799$, $p=0.001$, $d.f.=9$) and a significant decrease in the expression of IGF-1 ($t=2.37$, $p=0.0392$, $d.f.=10$) in Salb treated glial cells. No significant effect of Salb treatment was found in NT3 ($t=1.553$, $p=0.1514$, $d.f.=10$), NT4/5 ($t=0.0624$, $p=0.9515$, $d.f.=10$), TGF- β 1 ($t=2.195$, $p=0.0529$, $d.f.=10$), CNTF ($t=1.732$, $p=0.1215$, $d.f.=8$) or IL-10 ($t=1.193$, $p=0.2605$, $d.f.=10$). [Figure 3.39, $n=5-6$].

(a)



(b)

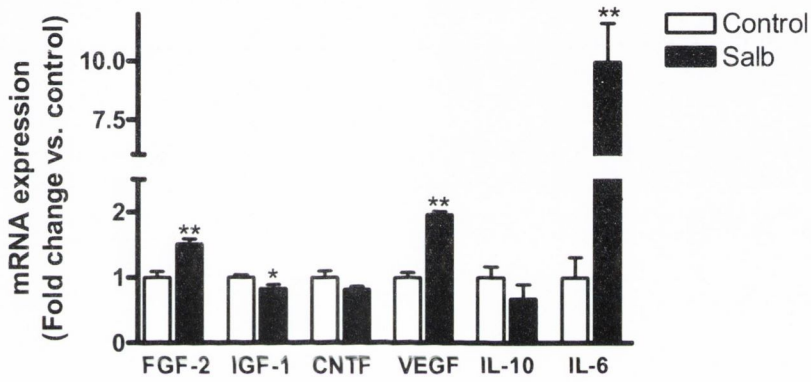


Figure 3.39: Salb treatment of glial cells leads to the increase in mRNA expression of several growth factors

Glial cells were treated for 6h with Salbutamol and then harvested for mRNA expression by qPCR. Salb increased the expression of GDNF, NGF- β , BDNF (a) and FGF-2, VEGF and IL-6 (b). Salb significantly reduced mRNA expression of IGF-1 (b). NT3, NT4/5, TGF- β 1, CNTF and IL-10 remained unchanged. Data expressed as means + SEM ($n=5-6$). * $p < 0.05$ vs. control, ** $p < 0.01$ vs. control (Student's t -test).

3.5.2 NA increases the release of growth factors from glial cells

In the previous sections, the growth factors GDNF, FGF-2, IL-6, NGF- β and BDNF were all shown to have increased mRNA expression following NA stimulation of primary mixed glial cells, it was therefore vital to ascertain whether NA stimulation of glial cells could induce the production of these factors for release into the CM. Therefore, glial cells were treated with NA (10 μ M) for 24h, after which time the CM was collected and analysed by ELISA for GDNF, NGF- β , IL-6, FGF-2, VEGF and BDNF.

3.5.2 NA stimulation enhances release of GDNF, FGF-2 and IL-6 from glial cells

A Student's *t*-test demonstrated a significant effect of NA on GDNF [$p=0.0065$, $t=3.422$, $d.f.=10$], FGF-2 [$p=0.0048$, $t=3.448$, $d.f.=12$]. IL-6 was not detected in control cultures, but clearly increased upon NA stimulation. There was no significant effect of NGF- β release [$p=0.1947$, $t=1.374$, $d.f.=12$] or VEGF release [$p=0.0893$, $t=1.848$, $d.f.=12$], while BDNF was undetected in both control and NA CM. [Figure 3.40].

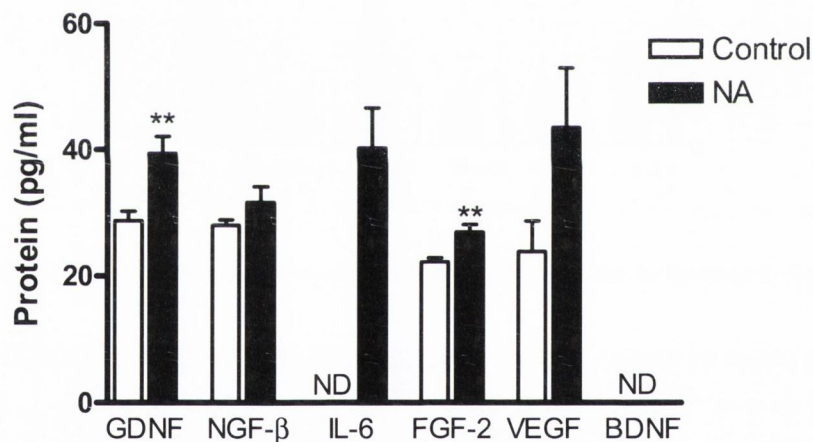


Figure 3.40: NA stimulation enhances release of GDNF, FGF-2 and IL-6 from glial cells

Glial cells were treated for 24h with NA (10 μ M), after which time the CM was analysed for protein release by ELISA. NA significantly increased the release of GDNF, IL-6 and FGF-2 from glial cells. There was no effect of NA on NGF- β or VEGF, and BDNF was undetected in the samples. Data expressed as means + SEM, $n=6-7$. ** $p<0.01$ vs. own control. ND=not detected. (Student's *t*-test).

3.5.3 GDNF increases neuronal complexity of primary cortical neurons

GDNF mRNA expression was significantly increased by both NA and Salb treatment of primary mixed glial cells. Therefore, the ability of GDNF to induce morphological changes in primary cortical neurons was assessed. Primary cortical neurons were treated with GDNF (1, 5, 10ng/ml) for 24h. As before, the neurons were stained using fluorescent immunocytochemistry for β III-tubulin and after image acquisition, were analysed by Sholl analysis specifically to determine the number of primary neurites extending from the cell soma, the number of neuritic branches and the length of the longest neurite.

3.5.3.1 GDNF increases all measures of neuronal complexity of primary cortical neurons

Primary Neurites

A one-way ANOVA demonstrated a significant effect of GDNF treatment on the number of primary neurites [$F_{(3,28)}=3.048$, $p=0.045$]. *Post-hoc* analysis revealed that GDNF 5ng/ml, ($p<0.01$) and 10ng/ml ($p<0.05$) treatment significantly increased the number of primary neurites extending from the cell soma as compared to control treated neurons. [Figure 3.41a, Fishers LSD, $n=8$].

Neuritic Branches

A one-way ANOVA demonstrated a significant effect of GDNF treatment on the number of neuritic branches [$F_{(3,28)}=3.96$, $p=0.018$]. *Post-hoc* analysis revealed that all doses of GDNF treatment significantly increased the number of neuritic branches compared to control treated neurons ($p<0.05$). [Figure 3.41b, Newman-Keuls, $n=8$].

Neuritic Length

A one-way ANOVA demonstrated a significant effect of GDNF treatment on the neuritic length [$F_{(3,28)}=11.41$, $p<0.0001$]. *Post-hoc* analysis revealed that all doses of GDNF treatment significantly increased the neuritic length compared to control treated neurons ($p<0.01$). [Figure 3.41c, Newman-Keuls, $n=8$].

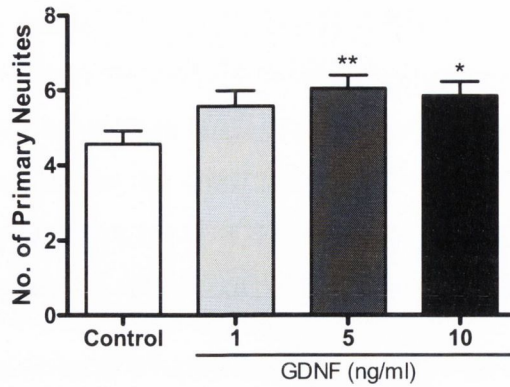
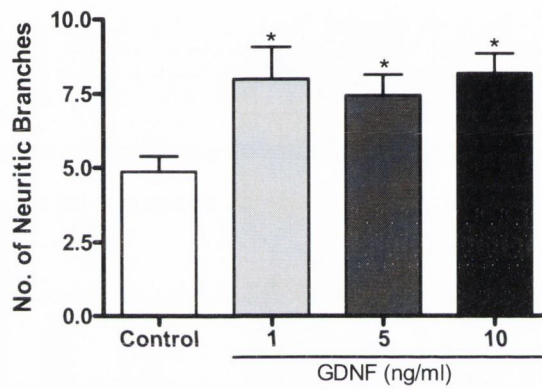
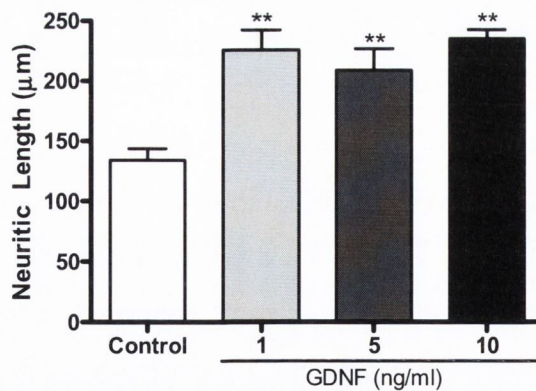
(a) Primary Neurites**(b) Neuritic Branches****(c) Neuritic Length**

Figure 3.41: GDNF increases all measures of neuronal complexity of primary cortical neurons

Primary cortical neurons were treated for 24h GDNF (1ng/ml, 5ng/ml, 10ng/ml). Sholl analysis was then performed on the neurons. GDNF significantly increased (a) number of primary neurites (b) number of neuritic branches and (c) neuritic length. Data expressed as mean + SEM ($n=8$). * $p<0.05$, ** $p<0.01$ vs. control (One-way ANOVA followed by *post-hoc* Newman-Keuls [b and c] or Fishers LSD [a]).

3.5.3.2 GDNF increases the Sholl profile of primary cortical neurons

A repeated measures two-way ANOVA demonstrated a significant effect of GDNF on the number of neuritic branches at specific distances from cell soma [$F_{(3,448)}=6.57$, $p=0.0017$]. ANOVA also demonstrated a significant effect of distance [$F_{(16,448)}=245.77$, $p<0.0001$] but no significant distance by treatment interaction. Furthermore, *post-hoc* analysis revealed that all doses of GDNF had significantly more branches ($p<0.05$ for 1ng/ml, $p<0.01$ for 5ng/ml and 10ng/ml) at 5, 15 and 25 μ m from the cell soma. In addition, GDNF (1ng/ml) had significantly more ($p<0.01$) branches at 35 μ m from the cell soma compared to control treated neurons. [Figure 3.42, Newman-Keuls, $n=8$].

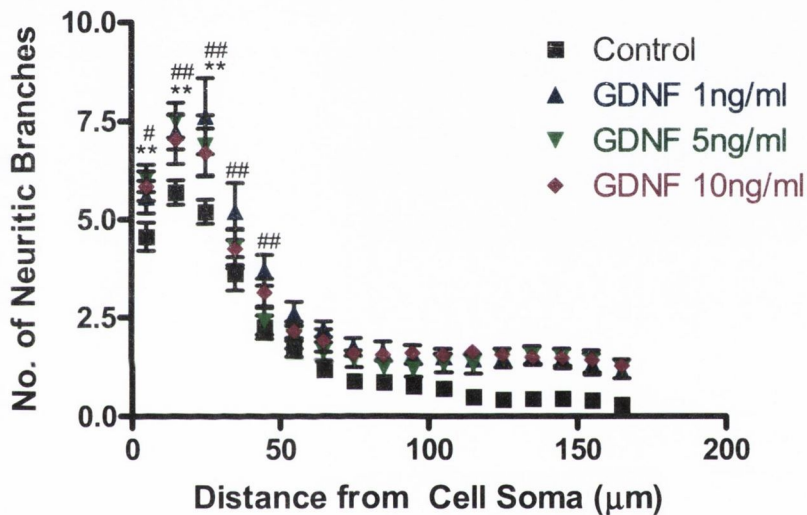


Figure 3.42: GDNF increases the Sholl profile of primary cortical neurons

Primary cortical neurons were treated for 24h with GDNF. Sholl analysis was then performed on the neurons. All doses of GDNF had significantly more branches at 5, 15 and 25 μ m from the cell soma. In addition, GDNF (1ng/ml) had significantly more branches at 35 μ m from the cell soma compared to control treated neurons. ** $p<0.01$ GDNF 5ng/ml and 10ng/ml vs. control, # $p<0.05$ GDNF 1ng/ml vs. control, ### $p<0.01$ GDNF 1ng/ml vs. control. Data expressed as means \pm SEM, $n=8$ (Two-way repeated measures ANOVA followed by *post-hoc* Newman-Keuls).

3.5.4 NGF- β increases neuronal complexity of primary cortical neurons

NGF- β mRNA expression was significantly increased by both NA and Salb treatment of primary mixed glial cells. Therefore, the ability of NGF- β to induce morphological changes in primary cortical neurons was assessed. Primary cortical neurons were treated with NGF- β (1, 5, 10ng/ml) for 24h. As before, the neurons were stained using fluorescent immunocytochemistry for β III-tubulin and after image acquisition, were analysed by Sholl analysis specifically to determine the number of primary neurites extending from the cell soma, the number of neuritic branches and the length of the longest neurite.

3.5.4.1 NGF- β increases all measures of neuronal complexity of primary cortical neurons

Primary Neurites

A one-way ANOVA demonstrated a significant effect of NGF- β treatment on the number of primary neurites [$F_{(3,27)}=3.85$, $p=0.0205$]. *Post-hoc* analysis revealed that all doses of NGF- β treatment increased the number of primary neurites extending from the cell soma as compared to control treated neurons ($p<0.05$). [Figure 3.43a, Newman-Keuls, $n=7-8$].

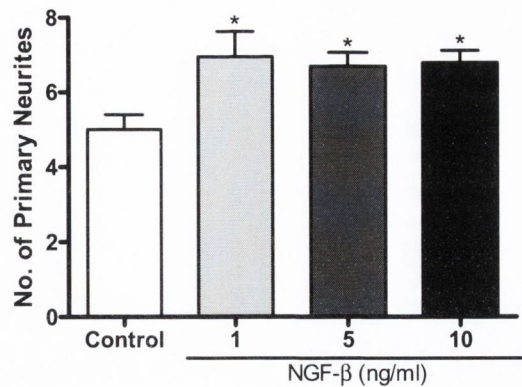
Neuritic Branching

A one-way ANOVA demonstrated a significant effect of NGF- β treatment on the number of neuritic branches [$F_{(3,27)}=5.907$, $p=0.0026$]. *Post-hoc* analysis revealed that all doses of NGF- β treatment increased the number of neuritic branches compared to control treated neurons ($p<0.05$). [Figure 3.43b, Newman-Keuls, $n=7-8$].

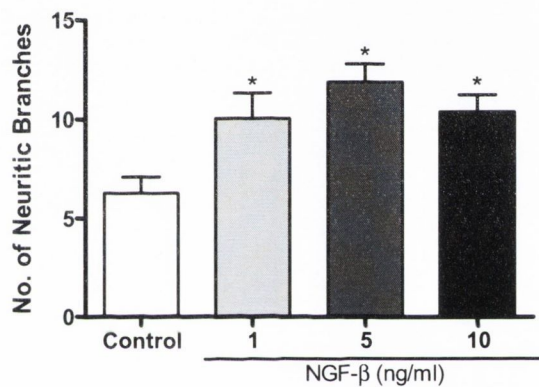
Neuritic Length

A one-way ANOVA demonstrated a significant effect of NGF- β treatment on the neuritic length [$F_{(3,27)}=5.052$, $p=0.0066$]. *Post-hoc* analysis revealed that all doses of NGF- β treatment significantly increased the neuritic length compared to control treated neurons ($p<0.05$). [Figure 3.43c, Newman-Keuls, $n=7-8$].

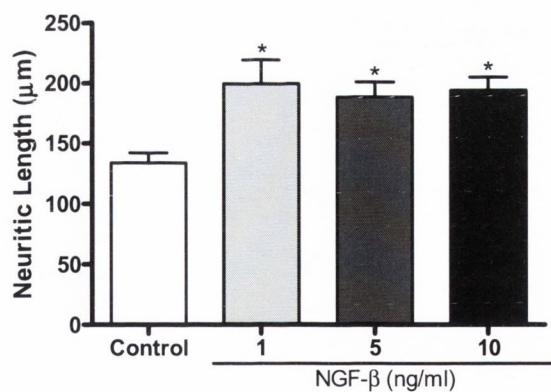
(a) Primary Neurites



(b) Neuritic Branches



(c) Neuritic Length

**Figure 3.43: NGF- β increases the complexity of primary cortical neurons**

Primary cortical neurons were treated for 24h NGF- β (1ng/ml, 5ng/ml, 10ng/ml). Sholl analysis was then performed on the neurons. NGF- β significantly increased (a) number of primary neurites (b) number of neuritic branches and (c) neuritic length. Data expressed as mean + SEM ($n=7-8$). * $p<0.05$ vs. control (One-way ANOVA followed by *post-hoc* Newman-Keuls).

3.5.4.2 NGF- β increases the Sholl profile of primary cortical neurons

A repeated measures two-way ANOVA demonstrated a significant effect of NGF- β on the number of neuritic branches at specific distances from cell soma [$F_{(3,432)}=11.33$, $p<0.0001$]. ANOVA also demonstrated a significant effect of distance [$F_{(16,432)}=286.79$, $p<0.0001$] and a significant distance by treatment interaction [$F_{(48, 432)}=4.75$, $p<0.0001$]. Furthermore *post-hoc* analysis revealed that all doses of NGF- β had significantly more branches than control at 5, 15, 25, 35 and 45 μm ($p<0.01$) from the cell soma while NGF- β (10ng/ml) in addition had significantly more branches at 55 μm ($p<0.05$) from the cell soma. [Figure 3.44, Newman-Keuls, $n=7-8$].

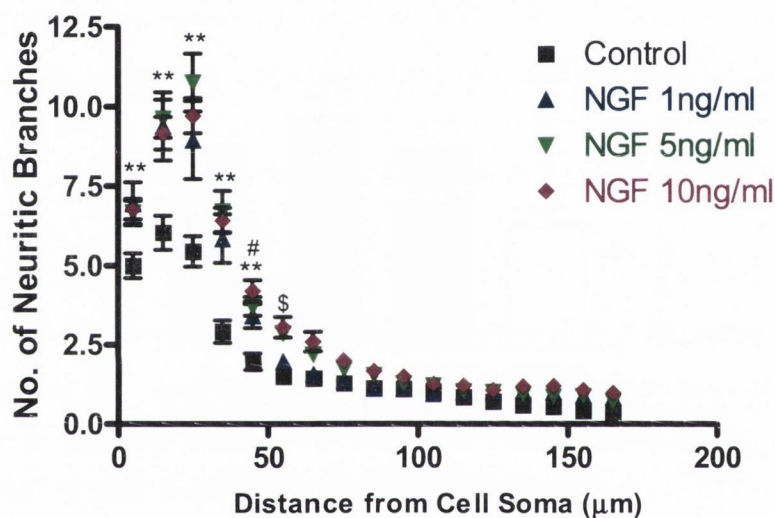


Figure 3.44: NGF- β treatment of neurons leads to an increase in Sholl profile complexity

Primary cortical neurons were treated for 24h with NGF- β . Sholl analysis was then performed on the neurons. All doses of NGF- β had significantly more branches at 5, 15, 25, 35 and 45 μm from the cell soma while NGF- β (10ng/ml) had significantly more branches in addition at 55 μm from the cell soma. Data expressed as means \pm SEM, $n=7-8$. # $p<0.05$ NGF- β (1ng/ml) vs. control, ** $p<0.01$ NGF- β (5ng/ml) vs. control, \$ $p<0.05$ NGF- β (10ng/ml) vs. control. (Two-way repeated measures ANOVA followed by *post-hoc* Newman-Keuls).

3.5.5 BDNF increases neuronal complexity of primary cortical neurons

BDNF mRNA expression was significantly increased by both NA and Salb treatment of primary mixed glial cells. Therefore, the ability of BDNF to induce morphological changes in primary cortical neurons was assessed. Primary cortical neurons were treated with BDNF (1, 5, 10ng/ml) for 24h. As before, the neurons were stained using fluorescent immunocytochemistry for β III-tubulin and after image acquisition, were analysed by Sholl analysis specifically to determine the number of primary neurites extending from the cell soma, the number of neuritic branches and the length of the longest neurite.

3.5.5.1 BDNF increases all measures of neuronal complexity of primary cortical neurons

Primary Neurites

A one-way ANOVA demonstrated a significant effect of BDNF treatment on the number of primary neurites [$F_{(3,20)}=12.93$, $p<0.0001$]. *Post-hoc* analysis revealed that all doses of IL-6 treatment ($p<0.05$ for 1ng/ml, $p<0.01$ for 5 and 10ng/ml) increased the number of neuritic branches compared to control treated neurons. [Figure 3.45a, Newman-Keuls, $n=6$].

Neuritic Branching

A one-way ANOVA demonstrated a significant effect of BDNF treatment on the number of neuritic branches [$F_{(3,20)}=3.53$, $p=0.0335$]. *Post-hoc* analysis revealed that IL-6 (5ng/ml) treatment significantly increased the number of neuritic branches compared to control treated neurons ($p<0.05$). [Figure 3.45b, Newman-Keuls, $n=6$].

Neuritic Length

A one-way ANOVA demonstrated a significant effect of BDNF treatment on the neuritic length [$F_{(3,20)}=8.86$, $p=0.0006$]. *Post-hoc* analysis revealed that all doses of IL-6 treatment significantly increased the neuritic length compared to control treated neurons ($p<0.01$). [Figure 3.45c, Newman-Keuls, $n=6$].

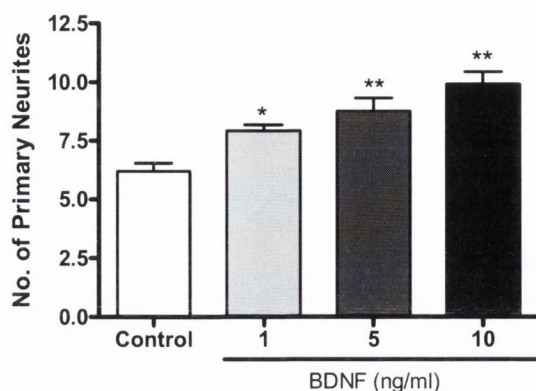
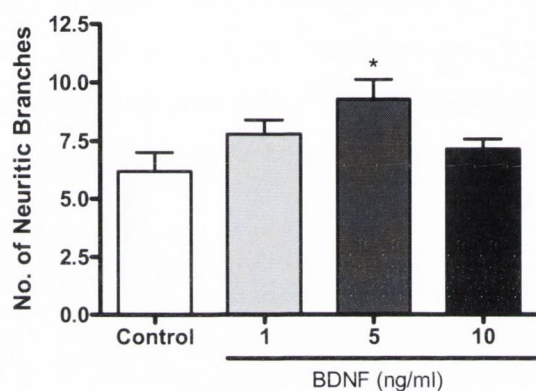
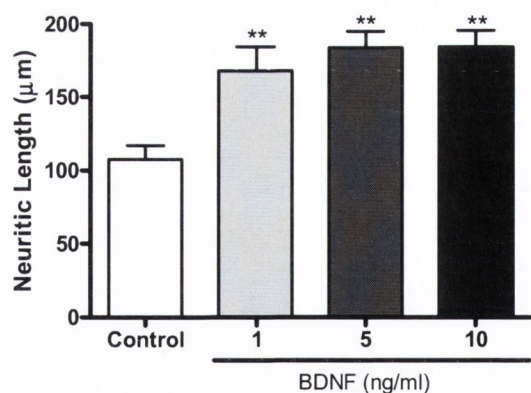
(a) Primary Neurites**(b) Neuritic Branches****(c) Neuritic Length**

Figure 3.45: BDNF increases all measures of neuronal complexity of primary cortical neurons

Primary cortical neurons were treated for 24h with BDNF (1ng/ml, 5ng/ml, 10ng/ml). Sholl analysis was then performed on the neurons. BDNF significantly increased (a) number of primary neurites (b) number of neuritic branches and (c) neuritic length. Data expressed as mean + SEM, $n=6$. ** $p<0.01$, * $p<0.05$ vs. control (One-way ANOVA followed by *post-hoc* Newman-Keuls).

3.5.5.2 BDNF increases the Sholl profile of primary cortical neurons

A repeated measures two-way ANOVA demonstrated a significant effect of BDNF on the number of neuritic branches at specific distances from cell soma [$F_{(3,320)}=8.826$, $p=0.0006$]. ANOVA also demonstrated a significant effect of distance [$F_{(16,320)}=434.289$, $p<0.0001$] and a significant distance by treatment interaction [$F_{(48,320)}=3.928$, $p<0.0001$]. Furthermore *post-hoc* analysis revealed that all doses of BDNF had significantly more branches than control at 5, 15 and 25 μm ($p<0.01$) from the cell soma while BDNF (1ng/ml and 5ng/ml) in addition had significantly more branches at 35 μm ($p<0.01$) and 45 μm ($p<0.05$) from the cell soma. [Figure 3.46, Newman-Keuls, $n=6$].

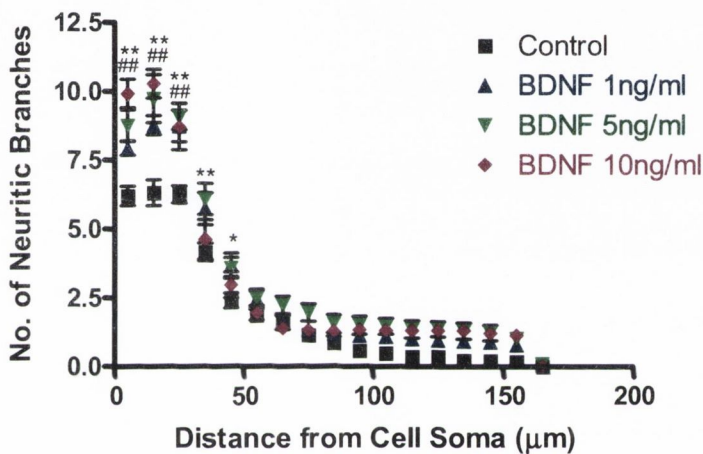


Figure 3.46: BDNF treatment of neurons leads to an increase in Sholl profile complexity

Primary cortical neurons were treated for 24h with BDNF. Sholl analysis was then performed on the neurons. All doses of BDNF had significantly more branches at 5, 15 and 25 μm , from the cell soma while BDNF (1ng/ml and 5ng/ml) also had significantly more branches at 35 μm and 45 μm from the cell soma. Data expressed as means \pm SEM ($n=6$), *, $p<0.05$, ** $p<0.01$ BDNF 1ng/ml and 5ng/ml vs. control, ### $p<0.01$ BDNF 10ng/ml vs. control (Two-way repeated measures ANOVA followed by *post-hoc* Newman-Keuls).

3.5.6 FGF-2 increases neuronal complexity of primary cortical neurons

FGF-2 mRNA expression was significantly increased by both NA and Salb treatment of primary mixed glial cells. Therefore, the ability of FGF-2 to induce morphological changes in primary cortical neurons was assessed. Primary cortical neurons were treated with FGF-2 (1, 5, 10ng/ml) for 24h. As before, the neurons were stained using fluorescent immunocytochemistry for β III-tubulin and after image acquisition, were analysed by Sholl analysis specifically to determine the number of primary neurites extending from the cell soma, the number of neuritic branches and the length of the longest neurite.

3.5.6.1 FGF-2 increases all measures of neuronal complexity of primary cortical neurons

Primary Neurites

A one-way ANOVA demonstrated a significant effect of FGF-2 treatment on the number of primary neurites [$F_{(3,20)}=9.395$, $p=0.0004$]. *Post-hoc* analysis revealed that all doses of FGF-2 treatment increased the number of neuritic branches compared to control treated neurons ($p<0.01$). [Figure 3.47a, Newman-Keuls $n=6$].

Neuritic Branching

A one-way ANOVA demonstrated a significant effect of FGF-2 treatment on the number of neuritic branches [$F_{(3,20)}=4.369$, $p=0.0161$]. *Post-hoc* analysis revealed that all doses of FGF-2 treatment significantly increased the number of neuritic branches compared to control treated neurons ($p<0.05$). [Figure 3.47b, Newman-Keuls, $n=6$].

Neuritic Length

A one-way ANOVA demonstrated a significant effect of FGF-2 treatment on the neuritic length [$F_{(3,20)}=4.318$, $p=0.0168$]. *Post-hoc* analysis revealed that all doses of FGF-2 treatment significantly increased the neuritic length compared to control treated neurons ($p<0.05$). [Figure 3.47c, Newman-Keuls, $n=6$].

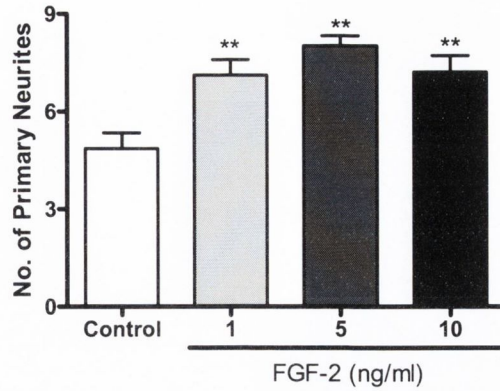
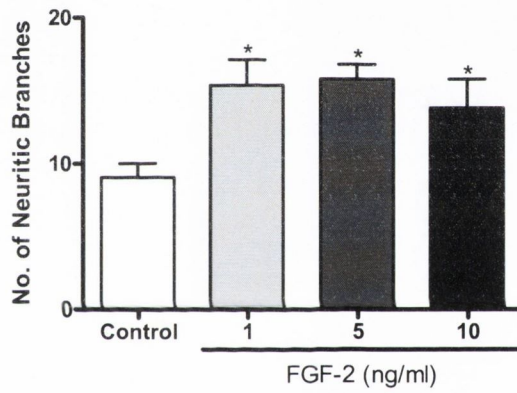
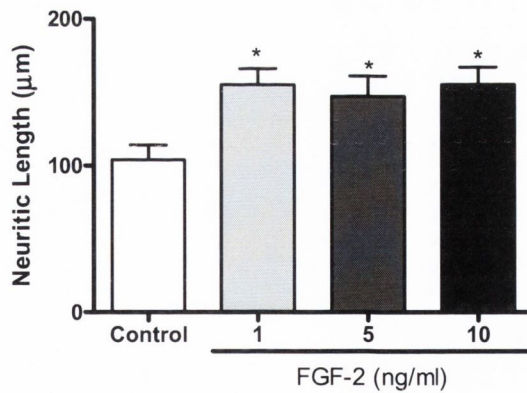
(a) Primary Neurites*(b) Neuritic Branches**(c) Neuritic Length*

Figure 3.47: Direct treatment of neurons with FGF-2 increases the complexity of primary cortical neurons

Primary cortical neurons were treated for 24h with FGF-2 (1ng/ml, 5ng/ml, 10ng/ml). Sholl analysis was then performed on the neurons. FGF-2 significantly increased (a) number of primary neurites (b) number of neuritic branches and (c) neuritic length. Data expressed as mean + SEM ($n=6$). ** $p<0.01$, * $p<0.05$ vs. control (One-way ANOVA followed by *post-hoc* Newman-Keuls).

3.5.6.2 FGF-2 increases the Sholl profile of primary cortical neurons

A repeated measures two-way ANOVA demonstrated a significant effect of FGF-2 on the number of neuritic branches at specific distances from cell soma [$F_{(3,320)}=4.622$, $p=0.013$]. ANOVA also demonstrated a significant effect of distance [$F_{(16,320)}=322.54$, $p<0.0001$] and a significant distance by treatment interaction [$F_{(48, 320)}=3.23$, $p<0.0001$]. Furthermore, *post-hoc* analysis revealed that all doses of FGF-2 had significantly more branches than control at 5, 15, 25 and 35 μ m from the cell soma ($p<0.01$), in addition FGF-2 had significantly more branches than control at 45 μ m for both 1ng/ml ($p<0.05$) and 5ng/ml ($p<0.01$). [Figure 3.48, Newman-Keuls, $n=6$].

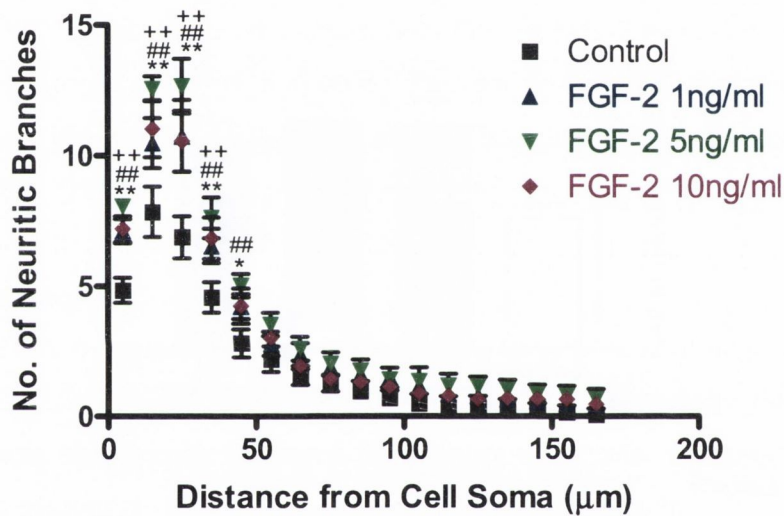


Figure 3.48: FGF-2 treatment of neurons show an enhanced Sholl profile

Primary cortical neurons were treated for 24h with FGF-2. Sholl analysis was then performed on the neurons. All doses of FGF-2 had significantly more branches at 5, 15, 25 and 35 μ m from the cell soma, in addition 1ng/ml and 5ng/ml had significantly more branches than control at 45 μ m from the cell soma. * $p<0.05$, ** $p<0.01$ FGF-2 1ng/ml vs. control, ## $p<0.01$ FGF-2 5ng/ml vs. control, ++ $p<0.01$ FGF-2 10ng/ml vs. control. Data expressed as means \pm SEM, $n=6$ (Two-way repeated measures ANOVA followed by *post-hoc* Newman-Keuls).

3.5.7 VEGF does not increase neuronal complexity of primary cortical neurons

VEGF mRNA expression was significantly increased by both NA and Salb treatment of primary mixed glial cells. Therefore, the ability of VEGF to induce morphological changes in primary cortical neurons was assessed. Primary cortical neurons were treated with VEGF (1, 5, 10ng/ml) for 24h. As before, the neurons were stained using fluorescent immunocytochemistry for β III-tubulin and after image acquisition, were analysed by Sholl analysis specifically to determine the number of primary neurites extending from the cell soma, the number of neuritic branches and the length of the longest neurite.

3.5.6.1 VEGF has no effect on the neuronal complexity of primary cortical neurons

Primary Neurites

A one-way ANOVA demonstrated no significant effect of VEGF treatment on the number of primary neurites [$F_{(3,20)}=2.08$, $p=0.135$]. [Figure 3.49a, $n=6$].

Neuritic Branching

A one-way ANOVA demonstrated no significant effect of VEGF treatment on the number of neuritic branches [$F_{(3,20)}=1.138$, $p=0.357$]. [Figure 3.49b, $n=6$].

Neuritic Length

A one-way ANOVA demonstrated no significant effect of VEGF treatment on the neuritic length [$F_{(3,20)}=1.81$, $p=0.178$]. [Figure 3.49c, $n=6$].

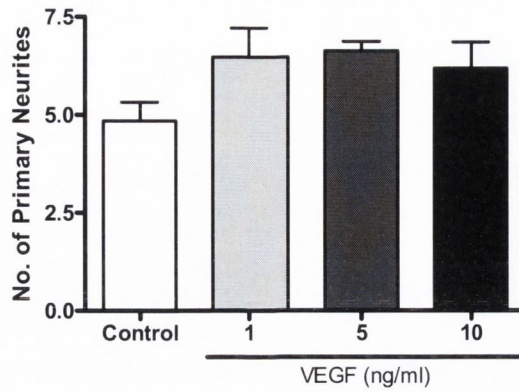
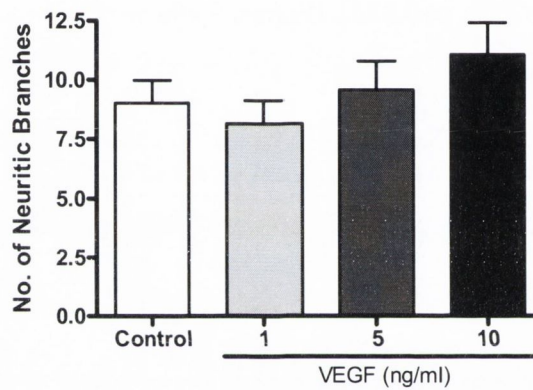
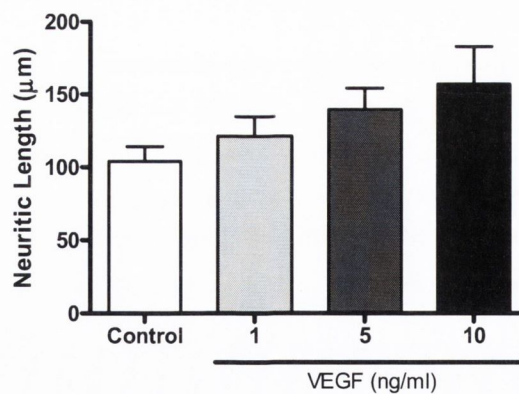
(a) Primary Neurites*(b) Neuritic Branches**(c) Neuritic Length*

Figure 3.49: Direct treatment of neurons with VEGF has no effect on the complexity of primary cortical neurons

Primary cortical neurons were treated for 24h with VEGF (1ng/ml, 5ng/ml, 10ng/ml). Sholl analysis was then performed on the neurons. VEGF had no effect on (a) number of primary neurites (b) number of neuritic branches and (c) neuritic length. Data expressed as mean + SEM, $n=6$ (One-way ANOVA).

3.5.7.2 VEGF increases the Sholl profile of primary cortical neurons

A repeated measures two-way ANOVA demonstrated no significant effect of VEGF on the number of neuritic branches at specific distances from cell soma [$F_{(3,320)}=0.905$, $p=0.4561$]. ANOVA demonstrated a significant effect of distance [$F_{(16,320)}=215.25$, $p<0.0001$] but no significant distance by treatment interaction. Furthermore, *post-hoc* analysis revealed that 1ng/ml VEGF had significantly more branches than control at 5 μ m from the cell soma ($p<0.05$), 5ng/ml VEGF had significantly more branches than control at 5 μ m ($p<0.05$) and 25 μ m ($p<0.01$) from the cell soma, while 10ng/ml VEGF had significantly more branches than control at 25 μ m ($p<0.01$) and 35 μ m ($p<0.05$) from the cell soma. [Figure 3.50, Newman-Keuls, $n=6$].

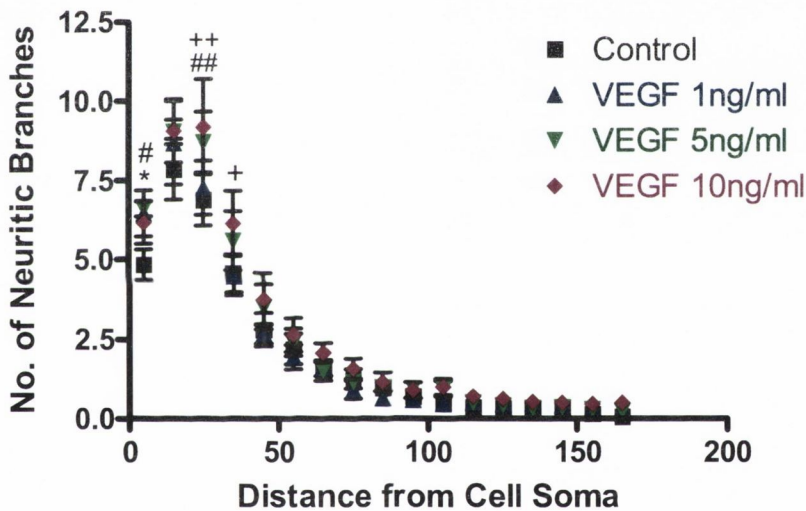


Figure 3.50: VEGF increases the Sholl profile of primary cortical neurons

Primary cortical neurons were treated for 24h with VEGF. Sholl analysis was then performed on the neurons. 1ng/ml VEGF had significantly more branches than control at 5 μ m from the cell soma, 5ng/ml VEGF had significantly more branches than control at 5 μ m and 25 μ m from the cell soma, while 10ng/ml VEGF had significantly more branches than control at 25 μ m and 35 μ m from the cell soma. * $p<0.01$ VEGF 1ng/ml vs. control, # $p<0.05$, ## $p<0.01$ VEGF 5ng/ml vs. control, + $p<0.05$, ++ $p<0.01$ VEGF 10ng/ml vs. control. Data expressed as means \pm SEM, $n=6$ (Two-way repeated measures ANOVA followed by *post-hoc* Newman-Keuls).

3.5.8 IL-6 increases neuronal complexity of primary cortical neurons

IL-6 mRNA expression was significantly increased by both NA and Salb treatment of primary mixed glial cells. Therefore, the ability of IL-6 to induce morphological changes in primary cortical neurons was assessed. Primary cortical neurons were treated with IL-6 (1, 5, 10ng/ml) for 24h. As before, the neurons were stained using fluorescent immunocytochemistry for β III-tubulin and after image acquisition were analysed by Sholl analysis specifically to determine the number of primary neurites extending from the cell soma, the number of neuritic branches and the length of the longest neurite.

3.5.8.1 IL-6 increases neuritic branching and neuritic length of primary cortical neurons

Primary Neurites

A one-way ANOVA revealed no effect of IL-6 treatment on the number of primary neurites [$F_{(3,20)}=1.019$, $p=0.405$]. [Figure 3.51a, $n=6$].

Neuritic Branching

A one-way ANOVA demonstrated a significant effect of IL-6 treatment on the number of neuritic branches [$F_{(3,20)}=12.28$, $p<0.0001$]. *Post-hoc* analysis revealed that all doses of IL-6 treatment increased the number of neuritic branches compared to control treated neurons ($p<0.01$). [Figure 3.51b, Newman-Keuls, $n=6$].

Neuritic Length

A one-way ANOVA demonstrated a significant effect of IL-6 treatment on the neuritic length [$F_{(3,20)}=11.09$, $p=0.0002$]. *Post-hoc* analysis revealed that all doses of IL-6 treatment significantly increased the neuritic length compared to control treated neurons ($p<0.01$). [Figure 3.51c, Newman-Keuls, $n=6$].

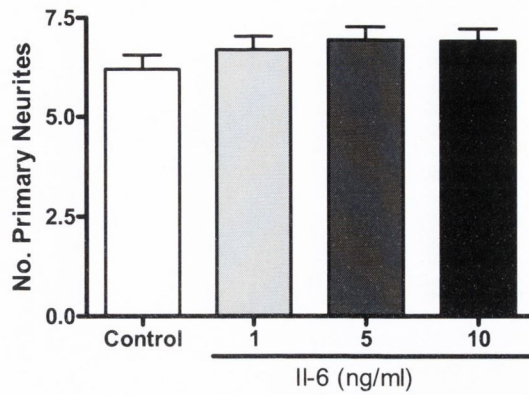
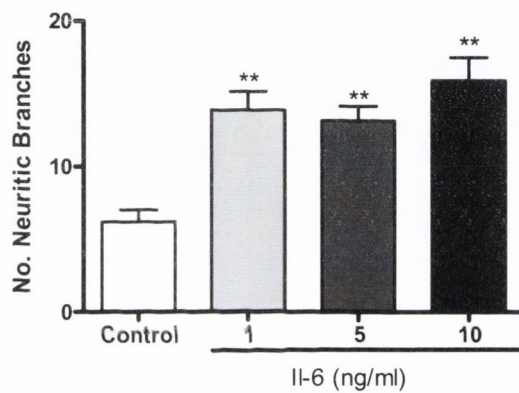
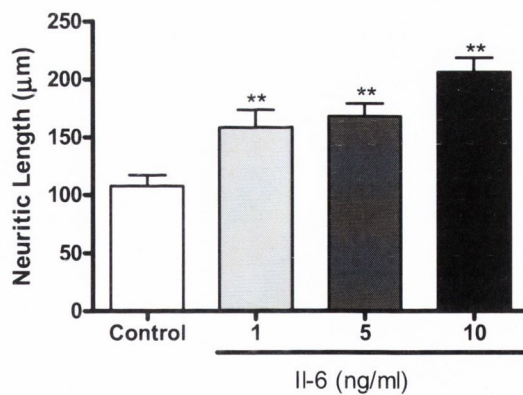
(a) Primary Neurites**(b) Neuritic Branches****(c) Neuritic Length**

Figure 3.51: IL-6 increases neuritic branching and neuritic length of primary cortical neurons

Primary cortical neurons were treated for 24h IL-6 (1ng/ml, 5ng/ml, 10ng/ml). Sholl analysis was then performed on the neurons. IL-6 had no effect on the number of neuritic branches (a) but significantly increased (b) number of neuritic branches and (c) neuritic length. Data expressed as mean + SEM, $n=6$.

** $p < 0.01$, * $p < 0.05$ vs. control. (One-way ANOVA followed by *post-hoc* Newman-Keuls).

3.5.8.2 IL-6 increases the Sholl profile of primary cortical neurons

A repeated measures two-way ANOVA demonstrated a significant effect of IL-6 on the number of neuritic branches at specific distances from cell soma [$F_{(3,320)}=8.25$, $p=0.0009$]. ANOVA also demonstrated a significant effect of distance [$F_{(16,320)}=362.106$, $p<0.0001$] and a significant distance by treatment interaction [$F_{(48, 320)}=2.72$, $p<0.0001$]. Furthermore *post-hoc* analysis revealed that IL-6 (1 and 5ng/ml) had significantly more branches at 15, 25, 35 μ m ($p<0.01$) and 45 μ m (1ng/ml at $p<0.05$, 5ng/ml at $p<0.01$) from the cell soma compared to control while IL-6 (10ng/ml) also had significantly more branches at 15, 25, 35 and 45 μ m ($p<0.01$) as well as at 95, 105, 115 μ m ($p<0.05$) from the cell soma compared to control neurons. [Figure 3.52, Newman-Keuls, $n=6$].

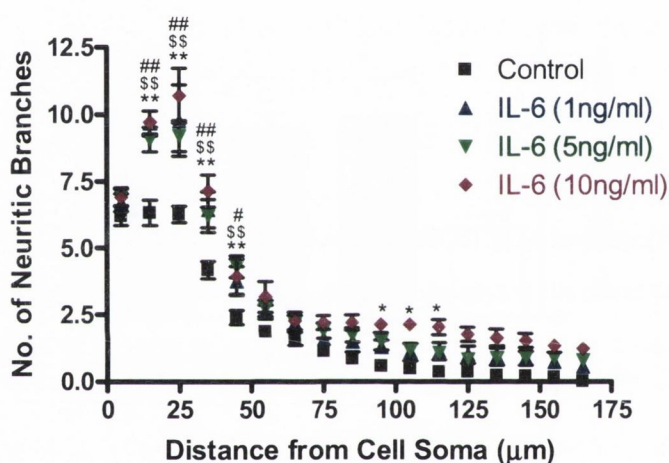


Figure 3.52: IL-6 increases the Sholl profile of primary cortical neurons

Primary cortical neurons were treated for 24h with IL-6. Sholl analysis was then performed on the neurons. All doses of IL-6 had significantly more branches at 15, 25, 35 and 45 μ m from the cell soma while IL-6 (10ng/ml) also had significantly more branches at 95, 105 and 115 μ m from the cell soma. Data expressed as means \pm SEM ($n=6$), # $p<0.05$, ## $p<0.01$ IL-6 (1ng/ml) vs. control, \$\$ $p<0.01$ IL-6 (5ng/ml) vs. control, * $p<0.05$, ** $p<0.01$ IL-6 (10ng/ml) vs. control. (Two-way repeated measures ANOVA followed by *post-hoc* Newman-Keuls).

3.5.9 Neutralization of GDNF attenuates some NA CM-induced increases in measures of neuronal complexity

As shown previously, GDNF treatment of primary cortical neurons enhanced neuronal complexity. In addition, NA stimulation of glial cells increases GDNF mRNA expression. To assess if GDNF was important for inducing NA CM-induced increases in neuronal complexity, a GDNF neutralizing antibody (nAB, 0.5 μ g/ml), or normal goat IgG (0.5 μ g/ml), was added to the CM for 30min. Neurons were then treated with the CM plus nAB or IgG for 24h, Sholl analysis was performed as before.

3.5.9.1 GDNF nAB attenuates NA CM-induced increases in neuritic length but not primary neurites or neuritic branching

Primary Neurites

A two-way ANOVA demonstrated a significant effect of NA CM on the number of primary neurites [$F_{(1,28)}=9.85$, $p=0.004$] but no significant effect of the GDNF nAB or any significant interaction between the two. *Post-hoc* analysis revealed that NA CM had significantly more primary neurites compared to control CM ($p<0.05$). GDNF nAB had no effect on the number of primary neurites either alone or in combination with NA CM. [Figure 3.53a, Fishers LSD, $n=8$].

Neuritic Branching

A two-way ANOVA demonstrated a significant effect of NA CM on the number of neuritic branches [$F_{(1,28)}=6.79$, $p=0.0145$] but no significant effect of the GDNF nAB or any significant interaction between the two. *Post-hoc* analysis revealed that NA CM had significantly more neuritic branches compared to control CM ($p<0.05$). GDNF nAB had no effect on the number of neuritic branches either alone or in combination with NA CM. [Figure 3.53b, Fishers LSD, $n=8$].

Neuritic Length

A two-way ANOVA demonstrated a significant effect of NA CM on the neuritic length [$F_{(1,28)}=35.63$, $p<0.0001$]. The GDNF nAb did not quite reach significance [$F_{(1,28)}=4.156$, $p=0.051$], however there was a significant interaction between the two [$F_{(1,28)}=4.32$, $p=0.0469$]. *Post-hoc* analysis revealed that NA CM had significantly longer neurites compared to control CM ($p<0.01$) while the GDNF nAb in combination with NA CM had significantly shorter neurites compared to NA CM alone ($p<0.01$). [Figure 3.53c, Newman-Keuls, $n=8$]

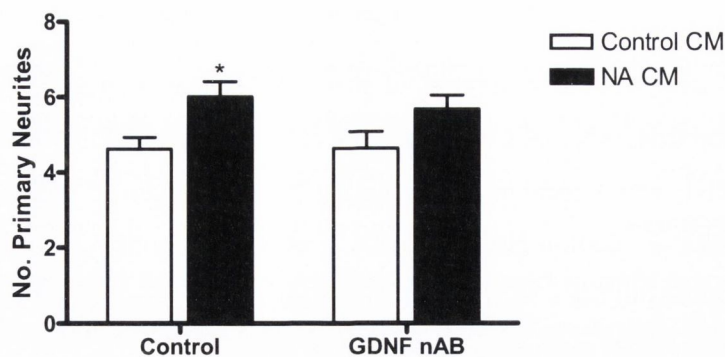
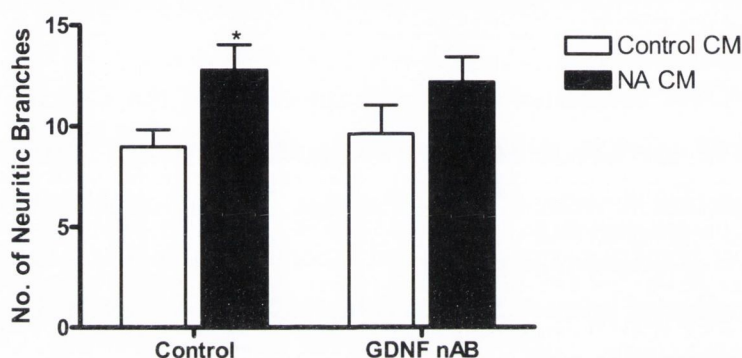
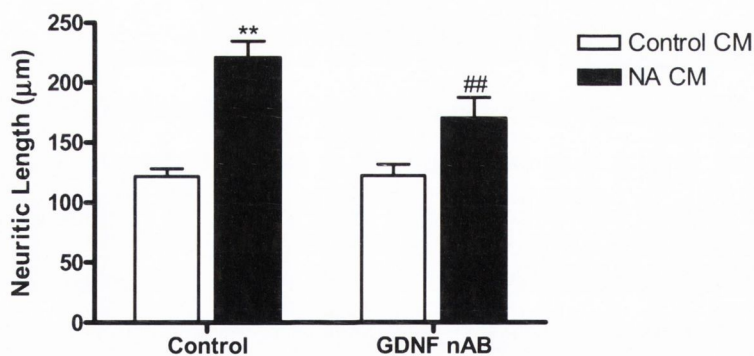
(a) Primary Neurites**(b) Neuritic Branches****(c) Neuritic Length**

Figure 3.53: GDNF nAB attenuates NA CM-induced increases in neuritic length but not primary neurites or neuritic branching

Primary cortical neurons were treated for 24h with NA CM ($10\mu\text{M}$) which had been incubated for 30min with the GDNF nAB ($0.5\mu\text{g/ml}$) or normal goat IgG ($0.5\mu\text{g/ml}$). Sholl analysis was then performed. NA CM significantly increased (a) primary neurites, (b) number of neuritic branches and (c) neuritic length. The GDNF nAB attenuated NA CM-induced increases in neuritic length (c) but not primary neurites or neuritic branching. Data expressed as means + SEM, $n=8$. ** $p<0.01$ vs. control CM, ## $p<0.01$ vs. NA CM alone (Two-way ANOVA followed by *post-hoc* Newman-Keuls (c) or Fishers LSD (a, b)).

3.5.9.2 GDNF nAB attenuates some NA CM-induced increases in the Sholl profile of primary cortical neurons

A three-way repeated measures ANOVA demonstrated a significant effect of NA CM treatment [$F_{(1,224)}=26.89$, $p=0.0001$] and distance [$F_{(16,224)}=221.57$, $p<0.0001$] but no significant effect of the GDNF nAB on the number of neuritic branches at points from cell the soma. ANOVA also demonstrated a significant treatment by distance interaction [$F_{(16,224)}=5.13$, $p=0<0.0001$]. In addition, *post-hoc* analysis revealed that NA CM had significantly more branches compared to control CM treated neurons at $5\mu\text{M}$ ($p<0.05$), 15, 25 and $35\mu\text{m}$ ($p<0.01$) from the cell soma and GDNF nAB + NA CM treatment had significantly less branches than NA CM alone treated neurons at $15\mu\text{m}$ ($p<0.05$). [Figure 3.54, Newman-Keuls, $n=8$].

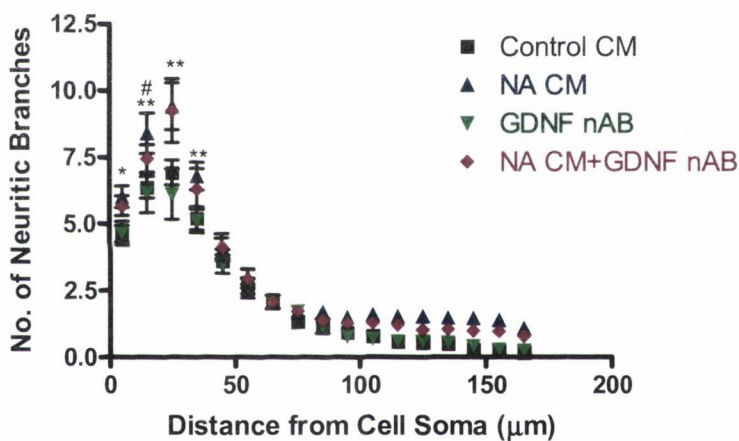


Figure 3.54: The GDNF nAB attenuates some NA CM-induced increases in the Sholl profile of primary cortical neurons

Primary cortical neurons were treated for 24h with NA CM ($10\mu\text{M}$) which had been incubated for 30min with the GDNF nAB ($0.5\mu\text{g/ml}$) or normal goat IgG ($0.5\mu\text{g/ml}$). Sholl analysis was then performed. NA CM had significantly more branches than control at 5, 15, 25 and $35\mu\text{m}$ from the cell soma. In addition, the GDNF nAB in combination with NA CM had significantly less branches than NA CM alone at $15\mu\text{m}$ from the cell soma. Data expressed as means \pm SEM, $n=8$. * $p<0.05$, ** $p<0.01$ NA CM vs. Control CM, # $p<0.05$ GDNF nAB + NA CM vs. NA CM alone. (Three-way repeated measures ANOVA followed by *post-hoc* Newman-Keuls).

3.5.10 Inhibition of NGF- β and BDNF signalling blocks NA CM-induced increases in neuronal complexity

As shown previously, NGF- β and BDNF treatment of primary cortical neurons enhanced neuronal complexity. In addition, NA stimulation of glial cells increases both NGF- β and BDNF mRNA expression. To assess if these neurotrophins were important for inducing NA CM-induced increases in neuronal complexity, a neurotrophin antagonist, Y1036 (40 μ M), was added to the CM for 30min. Y1036 is a small molecule inhibitor which binds both NGF- β ($K_D=3\mu$ M) and BDNF ($K_D=3.5\mu$ M) and prevents their binding to either Trk or p75 receptors (Eibl *et al.*, 2010). Neurons were then treated with the CM plus Y1036 for 24h and Sholl analysis was performed as before.

3.5.10.1 The neurotrophin antagonist, Y1036, blocks all NA CM-induced increases in neuronal complexity

Primary Neurites

A two-way ANOVA demonstrated a significant effect of NA CM on the number of primary neurites [$F_{(1,26)}=5.83$, $p=0.023$] but no significant effect of Y1036 or any significant NA by Y1036 interaction. *Post-hoc* analysis revealed that NA CM had significantly more primary neurites compared to control CM ($p<0.05$) and that Y1036 in combination with NA CM had significantly less primary neurites compared to NA CM alone ($p<0.05$). [Figure 3.55a, Newman Keuls, $n=7-8$].

Neuritic Branches

A two-way ANOVA demonstrated a significant effect of NA CM on the number of neuritic branches [$F_{(1,26)}=11.21$, $p=0.0025$], a significant effect of Y1036 [$F_{(1,26)}=6.21$, $p=0.0193$] and a significant NA CM by Y1036 interaction [$F_{(1,26)}=11.08$, $p=0.0026$]. *Post-hoc* analysis revealed that NA CM had significantly more neuritic branches compared to control CM ($p<0.01$) and that Y1036 in combination with NA CM had significantly less neuritic branches compared to NA CM alone ($p<0.01$). [Figure 3.55b, Newman-Keuls, $n=7-8$].

Neuritic Length

A two-way ANOVA demonstrated a significant effect of NA CM on the neuritic length [$F_{(1,26)}=11.88$, $p=0.0019$], a significant effect of Y1036 [$F_{(1,26)}=9.27$, $p=0.0053$] with no significant NA CM by Y1036 interaction. *Post-hoc* analysis revealed that NA CM had significantly longer neurites compared to control CM ($p<0.05$) while Y1036 in combination with NA CM had significantly shorter neurites compared to NA CM alone ($p<0.01$). [Figure 3.55c, Newman-Keuls, $n=7-8$].

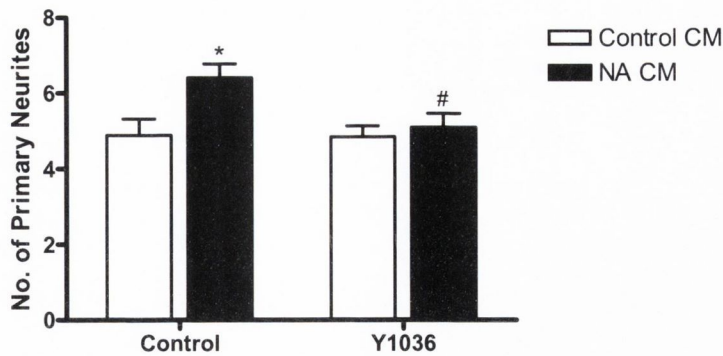
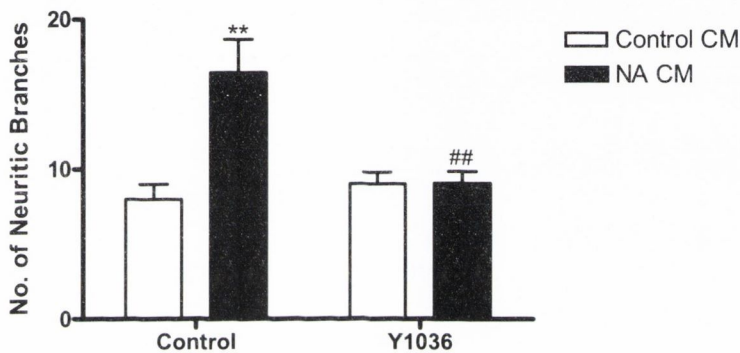
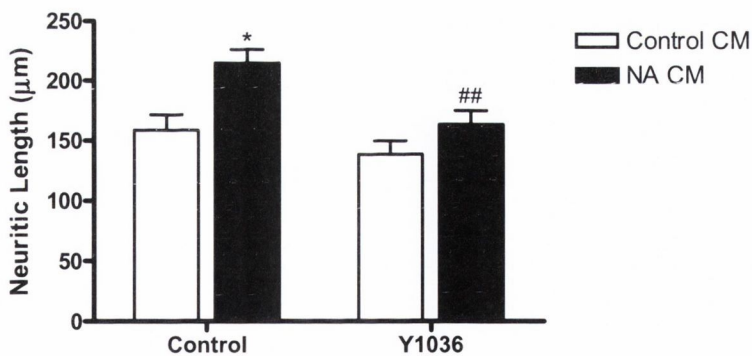
(a) Primary Neurites**(b) Neuritic Branches****(c) Neuritic Length**

Figure 3.55: The neurotrophin antagonist, Y1036, blocks all NA CM-induced increases in neuronal complexity

Primary cortical neurons were treated for 24h with NA CM (10μM) which had been incubated for 30min with Y1036 (40μM). Sholl analysis was then performed. NA CM significantly increased (a) primary neurites, (b) number of neuritic branches and (c) neuritic length. Y1036 attenuated all NA CM-induced increases in complexity. Data expressed as means + SEM, $n=8$. * $p<0.05$, ** $p<0.01$ NA CM vs. control CM, # $p<0.05$, ## $p<0.01$ vs. NA CM alone (Two-way ANOVA followed by *post-hoc* Newman-Keuls).

3.5.10.2 Neurotrophin antagonist, Y1036, blocks the NA CM induced increases in the Sholl profile

A three-way repeated measures ANOVA demonstrated a significant effect of NA CM treatment [$F_{(1,208)}=23.85$, $p=0.0003$], Y1036 treatment [$F_{(1,208)}=10.23$, $p=0.007$] and distance [$F_{(16,224)}=221.57$, $p<0.0001$] with significant interactions between NA CM and Y1036; [$F_{(1,208)}=8.56$, $p=0.0118$], NA CM and distance [$F_{(16,208)}=2.43$, $p=0.0022$], NA CM with Y1036 and distance [$F_{(16,208)}=3.95$, $p<0.0001$]. In addition, *post-hoc* analysis revealed that NA CM had significantly more branches compared to control CM at 5, 15, 25 and 35 μm ($p<0.01$) from the cell soma while Y1036 in combination with NA CM had significantly less branches than NA CM alone at 5, 15, 25 and 35 μm from the cell soma ($p<0.01$). [Figure 3.56, Newman-Keuls, $n=8$].

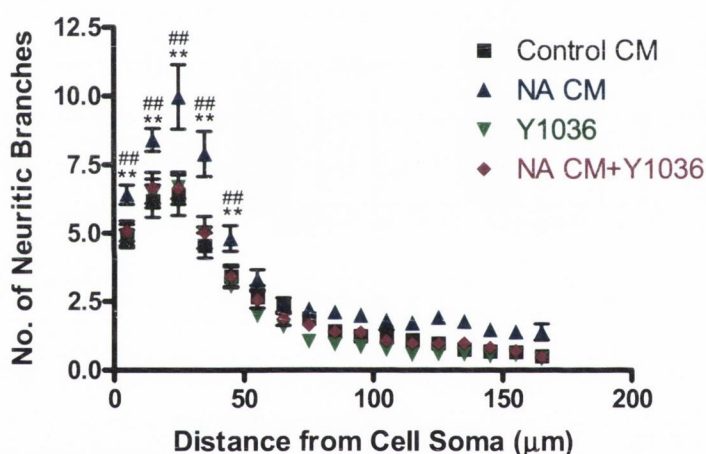


Figure 3.56: The neurotrophin antagonist, Y1036, blocks the NA CM-induced increases in the Sholl profile

Primary cortical neurons were treated for 24h with NA CM (10 μM) which had been incubated for 30min with Y1036 (40 μM). Sholl analysis was then performed. NA CM had significantly more branches than control at 5, 15, 25 and 35 μm from the cell soma. In addition, Y1036 in combination with NA had significantly less branches than NA CM alone at 5, 15, 25 and 35 μm from the cell soma. Data expressed as means \pm SEM, $n=7-8$. ** $p<0.01$ NA vs. control, ## $p<0.01$ Y1036 + NA CM vs. NA CM alone. (Three-way repeated measures ANOVA followed by *post-hoc* Newman-Keuls).

3.5.11 Neutralization of FGF-2 attenuates NA CM-induced increases in neuronal complexity

As shown previously, FGF-2 treatment of primary cortical neurons enhanced neuronal complexity. In addition, NA stimulation of glial cells increases FGF-2 mRNA expression. To assess if FGF-2 was important for inducing NA CM-induced increases in neuronal complexity, an FGF-2 neutralizing antibody (nAB, 2.5 μ g/ml), or the isotype control; mouse IgG1 κ (2.5 μ g/ml), has added to the CM for 30min. Neurons were then treated with the CM plus nAB or IgG for 24h, Sholl analysis was performed as before.

3.5.11.1 FGF-2 nAB reduces NA CM-induced increases in number of primary neurites and the neuritic length but not the number of branches

Primary Neurites

A two-way ANOVA demonstrated a significant effect of NA CM treatment on the number of primary neurites [$F_{(1,27)}=38.6$, $p<0.0001$]. There was no significant effect of the FGF-2 nAB [$F_{(1,27)}=2.82$, $p=0.1043$] or an interaction between the two [$F_{(1,27)}=3.77$, $p=0.063$]. *Post-hoc* analysis revealed that NA CM had significantly more primary neurites compared to control CM ($p<0.01$) and that the FGF-2 nAB in combination with NA CM had significantly less primary neurites compared to NA CM alone ($p<0.05$). [Figure 3.57a, Newman-Keuls, $n=7-8$].

Neuritic Branching

A two-way ANOVA demonstrated a significant effect of NA CM treatment on the number of neuritic branches [$F_{(1,27)}=59.25$, $p<0.0001$]. There was no significant effect of the FGF-2 nAB [$F_{(1,27)}=0.416$, $p=0.524$] or an interaction between the two [$F_{(1,27)}=2.42$, $p=0.13$]. *Post-hoc* analysis revealed that NA CM treatment significantly increased the number of neuritic branches compared to control CM treated neurons ($p<0.01$). [Figure 3.57b, Newman-Keuls, $n=7-8$].

Neuritic Length

A two-way ANOVA demonstrated a significant effect of NA CM treatment on the neuritic length [$F_{(1,27)}=53.07$, $p<0.0001$]. There was no significant effect of the FGF-2 nAB [$F_{(1,27)}=3.92$, $p=0.058$]. There was a significant interaction between the two [$F_{(1,27)}=7.52$, $p=0.0107$]. *Post-hoc* analysis revealed that NA CM treatment significantly increased the neuritic length compared to control treated neurons ($p<0.01$), while the FGF-2 nAB in combination with NA CM had significantly reduced neuritic length compared to NA CM alone ($p<0.01$). [Figure 3.57c, Newman-Keuls, $n=7-8$].

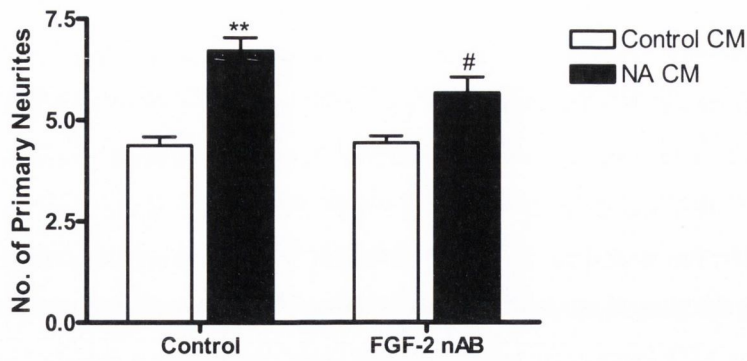
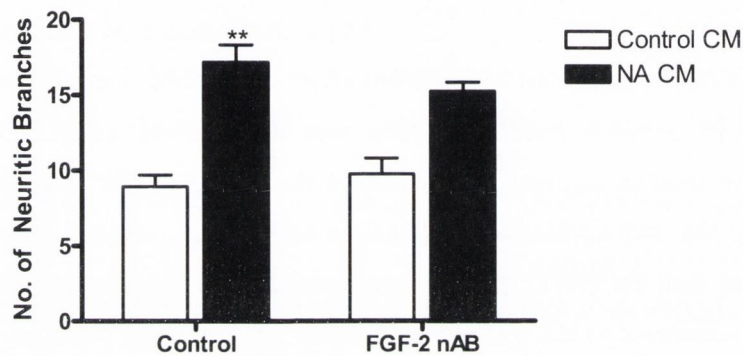
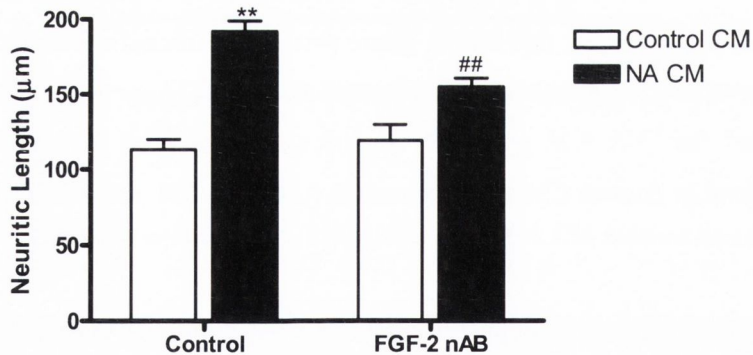
(a) Primary Neurites**(b) Neuritic Branches****(c) Neuritic Length**

Figure 3.57: FGF-2 nAB reduces NA CM-induced increases in number of primary neurites and the neuritic length but not the number of branches

Primary cortical neurons were treated for 24h with NA CM (10 μ M) which had been incubated for 30min with mouse IgG1 κ (2.5 μ g/ml) or the FGF-2 nAB (2.5 μ g/ml) for 30min, and then placed onto neurons. Sholl analysis was then performed. NA CM significantly increased (a) primary neurites, (b) number of neuritic branches and (c) neuritic length. The FGF-2 nAB attenuated NA CM-induced increases in (a) primary neurites and (c) neuritic length but not (b) neuritic branching. Data expressed as means + SEM, $n=6$. ** $p<0.01$ vs. control CM, # $p<0.05$, ## $p<0.01$ vs. NA CM alone (Two-way ANOVA followed by *post-hoc* Newman-Keuls).

3.5.11.2 FGF-2 nAB attenuates some NA CM-induced increases in the Sholl profile of primary cortical neurons

A three-way repeated measures ANOVA demonstrated a significant effect of NA CM on the number of neuritic branches at specific points from the cell soma [$F_{(1,224)}=70.7$, $p<0.0001$]. There was no significant effect of FGF-2 nAB but there was a significant NA CM by FGF-2 nAB interaction [$F_{(1, 224)}=4.99$, $p=0.0423$]. There was also a significant effect of distance [$F_{(16, 224)}=603.07$, $p<0.0001$] and a significant distance by NA CM interaction [$F_{(16,224)}=6.74$, $p<0.0001$]. Furthermore *post-hoc* analysis revealed that NA CM had significantly more branches than control CM at 5, 15, 25 ($p<0.01$) and 35 μ m ($p<0.05$) from the cell soma. The FGF-2 nAB in combination with NA CM had significantly less branches than NA CM alone at 15 μ m from the cell soma ($p<0.05$). [Figure 3.58, Newman-Keuls, $n=6$].

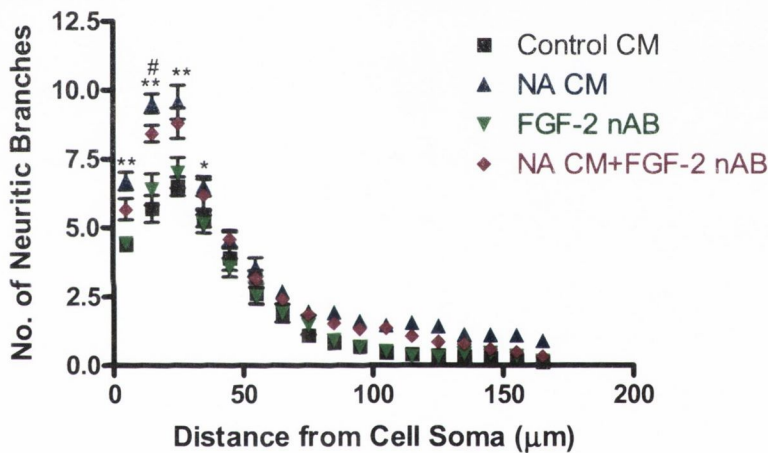


Figure 3.58: FGF-2 nAB attenuates some NA CM-induced increases in the Sholl profile of primary cortical neurons

Primary cortical neurons were treated for 24h with NA CM (10 μ M) which had been incubated for 30min with mouse IgG1 κ (2.5 μ g/ml) or the FGF-2 nAB (2/5 μ g/ml) for 30min, and then placed onto neurons. Sholl analysis was then performed. NA CM had significantly more branches than control at 5, 15, 25 and 35 μ m from the cell soma. The FGF-2 nAB in combination with NA had significantly less branches than NA alone at 15 μ m from the cell soma. Data expressed as means \pm SEM, $n=7-8$. * $p<0.05$, ** $p<0.01$ NA vs. control, # $p<0.05$ FGF-2 nAB + NA vs. NA alone (Three-way repeated measures ANOVA followed by *post-hoc* Newman-Keuls).

3.5.12 Inhibition of IL-6 Signalling blocks NA CM-induced increases in neuronal complexity

As shown previously, IL-6 treatment of primary cortical neurons enhanced neuronal complexity. In addition, NA stimulation of glial cells increases IL-6 mRNA expression. To assess if IL-6 was important for inducing NA CM-induced increases in neuronal complexity, an IL-6 receptor antibody (anti-IL6R, 0.1 μ g/ml) or the isotype control IgG2bk (0.1 μ g/ml), was added to the CM for 30min. Neurons were then treated with the CM plus anti-IL6R or IgG2bk for 24h, Sholl analysis was performed as before.

3.5.12.1 Inhibition of the IL-6R blocks NA CM-induced increases in neuronal complexity

Primary Neurites

A two-way ANOVA demonstrated a significant effect of NA CM treatment on the number of primary neurites [$F_{(1,27)}=7.51$, $p=0.0108$] There was also a significant effect of anti-IL6R [$F_{(1,27)}=5.54$, $p=0.0261$] but no significant interaction between the two [$F_{(1,27)}=0.0084$, $p=0.9278$]. *Post-hoc* analysis revealed no significant differences between the groups. [Figure 3.59a, Newman-Keuls, $n=7-8$].

Neuritic Branching

A two-way ANOVA demonstrated a significant effect of NA CM treatment on the number of neuritic branches [$F_{(1,27)}=7.51$, $p=0.0107$]. There was also a significant effect of anti-IL6R [$F_{(1,27)}=6.08$, $p=0.0203$] but no significant interaction between the two [$F_{(1,27)}=1.17$, $p=0.287$]. *Post-hoc* analysis revealed that NA CM treatment significantly increased the number of neuritic branches compared to control CM treated neurons ($p<0.05$) and that anti-IL6R in combination with NA CM had significantly less neuritic branches compared to NA CM alone ($p<0.05$). [Figure 3.59b, Newman-Keuls, $n=7-8$].

Neuritic Length

A two-way ANOVA demonstrated a significant effect of NA CM treatment on the neuritic length [$F_{(1,27)}=28.22$, $p=0.0001$]. There was also a significant effect of the IL-6R blocker [$F_{(1,27)}=32.9$, $p<0.0001$] and a significant interaction between the two [$F_{(1,27)}=9.278$, $p=0.0053$]. *Post-hoc* analysis revealed that NA CM treatment significantly increased the neuritic length compared to control treated neurons ($p<0.01$), while anti-IL6R in combination with NA CM had significantly reduced neuritic length compared to NA CM alone ($p<0.01$). [Figure 3.59c, Newman-Keuls, $n=7-8$].

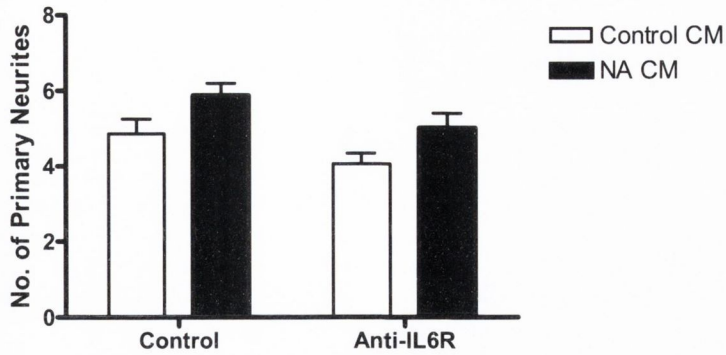
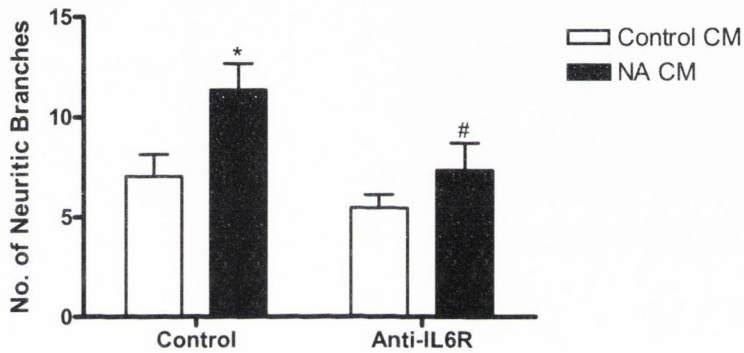
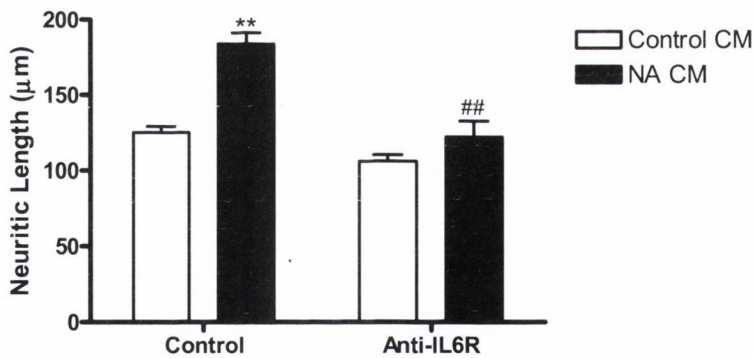
(a) Primary Neurites**(b) Neuritic Branches****(c) Neuritic Length**

Figure 3.59: Inhibition of the IL-6R reduces NA CM-induced increases in neuronal complexity

Primary cortical neurons were treated for 24h with NA CM ($10\mu\text{M}$) which had been incubated for 30min with IgG2b κ ($0.1\mu\text{g/ml}$) or anti-IL6R ($0.1\mu\text{g/ml}$) for 30min, and then placed onto neurons. Sholl analysis was then performed. Neither NA CM nor anti-IL6R had any significant effect on (a) the number of primary neurites. However, anti-IL6R significantly reduced the NA CM-induced increases in (b) number of neuritic branches and (c) neuritic length. Data expressed as mean + SEM, $n=7-8$. * $p<0.05$, ** $p<0.01$ vs. Control CM, # $p<0.05$, ## $p<0.01$ vs. NA CM alone. (Two-way ANOVA followed by *post-hoc* Newman-Keuls).

3.5.12.2 Anti-IL6R attenuates NA CM-induced increases in the Sholl profile of primary cortical neurons

A three-way repeated measures ANOVA demonstrated a significant effect of both NA CM [$F_{(1,224)}=5.10$, $p=0.04$] and anti-IL6R [$F_{(1, 224)}=13.41$, $p=0.0026$] on the number of neuritic branches at points from cell the soma. ANOVA also demonstrated a significant NA CM by distance interaction [$F_{(16,224)}=2.84$, $p=0.0003$], and distance by anti-IL6R interaction [$F_{(16, 224)}=1.97$, $p=0.0156$]. In addition, *post-hoc* analysis revealed that NA CM had significantly more branches compared to control CM at $15\mu\text{M}$ ($p<0.01$) from the cell soma and anti-IL6R + NA treatment had significantly less branches than NA CM alone at $15\mu\text{M}$ ($p<0.05$). Anti-IL6R also had significantly less branches than control CM at 15, 25 ($p<0.01$) and $35\mu\text{m}$ ($p<0.05$) from the cell soma. [Figure 3.60, Newman-Keuls, $n=7-8$].

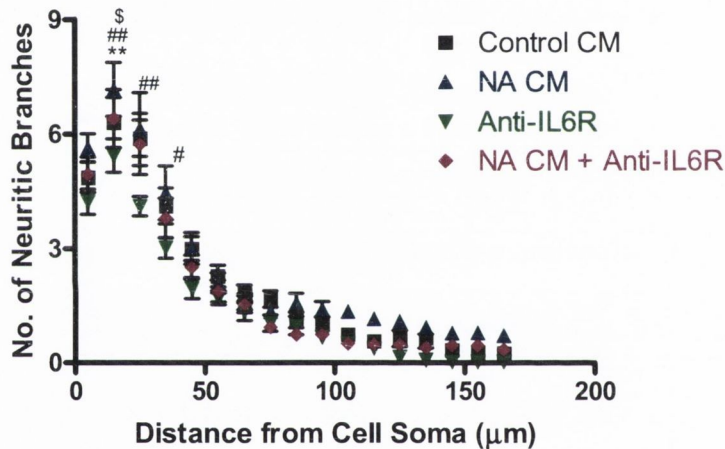


Figure 3.60: Anti-IL6R attenuates NA CM-induced increases in the Sholl profile of primary cortical neurons

Primary cortical neurons were treated for 24h with NA CM ($10\mu\text{M}$) which had been incubated for 30min with IgG2b κ ($0.1\mu\text{g/ml}$) or anti-IL6R ($0.1\mu\text{g/ml}$) for 30min, and then placed onto neurons. Sholl analysis was then performed. NA CM had significantly more branches than control at $15\mu\text{m}$ from the cell soma. Anti-IL6R had significantly less branches than control at 15, 25 and $35\mu\text{m}$ from the cell soma. In addition, anti-IL6R in combination with NA CM had significantly less branches than NA CM alone at $15\mu\text{m}$ from the cell soma. Data expressed as means \pm SEM, $n=7-8$. ** $p<0.01$ NA CM vs. Control CM, # $p<0.05$, ## $p<0.01$ anti-IL-6R vs. control, \$ $p<0.05$, NA CM + anti-IL-6R vs. NA CM alone. (Three-way repeated measures ANOVA followed by *post-hoc* Newman-Keuls).

3.6 Signalling pathways mediating the ability of NA CM to increase the complexity of primary cortical neurons

Increases in neuronal morphology have previously been associated with activation of the PI3K pathway (Ditlevsen *et al.*, 2003), the ERK1/2 MAPK pathway (Lee *et al.*, 2009c) and the STAT3 pathway (He *et al.*, 2005). As NA induces the release of several growth factors, all of which can signal via at least one of the above pathways, it was important to assess which pathway was primarily associated with the NA CM-induced increases in neuronal morphology of primary cortical neurons.

The aims of these studies were as follows:

- 1) To verify, using Western Immunoblotting, that the PI3K, ERK and STAT-3 signalling pathways are activated in primary cortical neurons after NA CM stimulation.
- 2) To ascertain the ability of inhibitors of the PI3K pathway, wortmannin and LY294002, to attenuate NA CM-induced increases in neuronal complexity.
- 3) To ascertain the ability of an inhibitor of the ERK1/2 pathway, PD98059, to attenuate NA CM-induced increases in neuronal complexity.
- 4) To ascertain the ability of an inhibitor of the STAT-3 pathway, S31-201, to attenuate NA CM-induced increases in neuronal complexity.

3.6.7 NA CM activates signaling pathways associated with neuronal growth in neurons

To assess the signalling pathways induced by NA CM in neurons, Western Immunoblotting was performed. Neurons were treated for 5min with control or NA CM and then prepared for Western Immunoblotting as described in the methods. Blots were probed for phosphorylated and total ERK1/2, AKT and STAT3.

- (a) A Student's *t*-test demonstrated a significant effect of NA CM on the ratio of the phosphorylated AKT to total AKT ($t=2.74$, $d.f.=10$, $p=0.0208$) [Figure 3.61a].
- (b) A Student's *t*-test demonstrated a significant effect of NA CM on the ratio of the phosphorylated STAT3 to total STAT3 ($t=2.311$, $d.f.=8$, $p=0.0496$) [Figure 3.61b].
- (c) A Student's *t*-test demonstrated a significant effect of NA CM on the ratio of the phosphorylated ERK1/2 to total ERK1/2 ($t=3.895$, $d.f.=8$, $p=0.0046$) [Figure 3.61c].

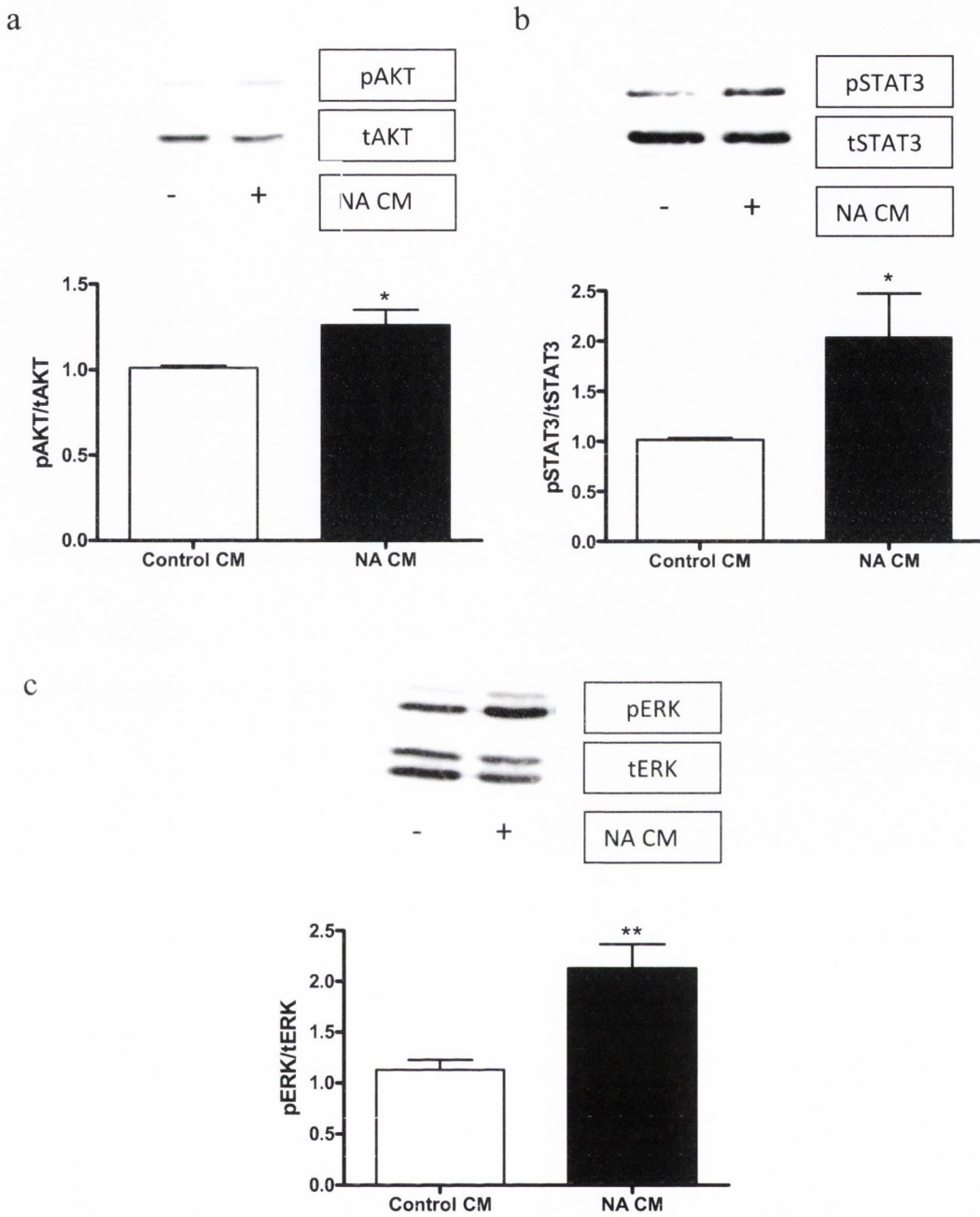


Figure 3.61: NA CM induces the phosphorylation of AKT, STAT3 and ERK

Primary cortical neurons were treated for 5min with the CM from NA treated glia or control CM. The neurons were harvested and western blotting was performed. NA CM increased phosphorylation of AKT (a), STAT3 (b) and ERK (c). * $p < 0.05$, ** $p < 0.01$ vs. control CM. Data expressed as means + SEM ($n=5-6$). (Student's *t*-test).

3.6.1 Inhibitors of the PI3K pathway blocks NA CM-induced increases in neuronal morphology

To assess the ability of NA CM to induce neuronal complexity via the PI3K pathway, primary cortical neurons were treated for 30min with wortmannin (Wort, 100nM) or LY294002 (LY, 10 μ M), highly selective inhibitors of PI3K signalling, followed by stimulation with NA CM. Sholl analysis was performed as before.

3.6.1.1 The PI3K inhibitors wortmannin and LY294002 block NA CM-induced increase in neuronal complexity

Primary Neurites

A two-way ANOVA demonstrated a significant effect of NA CM on the number of primary neurites extending from the cell soma [$F_{(1,39)}=4.308$, $p=0.0446$]. ANOVA also demonstrated a significant effect of inhibitor treatment [$F_{(2,39)}=4.725$, $p=0.0145$] and a significant NA CM by inhibitor interaction [$F_{(2,39)}=3.25$, $p=0.0492$]. Furthermore *post-hoc* analysis revealed that NA CM had significantly more primary neurites than control CM ($p<0.01$) and that both wortmannin and LY294002 reduced NA CM-induced increases in number of primary neurites ($p<0.05$). [Figure 3.62a, Newman-Keuls, $n=6-8$].

Neuritic Branching

A two-way ANOVA demonstrated a significant effect of NA CM on the number of neuritic branches of the primary neurons [$F_{(1,39)}=10.43$, $p=0.0025$]. ANOVA also demonstrated a significant effect of inhibitor treatment [$F_{(2,39)}=6.604$, $p=0.0034$] and a significant NA CM by inhibitor interaction [$F_{(2,39)}=7.374$, $p=0.0019$]. Furthermore *post-hoc* analysis revealed that NA CM had significantly more neuritic branches than control CM ($p<0.01$) and that both wortmannin and LY294002 reduced NA CM-induced increases in neuritic branches ($p<0.01$). [Figure 3.62b, Newman-Keuls, $n=6-8$].

Neuritic Length

A two-way ANOVA demonstrated a significant effect of NA CM on the neuritic length of the neurons [$F_{(1,39)}=35.506$, $p<0.0001$]. ANOVA also demonstrated a significant effect of inhibitor treatment [$F_{(2,39)}=10.237$, $p=0.0003$] and a significant NA CM by inhibitor interaction [$F_{(2,39)}=9.522$, $p=0.0004$]. Furthermore *post-hoc* analysis revealed that NA CM had significantly longer neurites than control CM ($p<0.01$) and that both wortmannin and LY294002 reduced NA CM-induced increases in neuritic length ($p<0.01$). [Figure 3.62c, Newman-Keuls, $n=6-8$].

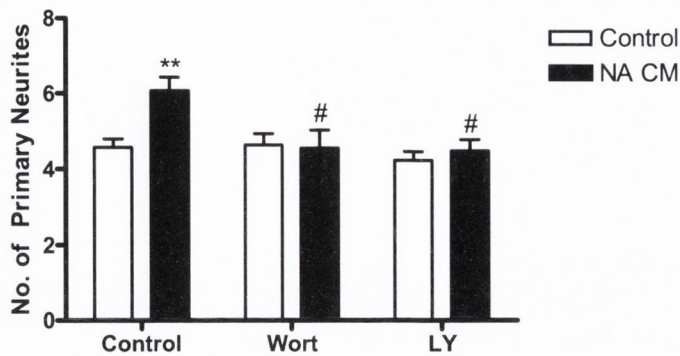
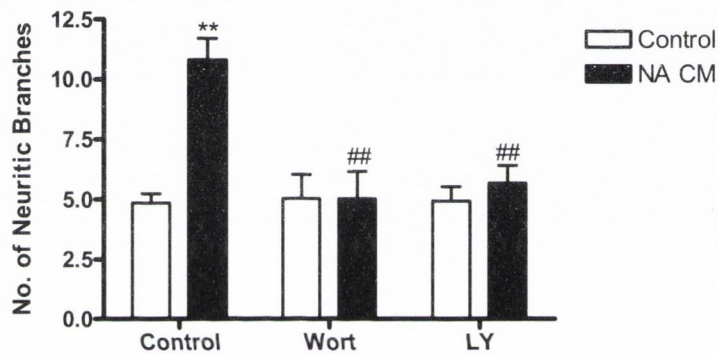
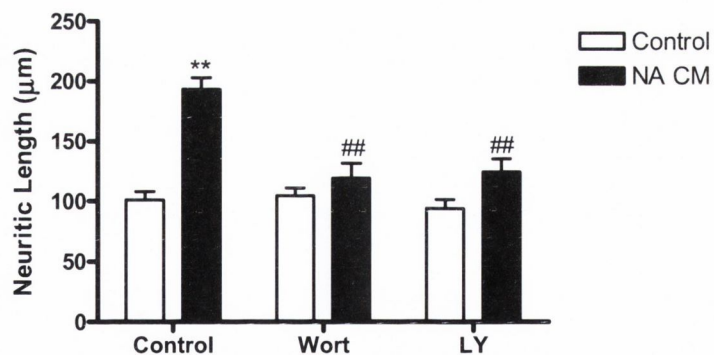
(a) Primary Neurites**(b) Neuritic Branches****(c) Neuritic Length**

Figure 3.62: The PI3K inhibitors wortmannin and LY294002 block NA CM-induced changes in neuronal morphology

Primary cortical neurons were treated for 30min with the PI-3K inhibitors Wort (100nM) and LY (10µM) and then treated for 24h with the CM from glial cells treated with NA (10µM). Sholl analysis was then performed. Both Wort and LY attenuated the NA CM-induced increases in (a) number of primary neurites, (b) number of neuritic branches and (c) neuritic length. Data expressed as means + SEM, $n=6-8$. ** $p<0.01$ vs. control CM, # $p<0.05$, ## $p<0.01$ vs. NA CM alone. (Two-way ANOVA followed by *post-hoc* Newman-Keuls).

3.6.1.2 The PI3K inhibitors wortmannin and LY block the NA CM-induced increases in the Sholl profile

A three-way repeated measures ANOVA demonstrated a significant effect of NA CM treatment [$F_{(1,448)}=17.35$, $p=0.001$], inhibitor treatment [$F_{(2,448)}=16.08$, $p<0.0001$] and distance [$F_{(16,448)}=532.86$, $p<0.0001$] on the number of neuritic branches at points from cell the soma. ANOVA also demonstrated significant interactions between NA CM and inhibitor treatments [$F_{(2,448)}=11.48$, $p=0.0002$], NA CM and distance [$F_{(16,448)}=4.19$, $p=<0.0001$] and inhibitor treatment and distance [$F_{(32,224)}=3.78$, $p<0.0001$]. In addition, *post-hoc* analysis revealed that NA CM had significantly more branches compared to control CM at 5, 15, 25 μ m ($p<0.01$), 35 and 45 μ m ($p<0.05$) from the cell soma. Wortmannin treatment significantly attenuated NA CM-induced increases at 5, 15, 25 ($p<0.01$), 35 and 45 μ m ($p<0.05$) while LY treatment also significantly attenuated the NA CM-induced increases in branches at 5, 15, 25, 35 μ m ($p<0.01$) and 45 μ m ($p<0.05$) from the cell soma. [Figure 3.63, Newman-Keuls, $n=6-8$].

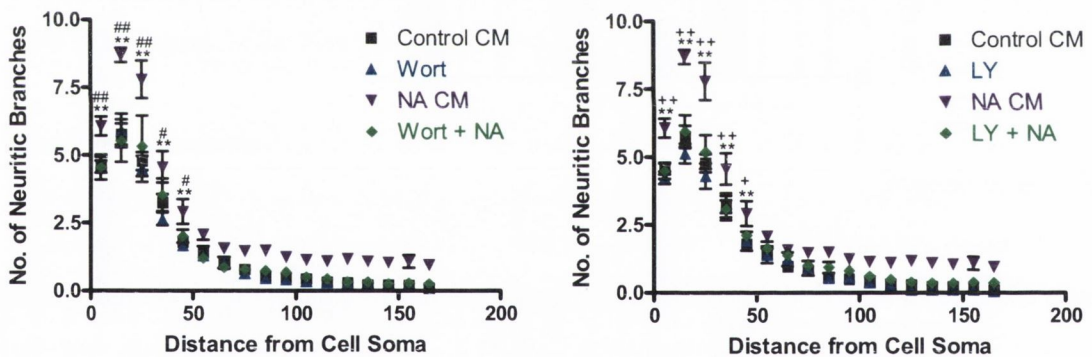


Figure 3.63: The PI3K inhibitors wortmannin and LY reduces the NA CM-induced increases in the Sholl profile

Primary cortical neurons were treated for 30min with the PI3K inhibitors Wort (100nM) or LY (10 μ M) and then treated for 24h with the CM from glial cells treated with NA (10 μ M). Sholl analysis was then performed. NA CM had significantly more branches than control at 5, 15, 25, 35 and 45 μ m from the cell soma. In addition; the PI3K inhibitor Wort and LY in combination with NA CM had significantly less branches than NA CM alone at 5, 15, 25, 35 and 45 μ m from the cell soma. Data expressed as means \pm SEM, $n=6-8$. ** $p<0.01$ NA vs. control, # $p<0.05$, ## $p<0.01$ Wort + NA vs. NA alone, + $p<0.05$, ++ $p<0.01$ LY + NA vs. NA alone. (Three-way repeated measures ANOVA followed by *post-hoc* Newman-Keuls).

3.6.2 An inhibitor of the MAPK pathway attenuates NA CM-induced increases in neuronal morphology

To assess the ability of NA CM to induce neuronal complexity via the ERK1/2 pathway, primary cortical neurons were treated for 30min with PD98059 (PD, 10 μ M), a highly selective inhibitor of MEK, followed by stimulation with NA CM. Sholl analysis was performed as before.

3.6.2.1 The MAPK kinase inhibitor PD98059 attenuates NA CM-induced changes in neuronal morphology

Primary Neurites

A two-way ANOVA demonstrated a significant effect of NA CM on the number of primary neurites extending from the cell soma [$F_{(1,27)}=5.210$, $p=0.0306$]. ANOVA showed no effect of PD treatment or any interaction. Furthermore *post-hoc* analysis revealed that NA CM had significantly more primary neurites than control CM ($p<0.05$) and that PD reduced NA CM-induced increases in number of primary neurites ($p<0.05$). [Figure 3.64a, Newman-Keuls, $n=7-8$].

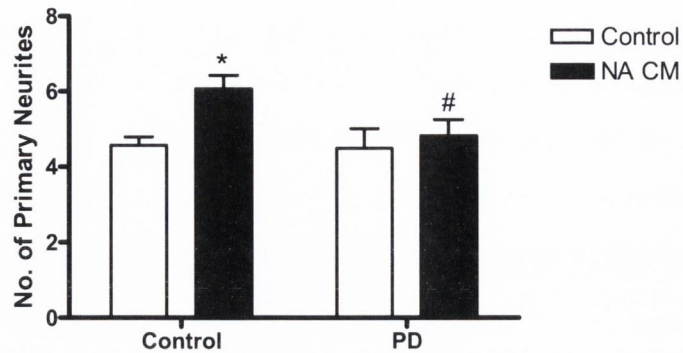
Neuritic Branches

A two-way ANOVA demonstrated a significant effect of NA CM on the number of neuritic branches of the primary neurons [$F_{(1,27)}=25.151$, $p<0.0001$]. ANOVA also demonstrated a significant effect of inhibitor treatment [$F_{(2,27)}=8.978$, $p=0.0058$] and a significant NA CM by inhibitor interaction [$F_{(2,27)}=4.783$, $p=0.0376$]. Furthermore *post-hoc* analysis revealed that NA CM had significantly more neuritic branches than control CM ($p<0.01$) and that PD reduced NA CM-induced increases in neuritic branches ($p<0.01$). [Figure 3.64b, Newman-Keuls, $n=7-8$].

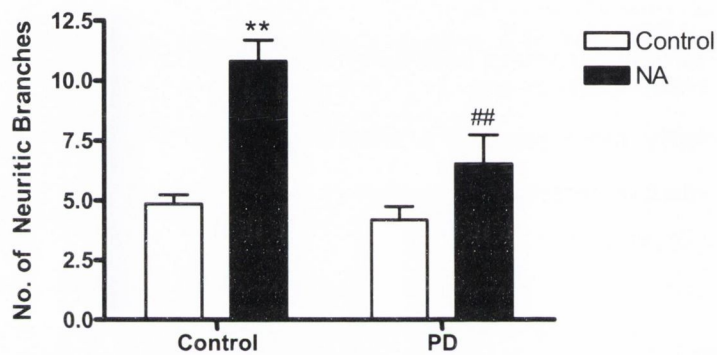
Neuritic Length

A two-way ANOVA demonstrated a significant effect of NA CM on the neuritic length of the neurons [$F_{(1,27)}=40.368$, $p<0.0001$]. ANOVA also demonstrated a significant effect of inhibitor treatment [$F_{(2,27)}=22.839$, $p<0.0001$] and a significant NA CM by inhibitor interaction [$F_{(2,27)}=23.546$, $p<0.0001$]. Furthermore *post-hoc* analysis revealed that NA CM had significantly longer neurites than control CM ($p<0.01$) and that PD reduced NA CM-induced increases in neuritic length ($p<0.01$). [Figure 3.64c Newman-Keuls, $n=7-8$].

(a) Primary Neurites



(b) Neuritic Branches



(c) Neuritic Length

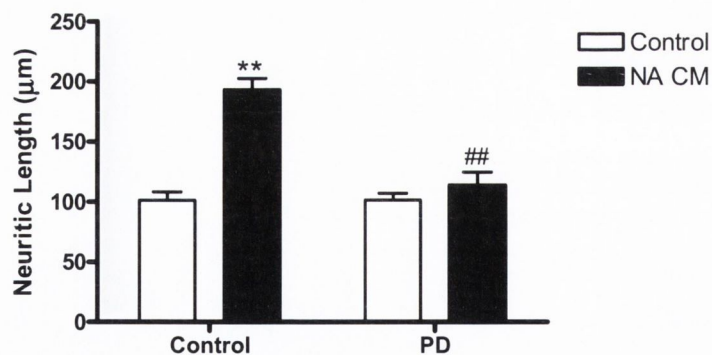


Figure 3.64: The MAPK inhibitor PD98059 blocks NA CM-induced increases in neuronal morphology Primary cortical neurons were treated for 30min with the MAPK inhibitor PD (10μM) and then treated for 24h with the CM from glial cells treated with NA (10μM). Sholl analysis was then performed. PD attenuated the NA CM-induced increases in (a) number of primary neurites, (b) number of neuritic branches and (c) neuritic length. Data expressed as means + SEM, $n=7-8$. * $p<0.05$, ** $p<0.01$ vs. control CM, # $p<0.05$, ## $p<0.01$ vs. NA CM alone. (Two-way ANOVA followed by *post-hoc* Newman-Keuls).

3.6.2.2 The MAPK inhibitor PD98059 blocks the NA CM-induced increases in the Sholl profile

A three-way repeated measures ANOVA demonstrated a significant effect of NA CM treatment [$F_{(1,224)}=18.30$, $p=0.0008$], PD treatment [$F_{(1,224)}=23.28$, $p=0.0003$] and distance [$F_{(16,224)}=271.27$, $p<0.0001$] on the number of neuritic branches at points from cell the soma. ANOVA also demonstrated significant interactions between NA CM and PD [$F_{(1,224)}=16.66$, $p=0.0011$], NA CM and distance [$F_{(16,224)}=4.67$, $p=0<0.0001$] and PD and distance [$F_{(16,224)}=3.81$, $p<0.0001$]. In addition, *post-hoc* analysis revealed that NA CM had significantly more branches compared to control at 5 μ M, 15, 25, 35 μ m ($p<0.01$) and 45 μ m ($p<0.05$) from the cell soma and PD significantly reduced the NA CM-induced increases in branches at 5, 15, 25 and 35 μ m ($p<0.01$) from the cell soma. [Figure 3.65, Newman-Keuls, $n=7-8$].

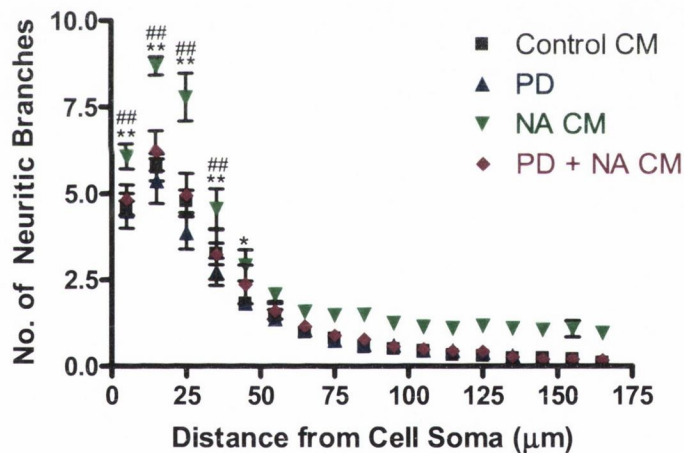


Figure 3.65: The MAPK inhibitor PD98059 blocks the NA CM-induced increases in the Sholl profile

Primary cortical neurons were treated for 30min with the MAPK inhibitor PD (10 μ M) and then treated for 24h with the CM from glial cells treated with NA (10 μ M). Sholl analysis was then performed. NA CM had significantly more branches than control at 5, 15, 25, 35 and 45 μ m from the cell soma. In addition; PD in combination with NA CM had significantly less branches than NA CM alone at 5, 15, 25 and 35 μ m from the cell soma. Data expressed as means \pm SEM, $n=7-8$. * $p<0.05$, ** $p<0.01$ NA vs. control, ### $p<0.01$ PD98059 + NA vs. NA alone. (Three-way repeated measures ANOVA followed by *post-hoc* Newman-Keuls).

3.6.3 An inhibitor of the STAT3 pathway blocks NA CM-induced increases in neuronal morphology

To assess the ability of NA CM to induce neuronal complexity via the STAT-3 pathway, primary cortical neurons were treated for 30min with S31-201 (10 μ M), a highly selective inhibitor of STAT-3 signalling, followed by stimulation with NA CM. Sholl analysis was performed as before.

3.6.3.1 The STAT3 inhibitor S31-201 blocks NA CM-induced changes in neuronal morphology

Primary Neurites

A two-way ANOVA demonstrated a significant effect of NA CM on the number of primary neurites extending from the cell soma [$F_{(1,20)}=15.83$, $p=0.0007$]. ANOVA also showed a significant effect of S31-201 treatment [$F_{(1,20)}=22.66$, $p<0.0001$] and a significant interaction between the two [$F_{(1,20)}=13.21$, $p=0.016$]. Furthermore *post-hoc* analysis revealed that NA CM had significantly more primary neurites than control CM ($p<0.01$) and that S31-201 reduced NA CM-induced increases in number of primary neurites ($p<0.01$). [Figure 3.66a, Newman-Keuls, $n=6$].

Neuritic Branches

A two-way ANOVA demonstrated a significant effect of NA CM on the number of neuritic branches of the primary neurons [$F_{(1,20)}=5.908$, $p=0.0246$]. ANOVA also demonstrated a significant effect of S31-201 treatment [$F_{(1,20)}=14.16$, $p=0.0012$] but no significant interaction between the two [$F_{(1,20)}=3.738$, $p=0.0675$]. Furthermore *post-hoc* analysis revealed that NA CM had significantly more neuritic branches than control CM ($p<0.01$) and that S31-201 treatment reduced NA CM-induced increases in neuritic branches ($p<0.01$). [Figure 3.66b Newman-Keuls, $n=6$].

Neuritic Length

A two-way ANOVA demonstrated a significant effect of NA CM on the neuritic length of the neurons [$F_{(1,20)}=12.17$, $p=0.0023$]. ANOVA also demonstrated a significant effect of inhibitor treatment [$F_{(1,20)}=14.86$, $p=0.001$] and a significant interaction between the two [$F_{(1,20)}=9.92$, $p=0.005$]. Furthermore *post-hoc* analysis revealed that NA CM had significantly longer neurites than control CM ($p<0.01$) and that S31-201 reduced NA CM-induced increases in neuritic length ($p<0.01$). [Figure 3.66c Newman-Keuls, $n=6$].

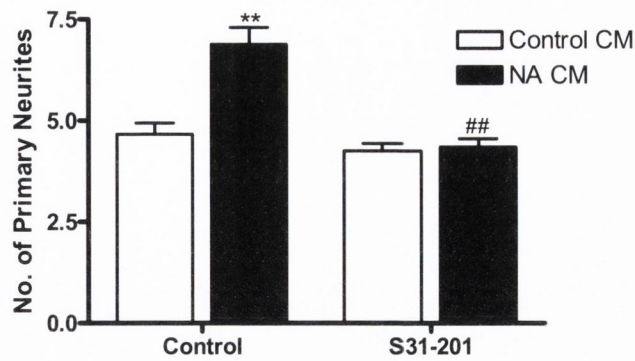
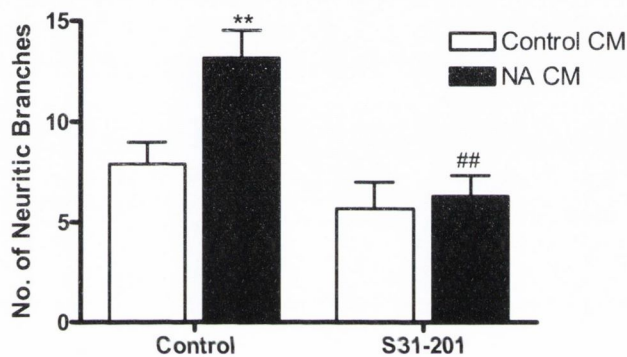
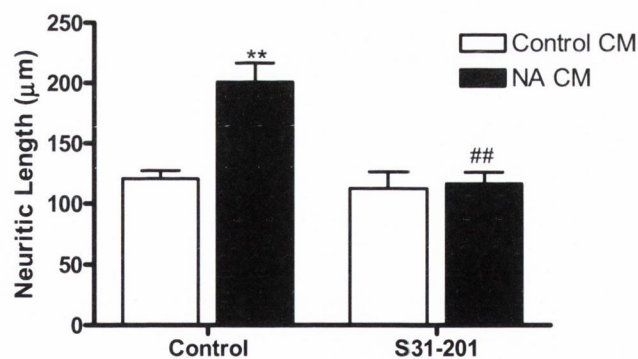
(a) Primary Neurites**(b) Neuritic Branches****(c) Neuritic Length**

Figure 3.66: The STAT3 inhibitor S31-201 blocks NA CM-induced changes in neuronal morphology

Primary cortical neurons were treated for 30min with S31-201 (10μM) and then treated for 24h with the CM from glial cells treated with NA (10μM). Sholl analysis was then performed. S31-201 treatment attenuated the NA CM-induced increases in (a) number of primary neurites, (b) number of neuritic branches and (c) neuritic length. Data expressed as means + SEM, $n=6$. ** $p<0.01$ vs. control CM, ## $p<0.01$ vs. NA CM alone. (Two-way ANOVA followed by *post-hoc* Newman-Keuls).

3.6.3.2 The STAT3 inhibitor S31-201 blocks the NA CM-induced increases in the Sholl profile

A three-way repeated measures ANOVA demonstrated a significant effect of NA CM treatment [$F_{(1,320)}=10.28$, $p=0.0044$], S31-201 treatment [$F_{(1,320)}=21.19$, $p=0.0002$] and distance [$F_{(16,320)}=195.13$, $p<0.0001$] on the number of neuritic branches at points from cell the soma. ANOVA also demonstrated significant interactions between NA CM and S31-201 [$F_{(1,320)}=14.25$, $p=0.0012$], NA CM and distance [$F_{(16,320)}=1.74$, $p=0.0383$] and S31-201 and distance [$F_{(16,224)}=5.66$, $p<0.0001$]. In addition, *post-hoc* analysis revealed that NA CM had significantly more branches compared than control at 5 μ M, 15, 25, 35 μ m ($p<0.01$) 45 μ m and 115 μ m ($p<0.05$) from the cell soma and S31-201 significantly reduced the NA CM-induced increases in branches at 5, 15, 25, 35, 45 μ m ($p<0.01$) and 115 μ m ($p<0.05$) from the cell soma. [Figure 3.67, Newman-Keuls, $n=6$].

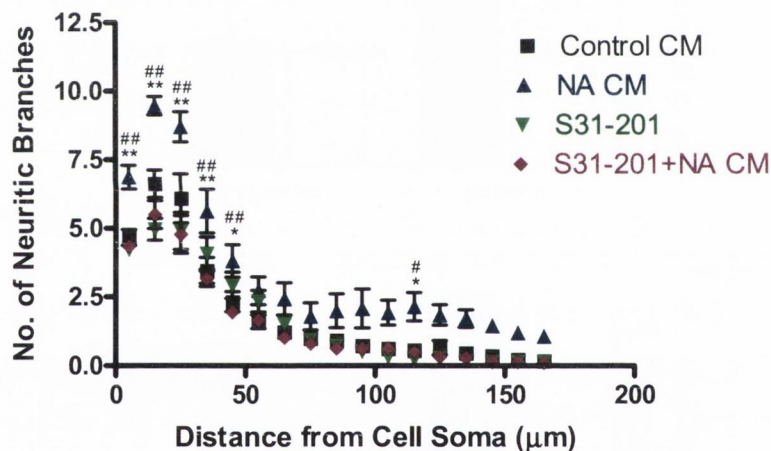


Figure 3.67: The STAT3 inhibitor S31-201 blocks the NA CM-induced increases in the Sholl profile

Primary cortical neurons were treated for 30min with the STAT3 inhibitor S31-201 (10 μ M) and then treated for 24h with the CM from glial cells treated with NA (10 μ M). Sholl analysis was then performed. NA CM had significantly more branches than control at 5, 15, 25, 35, 45 and 115 μ m from the cell soma. In addition; the STAT3 inhibitor in combination with NA CM had significantly less branches than NA CM alone at 5, 15, 25, 35, 45 and 115 μ m from the cell soma. Data expressed as means \pm SEM, $n=6$. * $p<0.05$, ** $p<0.01$ NA CM vs. control, ### $p<0.01$ S31-201 + NA CM vs. NA CM alone. (Three-way repeated measures ANOVA followed by *post-hoc* Newman-Keuls).

Chapter 4

Discussion

4 Discussion

The studies presented in this thesis examined the ability of CM from NA-treated primary mixed glial cells to induce neuritic growth in primary cortical neurons. An *in vitro* primary cell culture system was utilised in the present investigation as it allows for separation of CNS cell types, the study of neuronal growth in isolation and the manipulation of signalling pathways and growth factors *in situ*. The results presented in this thesis have revealed many novel and significant findings of the ability of NA to induce neuritic growth via an action on glial adrenoceptors. To start with, it is the first time that NA has been shown to have this growth-inducing ability. Secondly, the β -adrenoceptor, in particular the β_2 -adrenoceptor, has been shown to mediate the growth inducing ability of NA. The β_2 -adrenoceptor has previously been linked to the anti-inflammatory and neuroprotective properties of NA stimulation in glial cells (Junker *et al.*, 2002; McNamee *et al.*, 2010b), and so now enhancing neuritic growth can also be included in the functions of this receptor. The results presented here also show that an increase in intracellular cAMP in the glial cells, which is a downstream signalling event following β_2 -adrenoceptor activation, can mimic the ability of NA to induce neuritic growth. Again, this is in line with the many reports of β_2 -adrenoceptor mediated neuroprotection and down-regulation of inflammation via an increase in intracellular cAMP (McNamee *et al.*, 2010b). Furthermore, the results have demonstrated that astrocytes and not microglia are required for the ability of NA to induce neuritic growth. Astrocytes are the primary sources of neurotrophic factors in the CNS and CM from astrocytes has previously been shown to induce neuritic growth and favour neuronal survival (Spohr *et al.*, 2011), thus the results reported within this thesis are in line with the literature. In addition to this, the present work shows that NA stimulation of glial cells results in significantly increased secretion of GDNF, IL-6 and FGF-2, all of which have been shown to be required for NA CM-induced increases in neuritic growth, in combination with the presence of the neurotrophin NGF- β . Furthermore, the NA CM activates the PI3K, the MAPK and the STAT3 pathway in neurons, and inhibition of any of these three pathways inhibits NA CM-induced neuronal growth.

4.1 CM from NA treated glial cells but not a direct stimulation with NA, induces neuritic growth of primary cortical neurons

The ability of NA to impact upon cell viability of cortical neurons was firstly investigated. NA CM, but not direct treatment with NA, significantly enhanced neuronal viability as measured by the Alamar Blue mitochondrial colorimetric assay after 24h of treatment. This assay relies on the redox potential of the blue dye resazurin to be converted to resorufin by metabolic activity within the cells, and has previously been utilised to study neuronal viability in culture (White *et al.*, 1996). An increase in neuronal viability caused by NA CM without any pre-treatment of a toxic insult is a unique finding. Furthermore, this demonstrates one of several possible functions of the NA CM; firstly, that NA CM is inhibiting a basal level of cell loss within the primary neurons, or two; that NA CM is increasing neurogenesis or neuritic growth of the primary neurons, or three; that NA CM is increasing the metabolic activity of the same number of neurons. Any of these scenarios would increase the metabolic activity of the neurons and thus the Alamar Blue readout.

Following on from this, neuronal morphology was assessed in primary cortical neurons following treatment with the CM from primary mixed glial cells stimulated with NA, or after a direct treatment with NA. Specifically, the number of primary neurites, the number of neuritic branches, the neuritic length and changes in the Sholl profile were investigated. Interestingly, NA CM but not direct NA treatment, significantly enhanced the number of primary neurites extending from the cell soma, the number of neuritic branches and the neuritic length. To the best of my knowledge, this is the first time that NA, via an action on glial cells, has been demonstrated to alter the morphology of neurons. In addition to this, the Sholl profile-(a scatter-plot of the number of neuritic branches plotted against the distance from the cell soma) of each study design was investigated. The Sholl profile is a simple graphical representation of the overall morphology of the neuron. All doses of NA CM-treated neurons demonstrated significantly more branches than neurons treated with control CM at 5, 15 and 25 μ m from the cell soma while neurons treated with 1 μ M NA CM also had significantly more branches at 35 μ m. In the direct NA Sholl profile, both 1 μ M and 10 μ M NA had significantly less branches than control from 15-35 μ m from the cell soma. 5 μ M NA did not lead to any significant changes in the Sholl profile, the reasons for this are unknown. There is limited evidence in the literature supporting a role for NA to reduce neuritic growth. Inhibition of NA signalling via the β -adrenoceptor blocker,

propranolol, has been shown to increase sympathetic innervation to the rat heart. In the study, basal levels of NA acted to continuously inhibit neuritic outgrowth. The addition of exogenous β -adrenoceptor agonists had no effect on neuritic growth, but inhibition of endogenous NA synthesis increased the growth (Clarke *et al.*, 2010). This study therefore demonstrates that direct NA stimulation acts to reduce neuritic growth, similarly to the results demonstrated within this thesis. Thus it can be hypothesised that direct NA stimulation of the primary cortical neurons in the present work is attenuating basal levels of neuronal branching as reflected in the Sholl profile. A time course analysis of the growth of the neurons following direct NA treatment would need to be undertaken to confirm this.

However, NA CM had the opposite effect. The ability of the CM from NA treated glial cells to increase neuritic growth of neurons, but not direct NA, implies that the NA is stimulating the glial cells to release substances into the CM which act upon the neurons and result in morphological changes. Neurons *in vivo* co-exist with glial cells, and thus the action of NA on glia is more comparable to ongoing NA stimulation in the brain. Subsequent studies were then undertaken to ascertain potential mediators of these NA CM-induced neuronal changes.

4.2 5-HT does not induce neuritic growth

5-HT, a second monoaminergic neurotransmitter, has previously been shown to induce the expression of a wide range of neurotrophic factors (Pousset *et al.*, 1996; Hisaoka *et al.*, 2004; Juric *et al.*, 2006), has roles in neurogenesis (for review, see Azmitia, 2001) and thus might also alter the morphology of the primary cortical neurons investigated in this thesis. Neither a direct treatment of 5-HT, nor CM from 5-HT treated glial cells had any impact upon the gross parameters of neuronal morphology; primary neurites, neuritic branches or neuritic length. The Sholl profile for 5-HT CM does however show changes in neuronal morphology, specifically, all doses of 5-HT CM had significantly more branches than control between 5-45 μ m from the cell soma. In addition, 5 μ M but not 1 or 10 μ M of direct 5-HT led to significantly more branches than control at 15, 25 and 35 μ m from the cell soma.

The ability of 5-HT to induce neuritic growth in neurons and neuronal-like cells is controversial. There are some reports which have demonstrated that 5-HT stimulation

leads to an increase in neuritic growth. For example 5-HT increases both the neuritic outgrowth and neuritic length of mouse neuroblastoma cell line Neuro 2A cells (Fricker *et al.*, 2005) and PC12 cells (Homma *et al.*, 2006). Additionally, thalamic neurons show increases in primary neurites, neuritic branching and neuritic length upon 5-HT stimulation. However, this study treated the neurons for 72h, a much longer time-frame than that used in the present study (Persico *et al.*, 2006). Conversely, Haydon *et al.* in 1984 demonstrated that stimulation of primary neurons cultured from the snail with 5-HT showed a reduction in neuronal growth at the growth cone (Haydon *et al.*, 1984), which has since been replicated (McCobb *et al.*, 1988). To add to this confusion, the same culture of neurons can react differently to 5-HT depending on the neuronal phenotype; GABA containing glutamate decarboxylase positive neurons which represent 10% of the total neuronal population of primary rat cortical neurons, show increased axonal length, but glutamate decarboxylase negative neurons showed reductions in both axonal and dendritic lengths, upon 5-HT stimulation (Hayashi *et al.*, 2010). As this distinction was not made in the present study, it is possible that the mixed culture of neurons showed differential growth properties upon 5-HT stimulation which is masking any neuronal-specific effects.

Glial cells, however are known to express serotonergic receptors (for review, see Azmitia, 2001). Serotonin stimulation of astrocytes in culture has been shown to increase BDNF (Juric *et al.*, 2006), GDNF (Hisaoka *et al.*, 2004), IL-6 (Pousset *et al.*, 1996) but not NGF (Krzan *et al.*, 2001) production. However studies show that although 5-HT induces an increase in intracellular concentrations of BDNF in rat cortical astrocytes, the level of BDNF returned to baseline by 8h post stimulation, while NA-induced increases in BDNF required 24-36h for levels to return to baseline (Juric *et al.*, 2006). This might account for the NA vs. 5-HT differences in the present study. The production of trophic factors (either mRNA or protein) upon 5-HT stimulation was beyond the scope of this thesis, but it would be interesting to investigate any differences in noradrenergic and serotonergic stimulation of primary glial cells.

4.3 The NA/5-HT reuptake inhibitor, AMI, induces neuritic growth via both an action on glial cells and a direct action on neurons

AMI, an antidepressant which inhibits the uptake of both 5-HT and NA (Iversen, 2006), was investigated to establish if it would have any effect on the morphology of primary cortical neurons. Antidepressants have previously been shown to enhance neurogenesis in the hippocampus of adult rat brains (for review see Duman *et al.*, 2001). This however requires chronic treatment with antidepressants and so changes in neurogenesis are not seen for 2-4 weeks (Duman *et al.*, 2001). In the present studies, it is shown that a low dose ($1\mu\text{M}$, $5\mu\text{M}$) but not a high dose ($25\mu\text{M}$) of AMI leads to increases in neuritic morphology. Both the CM and the direct treatment of AMI led to increases in neuronal morphology. For the CM experiment, $5\mu\text{M}$ AMI increased the number of primary neurites and the neuritic length of the primary cortical neurons, while the direct treatment with AMI showed increases in the number of primary neurites, the number of neuritic branches and the neuritic length for $1\mu\text{M}$ only. $25\mu\text{M}$ AMI had no effect in either study design. Since a direct treatment of AMI led to significant changes in neuronal morphology, it remains to be seen whether the CM from AMI results in neuronal changes due to AMI present in the CM, or if AMI is inducing the production of growth factors into the CM which encourages neuritic growth. Astrocytes can take up AMI (Daniel, 2003) and therefore it is possible that much of the AMI is removed from the CM prior to media transfer. If a direct AMI treatment to neurons is resulting in neuronal morphological changes, removal of some of the antidepressant by the astrocytes could explain why a higher dose of AMI is required for CM ($5\mu\text{M}$) to induce neuronal changes compared to a lower direct dose ($1\mu\text{M}$). The highest dose utilised in this study, $25\mu\text{M}$, however might be neurotoxic; several studies have shown that a high dose of AMI can have toxic effects on neuronal cells. High dose AMI treatment ($20\mu\text{M}$ and $50\mu\text{M}$) to the cell lines HT22 and PC12 cells, show reduced cell viability compared to control, which may be attributed to oxidative stress (Post *et al.*, 2000; Bartholoma *et al.*, 2002). Furthermore, primary neurons, specifically primary sympathetic neurons, show reduced cell viability when treated with a wide dose range of AMI ($0.1\mu\text{M}$ to $500\mu\text{M}$). Indeed, in the study, a very high dose ($500\mu\text{M}$) led to neurons with significantly less axonal outgrowth compared to controls (Lirk *et al.*, 2006). In the present study, $25\mu\text{M}$ AMI had no effect on neuronal morphology (with the exception of $25\mu\text{M}$ CM AMI showing reduced branching compared to control CM at $25\mu\text{M}$ from the cell soma). Since lower doses of AMI increased neuritic

branching in the present study, and very high doses of AMI reduces axonal outgrowth (Lirk *et al.*, 2006), it is possible that at 25 μ M the neurotogenic potential of AMI is being balanced by the neurotoxic and growth-inhibiting potential of high dose AMI.

Interestingly, AMI has been shown to directly bind both TrkA and TrkB, but not TrkC receptors. AMI binding triggers both dimerisation of TrkA and heterodimerisation of TrkA to TrkB (see Figure 4.1). In addition, AMI treatment was able to induce neurite outgrowth of PC12 cells, which was prevented by blocking downstream targets of the Trk receptor such as the PI3K and MAPK pathway (Jang *et al.*, 2009). Thus in the present study it is possible that AMI-induced neuritic growth is somewhat attributable to activation of the Trk receptor. Furthermore, AMI has been shown to increase BDNF concentrations in depressed patients (Hellweg *et al.*, 2008), increase GDNF production from astrocytes (Hisaoka *et al.*, 2007) and frees FGF-2 from its plasma membrane anchor (Hisaoka *et al.*, 2011). Each of these growth factors has been shown in this thesis to increase neuritic growth of primary cortical neurons, and thus may account for the growth permitting properties of AMI.

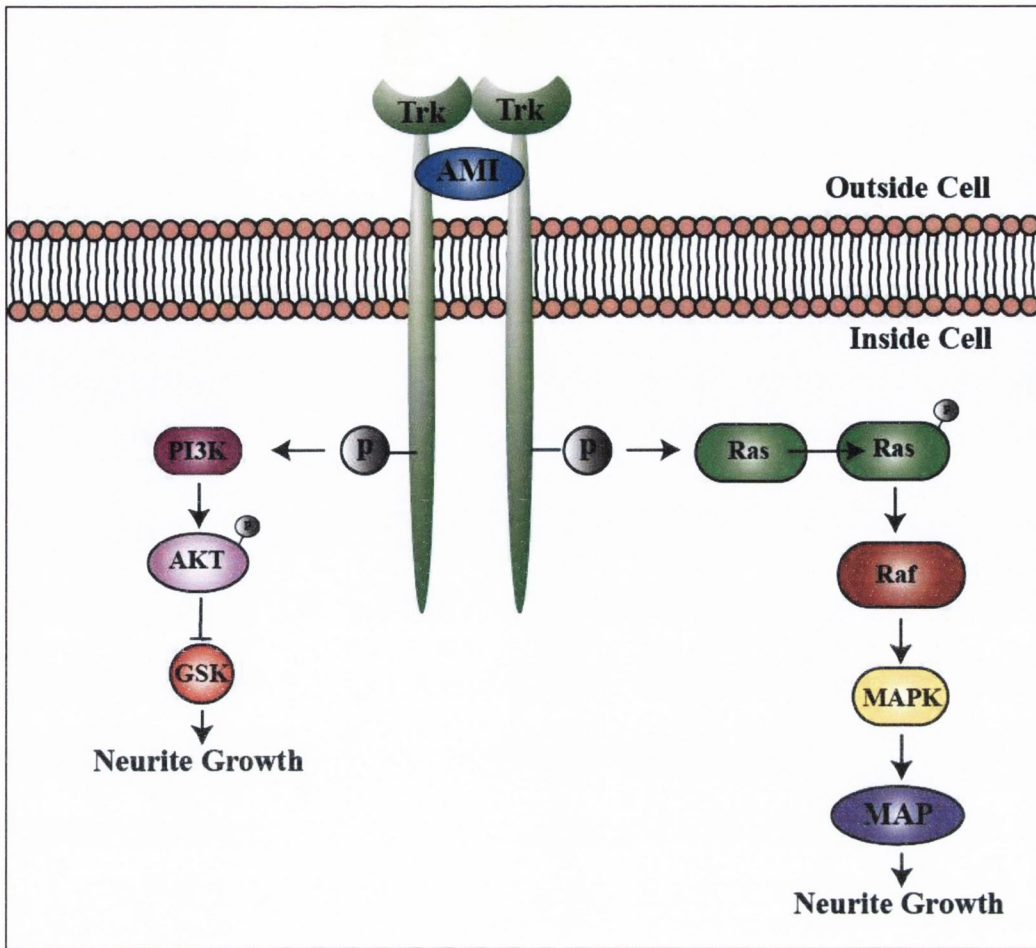


Figure 4.1: AMI leads to dimerisation of Trk receptors which may lead to neuritic growth via the PI3K and MAPK pathway

AMI has been shown to directly dimerise the Trk receptors, leading to the activation of the PI3K and the MAPK pathways, which are involved in neuritic growth. Trk, tropomyosin-receptor kinase; AMI, amitriptyline; P, phosphorylated residue; PI3K, phosphatidylinositol 3-kinase; GSK, glycogen synthase kinase; MAPK, mitogen-activated protein kinase; MAP, microtubule associated proteins.

4.4 The β_2 -adrenoceptor is involved in NA CM-induced neuritic outgrowth

NA can bind to either α - or β -adrenoceptors on the cell surface of astrocytes and microglia (for reviews, see Kimelberg, 1995; Pocock & Kettenmann, 2007). Therefore, this study investigated which of the adrenoceptors was primarily responsible for the NA CM-induced neuritic outgrowth. To do this, glial cells were pre-treated with Prop (a β -adrenoceptor antagonist) or Phent (an α -adrenoceptor antagonist) followed by stimulation with NA. Prop blocked NA CM-induced increases in the number of primary neurites, number of neuritic branches and the neuritic length of the cortical neurons. Phent however

showed some attenuation of NA CM-induced increases in neuritic length but had no effect on the number of primary neurites or the number of neuritic branches. Furthermore, Prop fully blocked all NA CM-induced increases in branch number as shown in the Sholl profile while Phent did not. Neither Prop nor Phent treatment of glia alone had any effect on gross neuronal morphology. These results therefore show that the NA CM-induced increases in neuritic growth are primarily attributed to the β -adrenoceptor.

To further study the role of the glial β -adrenoceptor in neuronal growth, the non-selective β -adrenoceptor agonist, Salb, was utilised to see if Salb CM could mimic NA CM-induced neuritic increases. Indeed, Salb CM (5 μ M and 10 μ M) led to significant increases in the number of primary neurites, number of neuritic branches and the neuritic length of the cortical neurons. Both doses also significantly increased the numbers of neuritic branches from 5 to 55 μ m from the cell soma, as represented in the Sholl profile.

The β -adrenoceptor can be further divided into the β_1 , β_2 , and β_3 subtypes, of which the β_1 and β_2 are associated with adrenergic mediated neuroprotection (Junker *et al.*, 2002). Therefore, the selective β_2 -adrenoceptor agonists' Salm and Clen, and the selective β_1 -adrenoceptor agonist Xam were examined for their ability to induce neuritic growth via glial activation. Salm CM and Clen CM but not Xam CM induced increases in the number of primary neurites, the number of neuritic branches and the neuritic length of the neurons. Furthermore, Salm CM increased neuritic branches at 5-45 μ m from the cell soma, while Clen CM increased neuritic branches at 5-35 μ m from the cell soma. Xam CM showed no changes in the Sholl profile from control CM.

As the β_2 -adrenoceptor primarily signals via the downstream messenger cAMP, it was then investigated if artificially increasing cAMP levels in the glial cells could also increase neuronal morphology. The cell permeable cAMP analogue dbcAMP, was therefore used. DbcAMP CM significantly increased the number of primary neurites, the number of neuritic branches and the neuritic length of the cortical neurons. dbcAMP CM also significantly increased the number of neuritic branches at 5-55 μ m from the cell soma as seen in the Sholl profile.

Overall, these results suggest that NA is acting primarily via the β_2 -adrenoceptor subtype to induce the production of various trophic factors from the glia into the CM to induce neuritic growth.

As previously discussed, this is the first time that NA has been shown to induce neuritic growth of primary neurons via an action on glial cells. However, NA has previously been shown to induce neuronal protection following various toxic insults. For example, primary rat astrocytes treated with NA (10 μ M) resulted in a CM which attenuated NMDA-dependent glutamate release from primary cortical neurons (Madrigal *et al.*, 2009). Furthermore, co-culture of NA-treated astrocytes with primary neurons protected the neurons from oxygen glucose deprivation, compared to untreated cultures, and this was attributed to an increase in MCP-1 (monocyte chemoattractant protein). It also appears that the β_2 -adrenoceptor is vital for NA-induced neuronal protection, as the β_2 -adrenoceptor antagonists, Prop and ICI 118551, inhibited this release of MCP-1 and thus the neuroprotection was provided via activation of the β_2 -adrenoceptor (Madrigal *et al.*, 2009). Similar results were also seen by Junker *et al.* (2002), who showed that mixed neuronal and astrocytic hippocampal cultures were protected from glutamate-induced neuronal toxicity by Clen stimulation. In addition, Clen attenuated neuronal damage following a stroke model in mice (Junker *et al.*, 2002), and has also been shown to be beneficial in a rat model of spinal cord injury (Zeman *et al.*, 1999), ischemic damage (Zhu *et al.*, 1998), and is associated with an increase in the expression of the anti-apoptotic proteins Bcl-2 and Bcl-xl following ischemia (Zhu *et al.*, 1999). Thus the ability of NA to induce neuritic growth via the glial β_2 -adrenoceptor fits with the already neuronal protective functions of this receptor.

4.5 Astrocytes and not microglia are involved in the NA CM-induced neuritic growth

Primary mixed glial cells are composed of predominantly astrocytes (approximately 80%), followed by microglia (10-20%); with minor contributions of neurons, oligodendrocytes and fibroblasts. As NA stimulation of mixed glial cells led to the induction of neuritic growth in primary neurons, it was of interest to investigate whether astrocytes, microglia, or both are involved in this process. Therefore, primary glial cultures were separated as described in the methods into separate cultures of astrocytes and microglia, and then stimulated with NA. The resultant CM was used to treat primary cortical neurons and measures of neuritic growth were taken by Sholl analysis. NA stimulation of primary enriched astrocyte cultures increased the number of primary neurites, the number of neuritic branches and the neuritic length of the primary cortical neurons. However, NA stimulation of primary enriched microglia actually reduced the number of primary

neurites, and had no effect on the number of neuritic branches or the neuritic length. This therefore demonstrates that astrocytes and not microglia are involved in NA CM-induced increases in neuritic growth.

These results are in line with the literature, which implicates the ability of astrocytes to provide protection to neurons and to secrete a variety of growth factors into the surrounding environment. For example CM from untreated primary astrocytes was shown to protect primary neurons from amyloid β -induced neuronal toxicity, although the study did not demonstrate what factors might be present in the CM, the neuroprotection relied on activation of the ERK1/2 pathway, which is induced by many trophic factors (Yamamuro *et al.*, 2003). Similarly, hydrogen peroxide neurotoxicity against primary neurons is attenuated upon the increasing presence of astrocytes in the culture (Desagher *et al.*, 1996). Astrocytes have also been previously demonstrated to be involved in encouraging neuritic growth of neurons. For example, neurons in co-culture with astrocytes show enhanced axonal growth compared to neurons grown with fibroblasts, demonstrating the neurite-promoting properties of astrocytes. However, in the study if the neurons were unable to contact the astrocytes, no stimulation of axonal growth was observed (Dijkstra *et al.*, 1999). In the present study, NA-stimulated astrocytes, but not un-stimulated astrocytes, led to observable differences in neuronal morphology. Both of these results therefore show that astrocytes need to be stimulated to increase production of trophic factors to induce neuritic growth; basal release of trophic factors is insufficient to induce morphological changes in neurons. In agreement with this, treatment of astrocytes with lysophosphatidic acid, a phospholipid derived from cell membranes, leads to a CM which induces neuritic growth of primary cortical neurons via activation of the MAPK pathway, while control CM had no effect (Spohr *et al.*, 2011).

Thus, both the literature and the present set of results demonstrate that astrocytes need to be stimulated to induce neuritic growth in neurons. In this thesis, it was also demonstrated that activation of the β -adrenoceptor via the agonist, Salb, and also an increase in intracellular cAMP via dbcAMP was sufficient to stimulate the astrocytes to result in the release of various mediators into the CM to induce neuritic growth of the neurons.

Although much evidence points to a neuronal growth permitting role of astrocytes, it is important to note that astrocytes are also associated with the inability of neurons to regenerate following neuronal lesion due to the formation of the glial scar. This glial scar

forms both a physical barrier to neuritic growth and also produces proteins which inhibit the growth of neurons (for review, see Fitch & Silver, 2008). Understanding the mechanisms which can switch astrocytes from a growth-inhibiting to a growth-permitting environment for neurons are essential in neuronal regenerative medicine.

4.6 The C6 glioma cell line cannot be used as a model for the ability of primary astrocytes *in vitro* to induce neuritic growth

In the present thesis, the possibility of utilising the readily available C6 glioma cell line as a model for the ability of NA to induce neuritic growth via an action on astrocytic cells was investigated. Cell lines are advantageous over primary cultures in that they are genetically identical thus reducing inter-experiment variability; they eliminate the need for animals; grow at a consistent rate relative to primary cells thus allowing for easier time management for experimentation; and are easier to manipulate in terms of genetic knock-down or knock-in experimentation.

The studies demonstrated in this thesis show that the C6 cells express the astrocytic markers S100 β and GFAP, and also show morphological characteristics similar to primary astrocytes. As the primary goal of this thesis was to investigate the role of the β_2 -adrenoceptor in inducing neuritic growth, it was essential to show that the cells express this receptor. Further to this, Western Immunoblotting clearly demonstrates that the C6 cells show protein expression of the receptor. Several reports have previously shown that C6 cells express the β -adrenoceptors (Homburger *et al.*, 1981; Neve *et al.*, 1985). However, NA stimulation of the C6 glioma cells did not result in a CM that induced neuritic growth in primary cortical neurons. This may seem surprising given that the cells clearly express the β_2 -adrenoceptor. As the receptor has previously been shown to be functional in C6 cells, via upregulation of cAMP (Homburger *et al.*, 1981; Neve *et al.*, 1985), it was assumed that it would also be functional in the present set of experiments. However, as C6 cells are continuously growing it is possible that other essential nutrients within the NBM required for neuritic growth are depleted by the glioma cells prior to CM transfer, thus although the NA stimulation may induce the same trophic factors, the availability of other nutrients would be diminished. To address this issue it would be necessary to calibrate a suitable density of C6 cells to utilise combined with an appropriate dilution of the CM to fresh NBM. This however was beyond the scope of this thesis. In addition to this, β_2 -adrenergic activation of C6 cells may not necessarily result in the

release of the same soluble factors as primary glial cells. For example, NA stimulation of C6 cells did not induce GDNF secretion (data not shown) unlike primary glial cells. The failure of the C6 cells to react similarly to primary astrocytes underlines the essential property of cell lines, in that they are transformed cancerous cells, which do not always react the same way as their parent cells (Lee *et al.*, 2006). It is important to keep this in mind as results derived from cell lines are commonly extrapolated to both primary cells and *in vivo* models.

4.7 Factors involved in inducing neuronal growth by NA CM

A huge number of growth factors, hormones, cytokines and synthetic molecules have been shown to modulate the morphology of neurons from both *in vitro* and *in vivo* models (Greene & Tischler, 1976; Walicke *et al.*, 1986; Patel & McNamara, 1995; Costantini & Isacson, 2000; Chao, 2003; Ditlevsen *et al.*, 2003; Paratcha *et al.*, 2003; Khaibullina *et al.*, 2004; Cui, 2006; Ducray *et al.*, 2006). Thus attempting to investigate the role of each of these in NA CM-induced increases in neuritic morphology was beyond the scope of this thesis. Instead, the mRNA expression, in glial cells, of a range of growth factors associated with neuritic outgrowth and/or induction by NA as determined by a literature search, was investigated following NA stimulation.

The neurotrophins, NGF- β , BDNF, NT3 and NT4/5, were therefore selected as they are considered important target-derived survival factors for neurons and have repetitively, in particular BDNF and NGF- β , been shown to induce neuritic outgrowth (for review, see Cui, 2006). GDNF, a newly-described neurotrophic factor, was also selected based on the ongoing research showing that GDNF is vital for dopaminergic survival (for review see Airaksinen & Saarna, 2002), and its potential for neuritic outgrowth (Hou *et al.*, 1996). As GDNF is a member of the larger TGF- β super-family of ligands (for review see Airaksinen *et al.*, 2006), it was decided to investigate the ability of NA to induce the classical member of this family, TGF- β 1. FGF-2 has been shown to be one of the most potent trophic factors for inducing neuritic outgrowth of primary neurons (Patel & McNamara, 1995), and thus was also selected. Similarly, VEGF, CNTF and IGF-1 have also been shown to induce neuritic outgrowth (Niblock *et al.*, 2000; Khaibullina *et al.*, 2004; Leibinger *et al.*, 2009). The cytokines, IL-6 and IL-10 have known roles in attenuating inflammation (for review, see Opal & DePalo, 2000), and as NA is an anti-

inflammatory agent (for review, see Marien *et al.*, 2004), they were therefore selected based on potential novel roles in neuronal protection.

Both NA and the β -adrenoceptor agonist, Salb, were shown to increase the mRNA expression of GDNF, NGF- β , BDNF, IL-6, VEGF and FGF-2. There was no effect on NT4/5, TGF- β 1, CNTF or IL-10, and the expression of IGF-1 and NT3 were reduced. Therefore, GDNF, NGF- β , BDNF, IL-6, VEGF and FGF-2 were all further assessed for their ability to induce morphological changes in primary cortical neurons, in addition to neutralisation of signalling by antibodies, and for the ability of NA to stimulate their secretion from glial cells.

4.7.1 GDNF contributes to the NA CM increases in neuronal complexity

GDNF treatment (1, 5, 10ng/ml) of primary cortical neurons for 24h increased the number of primary neurites, the number of neuritic branches, the neuritic length and the Sholl profile of the neurons. Furthermore, neutralisation of GDNF from NA CM by a GDNF neutralising antibody (nAB) attenuated NA CM-induced increases in neuritic length, but not primary neurites or neuritic branches. The GDNF nAB attenuated the NA CM-induced increase in the Sholl profile at 15 μ m from the cell soma only. Additionally, NA stimulation increased the release of GDNF from primary glial cells. It is of interest to point out that this is the first time that NA has been demonstrated to increase both the mRNA production of GDNF and to stimulate GDNF release from glial cells.

The results presented in this thesis are in line with many other studies in the literature which have demonstrated the ability of GDNF to induce increases in neuritic length. For example, cortical dopaminergic neurons show increased neuritic length which is associated with the interaction of GDNF with the NCAM receptor (Chao *et al.*, 2003; Cao *et al.*, 2008). Furthermore, GDNF is able to increase the neuritic length of hippocampal and cortical neurons which is also dependent on the NCAM and not RET receptor (Paratcha *et al.*, 2003; Nielsen *et al.*, 2009). In addition to this, the ability of GDNF to induce increases in neuritic length is associated with the activation of the PI3K pathway, as knockdown of this pathway via LY294002 inhibits GDNF-induced neuritic growth (Ditlevsen *et al.*, 2003). In line with this, the present study demonstrated that a direct treatment of GDNF induced increases in neuritic length and that the nAB reduced NA CM-induced increases in neuritic length.

However, the ability of GDNF to induce neuritic branching is more complex. Even in the present study, direct GDNF treatment induced neuritic branching, but the nAB failed to attenuate NA CM-induced neuritic branching. There are two important points to note regarding this result. Firstly, the NA CM contains many growth factors which are capable of inducing neuritic branching of primary cortical neurons. The inhibition of GDNF in the CM therefore must not be sufficient to inhibit NA CM-induced neuritic growth, due to redundancy of other factors. Secondly, the GDNF concentration released by NA stimulation of glial cells equalled to 40pg/ml, which is several fold lower than the lowest direct treatment of GDNF (1ng/ml). Interestingly, a study has shown that GDNF demonstrates two bell-shaped curves in its ability to induce neuritic lengthening of dopaminergic neurons. At the lower end, 50pg/ml showed a maximum induction of neuritic growth, while at the higher end, 0.5 to 10ng/ml showed maximum neuritic growth (Costantini & Isacson, 2000). Higher concentrations of GDNF (10ng/ml) which were utilised in the present study have also been shown to induce increases in both neuritic length and neuritic branching of primary serotonergic neurons (Ducray *et al.*, 2006). Thus higher concentrations of GDNF may stimulate neuritic branching, but the lower concentration contained in NA CM may only be sufficient to induce an increase in neuritic length.

4.7.2 The presence of the neurotrophins; NGF- β and BDNF, are required for NA CM-induced increases in neuronal complexity

In the present study, NGF- β administration to primary cortical neurons increased the number of primary neurites extending from the cell soma, the number of neuritic branches and the neuritic length of the neurons. All doses investigated showed increases in the Sholl profile compared to control treated neurons. BDNF administration to primary cortical neurons also increased the number of primary neurites extending from the cell soma, the number of neuritic branches (5ng/ml only) and the neuritic length of the neurons. All doses investigated showed increases in the Sholl profile compared to control treated neurons. Inhibition of neurotrophin signalling via the neurotrophin antagonist, Y1036, attenuated the ability of NA CM to induce increases in neuronal morphology; however, although NA increased mRNA expression of both NGF- β and BDNF in glial cells, it did not stimulate an increase in their release, with BDNF protein completely undetected in the CM.

The ability of direct treatments with both NGF- β and BDNF to increase neuritic morphology of the primary cortical neurons in this thesis is not surprising. The ability of NGF- β to induce neuritic growth is so well known that it is now routinely used to induce a neuritic phenotype in PC12 cells by stimulating neuritic outgrowth and neuritic lengthening (Greene & Tischler, 1976). Similarly there is a huge wealth of literature on the ability of BDNF to induce neuritic growth in neurons (for review, see Cohen-Cory *et al.*, 2010).

There is also much literature on the ability of NGF- β treatment to induce neuritic lengthening from primary neurons. For example, treatment of primary cortical neurons with 50ng/ml NGF- β for one week, produces neurons with increased neuritic length compared to control neurons (Lee *et al.*, 2009c). Furthermore, rat hippocampal neurons showed increased neurite outgrowth upon stimulation with NGF- β (Brann *et al.*, 1999). NGF- β is also associated with increased neuritic branching; localised addition of NGF- β onto primary chick dorsal root ganglion cells by the addition of NGF- β coated beads, induced collateral branching at the site of the bead (Gallo & Letourneau, 1998). In addition, NGF- β has been utilised to encourage re-growth following neuronal injury. For example, NGF- β treatment increases neuritic sprouting and innervation in the dentate gyrus following injury to the entorhinal cortex of the rat hippocampus. Indeed, use of NGF- β antibodies inhibits neuronal re-growth following injury (Van der Zee *et al.*, 1992).

Similarly, BDNF has been shown to increase neuritic length (Segal *et al.*, 1995) and neuritic branching (Horch & Katz, 2002) of primary neurons. Real-time imaging studies have also demonstrated that BDNF increases axonal length and branching *in vivo* (Alsina *et al.*, 2001), and axonal branching is significantly reduced in trigeminal neurons in BDNF knockdown in *Xenopus* (for review, see Cohen-Cory *et al.*, 2010). Furthermore, BDNF is involved in dendritic spine motility, important for creating functional networks during development (Luikart *et al.*, 2008). Furthermore, Eps8 has been shown to negatively regulate axonal branching, and this is inactivated by BDNF-induced MAPK signalling (Ketschek *et al.*, 2011).

Stimulation of neuritic growth by NGF- β and BDNF has been primarily attributed to the PI3K pathway (Jackson *et al.*, 1996; Gallo & Letourneau, 1998; Ketschek & Gallo, 2010), MAPK pathway (Dijkhuizen & Ghosh, 2005) and activation of NF κ B (Foehr *et al.*, 2000). Activation of the PI3K pathway by these neurotrophins increases the spontaneous

formation of F-actin patches along an axon. NGF- β increases the concentration of F-actin patches along an axon, while BDNF increases the likelihood that this patch will turn into a functional filopodia (Ketschek & Gallo, 2010; Ketschek *et al.*, 2011). Furthermore, inhibition of PI3K signalling by wortmannin and LY294002 attenuated NGF- β -induced increases in axon collateral formation (Gallo & Letourneau, 1998). Activation of NF κ B by NGF- β , although associated with neuritic outgrowth, is however not sufficient to induce growth alone (Foehr *et al.*, 2000). NGF- β -induced increases in axonal growth via TrkA in sympathetic neurons have been attributed to the downstream activation of the phosphatase calcineurin, and subsequent activation by dephosphorylation, of dynamin, resulting in axonal growth (Bodmer *et al.*, 2011).

In the present set of studies, inhibition of Trk signalling via the neurotrophin antagonist inhibited NA CM-induced increases in neuronal morphology, even though NA did not increase the release of BDNF or NGF- β from the glial cells. NGF- β however is present in the CM and therefore would be expected to bind to the TrkB receptor on neurons and thus lead to downstream signalling. Furthermore, this antagonist would prevent any endogenous BDNF from the neurons themselves binding to TrkA. A study by Jin *et al.* (2003) investigated the dendritic growth of cortical neurons in slice culture by BDNF. In their studies, blockade of BDNF in control cultures by a neutralising antibody for 5 days significantly reduced the levels of dendritic branching, demonstrating that endogenous BDNF is important for the ongoing growth of cortical neurons (Jin *et al.*, 2003). Similarly, blockade of TrkA for 36h by a neutralising antibody reduced dendritic complexity of cortical pyramidal neurons compared to control neurons again demonstrating the importance of endogenous BDNF for neuronal growth (McAllister *et al.*, 1997). It can therefore be hypothesised that BDNF is present in the neuronal media and that blockade of BDNF signalling is sufficient to down-regulate any beneficial consequences of NA CM-induced signalling. It is also of interest to note that astrocyte-derived BDNF has been attributed to neuronal degeneration (Colombo *et al.*, 2012). BDNF treatment of astrocytes leads to a CM which reduces neuritic branching and neuritic length of primary neurons via nitric oxide release (Colombo *et al.*, 2012). Furthermore, the importance of NGF- β in stimulating neuritic growth suggests that the NGF- β already present in the CM would in some part contribute to NA CM-induced increases in neuritic complexity. With this in mind, inhibition of Trk signalling via the neurotrophin antagonist demonstrates that the

presence of at least NGF- β , if not also BDNF, are necessary for NA CM to induce neuritic growth.

4.7.3 FGF-2 contributes to NA CM-induced increases in neuronal complexity

In the present study, FGF-2 administration to primary cortical neurons increased the number of primary neurites extending from the cell soma, the number of neuritic branches and the neuritic length of the neurons. All doses investigated showed increases in the Sholl profile compared to control treated neurons. Neutralisation of FGF-2 in the CM by a neutralising antibody to FGF-2 attenuated the ability of NA CM to induce increases in the number of primary neurites and neuritic length but not neuritic branches. Furthermore, NA increased the release of FGF-2 from glial cells.

The literature shows that FGF-2 has previously been shown to be associated with neuronal growth. An early study by Walicke *et al* demonstrated that FGF-2 bound to a heparin substrate significantly increased both survival and neurite outgrowth of primary hippocampal neurons (Walicke *et al.*, 1986). CM from astrocytes grown on an FGF-2 cross-linked nanofibre matrices for 48h led to a significant increase in neuronal growth compared to CM from astrocytes grown on plastic, which was attributed to be as a result of FGF-2 inducing its own secretion from the astrocytes (Delgado-Rivera *et al.*, 2009). Hippocampal neurons incubated with FGF-2 were shown to increase axonal branching and branch growth, but not to affect primary axon growth compared to control neurons (Aoyagi *et al.*, 1994). The present work did not distinguish between dendrites and axons, however it is demonstrated here that FGF-2 in the same dose range (1-10ng/ml) increases neuritic growth for primary cortical neurons. Similarly, dentate gyrus neurons treated with FGF-2 showed a significant increase in the number of neuritic branches per axon, while dendritic branching was not affected (Patel & McNamara, 1995). Other papers have also shown similar results (Szebenyi *et al.*, 2001). It would be interesting to distinguish in the present work if dendrites versus axons are differentially affected by addition of FGF-2.

A study by Abe *et al* (2001) demonstrated that the MAPK pathway is required for FGF-2-induced neuritic growth of primary cortical neurons. Primary rat hippocampal neurons demonstrated significant increases in the number of branch points per axon following FGF-2 exposure for 24h. This increase was attenuated by use of the MEK inhibitors U0126 and PD98059. FGF-2-induced ERK phosphorylation was shown to not be inhibited

by wortmannin or a protein kinase C inhibitor, however, unfortunately this study did not investigate if these inhibitors could attenuate the FGF-2-induced increases in neuritic branching (Abe *et al.*, 2001). Similarly, chick ciliary ganglion neurons demonstrate increases in neuritic growth upon FGF-2 exposure which was dependent on the PI3K and MAPK pathway, as well as the phospholipase C pathway (Gilardino *et al.*, 2009). Furthermore the microtubule inhibitors taxol and colchicine, significantly attenuated FGF-2-induced increases in neuronal branching of primary hippocampal neurons, demonstrating that microtubule polymerisation is required for FGF-2-induced neuritic branching (Aoyagi *et al.*, 1995). In the present work therefore, it is likely that FGF-2 present in the NA CM signals via both the PI3K and the MAPK pathways to contribute to the neuritic growth of the primary cortical neurons. Inhibition of FGF-2 signalling via the neutralising antibody failed to attenuate NA CM-induced neuritic branching, and this may be attributed to other factors in the CM.

4.7.4 VEGF does not contribute to the NA CM-induced increases in neuronal complexity

In the present study, VEGF (1-10ng/ml) did not lead to any morphological changes in the primary cortical neurons. A study by Khaibullina *et al* (2004) also using primary rat cortical neurons however, found that treatment with VEGF did in fact lead to increases in neuritic length. There are many differences between this study and the study reported in this thesis. Firstly the neurons in the study in this thesis were treated for 24h only with VEGF, while Khaibullina *et al* treated the primary neuronal cells for the duration of their culture life, totalling 3 days. Also, in this thesis, measurements of neuronal morphology were strictly only calculated in isolated neurons to minimise the confounding effects of cell-cell contact in inducing neuritic growth and thus to only examine the effects of soluble mediators present in the cellular medium. However, Khaibullina *et al* did not make this exclusion (Khaibullina *et al.*, 2004). It is therefore possible that VEGF assists in the induction of neuronal growth but perhaps is not sufficient to do so alone. A similar study by the same research group found that treatment of cortical explants for 3 days with VEGF (25 – 100ng/ml) increased expression of the microtubule protein MAP-2, and increased neuritic growth which was dependent on the VEGF receptor VEGFR2 and the downstream pathways of MAPK and PI3K (Rosenstein *et al.*, 2003). Again, this study used a much higher dose of VEGF for three times the duration of the present studies.

Direct treatment of primary cortical neurons with VEGF (1-10ng/ml) in this thesis did not lead to any gross morphological changes in the neurons as measured by primary neurite number, number of neuritic branches or neuritic length. However, VEGF did lead to increases in the Sholl profile compared to control neurons. This therefore demonstrates that VEGF must be interacting with its respective receptors on the cortical neurons and activating pathways to induce subtle changes in the morphology of the neurons. It is therefore feasible that a higher dose of VEGF as used in the above discussed studies could lead to more gross morphological changes. It is also possible that VEGF, which is present in both control and NA CM, could be contributing to NA CM-induced neuritic growth.

4.7.5 IL-6 is required for the NA CM-induced increases in neuronal complexity

In the present study, IL-6 administration to primary cortical neurons increased the number of neuritic branches and the neuritic length of the neurons, but failed to increase the number of primary neurites extending from the cell soma. All doses (1-10ng/ml) investigated showed increases in the Sholl profile compared to control treated neurons. Inhibition of IL-6 signalling via blockade of the IL-6 receptor by an antibody attenuated the ability of NA CM to induce increases in the neuritic branches and neuritic length. Furthermore, NA increased the release of IL-6 from glial cells.

Cytokines are more commonly associated with neuronal degeneration and thus there is only limited evidence of the ability of IL-6 to induce neuritic growth in neurons. Interestingly however, a sub-clone of PC12 cells, E2 cells, but not the native PC12 cells induce the formation of neurites following IL-6 stimulation in a similar manner to NGF- β stimulation, and this occurred via the JAK-STAT pathway (Wu & Bradshaw, 1996). This difference between clones of PC12 cells might be attributed to the expression of the IL-6 receptor and gp130 (Marz *et al.*, 1997). IL-6 has also been shown to induce neuritic growth from primary cortical neurons; IL-6 treatment for 1-3 days increased the primary neuritic length, the number of primary neurites and neuritic branching from rat hippocampal neurons (Sarder *et al.*, 1996). Further to this, IL-6 has been shown to have neuroregenerative properties. Blockade of IL-6 with a neutralising antibody completely inhibited re-growth of transected hippocampal slices and reduced GAP-43 expression, while exogenous IL-6 enhanced neuronal recovery and promoted axonal sprouting (Hakkoum *et al.*, 2007). IL-6 has also been shown to protect spinal motor neurons from axotomy-induced cell death (Ikeda *et al.*, 1996).

IL-6 has previously been shown to be induced by NA in astrocytes. In the study by Norris *et al.*, primary rat astrocytes maximally produced IL-6 in response to 10 μ M NA, the same concentration used here. In addition, microglial cells did not induce IL-6 upon NA exposure, and the effect on astrocytes was attributed primarily to the β_2 -adrenoceptor via cAMP expression (Norris & Benveniste, 1993).

Research into how IL-6 might be leading to neuritic growth is limited. However, IL-6 via STAT3, can lead to the transcription of RhoU, an atypical Rho GTPase which is associated with the actin cytoskeleton and can trigger filopodia formation (Schiavone *et al.*, 2009), and thus could lead to increased neuritic branching. In addition to this, the IL-6 receptor can also lead to the activation of both the PI3K and the MAPK pathway (Heinrich *et al.*, 2003), both of which are associated with neuritic growth.

4.7.6 Cross-talk between the neuritic growth-inducing factors

The ability of each trophic factor to induce neuronal morphological changes was investigated in isolation in the present study. However, the NA CM contains a combination of NGF- β , IL-6, FGF-2, GDNF and VEGF and potentially many more trophic factors which were not investigated here. Interactions between the above mentioned trophic factors therefore are more than likely contributing to the ability of NA CM to induce neuritic growth.

RET, the GDNF receptor, can also be activated by NGF- β in sympathetic neurons. NGF- β activated phosphorylation of the RET receptor, which was completely abolished by a TrkA antagonist, showing it to be TrkA dependent (Tsui-Pierchala *et al.*, 2002). Furthermore NGF- β is also capable of activating STAT3, which is more commonly associated with IL-6. However, NGF- β activation of STAT3 does not result in the regular tyrosine-phosphorylated STAT3, instead, NGF- β stimulation of both the sympathetic neuronal-like PC12 cells and primary cortical neurons led to the phosphorylation of a serine residue (serine⁷²⁷) on STAT3 but not the phosphorylation of tyrosine⁷⁰⁵. Additionally, this phosphoSTAT3 was located in the mitochondria, and was essential for NGF- β -induced neurite outgrowth of the PC12 cells. It is believed that NGF- β -induced STAT3 phosphorylation occurs via the MAPK and the tyrosine kinase Src pathways (Zhou & Too, 2011). Thus although NA does not increase the concentration of NGF- β released from the glial cells, the very presence of NGF- β in the CM can enhance

signalling for both GDNF and IL-6, both of which are increased by NA. Indeed, administration of both NGF- β and GDNF to peripheral dorsal root ganglion neurons resulted in increased axonal outgrowth as compared to either treatment alone (Madduri *et al.*, 2009). Similarly, NGF- β and IL-6 show synergistic neuronal survival abilities when co-treated to primary cholinergic neurons (Hama *et al.*, 1989). NGF- β might also enhance FGF-2-induced signalling. For example, primary olfactory neuroepithelium show an increase in neuritic growth when stimulated with a combination of IL-1 β , IL-6, NGF- β and FGF-2. The authors used many other combinations, and trophic factors alone, none of which significantly increased neuritic growth (Vawter *et al.*, 1996). Although IL-1 β was not investigated in the present study, it is interesting that a combination of IL-6, NGF- β and FGF-2 were required for this enhancement of neuritic growth.

Many trophic factors can induce their own and other trophic factor expression and release from cells. For example, BDNF can stimulate its own release from hippocampal neurons in culture, an action which is Trk-dependent (Canossa *et al.*, 1997). FGF-2 on the other hand can increase GDNF mRNA in C6 cells (Suter-Crazzolara & Unsicker, 1996) and can increase both the mRNA (Vige *et al.*, 1991) and the secretion of NGF- β from primary astrocytes in culture (Fukumoto *et al.*, 1991). The ability of FGF-2 to protect primary hippocampal neurons from glutamate toxicity has also been attributed to GDNF release by the neurons upon FGF-2 stimulation, and neutralisation of GDNF in the culture abolished FGF-2 mediated protection (Lenhard *et al.*, 2002). Additionally, GDNF has also been shown to induce the expression of FGF-2 from glial cells which was dependent on the MAPK pathway (Hauck *et al.*, 2006). A study by Drago *et al* discovered that blockage of IGF-1 by a neutralising antibody inhibited the ability of FGF-2 to induce neurogenesis of neuroepithelial cells (Drago *et al.*, 1991).

From these studies it is obvious that trophic factors often synergise and combine to create downstream effects. Often the abilities of one trophic factor rely on the presence of another. Thus in the present study, it is interesting that inhibition of any of the factors by antibody neutralisation, or via Y1036 attenuated to some degree the NA CM-induced increases in neuritic growth. It is clear that the neurons require the synergism of the combination of factors to grow in response to the CM. Interestingly, a combined therapy of artificially increasing cAMP along with the introduction of the neurotrophin, NT-3, led to a significant recovery of spinal cord neurons into lesion sites compared to control or either treatment alone (Lu *et al.*, 2004). As NA, and specifically activation of the β_2 -

adrenoceptor, leads to the production of growth factors involved in neuritic growth and an increase in intracellular cAMP, this could be an exciting candidate for neuronal regeneration.

4.8 Signalling Pathways involved in NA CM-induced increases in neuronal morphology

As the previous results have demonstrated, NA stimulates the release of GDNF, IL-6 and FGF-2 from the glial cells. Furthermore, these factors, in addition with neurotrophin signalling, contribute to NA CM-induced neuritic growth. These growth factors primarily signal via the PI3K, the MAPK and the STAT3 pathways, therefore the contribution of these pathways to NA CM-induced neuritic growth was investigated.

4.8.1 The PI3K pathway is involved in NA CM-induced increases in neuronal morphology

In the present set of studies, the ability of NA to induce neuritic growth via the PI3K, the MAPK/ERK and the STAT3 pathways were investigated. NA CM induced AKT phosphorylation in the primary cortical neurons. Furthermore, use of the PI3K inhibitors, wortmannin and LY294002 attenuated NA CM-induced increases in the number of primary neurites, number of neuritic branches and the neuritic length. Both wortmannin and LY294002 also attenuated all NA CM-induced increases in the Sholl profile at 5-45 μ m from the cell soma.

In general, the PI3K pathway is activated when the PI3K enzyme is recruited to phosphorylated residues, usually on activated receptor tyrosine kinases. PIP3 is then formed which recruits and leads to the phosphorylation of AKT, protein kinase C and the GTPase Rac. Activation of this pathway can occur in response to many stimuli, including NGF- β , GDNF, IL-6 and FGF-2 exposure (Takahashi, 2001; Chao, 2003; Heinrich *et al.*, 2003; Bottcher & Niehrs, 2005).

The substrate for wortmannin, a fungal metabolite, was first identified as the PI3K enzyme in 1993 (Arcaro & Wymann, 1993). LY294002, derived from a bioflavonoid, was soon after also identified as a specific inhibitor of PI3K (Vlahos *et al.*, 1994). Both wortmannin and LY294002 are commonly used tools for inhibiting the PI3K pathway; however, they are not as specific as first identified. LY294002 has been shown to not only inhibit PI3K,

but other kinases as well such as DNA-dependent protein kinase, casein kinase 2 and Pim-1. It might also inhibit Ca²⁺ signalling, the NF κ B pathway, the activation of casein kinase 2 (CK2), GSK3 β (Gharbi *et al.*, 2007), and also the mammalian target of rapamycin (mTOR) (Brunn *et al.*, 1996; Davies *et al.*, 2000). Wortmannin can also inhibit the myosin light chain kinase but does not inhibit CK2. (Davies *et al.*, 2000). Regardless of these facts, both remain useful molecular tools for inhibiting the PI3K pathway.

The induction of a neuronal phenotype by NGF- β in PC12 cells has proved instrumental in unravelling the role of the PI3K pathway in the formation and elongation of neurites. For example, soon after the specific inhibition on PI3K was discovered, wortmannin was identified as completely attenuating NGF- β -induced neuritic growth in PC12 cells, cementing the key role of this pathway in neuritic growth (Kimura *et al.*, 1994). Since then, PI3K has been associated with both the initiation (Jackson *et al.*, 1996) and the elongation (Kobayashi *et al.*, 1997) of NGF- β -induced neuritic growth in PC12 cells.

The importance of the PI3K pathway in neuritic growth has also been demonstrated in primary neurons. For example, PI3K induces increases in neuritic length of primary sympathetic neurons (Atwal *et al.*, 2000) and PI3K signalling via NGF- β coated beads induced collateral branching in primary dorsal root ganglion cells (Gallo & Letourneau, 1998). In addition, the formation of F-actin patches, precursors to neuritic branches, require PI3K signalling (Ketschek & Gallo, 2010; Ketschek *et al.*, 2011). Indeed, the pharmacological increase of PI-3K activity increased the concentration of F-actin patches in primary sensory neurons (Ketschek & Gallo, 2010). PI3K is also involved in spine motility which is important for creating functional networks during development (Luikart *et al.*, 2008). Furthermore, primary hippocampal neurons show increased dendritic branching and primary dendrites upon over-expression of PI3K and AKT. This also increased the dendritic length and the number of filopodia-like protrusions. Furthermore, inhibition of PI3K or AKT significantly reduced the dendritic length and the number of filopodia-like protrusions (Kumar *et al.*, 2005).

A major downstream function of phosphorylated AKT is in the inactivation of GSK3 β . GSK3 β is a serine/threonine kinase with a high basal activity in resting cells which is involved in many neuronal processes including neurogenesis, neuronal migration, neuronal polarisation, axonal growth and axon guidance. GSK3 β has a huge amount of substrates including CREB, the nuclear factor of activated T cells (NFAT) family,

SMAD1, c-Jun, β -catenin and regulates the activity of microtubules (for review, see Hur & Zhou, 2010). There is a vast amount of evidence linking the inactivation of GSK3 β to neuronal growth; global inhibition of GSK3 β induces the formation of multiple axons while over-expression prevents axonal development in neurons (Yoshimura *et al.*, 2005; Hur & Zhou, 2010). Furthermore local inactivation of GSK3 β can convert dendrites into axons (Jiang *et al.*, 2005). GSK3 β also activates many substrates involved in microtubule dynamics, such as collapsing response mediator protein 2, adenomatous polyposis coli, Tau and MAP1B. Overall, the inactivation of GSK results in the stabilisation of growing microtubules and promotion of microtubule assembly (for review, see Hur & Zhou, 2010). In addition to inactivation of GSK3 β , phosphorylated AKT can also activate a number of proteins which interact directly with the growing neurite (for excellent review see Read & Gorman, 2009). Another major target of the PI3K pathway is the Rho GTPases. These are family of guanine nucleotide binding proteins which switch between the active GTP-bound and the inactive GDP-bound state, facilitated by guanine nucleotide exchange factors. In particular the RhoA, Rac1 and Cdc42 members of the family have been associated with neuritic growth as they have functions in modulating the actin cytoskeleton, membrane trafficking, microtubule dynamics and transcriptional activity (for excellent review see Govek *et al.*, 2005).

Thus there is overwhelming evidence that the PI3K pathway, in particular the downstream phosphorylation of AKT, is involved in neuritic growth. Also, as the factors secreted by NA have been shown to induce PI3K signalling (Takahashi, 2001; Chao, 2003; Heinrich *et al.*, 2003; Bottcher & Niehrs, 2005), it comes as no surprise that NA CM both induced phosphorylation of AKT and that knock-down of PI3K signalling via both LY294002 and wortmannin was capable of blocking NA CM-induced neuritic growth.

4.8.2 The MAPK pathway is involved in NA CM-induced increases in neuronal morphology

NA CM induced ERK1/2 phosphorylation in the primary cortical neurons. Furthermore, use of the MEK inhibitor PD98059 attenuated NA CM-induced increases in the number of primary neurites, number of neuritic branches and the neuritic length. PD98059 also attenuated all NA CM-induced increases in the Sholl profile.

The MAPK/ERK pathway is commonly activated upon phosphorylation of an activated tyrosine kinase receptor, the subsequent activation of Ras and the ultimate activation of ERK1/2. The ERK1/2 pathway has been shown to be activated upon stimulation with NGF- β , GDNF, IL-6 and FGF-2 (Airaksinen *et al.*, 1999; Heinrich *et al.*, 2003; Reuss & von Bohlen und Halbach, 2003; Obara & Nakahata, 2010).

PD98059 was originally identified as a highly specific inhibitor of MEK activation by Raf or MEK kinase (Alessi *et al.*, 1995), however since then it has been found to also interfere directly with arachidonic acid metabolism via the inhibition of cyclooxygenases (Borsch-Haubold *et al.*, 1998). PD98059 has also been shown to inhibit both the activation of ERK1/2 and of ERK5 (which is activated by MKK5). (Davies *et al.*, 2000). However, Davies *et al.* (2000) did show that PD98059 was quite specific in inhibiting the MAPK pathway and did not inhibit the activation of any other protein kinase within its recommended concentration range (Davies *et al.*, 2000). PD98059 therefore remains a widely used tool for inhibiting the ERK1/2 pathway.

Again the NGF- β -induced neuritic growth of PC12 cells has proved instrumental in discovering the role of the MAPK pathway in encouraging neuritic growth. Early studies demonstrated that although both NGF- β and EGF resulted in activation of the ERK1/2 pathway, only NGF- β resulted in sustained activation of the pathway. As NGF- β and not EGF results in neuritic growth of PC12 cells, sustained activity of ERK1/2 appears to be essential (Traverse *et al.*, 1992). Later studies consolidated the role of ERK1/2 activation in PC12 neuritic growth, as increases in constitutive activity of the MAPK pathway induced neuritic growth and inhibition of the pathway blocked NGF- β -induced growth (Cowley *et al.*, 1994). Utilisation of the MEK inhibitor, PD98059, exploited in the present study, was also shown to significantly reduce neurite outgrowth in PC12 cells stimulated with NGF- β (Ihara *et al.*, 1997; Sole *et al.*, 2004).

Leading on from studies in PC12 cells, primary neurons were also shown to be dependent on the MAPK pathway for neuritic growth. The MAPK, ERK1/2 branch is involved in increasing neuritic length of primary sympathetic neurons (Atwal *et al.*, 2000). Furthermore, the ability of FGF-2, laminin and N-cadherin to induce neuritic outgrowth of primary embryonic chick retinal neurons all require the ERK1/2 branch of MAPK signalling (Perron & Bixby, 1999). In addition, primary rat hippocampal neurons, showed a low basal level of ERK phosphorylation. Inhibition of this basal activity by U0126 did

not show any changes in neuronal morphology. However, inhibition of FGF-2-induced MAPK activity significantly attenuated FGF-2 mediated neuritic branching, thus suggesting that a threshold level of MAPK activity is required for inducing changes in neuronal morphology (Abe *et al.*, 2001). Furthermore, activation stimulated neuritic growth of primary cortical neurons can be inhibited by the MEK inhibitor U0126 (Redmond *et al.*, 2002). Similarly, induction of neuritic outgrowth of again primary cortical neurons by a plant extract could also be prevented upon ERK inhibition by U0126 but not via a JNK or p38 inhibitor (Lee *et al.*, 2009c).

From the results reported within this thesis and the evidence above, it is clear that the MAPK pathway is essential for mediating neuritic growth of both neuronal cell lines and primary cortical neurons. However, how is activation of the MAPK pathway leading to these changes? Both CaM kinase IV and CREB-mediated gene expression are associated with the induction of dendritic complexity, and there are reports which suggest that ERK1/2 might take advantage of this pathway to induce neuritic growth (Redmond *et al.*, 2002). MAPK signalling is also known to directly phosphorylate microtubules associated with neuronal growth (Veeranna *et al.*, 1998). Activation of the MAPK pathway has also been shown to up-regulate the emergence of active filopodia from actin patches (for review, see Gallo, 2011).

4.8.3 The STAT3 pathway is involved in NA CM-induced increases in neuronal morphology

NA CM induced STAT3 phosphorylation in the primary cortical neurons. Use of the STAT3 inhibitor, S31-201, attenuated the NA CM-induced increases in the number of primary neurites, the number of neuritic branches and the neuritic length of the primary cortical neurons. S31-201 also attenuated all NA CM-induced increases in the Sholl profile.

The STAT-3 pathway is commonly associated with IL-6 signalling whereby phosphorylation of the gp130 molecules leads to the recruitment of Jaks and thus the phosphorylation, dimerisation and activation of STAT3 proteins which translocate to the nucleus and activate gene transcription (for review, see Spooren *et al.*, 2011). However, NGF- β can also lead to the activation of STAT3 (Zhou & Too, 2011). Furthermore, there is limited evidence that FGF-2 stimulation can lead to the activation of the STAT3

pathway (Yoshimatsu *et al.*, 2006) there is however little/no evidence that GDNF can activate this pathway. In the present thesis, STAT3 signalling is likely to be induced primarily via the induction of IL-6 by the glial cells.

The STAT3 inhibitor, S31-201, utilised in this study has been shown to selectively inhibit the DNA binding activity of STAT3 and thus to prevent any transcriptional activity (Siddiquee *et al.*, 2007).

Evidence in the literature that the STAT3 pathway is important for neuritic growth is limited compared to for PI3K and for the MAPK pathways. For example, inhibition of STAT3 activity by use of a dominant negative mutant completely abolished neurite outgrowth of Neuro-2A cells by stimulation with a cannabinoid agonist (He *et al.*, 2005). This parallels the results seen in the present thesis, whereby NA CM-induced increases in neuritic morphology were completely abolished by S31-201. S31-201 alone did not significantly reduce neuritic branching or length of control CM-treated neurons, thus demonstrating that the induction of STAT3 phosphorylation by NA CM is essential for NA CM-induced increases in neuronal morphology, but prevention of STAT3 signalling does not actively prune away existing branches, or interfere with basal levels of neuritic growth. Similar results were found by knocking down STAT3 for serotonin-induced neuritic outgrowth of Neuro-2A cells (Fricker *et al.*, 2005).

The ability of the STAT3 pathway to modify neuronal morphology may be related to the ability of STAT3 to bind to stathmin, a microtubule binding protein; and the promotion of microtubule formation by STAT3 (Verma *et al.*, 2009). In addition to this, activation of Jak-STAT signalling can often lead to the activation of the PI3K and the MAPK pathway (Heinrich *et al.*, 2003).

4.8.4 Cross-talk between the PI3K, MAPK and STAT3 Pathways

There is evidence in the literature concerning cross-talk between the three pathways investigated here. For example, over-expression of Ras, upstream of ERK1/2, leads to increases in dendritic length and filopodia, and inhibition of MEK via U0126, or PI3K via LY294002 blocked the ability of Ras to induce the dendritic changes, thus suggesting that Ras is essential in dendritic complexity formation and utilised both pathways for this ability (Kumar *et al.*, 2005). Furthermore, a study by Jang *et al.* (2009) demonstrated that blockade of the PI3K pathway via LY294002 and wortmannin as well as blockade of the

MEK pathway via PD98059 inhibited the NGF- β -induced increases in neurite outgrowth of PC12 cells. (Jang *et al.*, 2009). Moreover, activation of the MAPK pathway has been shown to result in the serine phosphorylation of STAT3 via ERK1/2, JNK and the p38 branch (for review, see Bowman *et al.*, 2000). Fricker *et al* show that 5-HT-induced neuritogenesis is dependent on all three of these pathways; PI-3K, MAPK and STAT3 (Fricker *et al.*, 2005). Lastly, a very insightful study by Liu *et al* (2001) showed that inhibition of the PI3K and the ERK1/2 pathway inhibited axonal outgrowth from control and NGF- β stimulated primary sensory embryonic neurons, while inhibition of the STAT pathway via JAK inhibition had no effect on axonal growth. However, using lesion-conditioned adult sensory neurons, (neurons which had been lesioned prior to culture preparation), inhibition of the PI3K and the ERK1/2 pathway was shown to have no effect on the regenerative potential of the neurons, but inhibition of the JAK pathway completely abolished the regenerative ability of the neurons. This was in concert with a large induction of STAT3 phosphorylation upon regeneration (Liu & Snider, 2001). This therefore demonstrates that each pathway has important but different roles in neuritic growth. In the present thesis, inhibition of any of the three pathways led to an attenuation of NA CM-induced neuritic growth. The growth factors which mediate the NA CM-induced neuritic growth can activate some if not all of the three pathways demonstrated in this thesis to be involved in NA CM-induced neuritic growth. As there is cross-talk between the growth factors and between the signalling pathways, it can be theorised that a threshold of signalling activation is required prior to neuritic growth.

4.9 The induction of neuritic growth; the answer to neuronal degeneration?

The inability of neurons to regenerate following brain trauma, infection, neuronal degenerative disorders or stroke underlies one of the most crucial medical challenges of our time. Perhaps then, understanding the mechanisms involved in encouraging neuritic growth can lead us closer to a cure for the above mentioned conditions.

Neuritic growth is associated with learning and memory, and thus perhaps encouragement of neuritic growth could ameliorate the symptoms associated with Alzheimer's disease (for review, see Holtmaat & Svoboda, 2009). Further to this, neuritic growth could prove beneficial for other conditions. Schizophrenia, for example, is associated with a down-regulation of AKT and many other molecules associated with neuritic growth e.g. GSK3 β , Wnt and Gap-43 to name but a few. This has led to a neurite patho-physiological model of

schizophrenia, in which abnormal neuritic pruning leads to the symptoms associated with the pathology. This abnormal pruning may also account for the most consistent findings in schizophrenia, that of reduced brain volume and ventricular enlargement (for review, see Emamian *et al.*, 2004; Bellon *et al.*, 2011). The study of the association of neurotrophins with schizophrenia and their possibility as a viable therapeutic is ongoing. It is also interesting to note that lesion sites in the CNS show signs of growth cone advancement but are inhibited by the non-permissive environment, primarily created by astrocytes (for review, see Fitch & Silver, 2008). Stimulation of astrocytes to encourage a growth-permitting environment is therefore essential for neuronal regeneration.

However, although neuritic growth might prove beneficial in some circumstances, neuritic growth can also be harmful. In the injured spinal cord, spontaneous formation of neuritic collaterals due to increased concentrations of neurotrophic factors is associated with pain, autonomic dysreflexia (overactivation of the sympathetic nervous system which can be life-threatening) and bladder dyssynergia. Indeed, blocking the function of NGF- β in spinal cord injury models can reduce these symptoms (for review, see Hagg, 2006). Furthermore, dysregulation of the FGF system is associated with juvenile spinal muscular atrophy (SMA), a monogenetic disease characterised by motoneuron loss in the spinal cord. A mouse model of SMA showed increased FGFRs in the mouse spinal cord which was associated with hyper-phosphorylation of both AKT and ERK1/2 (Hensel *et al.*, 2012). Thus the induction of neuritic growth, although might prove beneficial, needs to be highly regulated. Regardless of this, understanding the underlying mechanisms is important for the advancement of neuronal regeneration research.

4.10 Research Limitations and Future Directions

The results presented in this thesis are based on the ability of NA CM to induce neuritic growth via soluble mediators released by glial cells. To that end, neurons growing in isolation and not in contact with any other neuron were studied. It is important to note that all neurons *in vivo* are retained in a network, and thus have many additional signals through electrical activity and cell-contact to the soluble mediators investigated here. To address this issue, one could investigate the ability of NA CM to induce neuronal changes in a network, by analysing neuritic density *in vitro*. Additionally, live-cell imaging could be utilised to examine ongoing neuritic growth.

All structural changes in this thesis were examined via β III-tubulin staining, thus the preliminary changes that occur upon the initiation of growth cone advancement or neuritic branching via actin was not visualised. All positive staining with β III-tubulin represent filopodium that have already been invaded by neuronal microtubules, therefore it could be interesting to investigate early structural changes induced by NA CM by staining for F-actin. Furthermore, as β III tubulin is a global neuritic marker, it would be interesting to dissociate differences in growth patterns for axons and dendrites by staining for Tau and MAP-2 respectively.

In addition to the growth factors studied in this thesis, many others could potentially be involved in NA CM-induced neuritic growth. For example, MCP-1 has been shown to be induced by NA and to be involved in neuronal protection (Madrigal *et al.*, 2009), perhaps it too might be involved in NA CM-induced neuronal growth. Also perhaps the relatively newly discovered ERK5 branch of the MAPK pathway, which is induced by NGF- β and BDNF, and required for neuronal protection (Obara & Nakahata, 2010), could be involved in neuritic growth.

4.11 Conclusion

Understanding the mechanisms involved in the normal growth of a healthy neuron is imperative for further understanding the regenerative potential of CNS tissue. In this thesis, the ability of NA to encourage glial cells to promote neuronal growth has been investigated. This work raises the possibility that exploiting brain-permeable noradrenergic agonists could in the future be utilised to encourage repair after a brain trauma or infection.

The NA CM led to a robust induction of both mRNA and protein for IL-6, with only small increases for GDNF and FGF-2. Furthermore, inhibition of STAT3 signalling via S31-201 completely attenuated NA CM-induced neuritic growth. In addition to this, neutralisation of the IL-6 receptor led to a complete inhibition of neuritic growth in terms of both neuritic length and neuritic branching. Therefore, it is proposed that IL-6 is the prime candidate for NA CM-induced neuritic growth. In line with this proposal it is noteworthy that in addition to activating STAT3 signalling via the gp130 co-receptor, IL-6 can also activate the MAPK and PI3K pathways (Heinrich *et al.*, 2003; Spooren *et al.*, 2011). Thus IL-6 can induce activation of all three pathways which have been implicated in this thesis to be involved in NA CM-induced neuritic growth. In figure 4.2, a mechanism for NA CM-induced neuritic growth is displayed. NA binds to the β_2 -adrenoceptor on the astrocyte which upon activation of PKA leads to a massive release of IL-6, accompanied by a smaller release of GDNF and FGF-2 from the cell. These growth factors then bind to their respective receptors on the neuronal membrane. IL-6 signalling leads to the activation of the JAK-STAT pathway in addition to the MAPK and PI3K pathways. The PI3K and MAPK pathways are further activated by the presence of NGF- β , GDNF and FGF-2 in the environment, leading to a huge activation of these pathways. The three pathways then converge to together induce neuritic growth of the neuron.

As neuritic growth is important for functional recovery following neuronal degeneration, this novel ability of NA to induce neuritic growth predominantly via astrocyte-derived IL-6 should be thoroughly explored as a new strategy for neuronal repair.

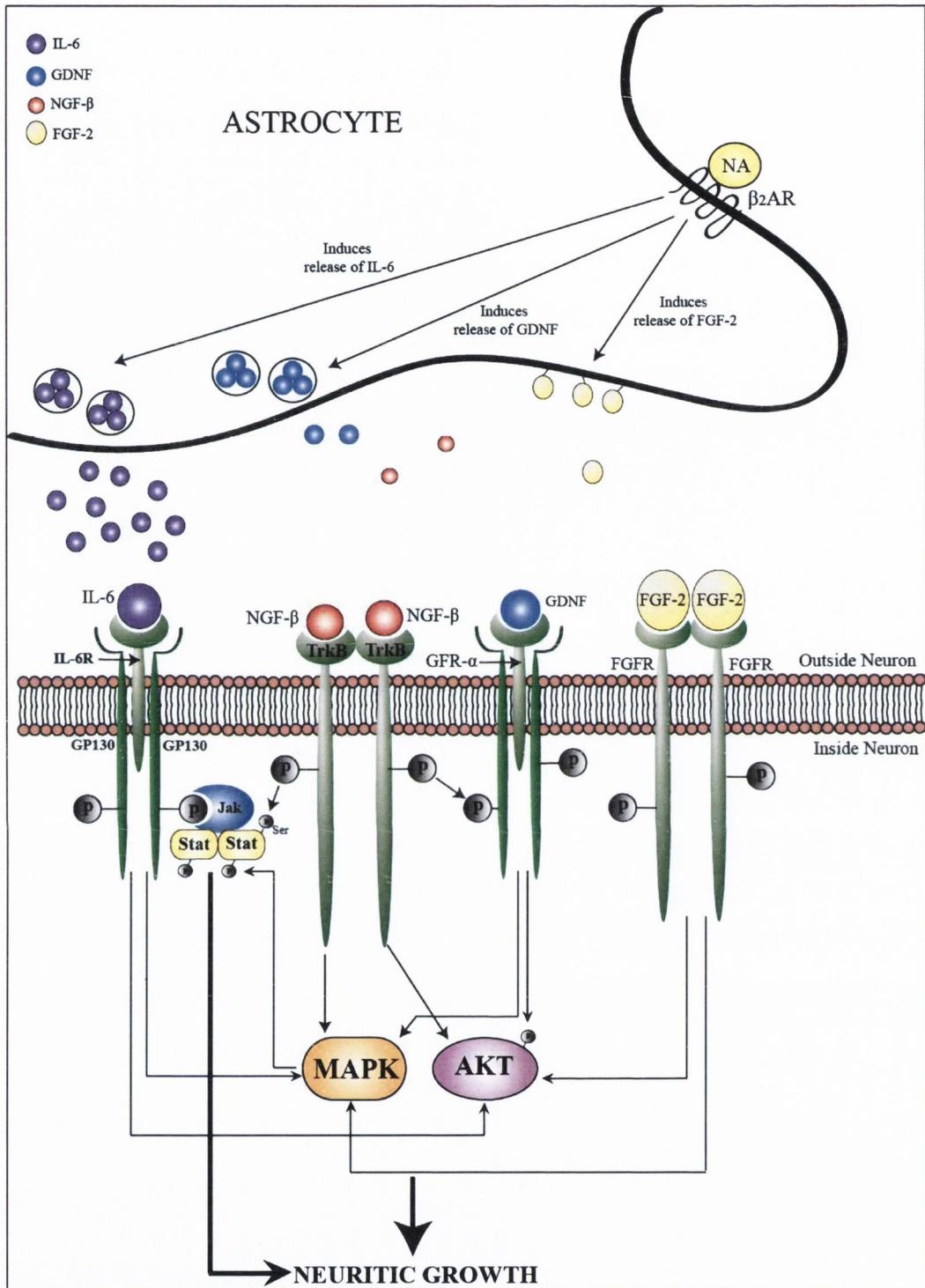


Figure 4.2: A unified theory for NA CM-induced neuritic growth

NA stimulation of astrocytes leads to the increased release of IL-6 and GDNF, the freeing of FGF-2 from the extracellular matrix (ECM) and the continued release of NGF- β from the astrocytes. These growth factors activate their respective receptors on the neurons to induce the activation of the STAT3, MAPK and PI3K pathway, which ultimately lead to neuritic growth of the neurons.

Chapter 5

References

- Abbott NJ, Ronnback L & Hansson E. (2006). Astrocyte-endothelial interactions at the blood-brain barrier. *Nat Rev Neurosci* **7**, 41-53.
- Abe K, Aoyagi A & Saito H. (2001). Sustained phosphorylation of mitogen-activated protein kinase is required for basic fibroblast growth factor-mediated axonal branch formation in cultured rat hippocampal neurons. *Neurochem Int* **38**, 309-315.
- Airaksinen MS, Holm L & Hatinen T. (2006). Evolution of the GDNF family ligands and receptors. *Brain Behav Evol* **68**, 181-190.
- Airaksinen MS & Saarma M. (2002). The GDNF family: signalling, biological functions and therapeutic value. *Nat Rev Neurosci* **3**, 383-394.
- Airaksinen MS, Titievsky A & Saarma M. (1999). GDNF family neurotrophic factor signaling: four masters, one servant? *Mol Cell Neurosci* **13**, 313-325.
- Alessi DR, Cuenda A, Cohen P, Dudley DT & Saltiel AR. (1995). PD 098059 is a specific inhibitor of the activation of mitogen-activated protein kinase kinase in vitro and in vivo. *J Biol Chem* **270**, 27489-27494.
- Aloisi F, Ria F & Adorini L. (2000). Regulation of T-cell responses by CNS antigen-presenting cells: different roles for microglia and astrocytes. *Immunol Today* **21**, 141-147.
- Alsina B, Vu T & Cohen-Cory S. (2001). Visualizing synapse formation in arborizing optic axons in vivo: dynamics and modulation by BDNF. *Nat Neurosci* **4**, 1093-1101.

Aoyagi A, Nishikawa K, Saito H & Abe K. (1994). Characterization of basic fibroblast growth factor-mediated acceleration of axonal branching in cultured rat hippocampal neurons. *Brain Res* **661**, 117-126.

Aoyagi A, Saito H & Abe K. (1995). Differential effects of microtubule inhibitors on axonal branching and elongation of cultured rat hippocampal neurons. *Jpn J Pharmacol* **68**, 223-226.

Appel E, Kolman O, Kazimirsky G, Blumberg PM & Brodie C. (1997). Regulation of GDNF expression in cultured astrocytes by inflammatory stimuli. *Neuroreport* **8**, 3309-3312.

Arcaro A & Wymann MP. (1993). Wortmannin is a potent phosphatidylinositol 3-kinase inhibitor: the role of phosphatidylinositol 3,4,5-trisphosphate in neutrophil responses. *Biochem J* **296 (Pt 2)**, 297-301.

Arenas E, Trupp M, Akerud P & Ibanez CF. (1995). GDNF prevents degeneration and promotes the phenotype of brain noradrenergic neurons in vivo. *Neuron* **15**, 1465-1473.

Asano A, Morimatsu M, Nikami H, Yoshida T & Saito M. (1997). Adrenergic activation of vascular endothelial growth factor mRNA expression in rat brown adipose tissue: implication in cold-induced angiogenesis. *Biochem J* **328 (Pt 1)**, 179-183.

Atwal JK, Massie B, Miller FD & Kaplan DR. (2000). The TrkB-Shc site signals neuronal survival and local axon growth via MEK and P13-kinase. *Neuron* **27**, 265-277.

Azmitia EC. (2001). Modern views on an ancient chemical: serotonin effects on cell proliferation, maturation, and apoptosis. *Brain Res Bull* **56**, 413-424.

Baecker PA, Lee WH, Verity AN, Eglen RM & Johnson RM. (1999). Characterization of a promoter for the human glial cell line-derived neurotrophic factor gene. *Brain Res Mol Brain Res* **69**, 209-222.

Baloh RH, Enomoto H, Johnson EM, Jr. & Milbrandt J. (2000). The GDNF family ligands and receptors - implications for neural development. *Curr Opin Neurobiol* **10**, 103-110.

Bardin L. (2011). The complex role of serotonin and 5-HT receptors in chronic pain. *Behav Pharmacol* **22**, 390-404.

Barker AJ & Ullian EM. (2008). New roles for astrocytes in developing synaptic circuits. *Commun Integr Biol* **1**, 207-211.

Barker RA. (2009). Parkinson's disease and growth factors - are they the answer? *Parkinsonism Relat Disord* **15 Suppl 3**, S181-184.

Barnes NM & Sharp T. (1999). A review of central 5-HT receptors and their function. *Neuropharmacology* **38**, 1083-1152.

Bartholoma P, Erlandsson N, Kaufmann K, Rossler OG, Baumann B, Wirth T, Giehl KM & Thiel G. (2002). Neuronal cell death induced by antidepressants: lack of correlation with Egr-1, NF-kappa B and extracellular signal-regulated protein kinase activation. *Biochem Pharmacol* **63**, 1507-1516.

Basu S & Yang ST. (2005). Astrocyte growth and glial cell line-derived neurotrophic factor secretion in three-dimensional polyethylene terephthalate fibrous matrices. *Tissue Eng* **11**, 940-952.

Batchelor PE, Porritt MJ, Martinello P, Parish CL, Liberatore GT, Donnan GA & Howells DW. (2002). Macrophages and Microglia Produce Local Trophic Gradients That Stimulate Axonal Sprouting Toward but Not beyond the Wound Edge. *Mol Cell Neurosci* **21**, 436-453.

Bellon A, Krebs MO & Jay TM. (2011). Factoring neurotrophins into a neurite-based pathophysiological model of schizophrenia. *Prog Neurobiol* **94**, 77-90.

Benaim E, Wang S., Hamilton D & Ando D. (2010). Plasmid gene transfer of zinc finger protein vegf-a transcription activator (SB-509) for treatment of amyotrophic lateral sclerosis (als) - a phase 2 clinical trial. *2010 Neuroscience Meeting Planner San Diego, CA: Society for Neuroscience, 2010, Online.*

Bodmer D, Ascano M & Kuruvilla R. (2011). Isoform-specific dephosphorylation of dynamin1 by calcineurin couples neurotrophin receptor endocytosis to axonal growth. *Neuron* **70**, 1085-1099.

Borsch-Haubold AG, Pasquet S & Watson SP. (1998). Direct inhibition of cyclooxygenase-1 and -2 by the kinase inhibitors SB 203580 and PD 98059. SB 203580 also inhibits thromboxane synthase. *J Biol Chem* **273**, 28766-28772.

Bottcher RT & Niehrs C. (2005). Fibroblast growth factor signaling during early vertebrate development. *Endocr Rev* **26**, 63-77.

Bowman T, Garcia R, Turkson J & Jove R. (2000). STATs in oncogenesis. *Oncogene* **19**, 2474-2488.

Boyle NT & Connor TJ. (2007). MDMA ("Ecstasy") suppresses the innate IFN-gamma response in vivo: a critical role for the anti-inflammatory cytokine IL-10. *Eur J Pharmacol* **572**, 228-238.

Bradford MM. (1976). A rapid and sensitive method for the quantitation of microgram quantities of protein utilizing the principle of protein-dye binding. *Anal Biochem* **72**, 248-254.

Brann AB, Scott R, Neuberger Y, Abulafia D, Boldin S, Fainzilber M & Futeran AH. (1999). Ceramide signaling downstream of the p75 neurotrophin receptor mediates the effects of nerve growth factor on outgrowth of cultured hippocampal neurons. *J Neurosci* **19**, 8199-8206.

Brunn GJ, Williams J, Sabers C, Wiederrecht G, Lawrence JC, Jr. & Abraham RT. (1996). Direct inhibition of the signaling functions of the mammalian target of rapamycin by the phosphoinositide 3-kinase inhibitors, wortmannin and LY294002. *EMBO J* **15**, 5256-5267.

Bruno MA & Cuello AC. (2006). Activity-dependent release of precursor nerve growth factor, conversion to mature nerve growth factor, and its degradation by a protease cascade. *Proc Natl Acad Sci U S A* **103**, 6735-6740.

Cajal S, R. (1937). *Recollections of My Life*. The MIT Press.

Canossa M, Griesbeck O, Berninger B, Campana G, Kolbeck R & Thoenen H. (1997). Neurotrophin release by neurotrophins: implications for activity-dependent neuronal plasticity. *Proc Natl Acad Sci U S A* **94**, 13279-13286.

Cantley LC. (2002). The phosphoinositide 3-kinase pathway. *Science* **296**, 1655-1657.

Cao JP, Wang HJ, Yu JK, Yang H, Xiao CH & Gao DS. (2008). Involvement of NCAM in the effects of GDNF on the neurite outgrowth in the dopamine neurons. *Neurosci Res* **61**, 390-397.

Carson MJ, Thomas EA, Danielson PE & Sutcliffe JG. (1996). The 5HT5A serotonin receptor is expressed predominantly by astrocytes in which it inhibits cAMP accumulation: a mechanism for neuronal suppression of reactive astrocytes. *Glia* **17**, 317-326.

Chalaris A, Garbers C, Rabe B, Rose-John S & Scheller J. (2011). The soluble Interleukin 6 receptor: generation and role in inflammation and cancer. *Eur J Cell Biol* **90**, 484-494.

Chao CC, Ma YL, Chu KY & Lee EH. (2003). Integrin α v and NCAM mediate the effects of GDNF on DA neuron survival, outgrowth, DA turnover and motor activity in rats. *Neurobiol Aging* **24**, 105-116.

Chao MV. (2003). Neurotrophins and their receptors: a convergence point for many signalling pathways. *Nat Rev Neurosci* **4**, 299-309.

Chen MJ, Nguyen TV, Pike CJ & Russo-Neustadt AA. (2007). Norepinephrine induces BDNF and activates the PI-3K and MAPK cascades in embryonic hippocampal neurons. *Cell Signal* **19**, 114-128.

Chlebova K, Bryja V, Dvorak P, Kozubik A, Wilcox WR & Krejci P. (2009). High molecular weight FGF2: the biology of a nuclear growth factor. *Cell Mol Life Sci* **66**, 225-235.

Civantos Calzada B & Aleixandre de Artinano A. (2001). Alpha-adrenoceptor subtypes. *Pharmacol Res* **44**, 195-208.

Clarke GL, Bhattacharjee A, Tague SE, Hasan W & Smith PG. (2010). ss-adrenoceptor blockers increase cardiac sympathetic innervation by inhibiting autoreceptor suppression of axon growth. *J Neurosci* **30**, 12446-12454.

Cohen-Cory S, Kidane AH, Shirkey NJ & Marshak S. (2010). Brain-derived neurotrophic factor and the development of structural neuronal connectivity. *Dev Neurobiol* **70**, 271-288.

Colangelo AM, Johnson PF & Mocchetti I. (1998). beta-adrenergic receptor-induced activation of nerve growth factor gene transcription in rat cerebral cortex involves CCAAT/enhancer-binding protein delta. *Proc Natl Acad Sci U S A* **95**, 10920-10925.

Colombo E, Cordiglieri C, Melli G, Newcombe J, Krumbholz M, Parada LF, Medico E, Hohlfeld R, Meinel E & Farina C. (2012). Stimulation of the neurotrophin receptor TrkB on astrocytes drives nitric oxide production and neurodegeneration. *J Exp Med* **209**, 521-535.

Conde C & Caceres A. (2009). Microtubule assembly, organization and dynamics in axons and dendrites. *Nat Rev Neurosci* **10**, 319-332.

Conner JM, Darracq MA, Roberts J & Tuszynski MH. (2001). Nontropic actions of neurotrophins: subcortical nerve growth factor gene delivery reverses age-related degeneration of primate cortical cholinergic innervation. *Proc Natl Acad Sci U S A* **98**, 1941-1946.

Costantini LC & Isacson O. (2000). Immunophilin ligands and GDNF enhance neurite branching or elongation from developing dopamine neurons in culture. *Exp Neurol* **164**, 60-70.

Counts SE & Mufson EJ. (2010). Noradrenaline activation of neurotrophic pathways protects against neuronal amyloid toxicity. *J Neurochem* **113**, 649-660.

Cowley S, Paterson H, Kemp P & Marshall CJ. (1994). Activation of MAP kinase kinase is necessary and sufficient for PC12 differentiation and for transformation of NIH 3T3 cells. *Cell* **77**, 841-852.

Cui Q. (2006). Actions of neurotrophic factors and their signaling pathways in neuronal survival and axonal regeneration. *Mol Neurobiol* **33**, 155-179.

Culmsee C, Stumm RK, Schafer MK, Weihe E & Kriegelstein J. (1999). Clenbuterol induces growth factor mRNA, activates astrocytes, and protects rat brain tissue against ischemic damage. *Eur J Pharmacol* **379**, 33-45.

Daaka Y, Luttrell LM & Lefkowitz RJ. (1997). Switching of the coupling of the beta2-adrenergic receptor to different G proteins by protein kinase A. *Nature* **390**, 88-91.

Daniel WA. (2003). Mechanisms of cellular distribution of psychotropic drugs. Significance for drug action and interactions. *Prog Neuropsychopharmacol Biol Psychiatry* **27**, 65-73.

Davalos D, Grutzendler J, Yang G, Kim JV, Zuo Y, Jung S, Littman DR, Dustin ML & Gan WB. (2005). ATP mediates rapid microglial response to local brain injury in vivo. *Nat Neurosci* **8**, 752-758.

Davies AM, Thoenen H & Barde YA. (1986). The response of chick sensory neurons to brain-derived neurotrophic factor. *J Neurosci* **6**, 1897-1904.

Davies SP, Reddy H, Caivano M & Cohen P. (2000). Specificity and mechanism of action of some commonly used protein kinase inhibitors. *Biochem J* **351**, 95-105.

Dechant G & Barde YA. (2002). The neurotrophin receptor p75(NTR): novel functions and implications for diseases of the nervous system. *Nat Neurosci* **5**, 1131-1136.

Delgado-Rivera R, Harris SL, Ahmed I, Babu AN, Patel RP, Ayres V, Flowers D & Meiners S. (2009). Increased FGF-2 secretion and ability to support neurite outgrowth by astrocytes cultured on polyamide nanofibrillar matrices. *Matrix Biol* **28**, 137-147.

Dent EW & Gertler FB. (2003). Cytoskeletal dynamics and transport in growth cone motility and axon guidance. *Neuron* **40**, 209-227.

- Desagher S, Glowinski J & Premont J. (1996). Astrocytes protect neurons from hydrogen peroxide toxicity. *J Neurosci* **16**, 2553-2562.
- Dijkhuizen PA & Ghosh A. (2005). BDNF regulates primary dendrite formation in cortical neurons via the PI3-kinase and MAP kinase signaling pathways. *J Neurobiol* **62**, 278-288.
- Dijkstra S, Bar PR, Gispen WH & Joosten EA. (1999). Selective stimulation of dendrite outgrowth from identified corticospinal neurons by homotopic astrocytes. *Neuroscience* **92**, 1331-1342.
- Ditlevsen DK, Kohler LB, Pedersen MV, Risell M, Kolkova K, Meyer M, Berezin V & Bock E. (2003). The role of phosphatidylinositol 3-kinase in neural cell adhesion molecule-mediated neuronal differentiation and survival. *J Neurochem* **84**, 546-556.
- Drago J, Murphy M, Carroll SM, Harvey RP & Bartlett PF. (1991). Fibroblast growth factor-mediated proliferation of central nervous system precursors depends on endogenous production of insulin-like growth factor I. *Proc Natl Acad Sci U S A* **88**, 2199-2203.
- Druse M, Tajuddin NF, Gillespie RA & Le P. (2005). Signaling pathways involved with serotonin1A agonist-mediated neuroprotection against ethanol-induced apoptosis of fetal rhombencephalic neurons. *Brain Res Dev Brain Res* **159**, 18-28.
- Ducray A, Krebs SH, Schaller B, Seiler RW, Meyer M & Widmer HR. (2006). GDNF family ligands display distinct action profiles on cultured GABAergic and serotonergic neurons of rat ventral mesencephalon. *Brain Res* **1069**, 104-112.

- Duman RS, Nakagawa S & Malberg J. (2001). Regulation of adult neurogenesis by antidepressant treatment. *Neuropsychopharmacology* **25**, 836-844.
- Dunn AJ & Swiergiel AH. (2008). The role of corticotropin-releasing factor and noradrenaline in stress-related responses, and the inter-relationships between the two systems. *Eur J Pharmacol* **583**, 186-193.
- Eibl JK, Chapelsky SA & Ross GM. (2010). Multipotent neurotrophin antagonist targets brain-derived neurotrophic factor and nerve growth factor. *J Pharmacol Exp Ther* **332**, 446-454.
- Eisenhofer G, Huynh TT, Hiroi M & Pacak K. (2001). Understanding catecholamine metabolism as a guide to the biochemical diagnosis of pheochromocytoma. *Rev Endocr Metab Disord* **2**, 297-311.
- Eketjall S, Fainzilber M, Murray-Rust J & Ibanez CF. (1999). Distinct structural elements in GDNF mediate binding to GFR α 1 and activation of the GFR α 1-c-Ret receptor complex. *EMBO J* **18**, 5901-5910.
- Emamian ES, Hall D, Birnbaum MJ, Karayiorgou M & Gogos JA. (2004). Convergent evidence for impaired AKT1-GSK3 β signaling in schizophrenia. *Nat Genet* **36**, 131-137.
- Feldman RS, Meyer JS & Quenzer LF. (1997). *Principles of Neuropsychopharmacology*. Sinauer Associates, Inc., Publishers, Sunderland, Massachusetts.

- Ferrara N, Gerber HP & LeCouter J. (2003). The biology of VEGF and its receptors. *Nat Med* **9**, 669-676.
- Fitch MT & Silver J. (2008). CNS injury, glial scars, and inflammation: Inhibitory extracellular matrices and regeneration failure. *Exp Neurol* **209**, 294-301.
- Foehr ED, Lin X, O'Mahony A, Gelezianas R, Bradshaw RA & Greene WC. (2000). NF-kappa B signaling promotes both cell survival and neurite process formation in nerve growth factor-stimulated PC12 cells. *J Neurosci* **20**, 7556-7563.
- Follesa P & Mocchetti I. (1993). Regulation of basic fibroblast growth factor and nerve growth factor mRNA by beta-adrenergic receptor activation and adrenal steroids in rat central nervous system. *Mol Pharmacol* **43**, 132-138.
- Fredriksson JM, Lindquist JM, Bronnikov GE & Nedergaard J. (2000). Norepinephrine induces vascular endothelial growth factor gene expression in brown adipocytes through a beta -adrenoreceptor/cAMP/protein kinase A pathway involving Src but independently of Erk1/2. *J Biol Chem* **275**, 13802-13811.
- Fricker AD, Rios C, Devi LA & Gomes I. (2005). Serotonin receptor activation leads to neurite outgrowth and neuronal survival. *Brain Res Mol Brain Res* **138**, 228-235.
- Fukumoto H, Kakihana M & Suno M. (1991). Recombinant human basic fibroblast growth factor (rhbFGF) induces secretion of nerve growth factor (NGF) in cultured rat astroglial cells. *Neurosci Lett* **122**, 221-224.
- Gage FH. (2002). Neurogenesis in the adult brain. *J Neurosci* **22**, 612-613.

- Galea I, Bechmann I & Perry VH. (2007). What is immune privilege (not)? *Trends Immunol* **28**, 12-18.
- Gallo G. (2011). The cytoskeletal and signaling mechanisms of axon collateral branching. *Dev Neurobiol* **71**, 201-220.
- Gallo G & Letourneau PC. (1998). Localized sources of neurotrophins initiate axon collateral sprouting. *J Neurosci* **18**, 5403-5414.
- Gauthier C, Rozec B, Manoury B & Balligand JL. (2011). Beta-3 adrenoceptors as new therapeutic targets for cardiovascular pathologies. *Curr Heart Fail Rep* **8**, 184-192.
- Gharbi SI, Zvelebil MJ, Shuttleworth SJ, Hancox T, Saghir N, Timms JF & Waterfield MD. (2007). Exploring the specificity of the PI3K family inhibitor LY294002. *Biochem J* **404**, 15-21.
- Gilardino A, Farcito S, Zamburlin P, Audisio C & Lovisolo D. (2009). Specificity of the second messenger pathways involved in basic fibroblast growth factor-induced survival and neurite growth in chick ciliary ganglion neurons. *J Neurosci Res* **87**, 2951-2962.
- Goddard AW, Ball SG, Martinez J, Robinson MJ, Yang CR, Russell JM & Shekhar A. (2010). Current perspectives of the roles of the central norepinephrine system in anxiety and depression. *Depress Anxiety* **27**, 339-350.
- Goldberg JL. (2003). How does an axon grow? *Genes Dev* **17**, 941-958.

- Gotoh N. (2008). Regulation of growth factor signaling by FRS2 family docking/scaffold adaptor proteins. *Cancer Sci* **99**, 1319-1325.
- Gottesmann C. (2008). Noradrenaline involvement in basic and higher integrated REM sleep processes. *Prog Neurobiol* **85**, 237-272.
- Govek EE, Newey SE & Van Aelst L. (2005). The role of the Rho GTPases in neuronal development. *Genes Dev* **19**, 1-49.
- Graeber MB, Li W & Rodriguez ML. (2011). Role of microglia in CNS inflammation. *FEBS Lett* **585**, 3798-3805.
- Greene LA & Tischler AS. (1976). Establishment of a noradrenergic clonal line of rat adrenal pheochromocytoma cells which respond to nerve growth factor. *Proc Natl Acad Sci U S A* **73**, 2424-2428.
- Griffin EW, Bechara RG, Birch AM & Kelly AM. (2009). Exercise enhances hippocampal-dependent learning in the rat: evidence for a BDNF-related mechanism. *Hippocampus* **19**, 973-980.
- Group TBS. (1999). A controlled trial of recombinant methionyl human BDNF in ALS: The BDNF Study Group (Phase III). *Neurology* **52**, 1427-1433.
- Gu H & Neel BG. (2003). The "Gab" in signal transduction. *Trends Cell Biol* **13**, 122-130.

Gu Q. (2002). Neuromodulatory transmitter systems in the cortex and their role in cortical plasticity. *Neuroscience* **111**, 815-835.

Guo S, Arai K, Stins MF, Chuang DM & Lo EH. (2009). Lithium upregulates vascular endothelial growth factor in brain endothelial cells and astrocytes. *Stroke* **40**, 652-655.

Guo Y, Xiao P, Lei S, Deng F, Xiao GG, Liu Y, Chen X, Li L, Wu S, Chen Y, Jiang H, Tan L, Xie J, Zhu X, Liang S & Deng H. (2008). How is mRNA expression predictive for protein expression? A correlation study on human circulating monocytes. *Acta Biochim Biophys Sin (Shanghai)* **40**, 426-436.

Gutierrez H & Davies AM. (2007). A fast and accurate procedure for deriving the Sholl profile in quantitative studies of neuronal morphology. *J Neurosci Methods* **163**, 24-30.

Gutierrez H, O'Keeffe GW, Gavalda N, Gallagher D & Davies AM. (2008). Nuclear factor kappa B signaling either stimulates or inhibits neurite growth depending on the phosphorylation status of p65/RelA. *J Neurosci* **28**, 8246-8256.

Gyires K, Zadori ZS, Torok T & Matyus P. (2009). alpha(2)-Adrenoceptor subtypes-mediated physiological, pharmacological actions. *Neurochem Int* **55**, 447-453.

Hagg T. (2006). Collateral sprouting as a target for improved function after spinal cord injury. *J Neurotrauma* **23**, 281-294.

Hakkoum D, Stoppini L & Muller D. (2007). Interleukin-6 promotes sprouting and functional recovery in lesioned organotypic hippocampal slice cultures. *J Neurochem* **100**, 747-757.

Hama T, Miyamoto M, Tsukui H, Nishio C & Hatanaka H. (1989). Interleukin-6 as a neurotrophic factor for promoting the survival of cultured basal forebrain cholinergic neurons from postnatal rats. *Neurosci Lett* **104**, 340-344.

Hamanoue M, Middleton G, Wyatt S, Jaffray E, Hay RT & Davies AM. (1999). p75-mediated NF-kappaB activation enhances the survival response of developing sensory neurons to nerve growth factor. *Mol Cell Neurosci* **14**, 28-40.

Hannon J & Hoyer D. (2008). Molecular biology of 5-HT receptors. *Behav Brain Res* **195**, 198-213.

Harada T, Harada C, Kohsaka S, Wada E, Yoshida K, Ohno S, Mamada H, Tanaka K, Parada LF & Wada K. (2002). Microglia-Muller glia cell interactions control neurotrophic factor production during light-induced retinal degeneration. *J Neurosci* **22**, 9228-9236.

Hauck SM, Kinkl N, Deeg CA, Swiatek-de Lange M, Schoffmann S & Ueffing M. (2006). GDNF family ligands trigger indirect neuroprotective signaling in retinal glial cells. *Mol Cell Biol* **26**, 2746-2757.

Hayashi T, Ohtani A, Onuki F, Natsume M, Li F, Satou T, Yoshikawa M, Senzaki K & Shiga T. (2010). Roles of serotonin 5-HT₃ receptor in the formation of dendrites and axons in the rat cerebral cortex: an in vitro study. *Neurosci Res* **66**, 22-29.

Haydon PG, McCobb DP & Kater SB. (1984). Serotonin selectively inhibits growth cone motility and synaptogenesis of specific identified neurons. *Science* **226**, 561-564.

Hayes VY, Isackson PJ, Fabrazzo M, Follesa P & Mocchetti I. (1995). Induction of nerve growth factor and basic fibroblast growth factor mRNA following clenbuterol: contrasting anatomical and cellular localization. *Exp Neurol* **132**, 33-41.

He JC, Gomes I, Nguyen T, Jayaram G, Ram PT, Devi LA & Iyengar R. (2005). The G alpha(o/i)-coupled cannabinoid receptor-mediated neurite outgrowth involves Rap regulation of Src and Stat3. *J Biol Chem* **280**, 33426-33434.

Heese K, Hock C & Otten U. (1998). Inflammatory signals induce neurotrophin expression in human microglial cells. *J Neurochem* **70**, 699-707.

Heinrich PC, Behrmann I, Haan S, Hermanns HM, Muller-Newen G & Schaper F. (2003). Principles of interleukin (IL)-6-type cytokine signalling and its regulation. *Biochem J* **374**, 1-20.

Hellweg R, Ziegenhorn A, Heuser I & Deuschle M. (2008). Serum concentrations of nerve growth factor and brain-derived neurotrophic factor in depressed patients before and after antidepressant treatment. *Pharmacopsychiatry* **41**, 66-71.

Hensel N, Ratzka A, Brinkmann H, Klimaschewski L, Grothe C & Claus P. (2012). Analysis of the fibroblast growth factor system reveals alterations in a mouse model of spinal muscular atrophy. *PLoS One* **7**, e31202.

Herdegen T & Leah JD. (1998). Inducible and constitutive transcription factors in the mammalian nervous system: control of gene expression by Jun, Fos and Krox, and CREB/ATF proteins. *Brain Res Brain Res Rev* **28**, 370-490.

Hirano T, Yasukawa K, Harada H, Taga T, Watanabe Y, Matsuda T, Kashiwamura S, Nakajima K, Koyama K, Iwamatsu A & et al. (1986). Complementary DNA for a novel human interleukin (BSF-2) that induces B lymphocytes to produce immunoglobulin.

Nature **324**, 73-76.

Hisaoka K, Maeda N, Tsuchioka M & Takebayashi M. (2008). Antidepressants induce acute CREB phosphorylation and CRE-mediated gene expression in glial cells: a possible contribution to GDNF production. *Brain Res* **1196**, 53-58.

Hisaoka K, Nishida A, Takebayashi M, Koda T, Yamawaki S & Nakata Y. (2004). Serotonin increases glial cell line-derived neurotrophic factor release in rat C6 glioblastoma cells. *Brain Res* **1002**, 167-170.

Hisaoka K, Takebayashi M, Tsuchioka M, Maeda N, Nakata Y & Yamawaki S. (2007). Antidepressants increase glial cell line-derived neurotrophic factor production through monoamine-independent activation of protein tyrosine kinase and extracellular signal-regulated kinase in glial cells. *J Pharmacol Exp Ther* **321**, 148-157.

Hisaoka K, Tsuchioka M, Yano R, Maeda N, Kajitani N, Morioka N, Nakata Y & Takebayashi M. (2011). Tricyclic antidepressant amitriptyline activates fibroblast growth factor receptor signaling in glial cells: involvement in glial cell line-derived neurotrophic factor production. *J Biol Chem* **286**, 21118-21128.

Holtmaat A & Svoboda K. (2009). Experience-dependent structural synaptic plasticity in the mammalian brain. *Nat Rev Neurosci* **10**, 647-658.

Homburger V, Lucas M, Rosenbaum E, Vassent G & Bockaert J. (1981). Presence of both beta1- and beta2-adrenergic receptors in a single cell type. *Mol Pharmacol* **20**, 463-469.

- Homma K, Kitamura Y, Ogawa H & Oka K. (2006). Serotonin induces the increase in intracellular Ca²⁺ that enhances neurite outgrowth in PC12 cells via activation of 5-HT₃ receptors and voltage-gated calcium channels. *J Neurosci Res* **84**, 316-325.
- Horch HW & Katz LC. (2002). BDNF release from single cells elicits local dendritic growth in nearby neurons. *Nat Neurosci* **5**, 1177-1184.
- Hornung JP. (2003). The human raphe nuclei and the serotonergic system. *J Chem Neuroanat* **26**, 331-343.
- Hou JG, Lin LF & Mytilineou C. (1996). Glial cell line-derived neurotrophic factor exerts neurotrophic effects on dopaminergic neurons in vitro and promotes their survival and regrowth after damage by 1-methyl-4-phenylpyridinium. *J Neurochem* **66**, 74-82.
- Hur EM & Zhou FQ. (2010). GSK3 signalling in neural development. *Nat Rev Neurosci* **11**, 539-551.
- Ihara S, Nakajima K, Fukada T, Hibi M, Nagata S, Hirano T & Fukui Y. (1997). Dual control of neurite outgrowth by STAT3 and MAP kinase in PC12 cells stimulated with interleukin-6. *EMBO J* **16**, 5345-5352.
- Ikeda K, Iwasaki Y, Shiojima T & Kinoshita M. (1996). Neuroprotective effect of various cytokines on developing spinal motoneurons following axotomy. *J Neurol Sci* **135**, 109-113.
- Inazu M, Takeda H & Matsumiya T. (2003). Functional expression of the norepinephrine transporter in cultured rat astrocytes. *J Neurochem* **84**, 136-144.

Iversen L. (2006). Neurotransmitter transporters and their impact on the development of psychopharmacology. *Br J Pharmacol* **147 Suppl 1**, S82-88.

Jackson TR, Blader IJ, Hammonds-Odie LP, Burga CR, Cooke F, Hawkins PT, Wolf AG, Heldman KA & Theibert AB. (1996). Initiation and maintenance of NGF-stimulated neurite outgrowth requires activation of a phosphoinositide 3-kinase. *J Cell Sci* **109 (Pt 2)**, 289-300.

Jang SW, Liu X, Chan CB, Weinshenker D, Hall RA, Xiao G & Ye K. (2009). Amitriptyline is a TrkA and TrkB receptor agonist that promotes TrkA/TrkB heterodimerization and has potent neurotrophic activity. *Chem Biol* **16**, 644-656.

Jiang H, Guo W, Liang X & Rao Y. (2005). Both the establishment and the maintenance of neuronal polarity require active mechanisms: critical roles of GSK-3 β and its upstream regulators. *Cell* **120**, 123-135.

Jin K, Mao XO & Greenberg DA. (2006). Vascular endothelial growth factor stimulates neurite outgrowth from cerebral cortical neurons via Rho kinase signaling. *J Neurobiol* **66**, 236-242.

Jin X, Hu H, Mathers PH & Agmon A. (2003). Brain-derived neurotrophic factor mediates activity-dependent dendritic growth in nonpyramidal neocortical interneurons in developing organotypic cultures. *J Neurosci* **23**, 5662-5673.

Johnson GL & Lapadat R. (2002). Mitogen-activated protein kinase pathways mediated by ERK, JNK, and p38 protein kinases. *Science* **298**, 1911-1912.

Johnson M. (2001). Beta2-adrenoceptors: mechanisms of action of beta2-agonists. *Paediatr Respir Rev* **2**, 57-62.

Johnson M. (2006). Molecular mechanisms of beta(2)-adrenergic receptor function, response, and regulation. *J Allergy Clin Immunol* **117**, 18-24; quiz 25.

Jones SA, Scheller J & Rose-John S. (2011). Therapeutic strategies for the clinical blockade of IL-6/gp130 signaling. *J Clin Invest* **121**, 3375-3383.

Junker V, Becker A, Huhne R, Zembatov M, Ravati A, Culmsee C & Krieglstein J. (2002). Stimulation of beta-adrenoceptors activates astrocytes and provides neuroprotection. *Eur J Pharmacol* **446**, 25-36.

Juric DM, Miklic S & Carman-Krzan M. (2006). Monoaminergic neuronal activity up-regulates BDNF synthesis in cultured neonatal rat astrocytes. *Brain Res* **1108**, 54-62.

Ketschek A & Gallo G. (2010). Nerve growth factor induces axonal filopodia through localized microdomains of phosphoinositide 3-kinase activity that drive the formation of cytoskeletal precursors to filopodia. *J Neurosci* **30**, 12185-12197.

Ketschek A, Spillane M & Gallo G. (2011). Mechanism of NGF-induced formation of axonal filopodia: NGF turns up the volume, but the song remains the same? *Commun Integr Biol* **4**, 55-58.

Khaibullina AA, Rosenstein JM & Krum JM. (2004). Vascular endothelial growth factor promotes neurite maturation in primary CNS neuronal cultures. *Brain Res Dev Brain Res* **148**, 59-68.

Kim B, Leventhal PS, Saltiel AR & Feldman EL. (1997). Insulin-like growth factor-I-mediated neurite outgrowth in vitro requires mitogen-activated protein kinase activation. *J Biol Chem* **272**, 21268-21273.

Kimelberg HK. (1995). Receptors on astrocytes--what possible functions? *Neurochem Int* **26**, 27-40.

Kimura K, Hattori S, Kabuyama Y, Shizawa Y, Takayanagi J, Nakamura S, Toki S, Matsuda Y, Onodera K & Fukui Y. (1994). Neurite outgrowth of PC12 cells is suppressed by wortmannin, a specific inhibitor of phosphatidylinositol 3-kinase. *J Biol Chem* **269**, 18961-18967.

Kiyota T, Ingraham KL, Jacobsen MT, Xiong H & Ikezu T. (2011). FGF2 gene transfer restores hippocampal functions in mouse models of Alzheimer's disease and has therapeutic implications for neurocognitive disorders. *Proc Natl Acad Sci U S A* **108**, E1339-1348.

Knowles JK, Rajadas J, Nguyen TV, Yang T, LeMieux MC, Vander Griend L, Ishikawa C, Massa SM, Wyss-Coray T & Longo FM. (2009). The p75 neurotrophin receptor promotes amyloid-beta(1-42)-induced neuritic dystrophy in vitro and in vivo. *J Neurosci* **29**, 10627-10637.

Kobayashi K & Yasoshima Y. (2001). The central noradrenaline system and memory consolidation. *Neuroscientist* **7**, 371-376.

Kobayashi M, Nagata S, Kita Y, Nakatsu N, Ihara S, Kaibuchi K, Kuroda S, Ui M, Iba H, Konishi H, Kikkawa U, Saitoh I & Fukui Y. (1997). Expression of a constitutively active

phosphatidylinositol 3-kinase induces process formation in rat PC12 cells. Use of Cre/loxP recombination system. *J Biol Chem* **272**, 16089-16092.

Kordower JH, Emborg ME, Bloch J, Ma SY, Chu Y, Leventhal L, McBride J, Chen EY, Palfi S, Roitberg BZ, Brown WD, Holden JE, Pyzalski R, Taylor MD, Carvey P, Ling Z, Trono D, Hantraye P, Deglon N & Aebischer P. (2000). Neurodegeneration prevented by lentiviral vector delivery of GDNF in primate models of Parkinson's disease. *Science* **290**, 767-773.

Krzan M, Wu VW & Schwartz JP. (2001). Serotonin regulation of nerve growth factor synthesis in neonatal and adult astrocytes: comparison to the beta-adrenergic agonist isoproterenol. *J Neurosci Res* **64**, 261-267.

Kumar V, Zhang MX, Swank MW, Kunz J & Wu GY. (2005). Regulation of dendritic morphogenesis by Ras-PI3K-Akt-mTOR and Ras-MAPK signaling pathways. *J Neurosci* **25**, 11288-11299.

Laming PR, Kimelberg H, Robinson S, Salm A, Hawrylak N, Muller C, Roots B & Ng K. (2000). Neuronal-glia interactions and behaviour. *Neurosci Biobehav Rev* **24**, 295-340.

Lee J, Kotliarova S, Kotliarov Y, Li A, Su Q, Donin NM, Pastorino S, Purow BW, Christopher N, Zhang W, Park JK & Fine HA. (2006). Tumor stem cells derived from glioblastomas cultured in bFGF and EGF more closely mirror the phenotype and genotype of primary tumors than do serum-cultured cell lines. *Cancer Cell* **9**, 391-403.

Lee JH, Park SM, Kim OS, Lee CS, Woo JH, Park SJ, Joe EH & Jou I. (2009a). Differential SUMOylation of LXRalpha and LXRbeta mediates transrepression of STAT1 inflammatory signaling in IFN-gamma-stimulated brain astrocytes. *Mol Cell* **35**, 806-817.

- Lee JS, Jang DJ, Lee N, Ko HG, Kim H, Kim YS, Kim B, Son J, Kim SH, Chung H, Lee MY, Kim WR, Sun W, Zhuo M, Abel T, Kaang BK & Son H. (2009b). Induction of neuronal vascular endothelial growth factor expression by cAMP in the dentate gyrus of the hippocampus is required for antidepressant-like behaviors. *J Neurosci* **29**, 8493-8505.
- Lee YK, Choi IS, Kim YH, Kim KH, Nam SY, Yun YW, Lee MS, Oh KW & Hong JT. (2009c). Neurite outgrowth effect of 4-O-methylhonokiol by induction of neurotrophic factors through ERK activation. *Neurochem Res* **34**, 2251-2260.
- Leibinger M, Muller A, Andreadaki A, Hauk TG, Kirsch M & Fischer D. (2009). Neuroprotective and axon growth-promoting effects following inflammatory stimulation on mature retinal ganglion cells in mice depend on ciliary neurotrophic factor and leukemia inhibitory factor. *J Neurosci* **29**, 14334-14341.
- Lenhard T, Schober A, Suter-Crazzolara C & Unsicker K. (2002). Fibroblast growth factor-2 requires glial-cell-line-derived neurotrophic factor for exerting its neuroprotective actions on glutamate-lesioned hippocampal neurons. *Mol Cell Neurosci* **20**, 181-197.
- Lessmann V & Brigadski T. (2009). Mechanisms, locations, and kinetics of synaptic BDNF secretion: an update. *Neurosci Res* **65**, 11-22.
- Levi-Montalcini R. (1964). Growth Control of Nerve Cells by a Protein Factor and Its Antiserum: Discovery of This Factor May Provide New Leads to Understanding of Some Neurogenetic Processes. *Science* **143**, 105-110.
- Lin LF, Doherty DH, Lile JD, Bektesh S & Collins F. (1993). GDNF: a glial cell line-derived neurotrophic factor for midbrain dopaminergic neurons. *Science* **260**, 1130-1132.

- Lirk P, Haller I, Hausott B, Ingorokva S, Deibl M, Gerner P & Klimaschewski L. (2006). The neurotoxic effects of amitriptyline are mediated by apoptosis and are effectively blocked by inhibition of caspase activity. *Anesth Analg* **102**, 1728-1733.
- Liu B & Hong JS. (2003). Role of microglia in inflammation-mediated neurodegenerative diseases: mechanisms and strategies for therapeutic intervention. *J Pharmacol Exp Ther* **304**, 1-7.
- Liu RY & Snider WD. (2001). Different signaling pathways mediate regenerative versus developmental sensory axon growth. *J Neurosci* **21**, RC164.
- Lu P, Yang H, Jones LL, Filbin MT & Tuszynski MH. (2004). Combinatorial therapy with neurotrophins and cAMP promotes axonal regeneration beyond sites of spinal cord injury. *J Neurosci* **24**, 6402-6409.
- Lucki I. (1998). The spectrum of behaviors influenced by serotonin. *Biol Psychiatry* **44**, 151-162.
- Luikart BW, Zhang W, Wayman GA, Kwon CH, Westbrook GL & Parada LF. (2008). Neurotrophin-dependent dendritic filopodial motility: a convergence on PI3K signaling. *J Neurosci* **28**, 7006-7012.
- Luo L. (2002). Actin cytoskeleton regulation in neuronal morphogenesis and structural plasticity. *Annu Rev Cell Dev Biol* **18**, 601-635.
- Madduri S, Papaloizos M & Gander B. (2009). Synergistic effect of GDNF and NGF on axonal branching and elongation in vitro. *Neurosci Res* **65**, 88-97.

Madrigal JL, Leza JC, Polak P, Kalinin S & Feinstein DL. (2009). Astrocyte-derived MCP-1 mediates neuroprotective effects of noradrenaline. *J Neurosci* **29**, 263-267.

Manni M, Granstein RD & Maestroni G. (2011). beta2-Adrenergic agonists bias TLR-2 and NOD2 activated dendritic cells towards inducing an IL-17 immune response. *Cytokine* **55**, 380-386.

Marien MR, Colpaert FC & Rosenquist AC. (2004). Noradrenergic mechanisms in neurodegenerative diseases: a theory. *Brain Res Brain Res Rev* **45**, 38-78.

Markiewicz I & Lukomska B. (2006). The role of astrocytes in the physiology and pathology of the central nervous system. *Acta Neurobiol Exp (Wars)* **66**, 343-358.

Marz P, Herget T, Lang E, Otten U & Rose-John S. (1997). Activation of gp130 by IL-6/soluble IL-6 receptor induces neuronal differentiation. *Eur J Neurosci* **9**, 2765-2773.

Marz P, Otten U & Rose-John S. (1999). Neural activities of IL-6-type cytokines often depend on soluble cytokine receptors. *Eur J Neurosci* **11**, 2995-3004.

Matsuoka I, Meyer M & Thoenen H. (1991). Cell-type-specific regulation of nerve growth factor (NGF) synthesis in non-neuronal cells: comparison of Schwann cells with other cell types. *J Neurosci* **11**, 3165-3177.

McAllister AK, Katz LC & Lo DC. (1997). Opposing roles for endogenous BDNF and NT-3 in regulating cortical dendritic growth. *Neuron* **18**, 767-778.

McCauslin CS, Heath V, Colangelo AM, Malik R, Lee S, Mallei A, Mocchetti I & Johnson PF. (2006). CAAT/enhancer-binding protein delta and cAMP-response element-binding protein mediate inducible expression of the nerve growth factor gene in the central nervous system. *J Biol Chem* **281**, 17681-17688.

McCobb DP, Cohan CS, Connor JA & Kater SB. (1988). Interactive effects of serotonin and acetylcholine on neurite elongation. *Neuron* **1**, 377-385.

McNamee EN, Ryan KM, Griffin EW, Gonzalez-Reyes RE, Ryan KJ, Harkin A & Connor TJ. (2010a). Noradrenaline acting at central beta-adrenoceptors induces interleukin-10 and suppressor of cytokine signaling-3 expression in rat brain: implications for neurodegeneration. *Brain Behav Immun* **24**, 660-671.

McNamee EN, Ryan KM, Kilroy D & Connor TJ. (2010b). Noradrenaline induces IL-1ra and IL-1 type II receptor expression in primary glial cells and protects against IL-1beta-induced neurotoxicity. *Eur J Pharmacol* **626**, 219-228.

Mele T, Carman-Krzan M & Juric DM. (2010). Regulatory role of monoamine neurotransmitters in astrocytic NT-3 synthesis. *Int J Dev Neurosci* **28**, 13-19.

Mitchell HA & Weinshenker D. (2010). Good night and good luck: norepinephrine in sleep pharmacology. *Biochem Pharmacol* **79**, 801-809.

Mori K, Ozaki E, Zhang B, Yang L, Yokoyama A, Takeda I, Maeda N, Sakanaka M & Tanaka J. (2002). Effects of norepinephrine on rat cultured microglial cells that express alpha1, alpha2, beta1 and beta2 adrenergic receptors. *Neuropharmacology* **43**, 1026-1034.

Mount HT, Dean DO, Alberch J, Dreyfus CF & Black IB. (1995). Glial cell line-derived neurotrophic factor promotes the survival and morphologic differentiation of Purkinje cells. *Proc Natl Acad Sci U S A* **92**, 9092-9096.

Nagahara AH, Merrill DA, Coppola G, Tsukada S, Schroeder BE, Shaked GM, Wang L, Blesch A, Kim A, Conner JM, Rockenstein E, Chao MV, Koo EH, Geschwind D, Masliah E, Chiba AA & Tuszynski MH. (2009). Neuroprotective effects of brain-derived neurotrophic factor in rodent and primate models of Alzheimer's disease. *Nat Med* **15**, 331-337.

Nagahara AH & Tuszynski MH. (2011). Potential therapeutic uses of BDNF in neurological and psychiatric disorders. *Nat Rev Drug Discov* **10**, 209-219.

Neve KA, Barrett DA & Molinoff PB. (1985). Selective regulation of beta-1 and beta-2 adrenergic receptors by atypical agonists. *J Pharmacol Exp Ther* **235**, 657-664.

Niblock MM, Brunso-Bechtold JK & Riddle DR. (2000). Insulin-like growth factor I stimulates dendritic growth in primary somatosensory cortex. *J Neurosci* **20**, 4165-4176.

Nickel W. (2010). Pathways of unconventional protein secretion. *Curr Opin Biotechnol* **21**, 621-626.

Nielsen J, Gotfryd K, Li S, Kulahin N, Soroka V, Rasmussen KK, Bock E & Berezin V. (2009). Role of glial cell line-derived neurotrophic factor (GDNF)-neural cell adhesion molecule (NCAM) interactions in induction of neurite outgrowth and identification of a binding site for NCAM in the heel region of GDNF. *J Neurosci* **29**, 11360-11376.

Nimmerjahn A, Kirchhoff F & Helmchen F. (2005). Resting microglial cells are highly dynamic surveillants of brain parenchyma in vivo. *Science* **308**, 1314-1318.

Norris JG & Benveniste EN. (1993). Interleukin-6 production by astrocytes: induction by the neurotransmitter norepinephrine. *J Neuroimmunol* **45**, 137-145.

O'Keeffe GW, Gutierrez H, Pandolfi PP, Riccardi C & Davies AM. (2008). NGF-promoted axon growth and target innervation requires GITRL-GITR signaling. *Nat Neurosci* **11**, 135-142.

Obara Y & Nakahata N. (2010). The signaling pathway leading to extracellular signal-regulated kinase 5 (ERK5) activation via G-proteins and ERK5-dependent neurotrophic effects. *Mol Pharmacol* **77**, 10-16.

Oh J, Recknor JB, Recknor JC, Mallapragada SK & Sakaguchi DS. (2009). Soluble factors from neocortical astrocytes enhance neuronal differentiation of neural progenitor cells from adult rat hippocampus on micropatterned polymer substrates. *J Biomed Mater Res A* **91**, 575-585.

Oosterink BJ, Korte SM, Nyakas C, Korf J & Luiten PG. (1998). Neuroprotection against N-methyl-D-aspartate-induced excitotoxicity in rat magnocellular nucleus basalis by the 5-HT_{1A} receptor agonist 8-OH-DPAT. *Eur J Pharmacol* **358**, 147-152.

Opal SM & DePalo VA. (2000). Anti-inflammatory cytokines. *Chest* **117**, 1162-1172.

- Ornitz DM, Xu J, Colvin JS, McEwen DG, MacArthur CA, Coulier F, Gao G & Goldfarb M. (1996). Receptor specificity of the fibroblast growth factor family. *J Biol Chem* **271**, 15292-15297.
- Paratcha G, Ledda F, Baars L, Coulpier M, Besset V, Anders J, Scott R & Ibanez CF. (2001). Released GFR α 1 potentiates downstream signaling, neuronal survival, and differentiation via a novel mechanism of recruitment of c-Ret to lipid rafts. *Neuron* **29**, 171-184.
- Paratcha G, Ledda F & Ibanez CF. (2003). The neural cell adhesion molecule NCAM is an alternative signaling receptor for GDNF family ligands. *Cell* **113**, 867-879.
- Park JA, Lee JY, Sato TA & Koh JY. (2000). Co-induction of p75^{NTR} and p75^{NTR}-associated death executor in neurons after zinc exposure in cortical culture or transient ischemia in the rat. *J Neurosci* **20**, 9096-9103.
- Patel MN & McNamara JO. (1995). Selective enhancement of axonal branching of cultured dentate gyrus neurons by neurotrophic factors. *Neuroscience* **69**, 763-770.
- Penn RD, Dalvi A, Slevin J, Young B, Gash D, Gerhardt G & Hutchinson M. (2006). GDNF in treatment of Parkinson's disease: response to editorial. *Lancet Neurol* **5**, 202-203.
- Perron JC & Bixby JL. (1999). Distinct neurite outgrowth signaling pathways converge on ERK activation. *Mol Cell Neurosci* **13**, 362-378.

Persico AM, Di Pino G & Levitt P. (2006). Multiple receptors mediate the trophic effects of serotonin on ventroposterior thalamic neurons in vitro. *Brain Res* **1095**, 17-25.

Pocock JM & Kettenmann H. (2007). Neurotransmitter receptors on microglia. *Trends Neurosci* **30**, 527-535.

Pong K, Xu RY, Baron WF, Louis JC & Beck KD. (1998). Inhibition of phosphatidylinositol 3-kinase activity blocks cellular differentiation mediated by glial cell line-derived neurotrophic factor in dopaminergic neurons. *J Neurochem* **71**, 1912-1919.

Post A, Crochemore C, Uhr M, Holsboer F & Behl C. (2000). Differential induction of NF-kappaB activity and neural cell death by antidepressants in vitro. *Eur J Neurosci* **12**, 4331-4337.

Pousset F, Fournier J, Legoux P, Keane P, Shire D & Soubrie P. (1996). Effect of serotonin on cytokine mRNA expression in rat hippocampal astrocytes. *Brain Res Mol Brain Res* **38**, 54-62.

Powers CJ, McLeskey SW & Wellstein A. (2000). Fibroblast growth factors, their receptors and signaling. *Endocr Relat Cancer* **7**, 165-197.

Qui MS & Green SH. (1992). PC12 cell neuronal differentiation is associated with prolonged p21ras activity and consequent prolonged ERK activity. *Neuron* **9**, 705-717.

Rang HP & Dale MM. (2003). *Pharmacology*. Church Livingstone, Edinburgh.

- Read DE & Gorman AM. (2009). Involvement of Akt in neurite outgrowth. *Cell Mol Life Sci* **66**, 2975-2984.
- Redmond L, Kashani AH & Ghosh A. (2002). Calcium regulation of dendritic growth via CaM kinase IV and CREB-mediated transcription. *Neuron* **34**, 999-1010.
- Reichardt LF. (2006). Neurotrophin-regulated signalling pathways. *Philos Trans R Soc Lond B Biol Sci* **361**, 1545-1564.
- Reuss B & von Bohlen und Halbach O. (2003). Fibroblast growth factors and their receptors in the central nervous system. *Cell Tissue Res* **313**, 139-157.
- Riva MA, Molteni R, Lovati E, Fumagalli F, Rusnati M & Racagni G. (1996). Cyclic AMP-dependent regulation of fibroblast growth factor-2 messenger RNA levels in rat cortical astrocytes: comparison with fibroblast growth factor-1 and ciliary neurotrophic factor. *Mol Pharmacol* **49**, 699-706.
- Rosenstein JM, Mani N, Khaibullina A & Krum JM. (2003). Neurotrophic effects of vascular endothelial growth factor on organotypic cortical explants and primary cortical neurons. *J Neurosci* **23**, 11036-11044.
- Sager JJ & Torres GE. (2011). Proteins interacting with monoamine transporters: current state and future challenges. *Biochemistry* **50**, 7295-7310.
- Sanders VM & Straub RH. (2002). Norepinephrine, the beta-adrenergic receptor, and immunity. *Brain Behav Immun* **16**, 290-332.

Sarder M, Abe K, Saito H & Nishiyama N. (1996). Comparative effect of IL-2 and IL-6 on morphology of cultured hippocampal neurons from fetal rat brain. *Brain Res* **715**, 9-16.

Satoh T, Nakamura S, Taga T, Matsuda T, Hirano T, Kishimoto T & Kaziro Y. (1988). Induction of neuronal differentiation in PC12 cells by B-cell stimulatory factor 2/interleukin 6. *Mol Cell Biol* **8**, 3546-3549.

Schafer DP & Stevens B. (2010). Synapse elimination during development and disease: immune molecules take centre stage. *Biochem Soc Trans* **38**, 476-481.

Schiavone D, Dewilde S, Vallania F, Turkson J, Di Cunto F & Poli V. (2009). The RhoU/Wrch1 Rho GTPase gene is a common transcriptional target of both the gp130/STAT3 and Wnt-1 pathways. *Biochem J* **421**, 283-292.

Schwartz JP & Costa E. (1977). Regulation of nerve growth factor content in C6 glioma cells by beta-adrenergic receptor stimulation. *Naunyn Schmiedebergs Arch Pharmacol* **300**, 123-129.

Scott EK & Luo L. (2001). How do dendrites take their shape? *Nat Neurosci* **4**, 359-365.

Segal RA, Pomeroy SL & Stiles CD. (1995). Axonal growth and fasciculation linked to differential expression of BDNF and NT3 receptors in developing cerebellar granule cells. *J Neurosci* **15**, 4970-4981.

Semkova I, Schilling M, Henrich-Noack P, Rami A & Kriegelstein J. (1996). Clenbuterol protects mouse cerebral cortex and rat hippocampus from ischemic damage and attenuates

glutamate neurotoxicity in cultured hippocampal neurons by induction of NGF. *Brain Res* **717**, 44-54.

Semkova I, Wolz P & Krieglstein J. (1998). Neuroprotective effect of 5-HT_{1A} receptor agonist, Bay X 3702, demonstrated in vitro and in vivo. *Eur J Pharmacol* **359**, 251-260.

Shang T, Uihlein AV, Van Asten J, Kalyanaraman B & Hillard CJ. (2003). 1-Methyl-4-phenylpyridinium accumulates in cerebellar granule neurons via organic cation transporter 3. *J Neurochem* **85**, 358-367.

Siddiquee K, Zhang S, Guida WC, Blaskovich MA, Greedy B, Lawrence HR, Yip ML, Jove R, McLaughlin MM, Lawrence NJ, Sebt SM & Turkson J. (2007). Selective chemical probe inhibitor of Stat3, identified through structure-based virtual screening, induces antitumor activity. *Proc Natl Acad Sci U S A* **104**, 7391-7396.

Sole C, Dolcet X, Segura MF, Gutierrez H, Diaz-Meco MT, Gozzelino R, Sanchis D, Bayascas JR, Gallego C, Moscat J, Davies AM & Comella JX. (2004). The death receptor antagonist FAIM promotes neurite outgrowth by a mechanism that depends on ERK and NF-kappa B signaling. *J Cell Biol* **167**, 479-492.

Sondell M, Sundler F & Kanje M. (2000). Vascular endothelial growth factor is a neurotrophic factor which stimulates axonal outgrowth through the flk-1 receptor. *Eur J Neurosci* **12**, 4243-4254.

Song HJ, Ming GL & Poo MM. (1997). cAMP-induced switching in turning direction of nerve growth cones. *Nature* **388**, 275-279.

Spoehr T, Dezonne RS, Rehen SK & Gomes FC. (2011). Astrocytes treated by lysophosphatidic acid induce axonal outgrowth of cortical progenitors through extracellular matrix protein and epidermal growth factor signaling pathway. *J Neurochem* **119**, 113-123.

Spooren A, Kolmus K, Laureys G, Clinckers R, De Keyser J, Haegeman G & Gerlo S. (2011). Interleukin-6, a mental cytokine. *Brain Res Rev* **67**, 157-183.

Stevens B, Allen NJ, Vazquez LE, Howell GR, Christopherson KS, Nouri N, Micheva KD, Mehalow AK, Huberman AD, Stafford B, Sher A, Litke AM, Lambris JD, Smith SJ, John SW & Barres BA. (2007). The classical complement cascade mediates CNS synapse elimination. *Cell* **131**, 1164-1178.

Suchanek B, Struppeck H & Fahrig T. (1998). The 5-HT_{1A} receptor agonist BAY x 3702 prevents staurosporine-induced apoptosis. *Eur J Pharmacol* **355**, 95-101.

Suter-Crazzolara C & Unsicker K. (1996). GDNF mRNA levels are induced by FGF-2 in rat C6 glioblastoma cells. *Brain Res Mol Brain Res* **41**, 175-182.

Szabo C, Hasko G, Zingarelli B, Nemeth ZH, Salzman AL, Kvetan V, Pastores SM & Vizi ES. (1997). Isoproterenol regulates tumour necrosis factor, interleukin-10, interleukin-6 and nitric oxide production and protects against the development of vascular hyporeactivity in endotoxaemia. *Immunology* **90**, 95-100.

Szebenyi G, Dent EW, Callaway JL, Seys C, Lueth H & Kalil K. (2001). Fibroblast growth factor-2 promotes axon branching of cortical neurons by influencing morphology and behavior of the primary growth cone. *J Neurosci* **21**, 3932-3941.

Takahashi M. (2001). The GDNF/RET signaling pathway and human diseases. *Cytokine Growth Factor Rev* **12**, 361-373.

Takano T, Oberheim N, Cotrina ML & Nedergaard M. (2009). Astrocytes and ischemic injury. *Stroke* **40**, S8-12.

Tan KS, Nackley AG, Satterfield K, Maixner W, Diatchenko L & Flood PM. (2007). Beta2 adrenergic receptor activation stimulates pro-inflammatory cytokine production in macrophages via PKA- and NF-kappaB-independent mechanisms. *Cell Signal* **19**, 251-260.

Tanabe K, Nishimura K, Dohi S & Kozawa O. (2009). Mechanisms of interleukin-1beta-induced GDNF release from rat glioma cells. *Brain Res* **1274**, 11-20.

Tanaka J, Toku K, Zhang B, Ishihara K, Sakanaka M & Maeda N. (1999). Astrocytes prevent neuronal death induced by reactive oxygen and nitrogen species. *Glia* **28**, 85-96.

Tanoue A, Koshimizu TA, Shibata K, Nasa Y, Takeo S & Tsujimoto G. (2003). Insights into alpha1 adrenoceptor function in health and disease from transgenic animal studies. *Trends Endocrinol Metab* **14**, 107-113.

Tao X, Finkbeiner S, Arnold DB, Shaywitz AJ & Greenberg ME. (1998). Ca²⁺ influx regulates BDNF transcription by a CREB family transcription factor-dependent mechanism. *Neuron* **20**, 709-726.

Thanos S, Bahr M, Barde YA & Vanselow J. (1989). Survival and Axonal Elongation of Adult Rat Retinal Ganglion Cells. *Eur J Neurosci* **1**, 19-26.

Tom VJ, Doller CM, Malouf AT & Silver J. (2004). Astrocyte-associated fibronectin is critical for axonal regeneration in adult white matter. *J Neurosci* **24**, 9282-9290.

Toyomoto M, Inoue S, Ohta K, Kuno S, Ohta M, Hayashi K & Ikeda K. (2005). Production of NGF, BDNF and GDNF in mouse astrocyte cultures is strongly enhanced by a cerebral vasodilator, ifenprodil. *Neurosci Lett* **379**, 185-189.

Traverse S, Gomez N, Paterson H, Marshall C & Cohen P. (1992). Sustained activation of the mitogen-activated protein (MAP) kinase cascade may be required for differentiation of PC12 cells. Comparison of the effects of nerve growth factor and epidermal growth factor. *Biochem J* **288 (Pt 2)**, 351-355.

Tremblay ME, Stevens B, Sierra A, Wake H, Bessis A & Nimmerjahn A. (2011). The role of microglia in the healthy brain. *J Neurosci* **31**, 16064-16069.

Trentin AG, De Aguiar CB, Garcez RC & Alvarez-Silva M. (2003). Thyroid hormone modulates the extracellular matrix organization and expression in cerebellar astrocyte: effects on astrocyte adhesion. *Glia* **42**, 359-369.

Tsai J, Grutzendler J, Duff K & Gan WB. (2004). Fibrillar amyloid deposition leads to local synaptic abnormalities and breakage of neuronal branches. *Nat Neurosci* **7**, 1181-1183.

Tsui-Pierchala BA, Milbrandt J & Johnson EM, Jr. (2002). NGF utilizes c-Ret via a novel GFL-independent, inter-RTK signaling mechanism to maintain the trophic status of mature sympathetic neurons. *Neuron* **33**, 261-273.

Turner CA, Akil H, Watson SJ & Evans SJ. (2006). The fibroblast growth factor system and mood disorders. *Biol Psychiatry* **59**, 1128-1135.

Tuszynski MH, Thal L, Pay M, Salmon DP, U HS, Bakay R, Patel P, Blesch A, Vahlsing HL, Ho G, Tong G, Potkin SG, Fallon J, Hansen L, Mufson EJ, Kordower JH, Gall C & Conner J. (2005). A phase 1 clinical trial of nerve growth factor gene therapy for Alzheimer disease. *Nat Med* **11**, 551-555.

Vaidya VA, Marek GJ, Aghajanian GK & Duman RS. (1997). 5-HT_{2A} receptor-mediated regulation of brain-derived neurotrophic factor mRNA in the hippocampus and the neocortex. *J Neurosci* **17**, 2785-2795.

van der Poll T, Jansen J, Endert E, Sauerwein HP & van Deventer SJ. (1994). Noradrenaline inhibits lipopolysaccharide-induced tumor necrosis factor and interleukin 6 production in human whole blood. *Infect Immun* **62**, 2046-2050.

Van der Zee CE, Fawcett J & Diamond J. (1992). Antibody to NGF inhibits collateral sprouting of septohippocampal fibers following entorhinal cortex lesion in adult rats. *J Comp Neurol* **326**, 91-100.

Vanhoutte P, Nissen JL, Brugg B, Gaspera BD, Besson MJ, Hipskind RA & Caboche J. (2001). Opposing roles of Elk-1 and its brain-specific isoform, short Elk-1, in nerve growth factor-induced PC12 differentiation. *J Biol Chem* **276**, 5189-5196.

Vaudry D, Stork PJ, Lazarovici P & Eiden LE. (2002). Signaling pathways for PC12 cell differentiation: making the right connections. *Science* **296**, 1648-1649.

Vawter MP, Basaric-Keys J, Li Y, Lester DS, Lebovics RS, Lesch KP, Kulaga H, Freed WJ, Sunderland T & Wolozin B. (1996). Human olfactory neuroepithelial cells: tyrosine phosphorylation and process extension are increased by the combination of IL-1beta, IL-6, NGF, and bFGF. *Exp Neurol* **142**, 179-194.

Veeranna, Amin ND, Ahn NG, Jaffe H, Winters CA, Grant P & Pant HC. (1998). Mitogen-activated protein kinases (Erk1,2) phosphorylate Lys-Ser-Pro (KSP) repeats in neurofilament proteins NF-H and NF-M. *J Neurosci* **18**, 4008-4021.

Verma NK, Dourlat J, Davies AM, Long A, Liu WQ, Garbay C, Kelleher D & Volkov Y. (2009). STAT3-stathmin interactions control microtubule dynamics in migrating T-cells. *J Biol Chem* **284**, 12349-12362.

Vige X, Costa E & Wise BC. (1991). Mechanism of nerve growth factor mRNA regulation by interleukin-1 and basic fibroblast growth factor in primary cultures of rat astrocytes. *Mol Pharmacol* **40**, 186-192.

Viollet C & Doherty P. (1997). CAMs and the FGF receptor: an interacting role in axonal growth. *Cell Tissue Res* **290**, 451-455.

Vlahos CJ, Matter WF, Hui KY & Brown RF. (1994). A specific inhibitor of phosphatidylinositol 3-kinase, 2-(4-morpholinyl)-8-phenyl-4H-1-benzopyran-4-one (LY294002). *J Biol Chem* **269**, 5241-5248.

Walicke P, Cowan WM, Ueno N, Baird A & Guillemin R. (1986). Fibroblast growth factor promotes survival of dissociated hippocampal neurons and enhances neurite extension. *Proc Natl Acad Sci U S A* **83**, 3012-3016.

Wang YM & Yang ZC. (2007). [The influence of terbutaline on VEGF gene expression in rat astrocytes after norepinephrine and burn serum induction]. *Zhonghua Shao Shang Za Zhi* **23**, 346-348.

Wang YQ, Cui HR, Yang SZ, Sun HP, Qiu MH, Feng XY & Sun FY. (2009). VEGF enhance cortical newborn neurons and their neurite development in adult rat brain after cerebral ischemia. *Neurochem Int* **55**, 629-636.

Wenzel-Seifert K & Seifert R. (2000). Molecular analysis of beta(2)-adrenoceptor coupling to G(s)-, G(i)-, and G(q)-proteins. *Mol Pharmacol* **58**, 954-966.

White MJ, DiCaprio MJ & Greenberg DA. (1996). Assessment of neuronal viability with Alamar blue in cortical and granule cell cultures. *J Neurosci Methods* **70**, 195-200.

Widmann C, Gibson S, Jarpe MB & Johnson GL. (1999). Mitogen-activated protein kinase: conservation of a three-kinase module from yeast to human. *Physiol Rev* **79**, 143-180.

Wood JN. (1995). Regulation of NF-kappa B activity in rat dorsal root ganglia and PC12 cells by tumour necrosis factor and nerve growth factor. *Neurosci Lett* **192**, 41-44.

Wu YY & Bradshaw RA. (1996). Induction of neurite outgrowth by interleukin-6 is accompanied by activation of Stat3 signaling pathway in a variant PC12 cell (E2) line. *J Biol Chem* **271**, 13023-13032.

- Yamamuro A, Ago Y, Takuma K, Maeda S, Sakai Y, Baba A & Matsuda T. (2003). Possible involvement of astrocytes in neuroprotection by the cognitive enhancer T-588. *Neurochem Res* **28**, 1779-1783.
- Yamashita H, Sato N, Kizaki T, Oh-ishi S, Segawa M, Saitoh D, Ohira Y & Ohno H. (1995). Norepinephrine stimulates the expression of fibroblast growth factor 2 in rat brown adipocyte primary culture. *Cell Growth Differ* **6**, 1457-1462.
- Yang EV, Donovan EL, Benson DM & Glaser R. (2008). VEGF is differentially regulated in multiple myeloma-derived cell lines by norepinephrine. *Brain Behav Immun* **22**, 318-323.
- York RD, Molliver DC, Grewal SS, Stenberg PE, McCleskey EW & Stork PJ. (2000). Role of phosphoinositide 3-kinase and endocytosis in nerve growth factor-induced extracellular signal-regulated kinase activation via Ras and Rap1. *Mol Cell Biol* **20**, 8069-8083.
- Yoshimatsu T, Kawaguchi D, Oishi K, Takeda K, Akira S, Masuyama N & Gotoh Y. (2006). Non-cell-autonomous action of STAT3 in maintenance of neural precursor cells in the mouse neocortex. *Development* **133**, 2553-2563.
- Yoshimura T, Kawano Y, Arimura N, Kawabata S, Kikuchi A & Kaibuchi K. (2005). GSK-3beta regulates phosphorylation of CRMP-2 and neuronal polarity. *Cell* **120**, 137-149.
- Zafra F, Lindholm D, Castren E, Hartikka J & Thoenen H. (1992). Regulation of brain-derived neurotrophic factor and nerve growth factor mRNA in primary cultures of hippocampal neurons and astrocytes. *J Neurosci* **12**, 4793-4799.

Zeman RJ, Feng Y, Peng H & Etlinger JD. (1999). Clenbuterol, a beta(2)-adrenoceptor agonist, improves locomotor and histological outcomes after spinal cord contusion in rats. *Exp Neurol* **159**, 267-273.

Zhang J, Roberts TM & Shivdasani RA. (2011). Targeting PI3K signaling as a therapeutic approach for colorectal cancer. *Gastroenterology* **141**, 50-61.

Zhou L & Too HP. (2011). Mitochondrial localized STAT3 is involved in NGF induced neurite outgrowth. *PLoS One* **6**, e21680.

Zhu Y, Culmsee C, Semkova I & Krieglstein J. (1998). Stimulation of beta2-adrenoceptors inhibits apoptosis in rat brain after transient forebrain ischemia. *J Cereb Blood Flow Metab* **18**, 1032-1039.

Zhu Y, Prehn JH, Culmsee C & Krieglstein J. (1999). The beta2-adrenoceptor agonist clenbuterol modulates Bcl-2, Bcl-xl and Bax protein expression following transient forebrain ischemia. *Neuroscience* **90**, 1255-1263.

